Konstantinos Grammatoglou

JAUNU METOŽU IZSTRĀDE PLP ATKARĪGO ENZĪMU INHIBITORU SINTĒZEI UN BAKTĒRIJU ENZĪMA O-ACETILSERĪNA SULFHIDRILĀZES KOVALENTĀS INHIBĪCIJAS POTENCIĀLA IZPĒTE

Promocijas darbs

THE DEVELOPMENT OF NEW METHODS FOR THE SYNTHESIS OF PLP-DEPENDENT ENZYME INHIBITORS AND EXPLORING COVALENT INHIBITION POTENTIAL OF BACTERIAL ENZYME O-ACETYLSERINE SULFHYDRYLASE
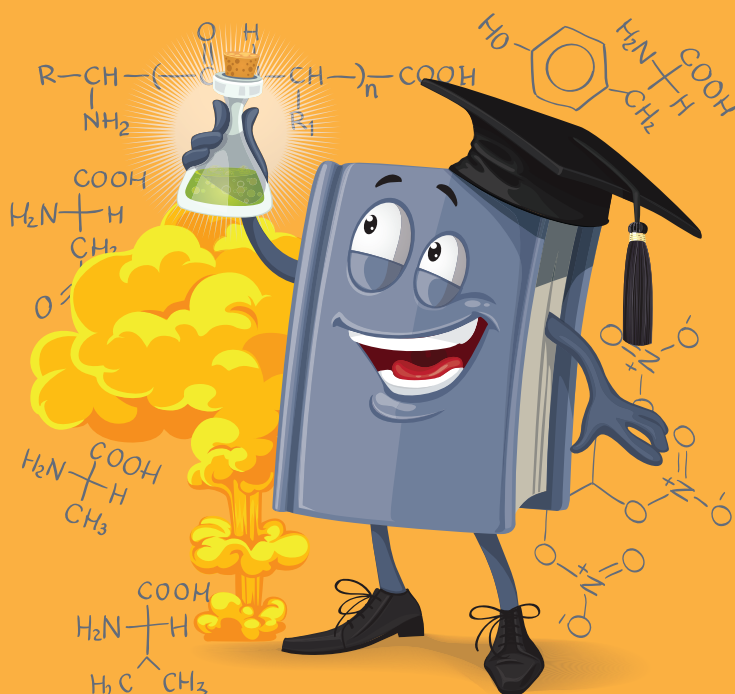
Doctoral Thesis

RĪGAS TEHNISKĀ UNIVERSITĀTE

Materiālzinātnes un lietišķās ķīmijas fakultāte
Organiskās ķīmijas tehnoloģijas institūts
Bioloģiski aktīvo savienojumu ķīmijas tehnoloģijas katedra

RIGA TECHNICAL UNIVERSITY

Faculty of Materials Science and Applied Chemistry
Institute of Technology of Organic Chemistry
Department of Chemical Technology of Biologically Active Compounds

Konstantinos Grammatoglou

Doktora studiju programmas "Ķīmija" doktorants
Student of the Doctoral Program "Chemistry"

Jaunu metožu izstrāde PLP atkarīgo enzīmu inhibitoru sintēzei un baktēriju enzīma O-acetilserīna sulfhidrilāzes kovalentās inhibīcijas potenciāla izpēte
The development of new methods for the synthesis of PLP dependent enzyme inhibitors and exploring covalent inhibition potential of bacterial enzyme O-acetylserine sulfhydrylase

Promocijas darbs
Doctoral Thesis

Zinātniskais vadītājs
Scientific supervisor

Profesors/Professor *Dr. chem.* AIGARS JIRGENSONS

RTU Izdevniecība
RTU Press
Rīga 2023

Pateicības

Īpašs paldies:

- Profesoram *Dr. chem.* A. Jirgensonam par zinātniskajām diskusijām, norādījumiem un vērtīgiem padomiem.
- *Dr. chem.* Annai Ņikitjukai par emocionālo atbalstu doktorantūras studiju gados un augsti novērtēto mana promocijas darba pārlasīšanu.
- Elīnai Līdumniecei, Jekaterinai Boļšakovai un Marijai Skvorcovai par komandas darbu.
- Visiem OSM grupas kolēģiem par izcilas darba vides radīšanu.
- Manai ģimenei par atbalstu un pacietību.

Acknowledgements

Special thanks to:

- Professor *Dr. chem.* A. Jirgensons for the scientific discussions, the guidance and fruitful advice.
- *Dr. chem.* Anna Nikitjuka for emotional support through the years of doctoral studies and deeply appreciated proof–reading of my Ph.D. Thesis.
- Elina Lidumniece, Jekaterina Bolsakova and Marija Skvorcova for their collaboration.
- All of the OSM group colleagues for creating an excellent working environment
- My family for the support and patience.

PROMOCIJAS DARBS IZVIRZĪTS ZINĀTNES DOKTORA GRĀDA IEGŪŠANAI RĪGAS TEHNISKAJĀ UNIVERSITĀTĒ

Promocijas darbs zinātnes doktora (*Ph. D.*) grāda iegūšanai tiek publiski aizstāvēts 2023. gada 14.jūnijā plkst. 14:00 Rīgas Tehniskās universitātes Materiālzinātnes un lietišķās ķīmijas fakultātē, Rīgā, Paula Valdena ielā 3, 272.auditorijā.

OFICIĀLIE RECENZENTI

Dr. chem. Mārtiņš Katkevičs Latvijas (Organiskās sintēzes institūts)

Dr. chem. Artis Kinēns (Latvijas Universitāte)

Dr. Marc Nazare (Leibnicas Molekulārās farmakoloģijas institūts (*Leibniz-Institute for Molecular Pharmacology*), Vācija)

APSTIPRINĀJUMS

Apstiprinu, ka esmu izstrādājis šo promocijas darbu, kas iesniegts izskatīšanai Rīgas Tehniskajā universitātē zinātnes doktora (*Ph. D.*) grāda iegūšanai. Promocijas darbs zinātniskā grāda iegūšanai nav iesniegts nevienā citā universitātē.

Konstantinos Grammatoglou ………………….(paraksts)

Datums …………………………

Promocijas darbs sagatavots kā tematiski vienota zinātnisko publikāciju kopa. Tas satur kopsavilkumu gan latviešu, gan angļu valodā. Promocijas darbs apvieno četras zinātniskas publikācijas, kas uzrakstītas angļu valodā, kopējais apjoms, ieskaitot elektroniski pieejamo informāciju, ir 301 lappuse.

SAĪSINĀJUMI

AIBN	α,α'–azobisizobutironitrils
Boc	*terc*-butoksikarbonil-
CADD	datorizēta zāļu izstrāde
CAN	cerija amonija nitrāts
CDI	1,1'-karbonildiimidazols
DCE	1,2-dihloretāns
DCM	dihlormetāns
DDQ	5,6-diciāno-2,3-dihloro-1,4-benzohinons
DFSI	asparagīnskābes–fenilalanīna–serīna–izoleicīna peptīds
DIPEA	diizopropiletilamīns
DMAP	4-dimetilaminopiridīns
EDC	1-etil-3-(3-dimetilaminopropil)karbodiimīds
HATU	heksafluorfosfāts azabenzotriazols tetrametiluronijs
HPLC	augstas veiktspējas šķidruma hromatogrāfija
IC_{50}	puse no maksimālās inhibējošās koncentrācijas
ist.t.	istabas temperatūra
LC/MS	šķidruma hromatogrāfija – masas spektrometrija
MeCN	acetonitrils
NBS	*N*-bromsukcinimīds
*n*Bu	*n*-butil-
NMO	*N*-metilmorfolīna *N*-oksīds
OASS	*O*-acetilserīna sulfhidrilāze
PDB	proteīnu datu banka
Ph	fenil-
PLP	piridoksāla 5'-fosfāts (B6 vitamīns)
PMB	*p*-metoksibenzil-
RCSB	strukturālās bioinformātikas pētījumu sadarbības centrs
PVO	Pasaules Veselības organizācija
SAR	struktūras–aktivitātes likumsakarības
SAT	serīna acetiltransferāze
TBA·BF$_4$	tetrabutilamonija tetrafluorborāts
*t*Bu	*terc*-butil-
TBS	*terc*-butildimetilsilil-
TFA	trifluoretiķskābe
THF	tetrahidrofurāns
triF-Ala	3,3,3-trifluoralanīns

SATURS

PROMOCIJAS DARBA VISPĀRĒJS RAKSTUROJUMS
Ievads

Antibiotiku attīstība 20. gadsimta pirmajā pusē, kad Aleksandra Fleminga 1928. gadā atklātais penicilīns bija visievērojamākais notikums, liecināja par revolucionāra laikmeta sākumu medicīnā (1. att.).[1a] Dzīves ilgums visās valstīs ievērojami palielinājās, slimības, kas līdz tam attīstītajās valstīs bija neārstējamas un letālas, tagad kļuva ārstējamas ar antibiotikām, sarežģītu ķirurģisku operāciju veikšana kļuva iespējama, cilvēkiem ar imūnsupresiju vai hroniskām slimībām izdevās cīnīties vai novērst infekcijas. Līdzīgi ieguvumi no antibiotiku lietošanas novēroti arī jaunattīstības valstīs, kur ārstētas ar piesārņotu pārtikas produktu saistītas un citas ar nabadzību saistītas infekcijas, samazinot saslimstību un mirstību.[1a] Selmans Vaksmans 30. gadu beigās definēja antibiotiku kā "savienojumu, kas izveidots ar mikrobu, lai iznīcinātu citus mikrobus". Vaksmans identificēja augsnē mītošos pavedienveida aktinomicītus kā pretmikrobu savienojumu ražotājus, tostarp neomicīnu un streptomicīnu, kas bija pirmie aktīvie savienojumi tuberkulozes ārstēšanai. Vaksmana darbs aizsāka antibiotiku zelta laikmetu no 40. līdz 60. gadu beigām, šajā laika posmā atklātas vairāk nekā 20 jaunas antibiotiku klases. Izstrādātas ne tikai makrolīdu, glikopeptīdu, cefalosporīnu, hinolonu, azolu u.c. klases, bet arī klases, kas ietver dabiskus produktus vai sintētiskas antibiotikas, kuru iedvesmas avots ir dabiski produkti (1. att.).[1b,1c]

Bažas par nepareizu penicilīna lietošanu Aleksandrs Flemings pauda jau 1945. gadā. Viņš atklāja stafilokokus, kas bija imūni pret penicilīnu, un paredzēja rezistentu baktēriju izplatīšanos. Antibiotiku rezistences rašanos izraisīja dažādi faktori, piemēram, pārmērīga antibiotiku lietošana, nepareiza antibiotiku izrakstīšana un plaša izmantošana lauksaimniecībā. Turklāt daudzu farmācijas uzņēmumu lēmums atteikties no jaunu antibiotiku izstrādes, kā arī pieaugošās grūtības iegūt normatīvo apstiprinājumu jaunajiem savienojumiem ir izraisījuši jaunatklāto antibiotiku tirdzniecības samazināšanos, kas tikai papildina konstatēto antibiotiku rezistences problēmu (1. att.).[1a,1d,1e]
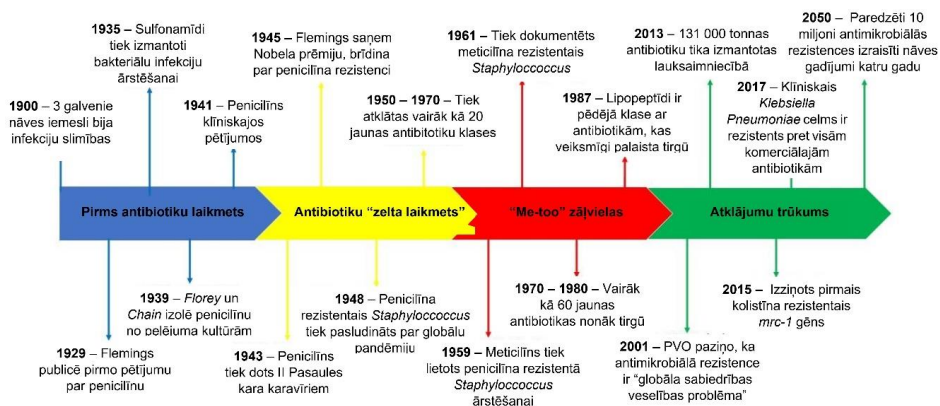

1. att. Mikrobiālās rezistences veidošanās laika skala.

Lai pārvarētu noteiktu antibiotiku neefektivitāti, ir izstrādātas "me-too" zāļvielas, kas radās esošo antibiotiku nelielu modifikāciju rezultātā. Diemžēl "me-too" zāļvielas darbības

mehānisms diezgan bieži bija identisks, kā rezultātā arī pret šiem savienojumiem ātri izveidojās rezistence.[1e] 2001. gadā Pasaules Veselības organizācija (PVO) pasludināja mikrobiālo rezistenci par "globālu sabiedrības veselības problēmu" un norādīja, ka zinātniskais izrāviens līdz mūsdienām šajā jomā nav noticis. Jaunatklāto antibiotiku skaits pēdējās desmitgadēs ir diezgan ierobežots, un lielākā daļa zāļu, kas nonāk klīnikā, strādā pēc tiem pašiem mehānismiem kā tradicionālās antibiotikas.[1e]

Meklējot jaunas, efektīvas antibiotikas, ir izmantotas dažādas stratēģijas, piemēram, hibrīdu pretmikrobu līdzekļu, membrānas aktīvu zāļu un baktēriju virulences un patoģenēzes inhibitoru izstrāde, kā arī alternatīvu metožu, piemēram, bakteriofāgu izmantošana. Cita jaunu antibiotiku izstrādes metode ir vērsta uz galvenajām baktēriju vielmaiņas funkcijām. Mērķēšana uz svarīgiem, bet nebūtiskiem gēnu produktiem var būt efektīvs līdzeklis baktēriju pielāgošanās un izdzīvošanas mazināšanai, kā rezultātā tiek uzlabota ārstēšana ar antibiotikām, saīsināti latentuma periodi, palielināta jutība pret tradicionālajām antibiotikām un tādējādi atvieglota saimnieka imūnsistēmas spēja izvadīt patogēnu.[3]

Sērs ir daudzu biomolekulu pamatkomponents, sākot no aminoskābēm, piemēram, cisteīnu, līdz kofaktoriem un savienojumiem, kas kontrolē redoks homeostāzi. Enzīmi, kas iesaistīti cisteīna biosintēzes ceļā un atrodami patogēnos un augos, bet nav sastopami zīdītājos, ir ļoti pievilcīgi antibakteriālie mērķi. Ir pierādīts, ka cisteīna biosintēzes inhibēšana ietekmē patogēnu spēju cīnīties ar oksidatīvo stresu, samazina to virulenci un rezistenci pret antibiotikām.[3,4] Cisteīna biosintēzes pēdējie posmi ietver divu enzīmu darbību – serīna acetiltransferāzes (SAT), kas acetilē serīnu, un O-acetilserīna sulfhidrilāzes (OASS), no piridoksāla 5'-fosfāta (PLP) atkarīgu enzīmu, kas veic β-aizvietošanas reakciju acetilserīnā (1. shēma).
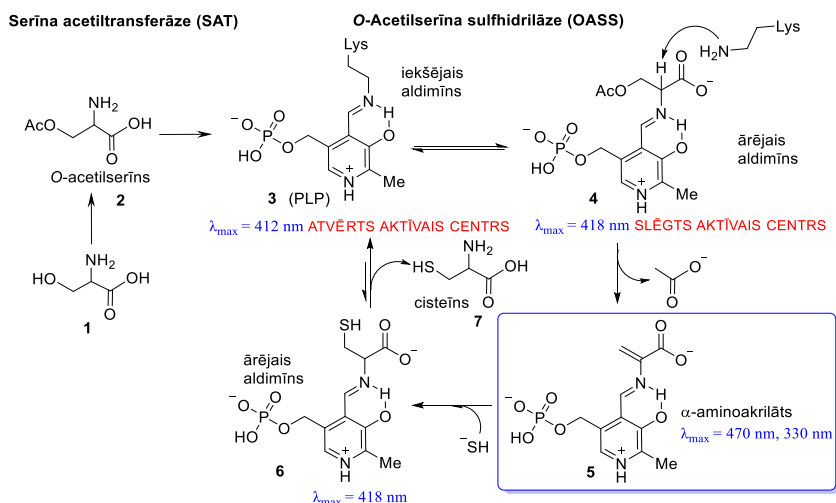
1. shēma. OASS katalītiskais cikls cisteīna (7) veidošanai.

OASS baktērijās atrodas divās izoformās, OASS-A un OASS-B, ko kodēšanas gēnos sauc arī par CysK un CysM. Serīna acetiltransferāze (SAT) spēj veidot augstas afinitātes kompleksu ar OASS-A, bet ne ar OASS-B.[5]

Lai izveidotu no PLP atkarīgu enzīmu inhibitorus, izmēģinātas vairākas pieejas, izmantojot struktūrā, ligandos vai mehānismā balstītu dizainu. Pirmie mēģinājumi bija vērsti uz dabiska pentapeptīda struktūrelementu atdarināšanu, veidojot OASS ligandus ar afinitāti mikromolārā diapazonā. Tā kā peptīdiskiem inhibitoriem nereti nepiemīt zāļvielām raksturīgās īpašības, izmantojot *in silico* un sintētiskās ķīmijas metodes, tika izveidoti dažādi aktīvi mazmolekulāri savienojumi (2. att.).[6]

K$_d$ *Hi*OASS-A = 1.45 µM

9

K$_d$ *St*OASS-A = 1.45 µM
K$_d$ *St*OASS-B = 148 µM

10

CysK1 inhibitor
IC$_{50}$ = 19 nM

8

K$_d$ *St*OASS-A = 0.067 µM
K$_d$ *St*OASS-B = 1.66 µM

11

K$_d$ *St*OASS-A = 0.028 µM
K$_d$ *St*OASS-B = 0.49 µM

12
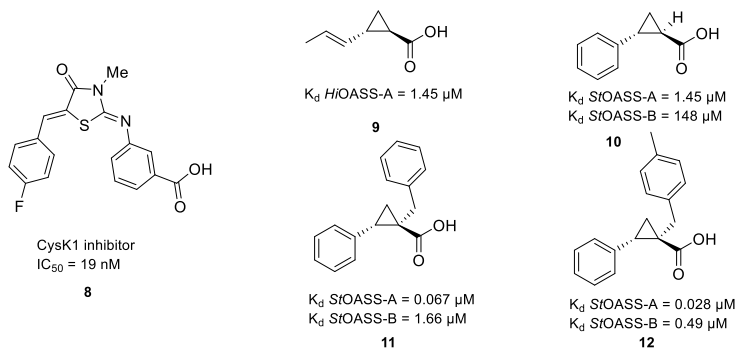
2. att. Zināmie OASS-A (CysK) inhibitori.

Mehānismā balstīti inhibitori ķīmiskas reakcijas rezultātā veido kovalentu neatgriezenisku proteīna–inhibitora kompleksu, kas kavē fermenta katalītisko darbību. Ir pētīts un ziņots par virkni kemotipu, kas darbojas kā mehānismā balstīti no PLP atkarīgu enzīmu inhibitori.[7]

Mikrobiālās rezistences pieaugums ir aktualizējis steidzamāku jaunu medikamentu mērķu noteikšanu. Lai gan PLP atkarīgie enzīmi veido apmēram 4% no Enzīmu Komisijas klasificētajiem enzīmiem, tikai neliels skaits no tiem ir identificēti kā potenciālie terapeitisko līdzekļu mērķi, un vēl mazāk ir tie, kuriem ir izstrādātas zāles. Šis ierobežotais skaits ir saistīts ar zināšanu trūkumu par PLP atkarīgo enzīmu saimi un to lomu dažādos bioloģiskos procesos. Tomēr tas, ka PLP piedalās dažādās reakcijās un ka dažādu PLP atvasinājumu spektrālās izmaiņas ievērojami palīdz kontolēt reakcijas gaitu, ir tikai divas no iezīmēm, kas padara šos enzīmus kā interesantus pētījumu objektus.[7d] Šajā aspektā enzīmi, kas iesaisti cisteīna biosintēzes ceļā ir ļoti aktuāli. OASS ir nozīmīgs cisteīna biosintēzes enzīms, kas ir potenciāls antibakteriālo zāļvielu mērķis, tāpēc ir svarīgi izstrādāt šī enzīma inhibitorus, lai izpētītu to lomu antibakteriālo zāļu atklāšanā. Ir nepieciešams identificēt jaunus kemotipus PLP atkarīgo enzīmu inhibēšanai un izstrādāt sintētiskās metodes šo jauno kemotipu iegūšanai.

Pētījuma mērķis un uzdevumi

Promocijas darba mērķis ir mehānismā balstītu no PLP atkarīgā enzīma *O*-acetilserīna sulfhidrilāzes (OASS) inhibitoru sintēze, balstoties uz esošajiem kemotipiem, jaunu kemotipu izpēte un jaunu sintētisko metožu izstrāde no PLP atkarīgu enzīmu potenciālo inhibitoru iegūšanai.

Darba mērķa īstenošanai izvirzīti šādi darba uzdevumi:

1. Izplānot un sintēzēt fokusētu potenciālo OASS inhibitoru bibliotēku.
2. Izstrādāt efektīvu metodi kvaternāro alkīnilglicīnolu sintēzei.
3. Izstrādāt sintētiskās metodes karbonskābes bioizostēra – tetrazola – ieviešanai molekulā.

Zinātniskā novitāte un galvenie rezultāti

Zinātnisko pētījumu ietvaros pārbaudīti vairāki zināmi un jauni savienojumi kā potenciāli baktēriju *O*-acetilserīna sulfhidrilāzes (OASS) inhibitori. Trifluoralanīns atklāts kā pirmais mehānismā balstītais OASS inhibitors. Izpētītas trifluoralanīna atvasinājumu struktūras aktivitātes likumsakarības (SAL).

Izstrādātas vairākas jaunas metodes no PLP atkarīgo enzīmu inhibitoru sintēzei:
1. *C*-Kvaternāro alkīnilglicīnolu sintēzes metode.
2. Metode tiešai tetrazolu C–H funkcionalizēšanai, izmantojot turbo Griņjāra reaģentu.
3. Metode tetrazolu funkcionalizēšanai ar elektroķīmiski nošķeļamu *N*-aizsarggrupu.
4. Metode stereoselektīvai aminoskābju analogu sintēzei, kas satur tetrazolu kā karbonskābes aizvietotāju.

Darba struktūra un apjoms

Promocijas darbs ir tematiski vienota zinātnisku publikāciju kopa. Publikācijās aprakstīta trifluoralanīna analogu sintēze un no PLP atkarīgu enzīmu inhibitoru sintēzes metožu izstrāde.

Publikācijas un darba aprobācija

Darba galvenie rezultāti apkopoti četrās publikācijās. Pētījuma rezultāti prezentēti astoņās konferencēs.

Zinātniskās publikācijas

1. **K. Grammatoglou**, J. Bolsakova, A. Jirgensons. C-Quaternary alkynyl glycinols *via* the Ritter reaction of cobalt complexed alkynyl glycols. *RSC Adv*. **2017**, *7*, 27530–27537.
2. N. Franko, **K. Grammatoglou**, B. Campanini, G. Costantino, A. Jirgensons, A. Mozzarelli. Inhibition of *O*-acetylserine sulfhydrylase by fluoroalanine derivatives. *J. Enzyme Inhib. Med. Chem.* **2018**, *33*(1), 1343–1351.
3. **K. Grammatoglou**, A. Jirgensons. Functionalization of 1*N*-Protected Tetrazoles by Deprotonation with the Turbo Grignard Reagent. *J. Org. Chem.* **2022**, *87*, 3810−3816.

4. **K. Grammatoglou**, M. Dārziņa, A. Jirgensons. Functionalization of Tetrazoles Bearing the Electrochemically Cleavable 1*N*-(6–Methylpyridyl–2–methyl) Protecting Group. *ACS Omega* **2022**, *7*, 18103−18109.

Dalība konferencēs

1. **K. Grammatoglou**, J. Sirotkina, A. Jirgensons. Synthesis of 4-Alkynyl 2-Oxazolines *via* the Ritter reaction. *9. Balticum Organicum Syntheticum konference (BOS 2016)*, Rīga, Latvija, 3.–6. jūlijs, **2016**, postera prezentācija.
2. **K. Grammatoglou**, J. Sirotkina. C-Quaternary Alkynyl Glycinols *via* the Ritter Reaction of Cobalt Complexed Alkynyl Glycols. *10. Paula Valdena simpozijs organiskajā ķīmijā*, Rīga, Latvija, 15.–16. jūnijs, **2017**, postera prezentācija.
3. N. Franko, J. Magalhães, **K. Grammatoglou**, B. Campanini, M. Pieroni, E. Azzali, G. Annunziato, G. Costantino, A. Jirgensons, A. Mozzarelli. Targeting enzymes of the sulfur assimilation pathway for the development of new antibiotics. *Proteine 2018 konferences materiāli (PROTEINE2018)*, Verona, Itālija, 28.–30. maijs, **2018**, postera prezentācija.
4. **K. Grammatoglou**, L. Levy, A. Jirgensons. Design and Synthesis of 3,3,3–trifluoroalanine Analogues as Potential Antibacterials. *10. Balticum Organicum Syntheticum konference (BOS 2018)*, Tallina, Igaunija, 1.–4. jūlijs, **2018**, postera prezentācija.
5. **K. Grammatoglou**. Design and synthesis of *O*-acetylserine sulfhydrylase inhibitors as potential antibacterials. *OUTREACH FINAL Konference ITN MSCA INTEGRATE "FIGHTING ESKAPE, THE BAD GANG"*, Parma, Itālija, 21.–23. novembris, **2018**, mutiska uzstāšanās.
6. **K. Grammatoglou**. Functionalization of 1*N*–protected tetrazoles by deprotonation with turbo Grignard reagent. *11. Paula Valdena simpozijs organiskajā ķīmijā*, Rīga, Latvija, 19.–20. septembris, **2019**, postera prezentācija.
7. **K. Grammatoglou**. Synthesis and Applications of Metalated 1*H*-tetrazoles. *Balticum Organicum Syntheticum konference (BOS 2022)*, Vilņa, Lietuva, 3.–6. jūlijs, **2022**, postera prezentācija.
8. **K. Grammatoglou**. Synthesis of PLP-dependent enzyme OASS inhibitors and the development of relevant synthetic methodologies. *Springboard vasaras skola "Major milestones in design and development of novel antimicrobials"*, Rīga, Latvija, 23.–25. augusts, **2022**, mutiska uzstāšanās.

PROMOCIJAS DARBA GALVENIE REZULTĀTI

1. Mehānismā balstītu OASS inhibitoru sintēze

Pētījuma sākumā izveidojām fokusētu bibliotēku no aminoskābēm, kas varētu būt no PLP atkarīgā enzīma OASS inhibitori (3. att.). Savienojumi **13**–**17** bija komerciāli pieejami, bet savienojumi **18**, **19** sintezēti citam, nesen publicētam projektam,[8] un savienojumus **20**–**22** sintezēja mūsu darba grupa. Bibliotēkas skrīnings pret OASS atklāja, ka triF-Ala (**13**) uzrāda inhibēšanas aktivitāti IC$_{50}$=132 µM (3. att.).
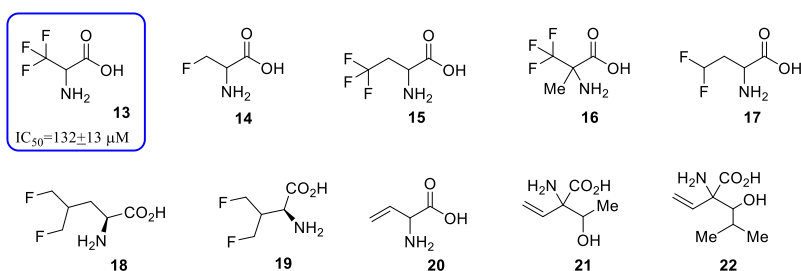
3. att. Mehānismā balstītu iespējamo OASS inhibitoru bibliotēka.

Alanīna halogēnatvasinājumi ir izmantoti kā vairāku no PLP atkarīgu enzīmu inhibitori.[5,9] Saskaņā ar iepriekš piedāvātajiem no PLP atkarīgu enzīmu inhibēšanas mehānismiem, triF-Ala (**13**) pievienojas enzīmam, un no iekšējā aldimīna **3** veidojas ārējais aldimīns **23** (2. shēma).
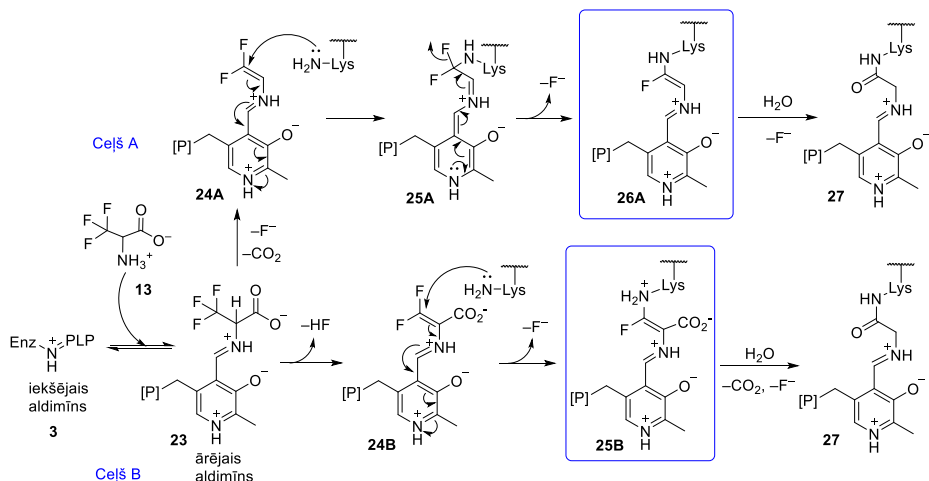

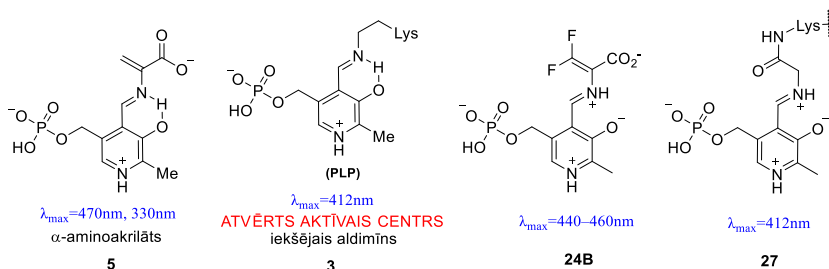**2. shēma. Iespējamie PLP atkarīgo enzīmu inaktivēšanas ceļi ar triF-Ala.**

Tālāk ir iespējami divi ceļi – ceļā A notiek fluorīdjona izšķelšana un dekarboksilēšana, veidojot starpproduktu **24A**. Otra fluora jona šķelšana un vienlaicīga enzīma aktīvajā centrā esošā lizīna uzbrukums elektrofīlā nepiesātinātā imīna dubultaitei ļauj iegūt

12

kovalenti saistītu un neaktīvu enzīma atvasinājumu **26A**. Ja nepiesātinātajam imīnam **26A** uzbrūk ūdens, tas pēc sekojošas HF izšķelšanas pārvēršas par amīdu **27**. Saskaņā ar ceļu B pēc sākotnējās transaldiminēšanas notiek HF eliminēšana, iegūstot starpproduktu **24B**, kas tiek pakļauts Maikla reakcijai ar aktīvā centra lizīnu un zaudē vēl vienu fluorīdjonu, veidojot neaktīvu kompleksu **25B**. Pēc ūdens pievienošanas kompleksam **25B** un secīgas dekarboksilēšanas un fluora zaudēšanas tiek iegūts amīds **27** (2. shēma).[5,10]

TriF-Ala mijiedarbība ar abām OASS, OASS-A (vai CysK) un OASS-B (vai CysM), enzīma izoformām pētīta ar absorbcijas un fluorescences spektroskopiju. Fotoķīmiski pētījumi parādīja, ka β,β,β-trifluoralanīns (triF-Ala, **13**) veido kovalentu savienojumu ar enzīmu, kas izraisa absorbcijas spektra izmaiņas, salīdzinot ar iekšējā aldimīna spektriem miera stāvoklī esošam enzīmam. Tas norāda, ka reakcija notiek ar kofaktoru. Kā jau minēts, OASS-A un OASS-B absorbcijas spektros ir josla pie 412 nm, kas raksturīga iekšējam aldimīnam **3** (5. att.). Pēc triF-Ala pievienošanas OASS-A spektrā parādījās divi maksimumi pie 440 un 466 nm un divas nelielas joslas pie 360 un 380 nm (4. att.), kas norāda uz starpsavienojumu ar garāku konjugācijas ķēdi (**24B**, 5. att.). Absorbcijas joslas pie 466 nm intensitāte lēnām samazinās, veidojoties joslai pie 412 nm. Mazāk intensīvas spektrālās izmaiņas novērotas triF-Ala reakcijā ar OASS-B diapazonā no 400 līdz 500 nm. Starpprodukta sadalīšanos, kuru pavada joslas intensitātes samazinājums pie 457 nm un absorbcijas palielināšanos diapazonā no 300 līdz 350 nm, iespējams, var saistīt ar difluorpiruvāta veidošanos.
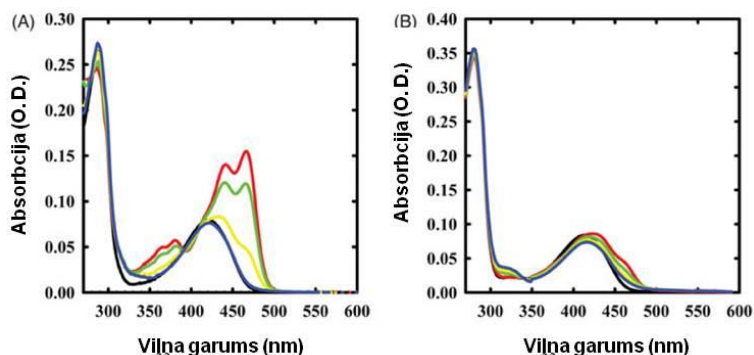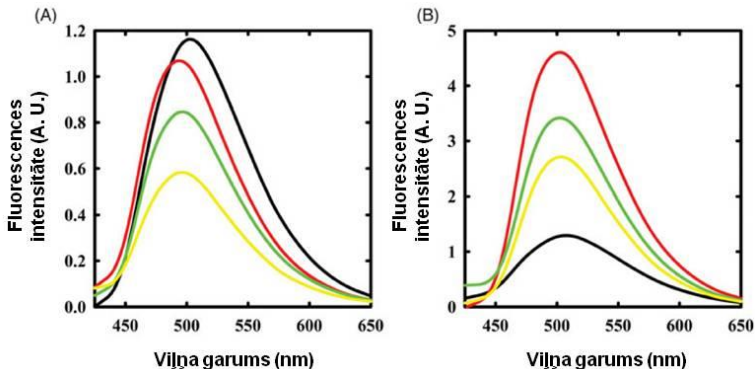

4. att. OASS absorbcijas spektri ar un bez 1 mM triF-Ala. A: OASS-A absorbcijas spektrs bez inhibitora (melna līnija), 1 min (sarkana līnija), 1 st (zaļa līnija), 3 st (dzeltena līnija) un 7 st (zila līnija) pēc inhibitora pievienošanas. B: OASS-B absorbcijas spektrs bez inhibitora (melna līnija), 1 min (sarkana līnija), 1 st (zaļa līnija), 3 st (dzeltena līnija) un 7 st (zila līnija) pēc inhibitora pievienošanas.

λ_{max}=470nm, 330nm
α-aminoakrilāts
5

λ_{max}=412nm
ATVĒRTS AKTĪVAIS CENTRS
iekšējais aldimīns
3

λ_{max}=440–460nm
24B

λ_{max}=412nm
27

5. att. Savienojumi un to absorbcijas maksimumi, kas novēroti OASS inhibēšanas procesā.

OASS-A reakcija pētīta arī ar fluorescences emisiju (6. att., A), un josla, kas parādās pēc ierosināšanas pie 412 nm, nobīdījās uz spektra daļu līdz 495 nm. Tas apstiprina, ka izveidojusies struktūra nav α-aminoakrilāts **5** (5. att.). Emisijas josla lēnām samazinās, bet pēc 6 stundu inkubēšanas, atšķirībā no absorbcijas spektroskopijas, kur novērota sākotnējā emisijas spektra atgūšana, šajā gadījumā tas nenotika. Tas liecina, ka savienojuma struktūra, kas absorbē pie 412 nm, atšķiras no iekšēja aldimīna **27** (5. att.). Pēc triF-Ala reakcijas ar OASS-B un ierosināšanas pie 412 nm emisijas intensitāte sākumā palielinās un pēc tam lēnām samazinās (6. att., B). To pavada neliela nobīde zilajā spektra apgabalā līdz 501 nm, kas pēc 7 stundu inkubēšanas lēnām pāriet atpakaļ uz 505 nm. Šīs izmaiņas var notikt ārējā aldimīna dēļ, un neliela nobīde uz zilo spektra daļu liecina par pārejoša starpprodukta veidošanos.


6. att. OASS fluorescences spektri ar vai bez 1 mM triF-Ala. Emisijas spektri reģistrēti pēc ierosināšanas pie 412 nm. A: OASS-A bez inhibitora (melna līnija), 1 min (sarkana līnija), 4 st (zaļa līnija) un 6 st (dzeltena līnija) pēc inhibitora pievienošanas. B: OASS-B bez inhibitora (melna līnija), 1 min (sarkana līnija), 3 st (zaļa līnija) un 7 st (dzeltena līnija) pēc inhibitora pievienošanas.

Turpinājumā tika veikts pētījums, lai novērtētu F-Ala un triF-Ala iespējamo inhibēšanas aktivitāti uz OASS-A un OASS-B izoformām. Šim nolūkam veikti divi dažādi eksperimenti. Vispirms abas enzīma izoformas pārbaudītas, apstrādājot ar pieaugošām F-Ala koncentrācijām. Noteiktās IC_{50} vērtības bija attiecīgi 480 ± 50 μM uz OASS-A un 1290 ± 230 μM uz OASS-B. TriF-Ala gadījumā rezultāti liecināja, ka

IC$_{50}$(OASS-A)=130 ± 10 µM un IC$_{50}$(OASS-B)=940 ± 60 µM. Lai noskaidrotu, vai triF-Ala ir neatgriezenisks OASS inhibitors, kā liecina dati par citiem no PLP atkarīgiem enzīmiem, tika izpētīta OASS-A kinētika dažādās triF-Ala koncentrācijās, un rezultāti bija atbilstoši enzīma neatgriezeniskās inhibēšanas substrātiem. Otrajā eksperimentā pārbaudīts enzīms pēc 85 stundu reakcijas ar 10 mM triF-Ala, kam sekoja pilnīga liganda izvadīšana un inkubācija pie paaugstinātas PLP koncentrācijas. Eksperimentu rezultāti liecināja par enzīma inhibēšanu, ko izraisīja kovalenta neatgriezeniska aktīvā centra atlikuma(-u) modificēšana triF-Ala dēļ.

Mūsu jaunie OASS inhibitoru meklējumi ietvēra datorizētās zāļvielu izveides (CADD) metožu izmantošanu. Mēs izmantojām datus par jau identificētajiem OASS inhibitoriem un strukturālo informāciju, kas iegūta no inhibitoru un enzīma kristalogrāfiskajiem datiem.[6d] DFSI peptīds **28**, kas sastāv no pēdējiem četriem SAT (CysE) enzīma aminoskābju atlikumiem, ir iepriekš identificēts kā OASS-CysK inhibitors. *Sriram* grupa ziņoja par OASS-CysK inhibitora **8** pētījumiem, kuram piemīt uzlabota aktivitāte salīdzinājumā ar dabisko peptīdu DFSI **28** (7. att.). Savienojumi **8** un **28** ir konkurējoši inhibitori, kas enzīma aktīvajā centrā saistās PLP kofaktora tuvumā.
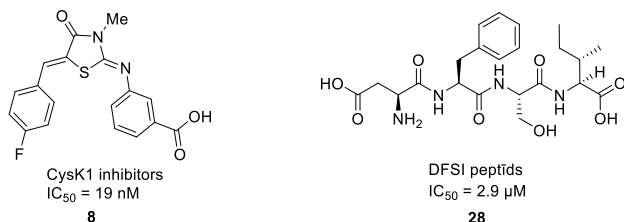
**7. att. OASS inhibitori, CysK1 inhibitors 8 un DFSI peptīds 28.**

Pamatojoties uz šiem datiem, mēs izveidojām proteīna modeli ar *Schrödinger Maestro* programmas palīdzību, lai veiktu ligandu bibliotēku virtuālo skrīningu. Tika izvēlēti divi proteīni no RCSB proteīnu datu bankas (PDB) – OASS holoenzīma 2Q3C struktūra no *Mycobacterium tuberculosis* kompleksa ar inhibējošo peptīdu DFSI un *Mycobacterium tuberculosis* OASS-CysK 3ZEI struktūra kompleksā ar mazmolekulāro inhibitoru **8** (8. att.).
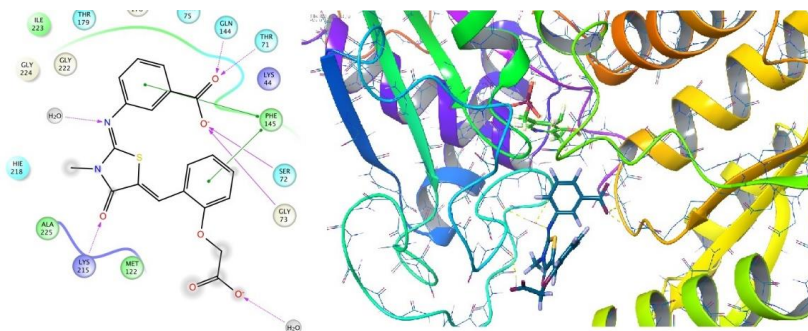

8. att. OASS-CysK komplekss ar inhibitoru 8.

Abas proteīna struktūras apstrādātas, izmantojot *Schrödinger* proteīnu sagatavošanas veidni (*Schrödinger's Protein Preparation Wizard*). Par pētījuma pamatu izvēlējamies

3ZEI proteīnu, jo komplekss ar zināmo inhibitoru ļāva mums noteikt galvenās mijiedarbības enzīma aktīvajā centrā. Sekojot iepriekš noskaidrotajām mijiedarbībām dokinga eksperimentā ar TriF-Ala, kas jau bija uzrādījis afinitāti pret PLP, noteicām tā svarīgākās mijiedarbības enzīma aktīvajā centrā un arī atšķirību no iepriekšējiem inhibitoriem, jo novērojām TriF-Ala mijiedarbību ar PLP (9. att.).
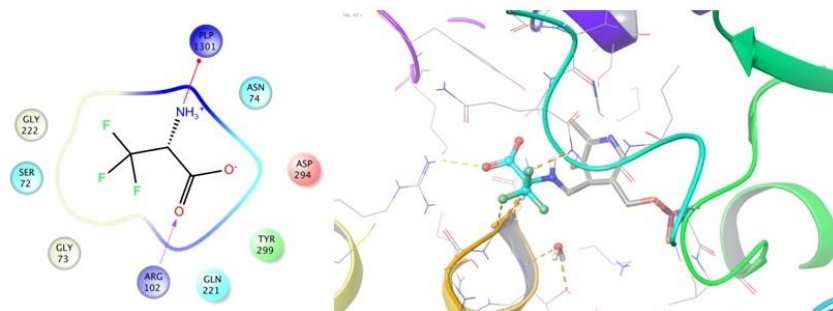
9. att. TriF-Ala mijiedarbība ar OASS proteīna atlikumiem un PLP.

   Tā kā mūsu mērķis bija sintezēt OASS kovalentos inhibitorus, ieprogrammētais reakcijas modelis bija jāizveido tā, lai tas ievēro reakciju starp substrātu un PLP, tāpēc tas bija jāuzstāda *Schrödinger* programmu komplektā modelēšanas eksperimentu veikšanai. Šim mērķim tika sagatavots jauns pielāgots reakcijas modeļa fails, kas veicina kovalentās saites veidošanos virtuālo eksperimentu laikā. Kad enzīms un reakcijas modelis bija sagatavoti, mēs turpinājām ar komerciālo bibliotēku (kompānijas *Enamine* "Skrīninga savienojumu kolekcija", *MolPort* "Skrīninga savienojumu datu bāze" un *eMolecules* datubāze) un *Schrödinger* programmas nodrošināto fragmentu bibliotēku pielāgošanu eksperimentam. Tika apkopota 140 000 savienojumu bibliotēka, kur pēc savienojumu atlases, izvēlējamies tikai tos, kas teorētiski var stāties mūs interesējošajā mijiedarbībā, un nonācām pie 200 savienojumu bibliotēkas. Šie savienojumi tika pakļauti kovalentā dokinga eksperimentiem, kas radīja aptuveni 2000 modelētās saistīšanās pozas. Apvienojot molekulārā dokinga *Glide* programmas rezultātus un struktūru fragmentu iedalījumu kategorijās, mēs nonācām pie vispārīgām struktūrām kā potenciālajiem mērķiem mūsu sintētiskajam darbam (10. att.).
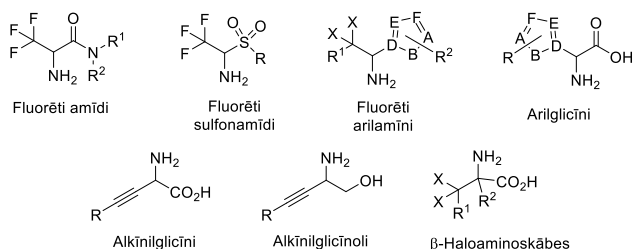
**10. att. Potenciālo OASS inhibitoru struktūras.**

2. Trifluoralanīna analogu sintēze

Vispirms veicām TriF-Ala (**13**) karbonskābes daļas aizvietošanu ar bioizostēriem, sintezējot vairākus amīdus **32a–f** un hidroksamskābi **35a** (3. shēma). Boc aizsargātais triF-Ala **29** tika kondensēts ar dažādiem amīniem, izmantojot HATU, un pēc Boc grupas nošķelšanas skābā vidē ieguvām amīdus **32a–f** ar augstiem iznākumiem. Hidroksamskābes **35a** sintēzei vispirms ar izcilu iznākumu ieguvām starpproduktu **34a**, izmantojot CDI kā kondensēšanas reaģentu, kas pēc aizsarggrupas nošķelšanas deva savienojumu **35a**.
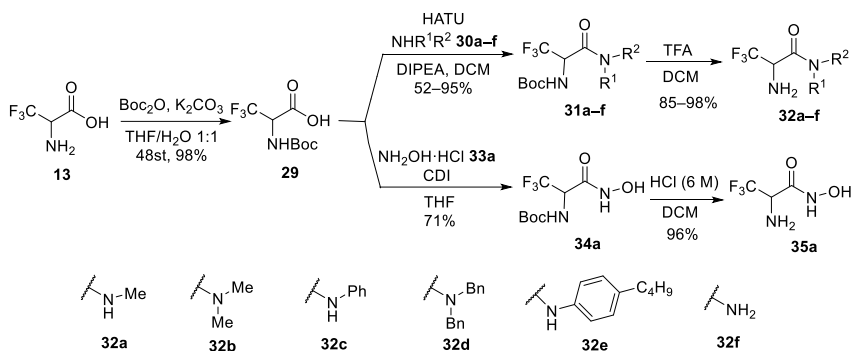

3. shēma. No TriF-Ala atvasinātu amīdu 32a–f un hidroksamskābes 35a sintēze.

Paplašinot triF-Ala analogu bibliotēku, mēs pievērsāmies paralēlajai sintēzei. Sintētiskos protokolus, kas būtu piemēroti paralēlās sintēzes metodes izmatošanai, izveidojām, izmantojot modeļreakcijas. Hidroksāmskābju **35b–d** sintēzei vislabākā izvēle izrādījās skābes **29** un hidroksilamīnu **33b–d** kondensācija CDI klātbūtnē. Acilsulfonamīda **38a** sintēzei izmantojām DMAP un EDC. Amīda **32g** sintēzei piemērojām agrāk izveidoto protokolu ar HATU un DIPEA (4. shēma).
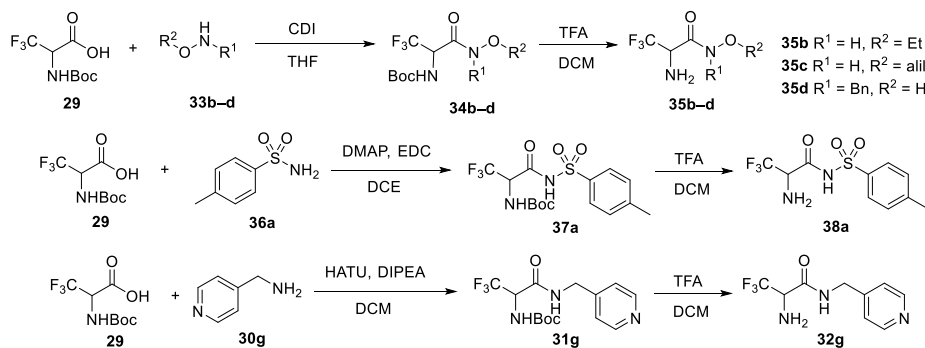

4. shēma. Modeļsavienojumu 35b–d, 38a, 32g reakciju protokolu validācija paralēlajai sintēzei.

Kad protokoli bija izveidoti, turpinājām savienojumu sintēzi ar paralēlās sintēzes bloku. Šajā iekārtā mēs varējām veikt vairākas reakcijas reizē 48 mēģeņu blokā, filtrēt visu komplektu caur mikrotitru plāksni ar stikla filtru analītiskajā 48 mikrotitru plāksnē. Iegūtos reakciju maisījumus pēc tam attīrījām ar preparatīvo HPLC (11. att.).
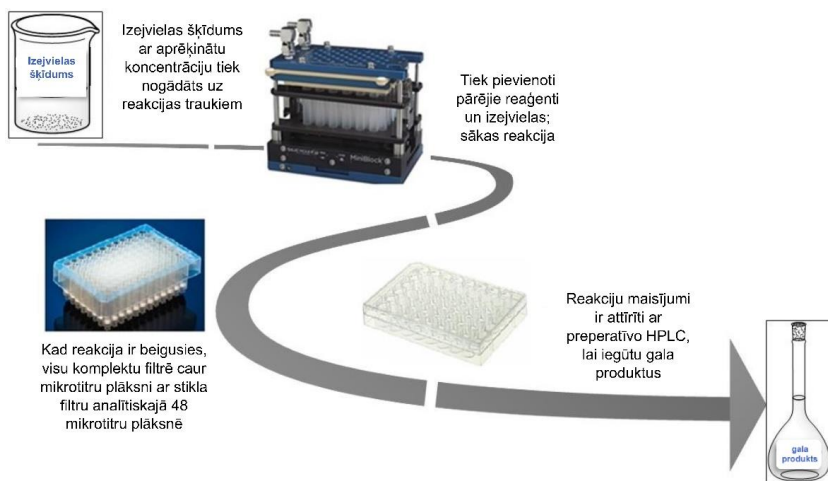
11. att. Paralēlās sintēzes procesa shēma.

Īstenojot šo procesu, īsā laikā mums izdevās sintezēt un izolēt kopumā 42 savienojumus. Starp tiem, veiksmīgi tika sintezēti un izolēti 11 hidroksamskābju atvasinājumi **35b–l** (papildus iepriekš sintezētajai skābei **35a**), ietverot arī aromātiskos un alifātiskos *N*- un *O*-aizvietotos produktus (12. att.).
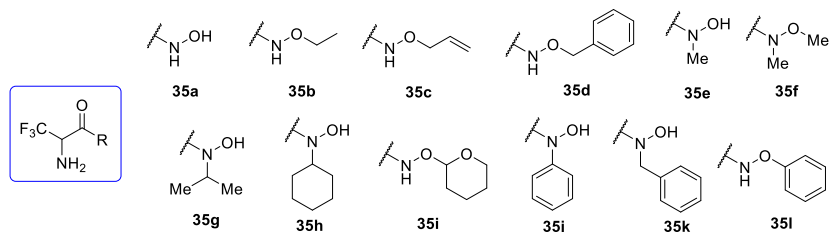
**12. att. Hidroksāmskābes 35a–l, kas iegūtas ar paralēlās sintēzes pieeju.**

Ieguvām arī dažādus *N*-acilsulfonamīdus **38b–p** (papildus iepriekš sintezētajam *N*-acilsulfonamīdam **38a**), vairums no tiem saturēja aromātisku vai heteroaromātisku fragmentu ar dažādiem aizvietotājiem, piemēram, halogēniem (**38e**, **38f**, **38h**, **38k, 38m**), cianogrupu (**38n**) vai nitrogrupu (**38k**, **38l**) (13. att.).
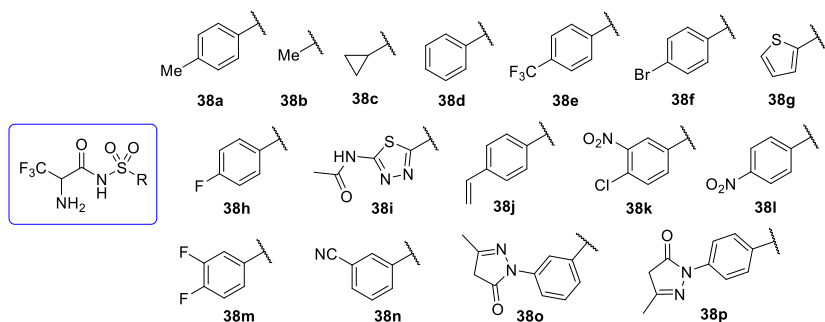
13. att. *N*-Acilsulfonamīdi 38a–p, kas iegūti ar paralēlās sintēzes pieeju.

Izmantojot paralēlās sintēzes metodi tika sintezēti 15 amīdi **32h–u** (papildus iepriekš sintezētajam amīdam **32g**), veidojot daudzpusīgu savienojumu grupu, piemēram, iegūti amīdi ar halogēn- vai ar metilgrupu aizvietotu piridīnu (**32h**, **32j**, **32o**, **32t**), piridīnmetilamīdi (**32g**, **32u**), dažādi 5-locekļu heterociklus saturoši amīdi u.c. (14. att.).
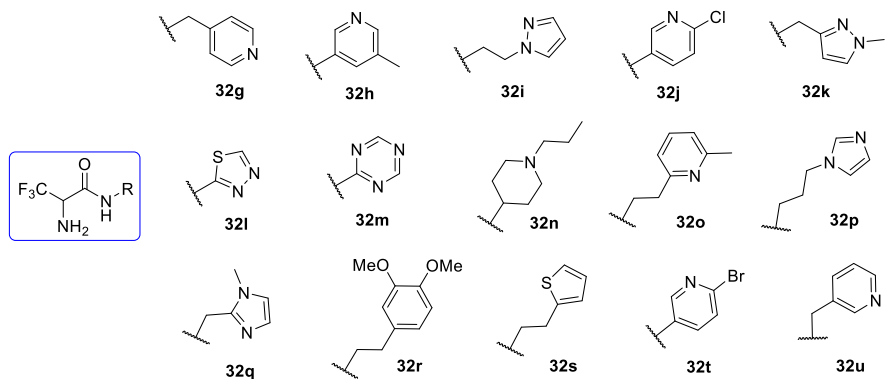
**14. att. Amīdi 32g–u, kas iegūti ar paralēlās sintēzes pieeju.**

TriF-Ala analogu klāstā tika izvirzīts mērķis iegūt arī difluoraspargīnskābes monoesteri **45**. Šim nolūkam spirtu **41** sintēzējām Barbjē tipa reakcijā starp benzaldehīdu (**39**) un bromdifluoretiķskābes etilesteri (**40**). Spirta **41** mezilēšana un aizvietošana ar azīdu nodrošināja starpprodukta **42** veidošanos. Azīda grupa tika reducēta par amīnu, kas tika aizsargāts ar Boc grupu *in situ*, lai iegūtu savienojumu **43**. Tas tika pakļauts aromātiskai oksidēšanai ar nātrija perjodātu un rutēnija hlorīdu, lai pārveidotu fenilgrupu par karboksilgrupu. No iegūtās skābes **44** nošķelta Boc aizsarggrupa, lai iegūtu vēlamo difluoraspargīnskābes monoesteri **45**. Lai paplašinātu triF-Ala analogu bibliotēku, Boc aizsargātais amīns **43** tika pārvērsts par brīvu amīnu **46** (5. shēma).
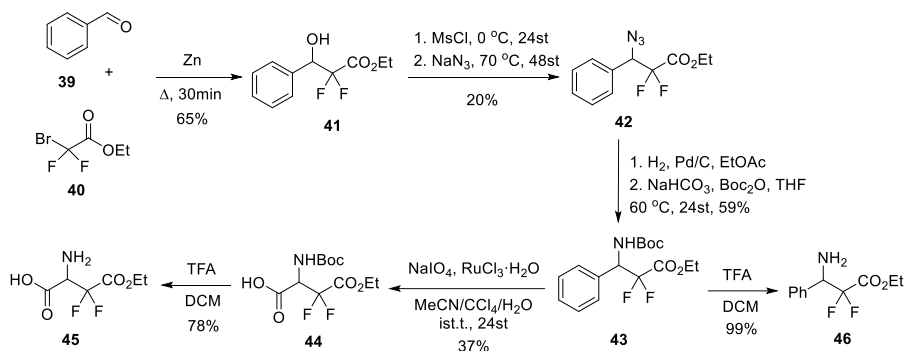
**5. shēma. Difluoraspargīnskābes monoestera 45 sintēze.**

Mēs pieņemām, ka difluoraspargīnskābes monoesteris **45** varētu darboties kā mehānismā balstīts inhibitors (6. shēma) divos dažādos veidos: ar dekarboksilēšanu sākumposmā (**48B**–**52B**, ceļš B) vai beigās (**48A**–**53A**, ceļš A), saskaņā ar piedāvāto mehānismu.
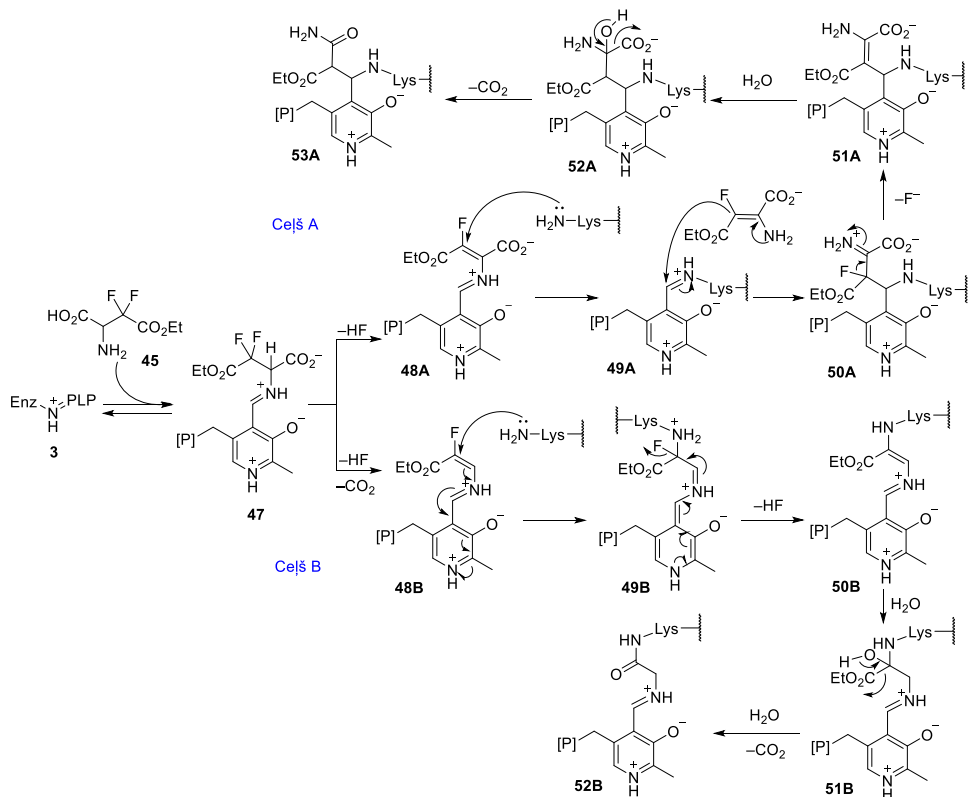

6. shēma. Iespējamie mehānismi OASS inhibēšanai ar difluoraspargīnskābes monoesteri 45.

Citi sintētiskie mērķi triF-Ala analogu klāstā bija savienojumi, kuros karbonskābe aizstāta ar triazolu **54** un tetrazolu **55** (15. att.).
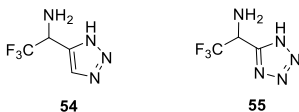
15. att. TriF-Ala triazola un tetrazola analogi.

Lai sintezētu mērķa savienojumus **54** un **55**, mēs vispirms ieguvām imīnu **58**, kondensējot *p*-metoksibenzilamīnu (**56**) ar trifluoracetaldehīda hemiacetālu **57**. TMS-acetilēnīda jona nukleofīlā pievienošanās imīnam **58** un desililēšana veidoja alkīnu **59**, kas stājās vara katalizētā [2+3] ciklopievienošanās reakcijā ar *p*-metoksibenzilazīdu (**60**), lai iegūtu aizsargāto triazolu **61**. PMB aizsarggrupas nošķelšana ar TFA, diemžēl, notika tikai no aminogrupas, kā rezultātā ieguvām triazolu **62** (7. shēma).
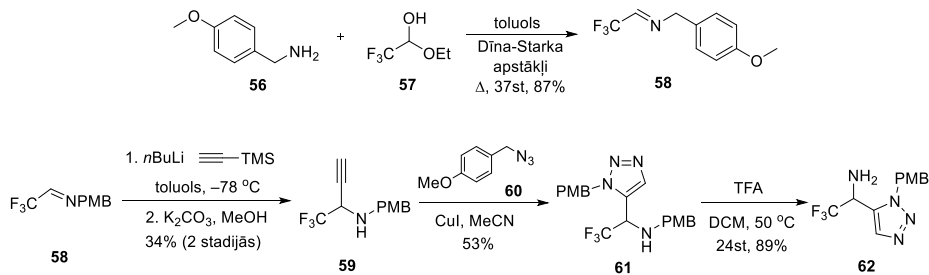
7. shēma. Triazola 62 sintēze.

Mērķa savienojuma **55** sintēzei sākotnēji vajadzēja iegūt PMB aizsargātu tetrazolu **63**, izmantojot klasiskos literatūrā aprakstītos reakcijas apstākļus. Starpprodukts **63** tika deprotonēts ar *i*PrMgCl un pievienots imīnam **58**, veidojot tetrazolu **64** ar zemu iznākumu (8. shēma). Mūsu centieni nošķelt aizsarggrupu tetrazolā **64** dažādos apstākļos (TFA/DCM, tīra TFA 60 °C, H2/Pd, CAN, DDQ) izraisīja tetrazola sadalīšanos (galvenais identificētais produkts bija *p*-metoksibenzilamīns **56**) vai sarežģīta produktu maisījuma veidošanos, kas sastāvēja no tetrazola **64** un produkta ar daļēji nošķeltu aizarggrupu.
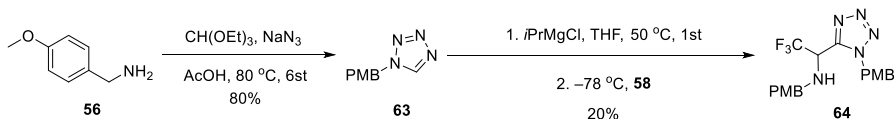
**8. shēma. Tetrazola 64 sintēze.**

3. Trifluoralanīna analogu inhibēšanas spēju noteikšana

Sintezētajiem savienojumiem **32a–u**, **35a–l**, **38a–p**, **45**, **46**, **62** (16. att.) tika noteikta reaģētspēja ar OASS-A un OASS-B izoformām, kā arī enzīmu inhibēšanas spēja un kinētika. Testi veikti ar *Salmonella Typhimurium* CysK un CysM, kas rekombinanti

ekspresēti *Escherichia coli*. Enzīms inkubēts ar savienojumiem 1 mM koncentrācijā, un enzimatiskā aktivitāte mērīta laika intervālos.
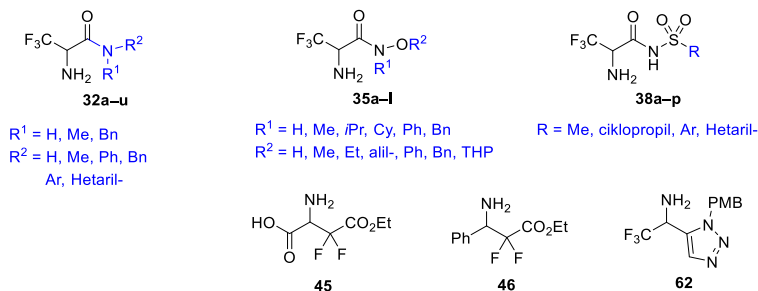
**16. att. Sintezēto savienojumu bibliotēka ar savienojumiem, kuriem pārbaudīta reaģētspēja ar OASS.**

Lai izpētītu triF-Ala analogu aktivitāti, tika analizēti savienojumu **3**–**5** (3. att.) un **45**, **46** (5. shēma) reaģētspēja ar OAAS-A un OAAS-B izoformām. Neviens no šiem savienojumiem neuzrādīja reaģētspējas uzlabošanos, salīdzinot ar sākotnējo savienojumu TriF-Ala **13**.

Pēc tam pārbaudījām karbonskābes bioizostērās aizvietošanas ietekmi. Pārbaudot pirmo savienojumu grupu **32a**–**f** (16. att.) un **35a** (12. att.), tika novērota nenozīmīga ietekme uz reaģētspēju ar enzīmu. Jāatzīmē, ka hidroksāmskābe **35a** izraisīja nelielas izmaiņas OASS-A absorbcijas spektrā (17. att.) un aptuveni 14% enzīma aktivitātes samazināšanos.[5]
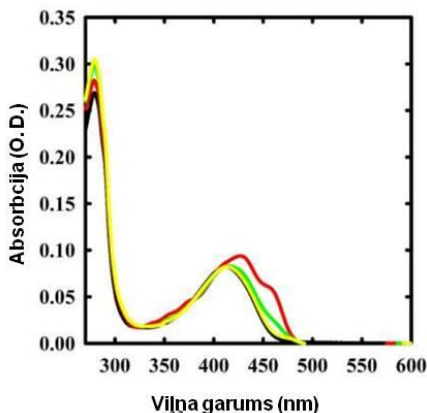
17. att. Spektrālās izmaiņas reakcijā starp OASS-A un 1 mM savienojuma 35a. OASS-A bez inhibitora (melna līnija) un 1 min (sarkana līnija), 30 min (zaļa līnija) un 1 st (dzeltena līnija) pēc inhibitora 35a pievienošanas.

No nākamās savienojumu grupas **35b**–**l**, **38a**–**p** un **32g**–**u** (16. att.) 5 savienojumi uzrādīja vērā ņemamas OASS-A inhibēšanas īpašības (18. att.). Savienojumi **38i**, **38p** un **32h** uzrāda vāju saistību ar enzīmu un neizraisa būtisku enzīma aktivitātes samazināšanos, tomēr hidroksāmskābes atvasinājums **35k** un sulfonamīds **38b** ir spēcīgākie savienojumi no šīs mazās bibliotēkas.
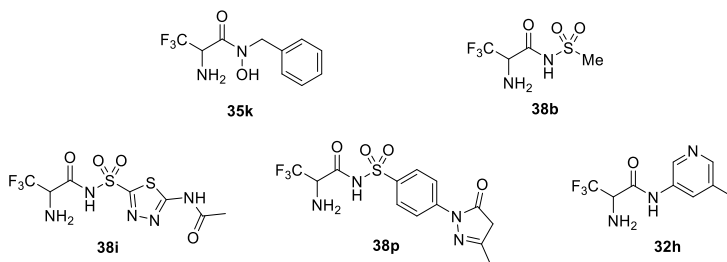
18. att. TriF-Ala analogi ar OASS inhibējošu aktivitāti.

Hidroksāmskābe **35k** uzrādīja OASS-A inhibēšanas spēju ar konstanti $IC_{50}=177 \pm 29$ µM, kā arī inhibēšanas testā pirmajā laika punktā tika novērota aptuveni 15% enzīma aktivitātes samazināšanās, lai gan vēlāk tā pazuda, iespējams, starpprodukta hidrolīzes rezultātā (19. att).
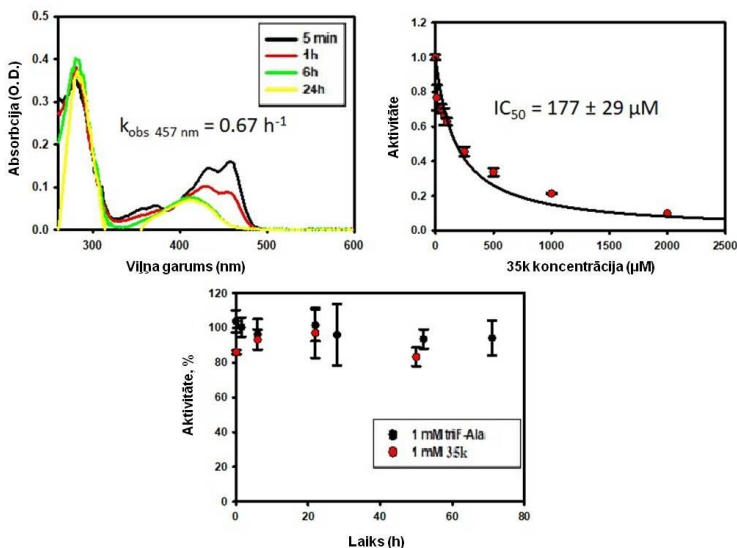
19. att. Inhibitors 35k 1 µM koncentrācijā, testam 5000 reizes liels atšķaidījums (inhibitora koncentrācija testā 0.2 µM), divos atkārtojumos.

Sulfonamīds **38b** arī uzrādīja OASS-A inhibēšanu ar konstanti $IC_{50}=179 \pm 22$ µM. Enzīma aktivitāte testā pirmajā laika punktā ir pazemināta par aptuveni 20%, lai gan atkal šis efekts vēlāk pazuda, iespējams, starpprodukta hidrolīzes rezultātā (20. att.).
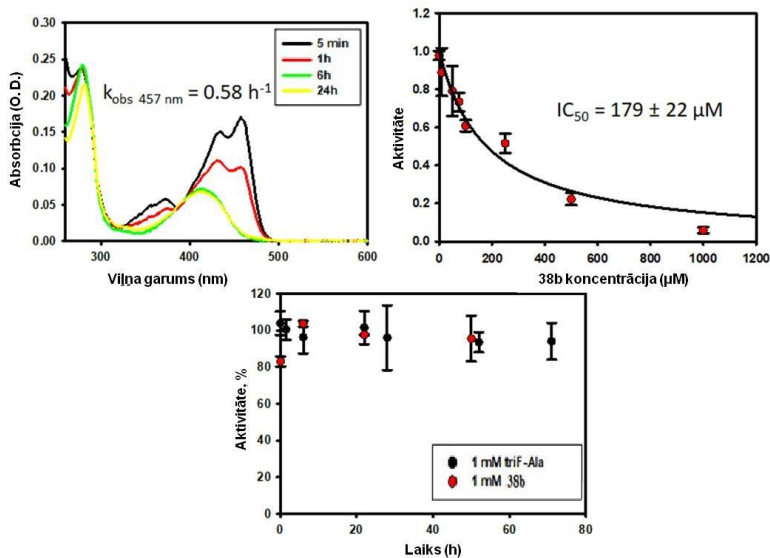
20. att. Inhibitors 38b 1 µM koncentrācijā, testam 5000 reizes liels atšķaidījums (inhibitora koncentrācija testā 0.2 µM), divos atkārtojumos.

Pamatojoties uz spektrālajiem un kinētikas datiem, kas iegūti no TriF-Ala reaģētspējas eksperimentiem ar OASS, un ņemot vērā jau piedāvātos mehānismus triF-Ala reakcijai ar citiem no PLP atkarīgiem enzīmiem, mēs izvirzījām hipotēzi, ka OASS-A inhibēšanas mehānisms ir līdzīgs iepriekš piedāvātajam (2. shēma). Mēs pieņemam, ka mehānisms seko B ceļam, nevis A ceļam, jo OASS katalītiskajā ciklā dekarboksilēšana nenotiek.

Inhibitori **35k** un **38b** ir daudzsološi bāzes savienojumi to turpmākai attīstībai. Atšķirībā no izejas inhibitora triF-Ala (**13**), šie savienojumi satur funkcionālās grupas, kuras atvasinot var iegūt papildus mijiedarbības ar OASS. Darbs šajā virzienā tika apturēts, jo beidzās projekta termiņš un savienojumu bioloģiskā pārbaude vairs nebija pieejama.

4. Jaunu metožu izstrāde no PLP atkarīgu enzīmu inhibitoru sintēzei

4.1. Jauna pieeja C-kvarternāro alkīnilglicīnolu sintēzei

Viens no kemotipiem, ko atklājām kā potenciālu no PLP atkarīgu enzīmu inhibitoru, bija alkīnilglicīnols **65**, kas kopā ar sintētiski līdzvērtīgiem alkīnilglicīna atvasinājumiem **66** (21. att.) ir ļoti noderīgi būvbloki sarežģītu bioloģiski aktīvu savienojumu sintēzei. Ir zināmas tikai dažas metodes alkīnilglicīnolu tiešai sintēzei, kurās netiek izmantota karboksilgrupas reducēšana glicīnos **66**.
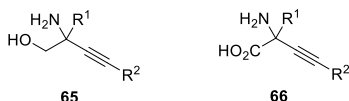

21. att. Alkīnilglicīnoli 65 un alkīnilglicīni 66.

Kā viena no metodēm alkīnilglicīnolu **65** iegūšanai tika pārbaudīta 1,2-diolu Ritera reakcija, sākotnēji veidojot attiecīgos oksazolīnus. Pirmais mēģinājums iegūt oksazolīnu **70** deva sliktu produkta iznākumu, zem 10% (9. shēma). Atklājām, ka kobalta kompleksētu alkīnilglicīnolu **68** izmantošana var efektīvi stabilizēt starpproduktu – karbēnija jonu A – un pēc kobalta kompleksa nošķelšanas nodrošināt veiksmīgu oksazolīnu **70** iegūšanu.
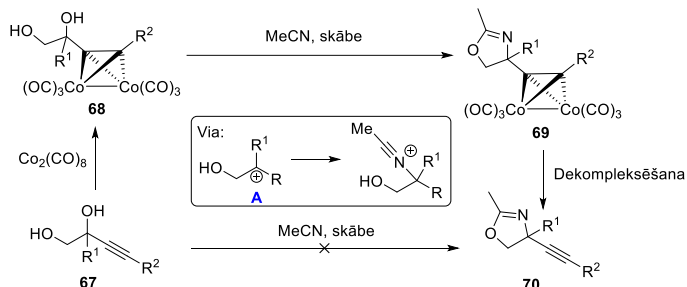
9. shēma. Oksazolīnu 70 sintēze Ritera reakcijā.

Kobalta kompleksētu alkīnilglikolu **68** un **73** sintēzi veicām divās stadijās, vispirms pievienojot litija acetilēnīdu α-hidroksiketona atvasinājumiem **71** un pēc tam apstrādājot iegūtos alkīnildiolus **72** ar $Co_2(CO)_8$ (10. shēma).

10. shēma. Alkīnilglikolu kobalta kompleksu 68 un 73 iegūšana.

Ritera reakcijā izmantojot H_2SO_4 vai $BF_3 \cdot Et_2O$, alkīnilglikola kobalta kompleksi **68** reakcijā ar MeCN veidoja atbilstošos oksazolīnus **69**. Reakcijā iespējams izmantot plašu substrātu klāstu ar dažādiem aizvietotājiem R^2 pozīcijā, savukārt substrāti, kuriem R^1 pozīcijā bija fenilgrupa, nedeva gaidītos oksazolīnus (11. shēma).

$R^1 = H$, Me, CH_2OH
$R^2 = Ph$, *n*Pentil, Me, 4-$MeOC_6H_4$, CH_2OBn,
       *t*Bu, TMS, 2-ClC_6H_4

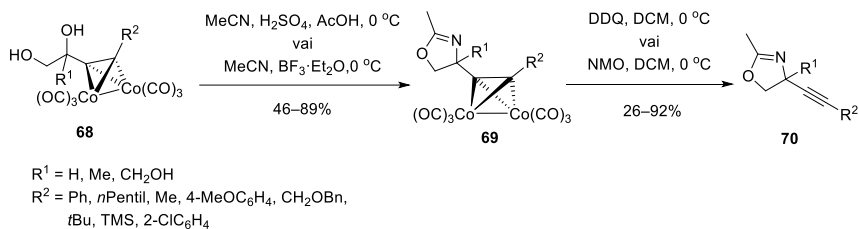**11. shēma. Substrātu 68 Ritera reakcija un tai sekojoša kobalta kompleksa šķelšana oksazolīnu 70 iegūšanai.**

Lai gan galvenā sintēzes metode paredz spirta TBS aizsarggrupas nošķelšanu pirms kobalta kompleksa veidošanas, parādījām arī veiksmīgus piemērus, kuros aizsargāti spirti tiek pakļauti Ritera reakcijai ar vienlaicīgu TBS grupas šķelšanu (12. shēma).

$R^2 = $ Me, Ph, *n*Pentil
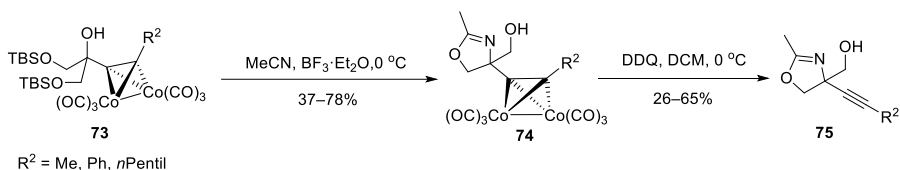
12. shēma. Oksazolīnu 75 iegūšana no substrāta 73 Ritera reakcijas un kompleksa šķelšanas rezultātā.

Vairumā gadījumu alkīnilglicīnolu kobalta kompleksa šķelšanai DDQ izmantošana izrādījās efektīvāka salīdzinājumā ar NMO. Jāatzīmē, ka tas ir pirmais piemērs, kas demonstrē DDQ pielietošanu šādas reakcijas veikšanai (11. un 12. shēmas).

Izvēlētie oksazolīni tika pakļauti skābes ierosinātai hidrolīzei maigos apstākļos, lai iegūtu aminospirtus **76** ar labiem iznākumiem (13. shēma).

$R^1 = $ Me, CH_2OH
$R^2 = Ph$, *n*Pentil, Me, CH_2OBn
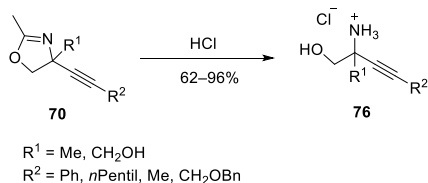
13. shēma. Oksazolīnu 70 hidrolīze par aminospirtiem 76.

4.2. 1*N*-PMB aizsargātu tetrazolu funkcionalizēšana

Mūsu mēģinājums sintezēt tetrazolu saturošu TriF-Ala analogu **64** (8. shēma) bija sākumpunkts, lai izstrādātu jaunu metodi tiešai tetrazola C–H funkcionalizēšanai, kas dotu labāku iznākumu, salīdzinot ar mūsu sākotnējiem centieniem (20%). No literatūras zināms, ka paralēli vēlamajai reakcijai notiek metalētā starpprodukta retro [2+3] ciklopievienošanās reakcija, kas veido ciānamīdu **80** (14. shēma). Metalēts tetrazols **78** var būt nestabils pat –98 °C temperatūrā, kas ir galvenais šķērslis tetrazola atvasinājumu iegūšanai C–H deprotonēšanas ceļā.

Met = Li, K, MgX

14. shēma. Metalētu tetrazolu retro [2+3] ciklopievienošanās reakcija.
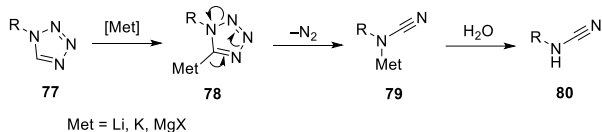
Literatūrā ir zināmi tetrazolu saturoši Griņjāra reaģenti, kas iegūti halogēna–metāla apmaiņas rezultātā, un tie uzrāda augstāku stabilitāti salīdzinājumā ar litijētajiem analogiem.[11] Tas rosināja mūs iegūt Griņjāra reaģentus C–H deprotonēšanas ceļā. Šim nolūkam mēs sintezējām 1*N*-PMB aizsargātu tetrazolu **63**, kurš tika pakļauts dažādiem deprotonēšanas apstākļiem (1. tabula). Lai noteiktu deprotonēšanas efektivitāti, mēs pārbaudījām dažādus Griņjāra reaģentus, izmantojot reakciju ar deitērētu metanolu. Konstatējām, ka turbo Griņjārs (*i*PrMgCl·LiCl) ir visefektīvākais un nodrošina pat 99% deitērija iekļaušanu molekulā (1. tabula, 1., 2. aile). Jāatzīmē, ka šajos apstākļos retro [2+3] ciklopievienošanās produkts **81b** netika novērots pat pēc 1 stundas –60 °C temperatūrā. Izpētīti arī citi Griņjāra reaģenti, piemēram, *i*PrMgCl un *i*PrMgBr, tomēr tie izrādījās mazāk efektīvi, salīdzinot ar turbo Griņjāru (1. tabula, 3.–6. aile).

1. tabula. Dažādu Griņjāra reaģentu deprotonēšanas spēju izvērtēšana.
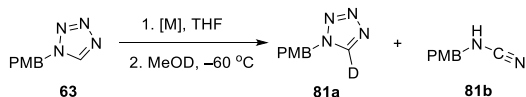
Nr. p. k.	[M]	Laiks, min	81a iznākums[a], %	81b
1	*i*PrMgCl·LiCl	15	98	n.n.[b]
2	*i*PrMgCl·LiCl	60	99	n.n.
3	*i*PrMgCl	15	53	n.n.
4	*i*PrMgCl	60	76	n.n.
5	*i*PrMgBr	15	57	n.n.
6	*i*PrMgBr	60	69	n.n.

[a]Iznākumi aprēķināti, pamatojoties uz sausā atlikuma svaru; KMR bez **81a** netika novēroti citi savienojumi
[b]n.n. = nav novērots

Pēc tam pārbaudījām tetrazola **63** reakciju ar anīsaldehīdu (**82a**) dažādos šķīdinātājos. Izmantojot THF, spirts **83a** tika iegūts ar ļoti labu iznākumu (2. tabula, 1. aile). Reakcijas iznākums būtiski nesamazinājās, ja reakcijas maisījumu tika atsildīts līdz istabas

temperatūrai pēc anīsaldehīda pievienošanas (2. tabula, 2. aile). Citu šķīdinātāju (Et₂O, toluola) izmantošana pazemināja reakcijas iznākumu (2. tabula, 3., 4. aile).

2. tabula. Reakcijas apstākļu optimizācija.
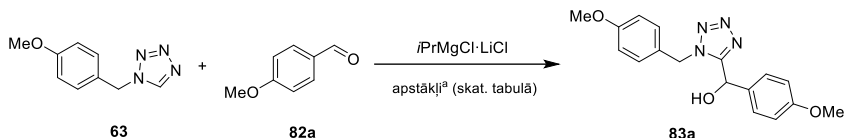
Nr. p. k.	Šķīdinātājs	Temperatūra, $^\circ$C	Laiks, st	83a iznākums, %
1	THF	–60 $^\circ$C	5	78[b]
2	THF	ist.t.	24[c]	76
3	Et₂O	–60 $^\circ$C	5	47
4	Toluols	–60 $^\circ$C	5	22

[a]Tetrazols **63** (1.1 ekviv.), *i*PrMgCl·LiCl (1.3 ekviv.) 2 mmol mērogā. Pēc *i*PrMgCl·LiCl pievienošanas reakciju maisa 30 min un tad pievieno aldehīdu **82a**.
[b]Produkts **83a** iegūts ar 88% iznākumu, veicot reakciju 5 mmol mērogā
[c]Aldehīda **82a** pievienošana veikta –60 °C, pēc tam reakcijas maisījums atsildīts līdz ist.t.

Substrāta klāsta izpētei izmantojām dažādus aromātiskus (**82b**–**e**) un alifātiskus (**82f**–**g**) aldehīdus, kā arī strukturāli daudzveidīgus ketonus (**82h**–**n**). Šo subtrātu reakcijās ar Griņjāra reaģentu, kas atvasināts no tetrazola **63** ieguvām atbilstošus spirtus **83b**–**n** ar labiem līdz izciliem iznākumiem (15. shēma).
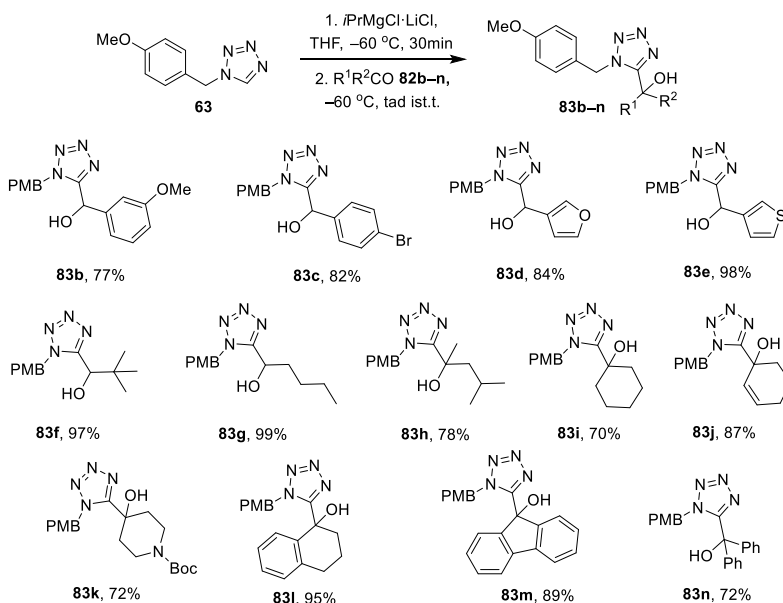
15. shēma. Tetrazola 63 pievienošanas produkti aldehīdiem un ketoniem.

Izpētījām arī citus elektrofīlus reakcijai ar Griņjāra reaģentiem, kas atvasināti no tetrazola **63**. Veinreba amīdi **84a**–**c** var tikt veiksmīgi izmantoti kā reakcijas komponentes,

nodrošinot atbilstošo ketonus **85a–c** veidošanos ar labiem iznākumiem. Reakcija ar jodu deva atvasinājumu **86** ar gandrīz kvantitatīvu iznākumu (16. shēma).
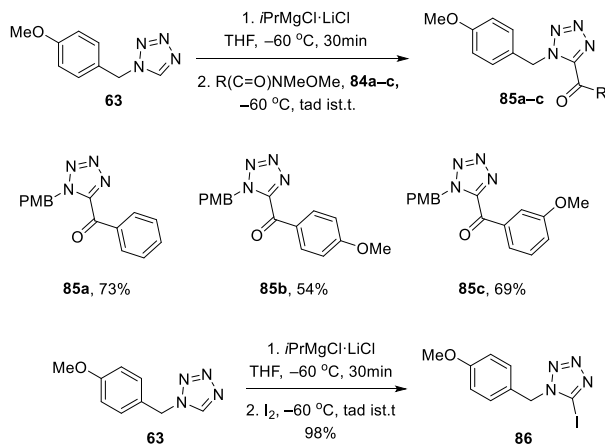
16. shēma. Tetrazola 63 pievienošana Veinreba amīdiem un jodēšana.

1*N*-PMB aizsarggrupas nošķelšanai izmantojām trīs dažādas metodes – oksidējošo šķelšanu ar CAN MeCN/H$_2$O maisījumā (metode A), katalītisko hidrogenēšanu ar H$_2$/PdCl$_2$ etanolā (metode B) un šķelšanu ar trifluoretiķskābi dihlormetānā (metode C). Katra no šīm metodēm nodrošināja vēlamo neaizargoto tetrazolu **87a–i** iegūšanai ar labiem vai izciliem iznākumiem (17. shēma).
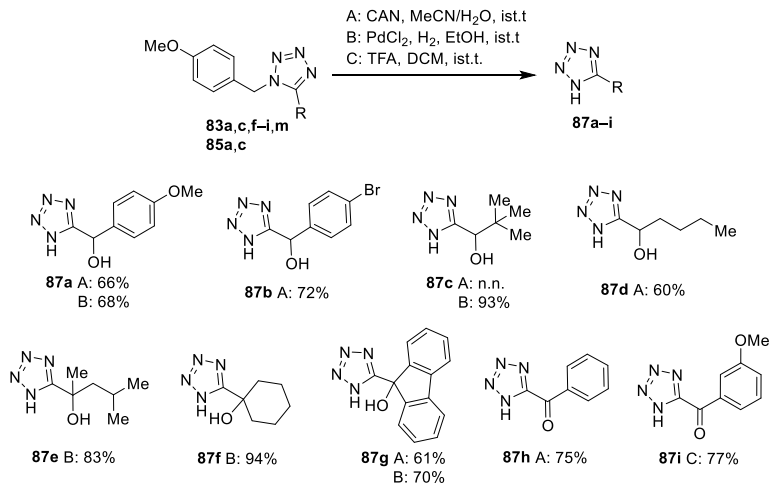
17. shēma. PMB aizsarggrupas šķelšanas apstākļi un iegūtie produkti 87a–i.

4.3. Elektroķīmiski nošķeļamas 1*N*-6-metilpiridil-2-metil- aizsarggrupas saturošu tetrazolu, funkcionalizēšana

Lai paplašinātu tetrazolu funkcionalizēšanas metodes pielietojamību, mēs centāmies ievadīt jaunu, elektroķīmiski nošķeļamu tetrazolu aizsarggrupu. Šim nolūkam sagatavojām divus substrātus – ar piridilmetilgrupu aizsargātu tetrazolu **89**, kas iegūts no atbilstošā 2-aminometilpiridīna (**88**) un ar 6-metilpiridilmetilgrupu aizsargātu tetrazolu **93**, kas iegūts no 2,6-lutidīna (**90**) ar bromēšanu un sekojošu tetrazola **92** alkilēšanu (18. shēma).
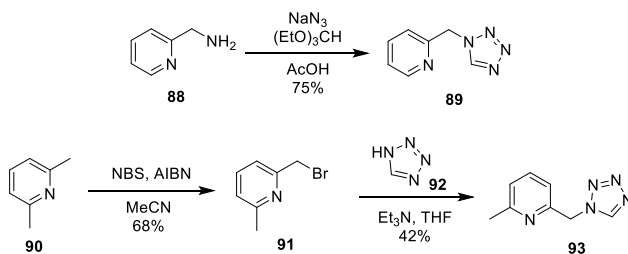
18. shēma. Ar piridilmetilgrupu aizsargātu tetrazolu sintēze.

Turbo Griņjāra izmantošana tetrazolu **89** un **93** piektās pozīcijas deprotonēšanai rezultējās ar minimālu retrociklopievienošanās produktu veidošanās vai arī tie neveidojās vispār. Nelielos daudzumos izveidotais tetrazolu **89** un **93** sadalīšanās produkts, ciānamīds **94a**, ciklizējās par pirazolopiridīnu **94c** (19. shēma).
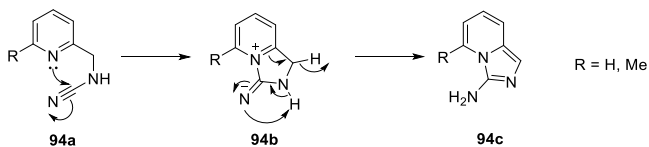
19. shēma. Piedāvātais blakusprodukta 94c veidošanās mehānisms.

Piridilmetil- aizsargāta tetrazola **89** metalēšanas/deiterēšanas reakcijā ieguvām nepilnīgu deitērija iekļaušanos tetrazola piektajā pozīcijā (40–60%), kopā ar konkurējošu deiterēšanas produktu CH$_2$ grupā un neizreaģējušu izejvielu. Deiterēšanas selektivitāte ievērojami uzlabojās, kad deiterēšanas eksperimentos izmantojām 6-metilpiridilmetil-aizsargātu tetrazolu **93** (deitērija iekļaušanās 97–98%). Svarīgi, ka netika novērots ne konkurējošas deiterēšanas, ne sadalīšanās produkts. Mēs pieņēmām, ka metilgrupa piridīna C-6 pozīcijā savienojumā **93** bloķē relatīvi skābo piridīna C–H funkciju, kas var izraisīt vairāku metalētu daļiņu līdzsvara maisījuma rašanos.

No 6-metilpiridilmetil-aizsargāta tetrazols **93** atvasināts Griņjāra reaģents stājās reakcijā ar aromātiskajiem, alifātiskajiem un heteroaromātiskajiem aldehīdiem **95a**–**e**, veidojot spirtus **96a**–**e** ar labiem līdz izciliem iznākumiem. Reakcijā ar ketoniem **95f**–**j** atbilstošie spirti **96f**–**j** tika iegūti ar mēreniem vai labiem iznākumiem (20. shēma).
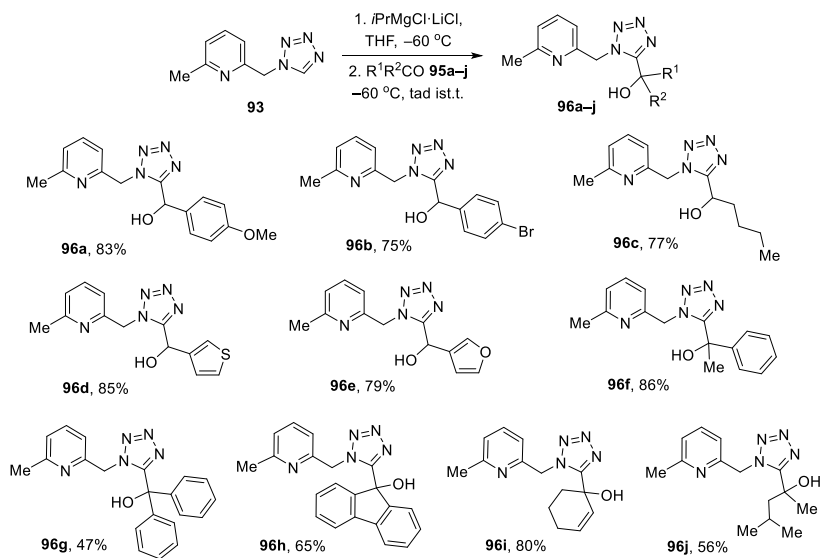
20. shēma. Tetrazola 93 pievienošanas produkti aldehīdiem un ketoniem.

Literatūrā 6-metilpiridilmetilgrupa ir aprkastīta kā elektroķīmiski nošķeļama aizsarggrupa no tioliem, karbonskābēm un spirtiem.[14] Līdzīgus elektroķīmiskos apstākļus piemērojām arī 6-metilpiridilmetilgrupas reducējošai nošķelšanai no tetrazola, izmantojot savienojumu **96a** kā modeļsubstrātu. Mēs izpētījām elektrodu un elektrolītu klāstu pie fiksētas strāvas un elektriskā lādiņa. Labākais rezultāts tika sasniegts, izmantojot svinu saturošu bronzas elektrodu kā katodu un šķīstošo cinka elektrodu kā anodu, kā arī TBA·BF$_4$, nodrošinot neaizsargāta tetrazola **97a** veidošanos ar 67% izolēto iznākumu. Šie optimizētie aizsarggrupas nošķelšanas apstākļi tika piemēroti tetrazoliem **96a–c** un **96e–h**, lai iegūtu 1*H*-tetrazolus **97b–g** ar vidējiem iznākumiem. Augstākus tetrazolu iznākumus neizdevās sasniegt, jo to ļoti polārās dabas dēļ bija apgrūtināts produktu izolēšanas process (21. shēma).
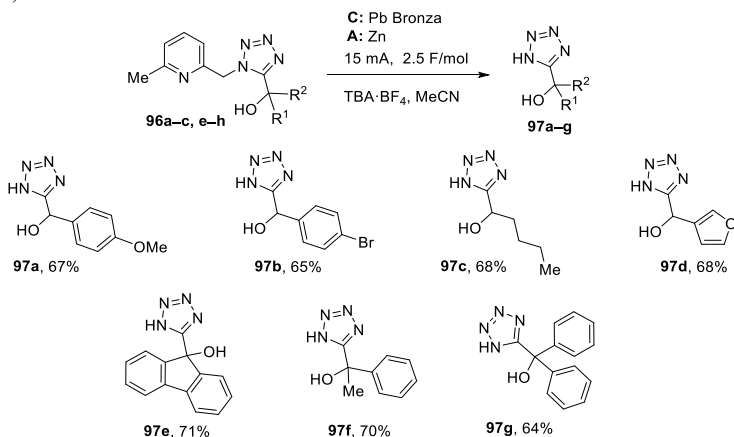
21. shēma. 6-Metilpiridilmetil- aizsarggrupas elektroķīmiskā nošķelšana.

31

Piedāvātais mehānisms tetrazola **96** 6-metilpiridilmetil-aizsarggrupas elektroķīmiskai noškelšanai ir attēlots 22. shēmā. Tas sākas ar 6-metilpiridilmetilgrupas reducēšanu pie katoda, oksidējot Zn anodu, kas noved pie anjona radikāļa **96A**. Tas sadalās par radikāli **97B** un tetrazola anjonu [**97**]⁻. Radikālis **97B** tiek pakļauts turpmākām reakcijām, piemēram, ūdeņraža atoma abstrakcijai, dimerizēšanās, oksidēšanās un/vai reducēšanās reakcijām, kas veido blakusproduktu maisījumu. Piridilmetilradikāļa **97B** veidošanos apstiprina 2,6-lutidīna detektēšana LC/MS analīzēs neapstrādātam reakcijas maisījumam. Šāds blakusprodukts var veidoties no piridilmetilradikāļa **97B** vai nu ūdeņraža atoma abstrakcijas rezultātā vai arī to reducējot par anjonu ar sekojošu protonēšanu.
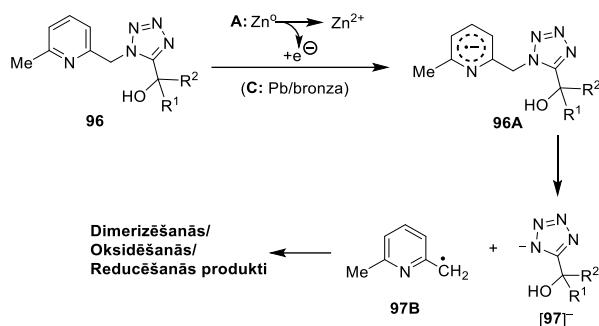
22. shēma. 6-Metilpiridilmetil- aizsarggrupas elektroķīmiskas noškelšanas iespējamais mehānisms.

4.4. Tetrazolu pievienošana imīniem, aminoskābju analogu sintēze

Mēs izpētījām metalētā tetrazola izmantošanu, lai iegūtu aminoskābju analogus, kuri satur tetrazolu kā karbonskābes bioizostēru. Literatūrā ir zināms, ka metālorganiskos reaģentus var pievienot *t*-butilsulfīnilimīniem diastereoselektīvā veidā (23. shēma).[12] Šāda tipa reakciju diastereoselektivitāte uzlabojas, ja kā šķīdinātāju izmanto DCM.
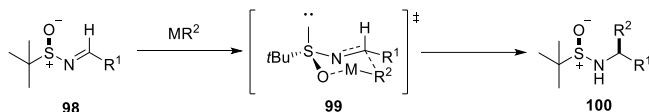
23. shēma. Metālorganisko savienojumu diastereoselektīva pievienošanās *t*-butilsulfīnilimīniem 98.

Kā modeļsubstrātu pirmajām testa reakcijām izvēlējamies imīnu **102a**, kas tika sintezēts saskaņā ar literatūrā aprakstīto metodi (24. shēma).[13]
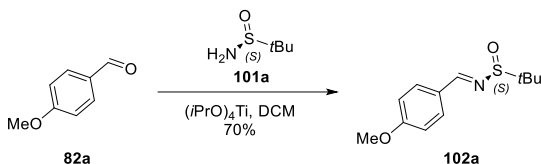
24. shēma. *t*-Butilsulfīnilimīna 102a sintēze.

1*N*-PMB aizsargātā tetrazola **63** deprotonēšanu veicām, izmantojot turbo Griņjāra reaģentu, kam sekoja metalētā starpprodukta pievienošana *t*-butilsulfīnilimīnam **102a**, izmantojot DCM kā šķīdinātāju. Rezultātā ieguvām tikai pamatproduktu **103a** ar augstu iznākumu. [1]H un ^{13}C KMR spektri, metodes jutības robežās uzrādīja tikai viena diastereomēra klātbūtni (25. shēma). Saskaņā ar stereoindukcijas mehānismu, kas parādīts 23. shēmā, pieņēmām, ka jaunizveidotā stereocentra konfigurācija produktā **103a** ir *S*, produkta konfigurācijas pierādīšanai ir nepieciešami papildus eksperimenti.
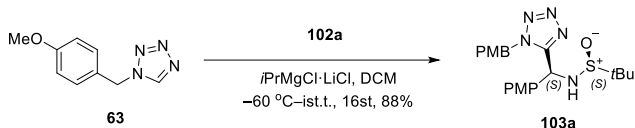
25. shēma. Tetrazola 63 pievienošana *t*-butilsulfīnilimīnam 102a.

Pēc pirmajiem daudzsološajiem rezultātiem mēs pievērsāmies reakcijas produktu klāsta paplašināšanai, tāpēc sintezējām vairākus *t*-butilsulfīnilimīnus **102b–l**, kurus varētu izmantot tetrazola **63** pievienošanai (26. shēma).
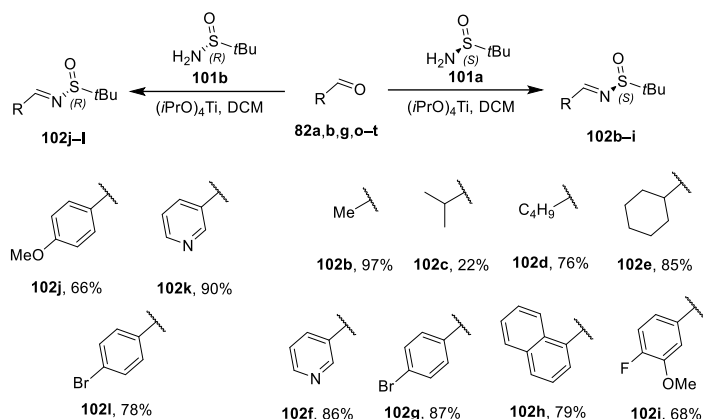
26. shēma. *t*-Butilsulfīnilimīnu **102b–l** sintēze.

Piemērojot optimizētos reakcijas apstākļus *t*-butilsulfīnilimīnu **102b–l** reakcijai ar tetrazolu **63**, ieguvām pievienošanās produktus **103b–l** ar labiem līdz izciliem iznākumiem (27. shēma).
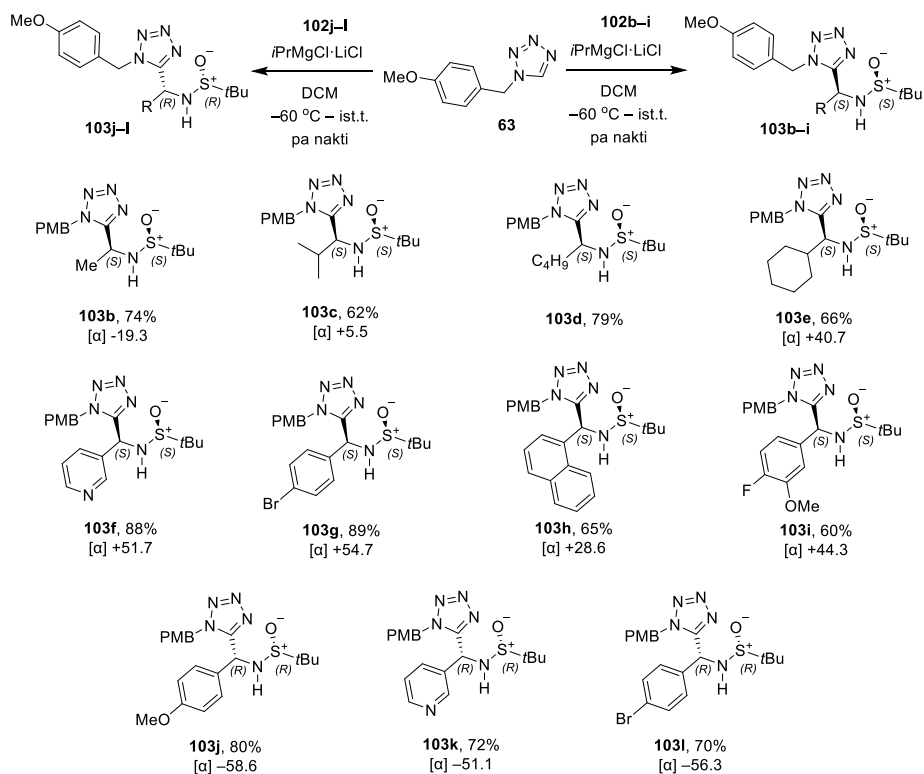
27. shēma. Tetrazola **63** pievienošanas produkti *t*-butilsulfīnilimīniem **102b–l**.

Noskaidrojām, ka tetrazolu **63** var pievienot arī *t*-butil- (*E*)-(4-metoksibenzilidēn)karbamātam (**105**), kas tika iegūts reakcijā starp *p*-anīsaldehīdu (**82a**)

un *t*-butilkarbamātu (**104**). Pievienošanas reakcijas rezultātā veidojās savienojums **106** (28. shēma).
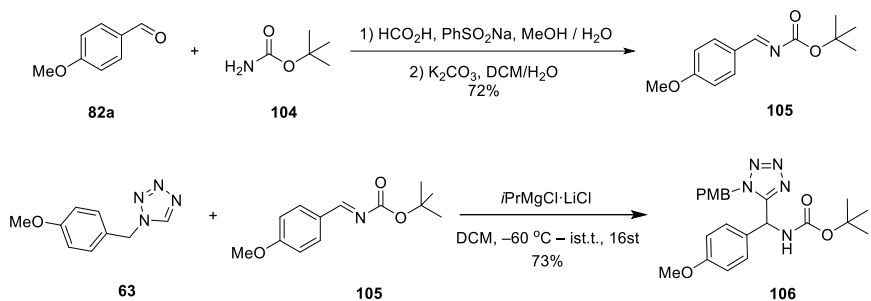
28. shēma. Tetrazolu saturoša aminoskābes analoga 106 sintēze.

Sumējot iegūtos rezultātus, turbo Griņjāra izmantošana 1*N*-PMB aizsargāta tetrazola **63** deprotonēšanai un sekojoša pievienošana *t*-butilsulfīnilimīniem **102a–l** ļāva iegūt savienojumus **103a–l**, kas ir prekursori tetrazolu saturošiem aminoskābju analogiem **107** (29. shēma).
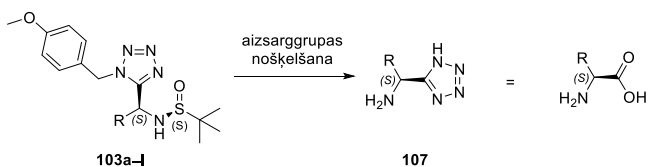
29. shēma. Piedāvātais aminoskābju analogu 107 sintēzes ceļš.

SECINĀJUMI

1. Identificēti jauni kemotipi kā potenciālie no PLP atkarīgu enzīmu kovalentie inhibitori. TriF-Ala analogi, kas satur hidroksāmskābi un sulfonamīdu, uzrādīja augstāko OASS inhibēšanas aktivitāti (mikromolārā līmenī).

2. Izstrādāta jauna metode C-kvarternāro alkīnilglicīnolu sintēzei. Tā realizēta izmantojot Ritera reakciju starp alkīnilglikola kobalta kompleksu un acetonitrilu, iegūstot oksazolīnu.
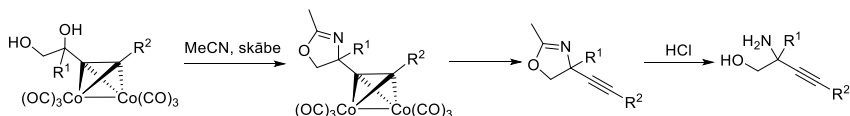
3. Tiešu tetrazolu C–H funkcionalizēšanu var panākt, izmantojot turbo Griņjāra reaģentu (*i*PrMgCl·LiCl kompleksu). Turbo Griņjāra reaģenta izmantošana nodrošina stabilāku metalētu starpproduktu, izvairoties no retro [2+3] ciklopievienošanās, kas ļauj realizēt reakcijas ar elektrofīliem, tai skaitā aldehīdiem un ketoniem.
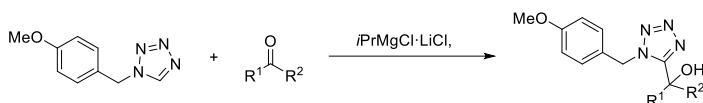
4. 6-Metilpiridilmetil- aizsargātus tetrazolus var pakļaut C–H deprotonēšanai, izmantojot turbo Griņjāra reaģentu, un sekojošai reakcijai ar elektrofīliem. 6-Metilpiridilmetilgrupu var nošķelt reducējošos elektroķīmiskos apstākļos.
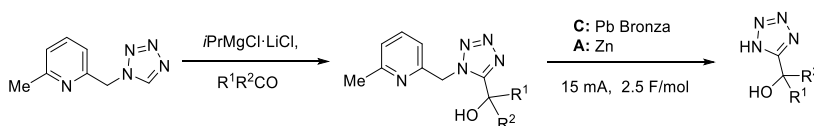
5. Deprotonētu tetrazolu reakcijā ar enantiomēri bagātinātiem *t*-butilsulfīnilimīniem var diastereoselektīvi iegūt atbilstošus pievienošanās produktus. Šī metode nodrošina piekļuvi aminoskābju analogiem, kas satur tetrazola fragmentu kā karbonskābes bioizostēru.
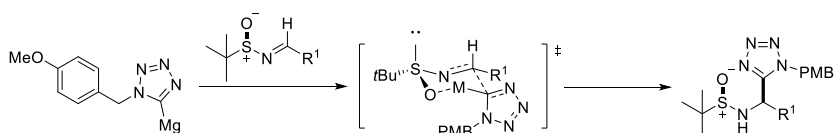
DOCTORAL THESIS PROPOSED TO RIGA TECHNICAL UNIVERSITY FOR THE PROMOTION TO THE SCIENTIFIC DEGREE OF DOCTOR OF SCIENCE

To be granted the scientific degree of Doctor of Sciences (Ph.D.), the present Doctoral Thesis has been submitted for the defence at the open meeting of RTU Promotion Council on June 14, 2023 at 14:00 at Riga Technical University Faculty of Materials Science and Applied Chemistry, Paula Valdena Street 3, Auditorium 272, Riga.

OFFICIAL REVIEWERS

Dr. chem. Mārtiņš Katkevičs (Latvian Institute of Organic Synthesis)

Dr. chem. Artis Kinēns (University of Latvia)

Dr. Marc Nazare (Leibniz-Institute for Molecular Pharmacology, Germany)

DECLARATION OF ACADEMIC INTEGRITY

I hereby declare that the Doctoral Thesis submitted for the review to Riga Technical University for the promotion to the scientific degree of Doctor of Science (*Ph. D.*) is my own. I confirm that this Doctoral Thesis had not been submitted to any other university for the promotion to a scientific degree.

Konstantinos Grammatoglou ....
(*signature*)

Date ....

The Doctoral Thesis has been prepared as a collection of thematically related scientific publications complemented by summaries in both Latvian and English. The Doctoral Thesis unites four scientific publications that have been written in English, with a total volume of 301 pages, including supplementary data.

ABBREVIATIONS

AIBN	α,α'–Azobisisobutyronitrile
Boc	*t*–Butoxycarbonyl
CADD	Computer Assisted Drug Design
CAN	Ceric ammonium nitrate
CDI	1,1'–Carbonyldiimidazole
DCE	1,2–Dichloroethane
DCM	Dichloromethane
DDQ	2,3–Dichloro–5,6–dicyano–1,4–benzoquinone
DFSI	Aspartic acid–Phenylalanine–Serine–Isoleucine peptide
DIPEA	Diisopropylethylamine
DMAP	4–Dimethylaminopyridine
EDC	1–Ethyl–3–(3–dimethylaminopropy)carbodiimide
HATU	Hexafluorophosphate Azabenzotriazole Tetramethyl Uronium
HPLC	High Performance Liquid Chromatography
IC_{50}	Half–maximal inhibitory concentration
LC/MS	Liquid chromatography–mass spectrometry
MeCN	Acetonitrile
NBS	*N*–Bromosuccinimide
nBu	n–Butyl
NMO	*N*–Methylmorpholine–*N*–oxide
OASS	*O*–acetylserine sulfhydrylase
PDB	Protein Data Bank
Ph	Phenyl
PLP	Pyridoxal 5'–phosphate (vitamin B6)
PMB	*p*–Methoxybenzyl
RCSB	Research Collaboratory for Structural Bioinformatics
r.t.	Room temperature
SAR	Structure–Activity Relationship
SAT	Serine acetyl transferase
TBA·BF$_4$	Tetrabutylammonium tetrafluoroborate
*t*Bu	tert–Butyl
TBS	tert–Butyldimethylsilyl
TFA	Trifluoroacetic acid
THF	Tetrahydrofurane
triF–Ala	3,3,3–Trifluoro–alanine
WHO	World Health Organization

Contents

GENERAL OVERVIEW OF THE THESIS

Introduction

The development of antibiotics in the first half of the 20th century, with penicillin discovery by Alexander Fleming in 1928 being the most prominent event, has signalized the beginning of a revolutionary era in medicine (Fig. 1).[1a] Life expectancy rose significantly in all the developed countries, diseases that were until then untreatable and fatal were afterwards treatable by the use of antibiotics, the performance of complex surgical operations was made viable, people under immunosuppression or with chronic diseases managed to fight or prevent infections. Similar benefits from the use of antibiotics were observed in developing countries where food–borne and other poverty–related infections were treated, leading to decrease of morbidity and mortality.[1a] Selman Waksman, in the late 30's, defined an antibiotic as "*a compound made by a microbe to destroy other microbes*". Waksman identified soil–dwelling filamentous actinomycetes as producers of antimicrobial compounds, including neomycin and streptomycin, the first agent active against tuberculosis. Waksman's work initiated the Golden age of antibiotics, from the 40's until the late 60's, a period during which more than 20 new antibiotic classes were discovered. Amongst other Macrolides, Glycopeptides, Cephalosporins, Quinolones, Azoles etc., classes that include natural products or synthetic antibiotics inspired by natural products, were developed (Fig. 1).[1b,1c]

Alexander Fleming expressed his concerns about the improper use of penicillin as early as in 1945, he had already discovered staphylococci that were immune to penicillin and predicted the spread of resistant bacteria. The emergence of antibiotic resistance was caused by different factors like overuse of antibiotics, incorrect prescription of antibiotics, and extensive use in agriculture. Additionally, the decision of many companies to withdraw from the development of new antibiotics, as well as the increased difficulties in obtaining regulatory approval for new developments has led to diminished marketing of new antibiotics, adding to the established antibiotics resistance problem (Fig. 1).[1a,1d,1e]
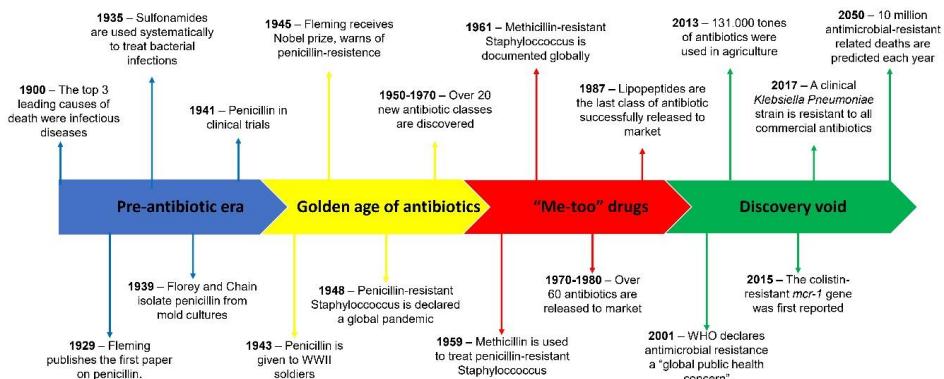
Fig. 1. The antibiotic–resistance timeline.

To overcome the ineffectiveness of certain antibiotics, "me–too" drugs were developed, which were the result of minor modifications made to existing antibiotics. The fact, however, that the mechanism of action of "me–too" drugs was, quite often, identical, resulted in rapid resistance to these compounds too.[1e] The World Health Organization (WHO) declared antimicrobial resistance a "global public health concern" in 2001, and indicates a discovery void until today. The number of innovative new leads, during this period, is quite limited and most of the drugs that enter the clinical pipeline aim to act on the same targets as traditional antibiotics.[1e]

In the search of novel, effective antibiotics, various strategies have been exploited like the development of hybrid antimicrobial agents, membrane–active drugs, and inhibitors of bacterial virulence and pathogenesis, and exploitation of alternative methods like the use of bacteriophages.[2] Another strategy for the development of new antibiotics is focused on key metabolic functions of bacteria. Targeting important but non–essential gene products can be an effective means of reducing bacterial fitness, resulting in enhanced antibiotic treatments, shortened latency periods, increased susceptibility to traditional antibiotics and thereby facilitating clearance of the pathogen by the host immune system.[3]

Sulfur is a fundamental component of many biomolecules, from amino acids, such as cysteine, to cofactors and compounds that control the redox homoeostasis. Therefore, the enzymes involved in the cysteine biosynthetic pathway, which is present in pathogens and plants but absent in mammals, are very attractive antibacterial targets. Inhibition of cysteine biosynthesis has been proven to affect the ability of pathogens to fight oxidative stress, it reduces their virulence and leads to decreased antibiotic resistance.[3–4] The final steps of the cysteine biosynthesis involve the action of two enzymes, serine acetyl transferase (SAT) which acetylates serine, and O–acetylserine sulfhydrylase (OASS), a pyridoxal 5'–phospate (PLP) dependent enzyme that carries out a β–replacement reaction on acetyl serine (Scheme 1).
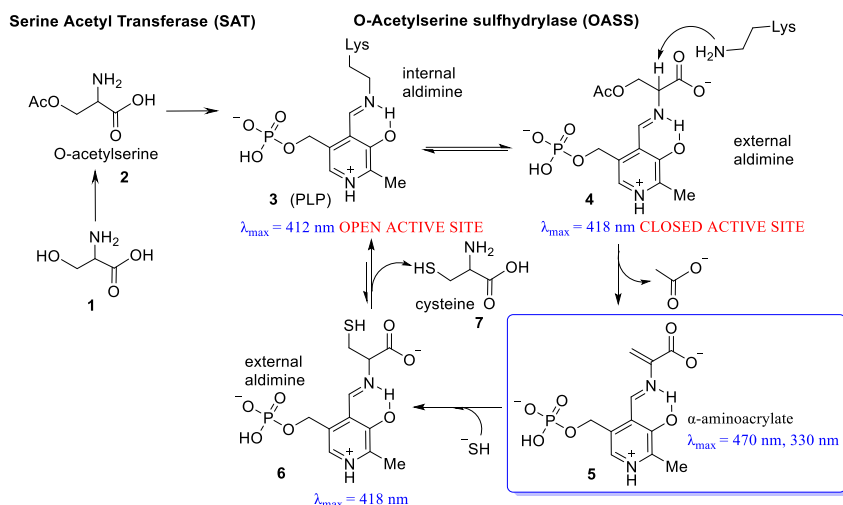
Scheme 1. Catalytic cycle of OASS to produce cysteine.

OASS is present in bacteria as two isoforms, OASS–A and OASS–B, also named CysK and CysM after the coding genes. Serine acetyltransferase (SAT), is able to form a high–affinity complex with OASS–A but not with OASS–B.[5]

Several efforts have been made to develop inhibitors of PLP–dependent enzymes, either following the structure–based, ligand–based, or mechanism–based design. The first attempts were focused in mimicking the nature developing pentapeptides with affinities in the micromolar range. In order to overcome the unfavorable drug–like properties of peptide inhibitors, and using *in silico* and synthetic chemistry techniques various active small molecules were prepared (Fig. 2).[6]

K_d *Hi*OASS-A = 1.45 µM

9

K_d *St*OASS-A = 1.45 µM
K_d *St*OASS-B = 148 µM

10

CysK1 inhibitor
IC_{50} = 19 nM

8

K_d *St*OASS-A = 0.067 µM
K_d *St*OASS-B = 1.66 µM

11

K_d *St*OASS-A = 0.028 µM
K_d *St*OASS-B = 0.49 µM

12
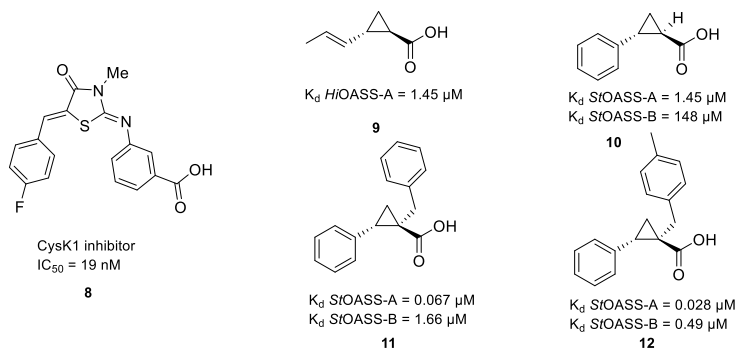
Fig. 2. Known inhibitors of OASS–A (CysK).

Mechanism–based inhibitors cause the inactivation of the enzyme through a chemical reaction that leads to an irreversible protein–inhibitor complex impeding the catalytic action of the enzyme. A range of chemotypes acting as mechanism–based inhibitors of PLP–dependent enzymes have been studied and reported.[7]

The rise of antimicrobial resistance made the identification of new druggable targets more urgent. Although PLP-dependent enzymes represent about 4% of the enzymes classified by the Enzyme Commission, only a small number of them have been identified as potential targets for therapeutic agents, and even less are those for which drugs have been developed. These limited numbers are associated with the lack of knowledge regarding the family of PLP-dependent enzymes and the role played by them in a variety of biological processes. However, the fact that PLP carries out a variety of reactions and the spectral changes attributed to different PLP-substrate derivatives that help monitoring the reaction progress, are just two of the features that make PLP-dependent enzymes interesting targets.[7d] In this aspect, the enzymes of the cysteine biosynthetic pathway attract enough interest. OASS is an important enzyme that could possibly be a target of antibacterials. Therefore, there is a need for the development of OASS inhibitors in order to investigate its importance for the antibacterial drug discovery. Furthermore, it is necessary to identify new chemotypes, from the unexplored chemical space, for PLP dependent enzymes' inhibitors. In addition, the requirement for the development of synthetic methods for these new chemotypes arises.

Aims and objectives

The aim of the thesis is the synthesis of mechanism–based inhibitors–inactivators of PLP–dependent enzyme *O*–acetylserine sulfhydrylase (OASS) based on existing chemotypes, the investigation of new chemotypes, and the development of synthetic methods to facilitate the construction of potential PLP dependent enzyme inhibitors.

The following tasks were set:

1. Design and synthesis of small library of potential OASS inhibitors.
2. Development of efficient protocol for the synthesis of quaternary alkynyl glycinols.
3. Development of synthetic methods to introduce terazole as a carboxylic acid bioisoster.

Scientific novelty and main results

As a part of scientific efforts, a number of known and new compounds were tested as potential inhibitors of bacterial *O*–acetylserine sulfhydrylase (OASS). Trifluoroalanine was found as the first mechanism–based inhibitor of OASS. SAR of triF–Ala derivatives was explored.

Additionally, several new methods were developed for the synthesis of PLP dependent enzyme inhibitors:

1. Method for the synthesis of *C*–quaternary alkynyl glycinols.
2. Method for the direct C–H functionalization of tetrazoles using turbo Grignard reagent.
3. Introduction of electrochemically cleavable *N*–protecting group for tetrazole, facilitating its functionalization.
4. Stereoselective synthesis of amino acid analogues bearing tetrazole as carboxylic acid replacement.

Structure of the thesis

The thesis is a collection of scientific publications focused on the synthesis of triF–Ala analogues and the development of methods for the synthesis of PLP–dependent enzyme inhibitors.

Publications and approbation of the thesis

Main results of the thesis were summarized in four publications. In addition, results of the research were presented in seven conferences.

Scientific publications

1. **K. Grammatoglou**, J. Bolsakova, A. Jirgensons, C–Quaternary alkynyl glycinols *via* the Ritter reaction of cobalt complexed alkynyl glycols. *RSC Adv.* **2017**, *7*, 27530–27537.
2. N. Franko, **K. Grammatoglou**, B. Campanini, G. Costantino, A. Jirgensons, A. Mozzarelli, Inhibition of *O*–acetylserine sulfhydrylase by fluoroalanine derivatives. *J. Enzyme Inhib. Med. Chem.* **2018**, *33*, 1, 1343–1351.
3. **K. Grammatoglou**, A. Jirgensons, Functionalization of 1N-Protected Tetrazoles by Deprotonation with the Turbo Grignard Reagent. *J. Org. Chem.* **2022**, *87*, 3810−3816.
4. **K. Grammatoglou**, M. Dārziņa, A. Jirgensons, Functionalization of Tetrazoles Bearing the Electrochemically Cleavable 1*N*-(6–Methylpyridyl–2–methyl) Protecting Group. *ACS Omega* **2022**, *7*, 18103−18109.

Participation in conferences

1. **K. Grammatoglou**, J. Sirotkina, A. Jirgensons, Synthesis of 4–Alkynyl 2–Oxazolines *via* the Ritter reaction. *9th Balticum Organicum Syntheticum conference (BOS 2016)*, Riga, Latvia, July 3–6, **2016**, poster presentation.
2. **K. Grammatoglou**, J. Sirotkina, C–Quaternary Alkynyl Glycinols *via* the Ritter Reaction of Cobalt Complexed Alkynyl Glycols. *Paul Walden 10th Symposium on Organic Chemistry*, Riga, June 15–16, **2017**, poster presentation.
3. N. Franko, J. Magalhães, **K. Grammatoglou**, B. Campanini, M. Pieroni, E. Azzali, G. Annunziato, G. Costantino, A. Jirgensons, A. Mozzarelli, Targeting enzymes of the sulfur assimilation pathway for the development of new antibiotics. *Proceedings of the Proteine 2018 conference (PROTEINE2018),* Verona, Italy, May 28–30, **2018**, poster presentation.
4. **K. Grammatoglou**, L. Levy, A. Jirgensons, Design and Synthesis of 3,3,3–trifluoroalanine Analogues as Potential Antibacterials. *10th Biannual Balticum Organicum Syntheticum conference (BOS 2018)*, Tallinn, Estonia, July 1–4, **2018**, poster presentation.
5. **K. Grammatoglou**, Design and synthesis of *O*–acetylserine sulfhydrylase inhibitors as potential antibacterials. *OUTREACH FINAL Conference ITN MSCA INTEGRATE "FIGHTING ESKAPE, THE BAD GANG"*, Parma, Italy, November 21–23, **2018**, oral presentation.
6. **K. Grammatoglou**, Functionalization of 1*N*–protected tetrazoles by deprotonation with turbo Grignard reagent. *Paul Walden 11th Symposium on Organic Chemistry*, Riga, September 19–20, **2019**, poster presentation.
7. **K. Grammatoglou**, Synthesis and Applications of Metalated 1*H*–tetrazoles. *Balticum Organicum Syntheticum conference (BOS 2022)*, Vilnius, Lithuania, July 3–6, **2022**, poster presentation.
8. **K. Grammatoglou,** Synthesis of PLP–dependent enzyme OASS inhibitors and the development of relevant synthetic methodologies. *Springboard Summer*

School "Major milestones in design and development of novel antimicrobials", Riga, August 23–25, **2022**, oral presentation.

MAIN RESULTS OF THE THESIS

1. Synthesis of mechanism–based OASS inhibitors.

A focused library of amino acids – potential mechanism–based inhibitors of OASS as PLP dependent enzyme was assembled (Fig. 3). Compounds **13–17** were purchased as they were commercially available while compounds **18–19** were synthesized for a different, recently published project,[8] and compounds **20–22** were synthesized by our workgroup. The screening of the library against OASS revealed that triF–Ala (**13**) exhibited inhibitory potency with $IC_{50}=132$ μM (Fig. 3).
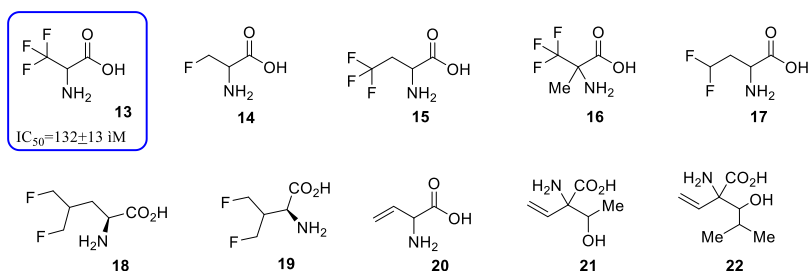
Fig. 3. Library of potential mechanism–based inhibitors of OASS.

Halogenated alanines have been exploited as inhibitors of various PLP–dependent enzymes.[5,9] Based on previously reported mechanisms for the inactivation of PLP–dependent enzymes, addition of triF–Ala (**13**) to the resting enzyme leads to initial transaldimination forming the external aldimine (**23**) (Scheme 2).
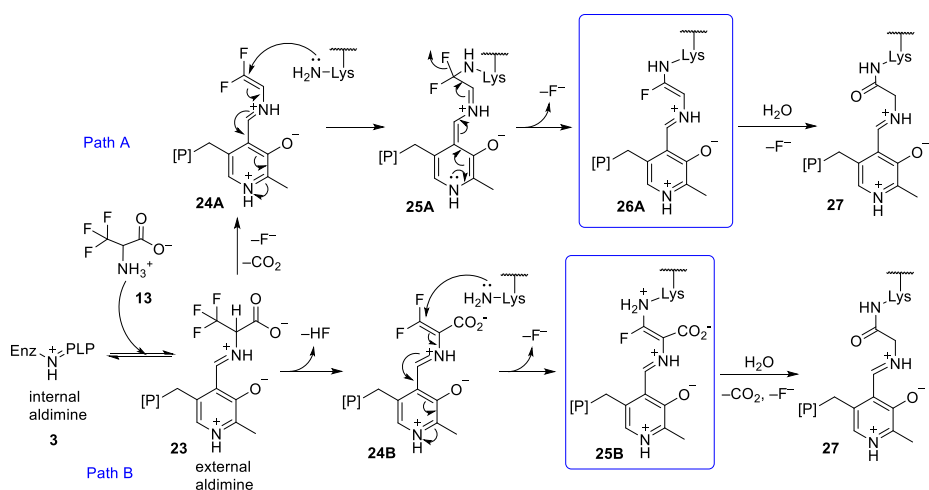
Scheme 2. Possible inactivation pathways of PLP dependent enzymes by triF–Ala.

Two possible paths have been proposed after that, path A describes the loss of fluoride and decarboxylation to intermediate **24A**. Elimination of the second fluoride ion and concomitant attack of an enzyme active site lysine on the olefinic terminus of the electrophilic unsaturated imine, leads to the enzyme inactivation. The resultant inactive complex **26A**, would be covalently bound to the enzyme through the lysine residue. Unsaturated imine **26A** is attacked by water and after further loss of HF it gives the amide **27**. According to path B after the initial transaldimination, elimination of HF occurs to give intermediate **24B**, which is more active towards Michael attack by active site lysine. Further elimination of the second fluoride ion gives rise to the inactive complex **25B**, which would be covalently bound to the enzyme through the lysine residue. **25B** is attacked by water and after further loss of HF and CO_2, it gives the amide **27** (Scheme 2).[5,10]

Photochemical investigations showed that β,β,β–trifluoroalanine (triF–Ala, **13**), a known suicide substrate of PLP–dependent enzymes, forms an adduct with the enzyme which causes changes to the absorbance spectra compared to the spectra of the internal aldimine of the resting enzyme, an indication of the reaction taking place on the co–factor. The interactions of triF–Ala with both isozymes of OASS, OASS–A (or Cys–K) and OASS–B (or Cys–M) were investigated by absorbance and fluorescence spectroscopy.

As it has already been noted, the absorption spectra of OASS–A and OASS–B exhibit a band at 412 nm, attributed to the internal aldimine (**3**, Fig. 5). After addition of triF–Ala to OASS–A two peaks appeared at 440 and 466 nm, and two minor bands at 360 and 380 nm (Fig. 4), indicating a species with extended conjugation (**24B**, Fig. 5). The intensity of 466 nm absorbance slowly decreased with the formation of a band at 412 nm. Less intense spectral changes were observed at the reaction of triF–Ala with OASS–B in the range of 400–500 nm. The decomposition of the intermediate along with the decrease at 457 nm was accompanied by the increase in absorbance in the range of 300–350 nm, possibly attributed to the production of difluoropyruvate.
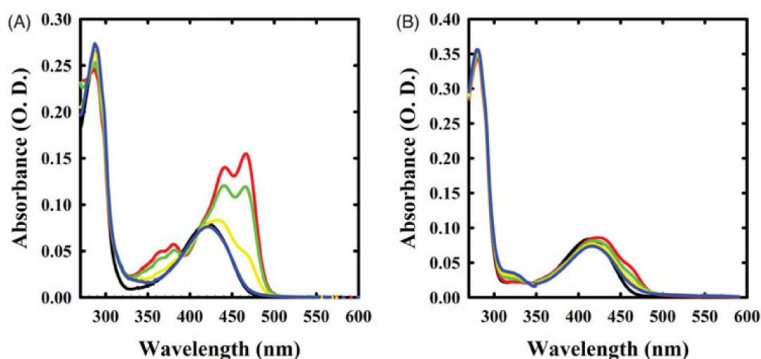
Fig. 4. Absorbance spectra of OASS in the absence and presence of 1 mM triF–Ala. Panel A: absorbance spectrum of OASS–A in the absence of reagent (black line), 1 min (red line), 1 h (green line), 3 h (yellow line), and 7 h (blue line) after addition of the reagent. Panel B: absorbance spectrum of OASS–B in the absence of reagent (black line), 1 min (red line), 1 h (green line), 3 h (yellow line), and 7 h (blue line) after addition of the reagent.
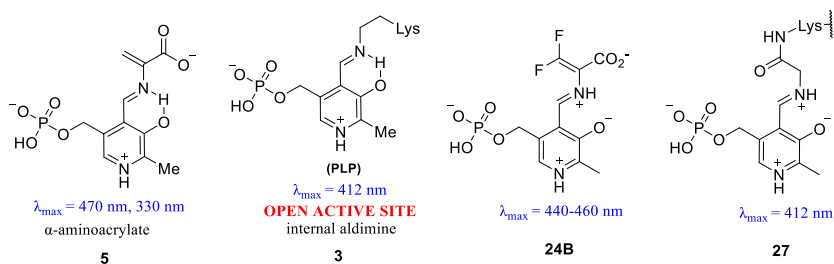
Fig. 5. Structures attributed to absorbance bands observed during OASS inactivati–on process.

Next, the reaction of OASS–A was monitored by fluorescence emission (Fig. 6), and the band measured upon excitation at 412 nm was blue shifted to 495 nm. This confirms that the species formed is not the α–aminoacrylate (**5**, Fig. 5). The emission band slowly decreased but after 6 hours incubation, in contrast to what was observed by absorbance spectroscopy, there was no recovery of the initial emission spectrum. The later suggests that this species that absorbs at 412 nm is different than the internal aldimine **27** (Fig. 5). Upon excitation at 412 nm of the reaction of triF–Ala with OASS–B, the intensity of emission is primarily increased and then slowly decreased. This is accompanied by a small blue shift to 501 nm which slowly shifts back to 505 nm after incubation of 7 hours. These changes may refer to an external aldimine, and the small blue shift suggests the formation of a transient species.
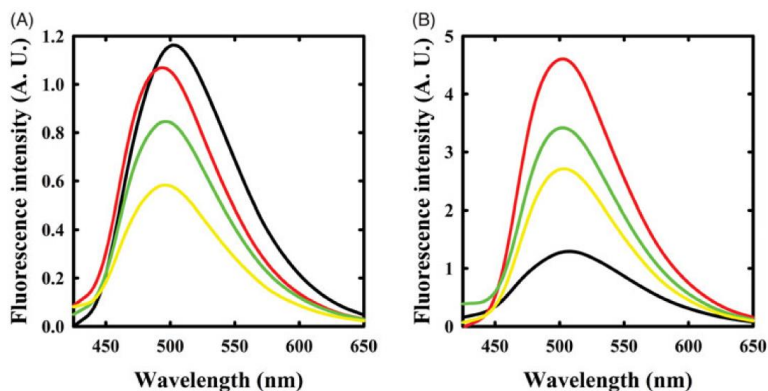
Fig. 6. Fluorescence emission spectrum of OASS in the absence and presence of 1 mM triF–Ala. Emission spectra were recorded upon excitation at 412 nm. Panel A: OASS–A in the absence of reagent (black line), 1 min (red line), 4 h (green line), and 6 h (yellow line) after addition of the reagent. Panel B: OASS–B in the absence of reagent (black line), 1 min (red line), 3 h (green line), and 7 h (yellow line) after addition of the reagent.

Further investigation was performed to evaluate the potential inhibitory action of F–Ala and triF–Ala on OASS–A and OASS–B. Two different experiments were conducted for this purpose; first the two isozymes were assayed after exposure to increasing concentrations of F–Ala determining IC_{50} values of 480 ± 50 μM and 1290 ± 230 μM for OASS–A and OASS–B respectively, and for triF–Ala IC_{50} values of 130 ± 10 μM and 940 ± 60 μM were determined. To detect whether triF–Ala is irreversible inhibitor of OASS, as it is reported

for other PLP–dependent enzymes, the kinetics of OASS–A in the presence of different concentrations of triF–Ala were monitored, and the results were in agreement to what is expected by the suicide substrates. The second experiment involved assaying the enzyme after 85–hour reaction with 10 mM triF–Ala, the complete removal of ligand, and incubation in the presence of saturating PLP concentration. The results of the latter experiment were indicative of the inactivation caused by irreversible covalent modification of active site residue(s) that was brought about by triF–Ala.

Our research for new OASS inhibitors involved the use of Computer Assisted Drug Design (CADD) methods. We relied on the data already reported about identified OASS inhibitors, and the structural information retrieved from the crystallographic data of the inhibitors and the enzyme.[6d] The Natural peptide DFSI **28**, which consists of the last four residues of SAT (CysE) enzyme, has been previously identified as OASS–CysK inhibitor. Sriram et.al. reported the development of OASS–CysK inhibitor **8** with improved activity compared to the natural peptide, DFSI (**28**, Fig. 7). Inhibitor **8**, as well as **28**, are competitive inhibitors which bind in the proximity of PLP cofactor in the active site cleft of the enzyme.
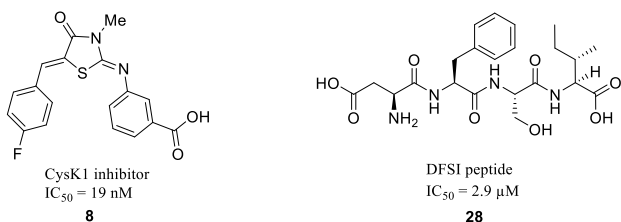
Fig. 7. OASS inhibitors, CysK1 inhibitor 8 and DFSI peptide 28.

Based on these data we proceeded to construction of a protein model on Schrödinger Maestro suite in order to perform virtual screening of ligand libraries. Two proteins were chosen from RCSB Protein Data Bank (PDB), 2Q3C crystal Structure of OASS holoenzyme from *mycobacterium tuberculosis* in complex with the inhibitory peptide DFSI and 3ZEI structure of the *mycobacterium tuberculosis* OASS–CysK in complex with the small molecule inhibitor **8** (Fig. 8).
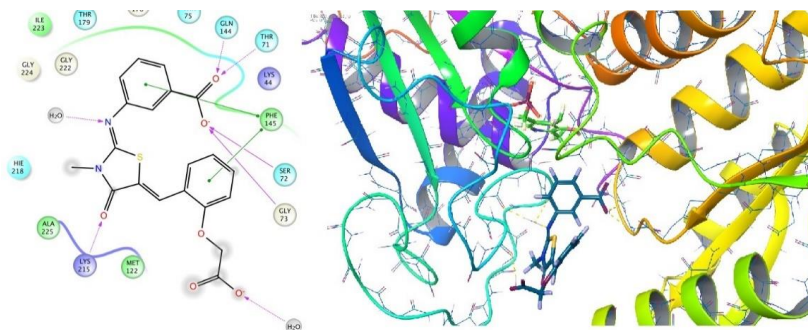
Fig. 8. OASS–CysK complex with inhibitor 8.

Both protein structures were prepared using Schrödinger's Protein Preparation Wizard. The 3ZEI protein was chosen as the base for our study as the complex with the known

inhibitor allowed us to identify the main interactions in the enzyme pocket. Docking of triF–Ala, that had already shown affinity to PLP, followed the interactions revealed above, pointed out the most important ones and also the difference from previous inhibitors, as the interaction with PLP is observed (Fig. 9).
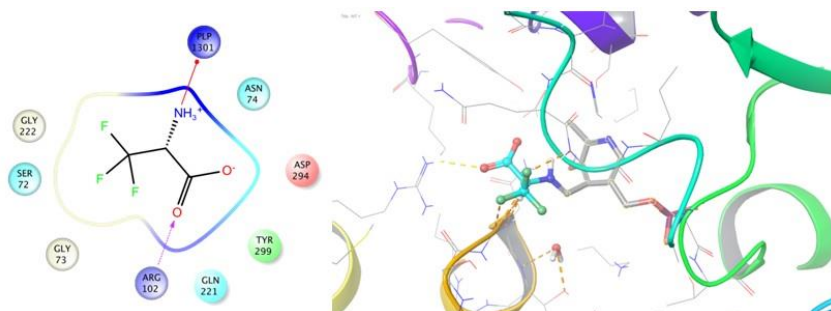
Fig. 9. Interactions of triF–Ala with OASS protein residues and PLP.

As our aim was to synthesize covalent inhibitors of OASS, we aimed for the substrates to perform a reaction with PLP. This had to be programmed in Schrödinger suite in order to perform the docking experiments with this function. Therefore, the docking motif had to be reprogrammed to address the reaction between the substrate and PLP, and a new custom reaction file was prepared to facilitate this covalent bond during the virtual experiments. Having the protein and the reaction motif prepared we proceeded to the covalent docking of commercial libraries (Enamine's "Stock Screening Compounds Collection", MolPort's "Screening Compound Database", and eMolecules database) and the fragment library provided by Schrödinger software. A library containing 140000 compounds was compiled and after selection of the compounds that fulfilled the verified interactions, we ended up with a library of 200 compounds. These compounds were submitted to covalent docking experiments producing approximately 2000 docking poses. Combining the scoring given by the molecular docking program Glide, and the categorization based on structural motifs, we ended up with generic structures as indicative targets for our synthetic work (Fig. 10).
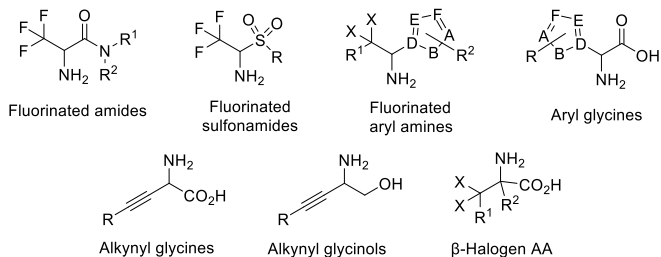
Fig. 10. Chemotypes promoted for synthetic realization.

2. Synthesis of trifluoroalanine analogues

The substitution of the carboxylic acid moiety of triF–Ala (**13**) with bioisosters was attempted first by synthesizing several amides and hydroxamic acid (Scheme 3). Boc–protected triF–Ala **29** underwent coupling with different amines using HATU, and after acidic removal of Boc group amides **32a–f** were obtained in high yields. For the synthesis of hydroxamic acid **35a** the use of CDI as a coupling agent afforded the required product **34a** in excellent yield, which was deprotected to give **35a**.
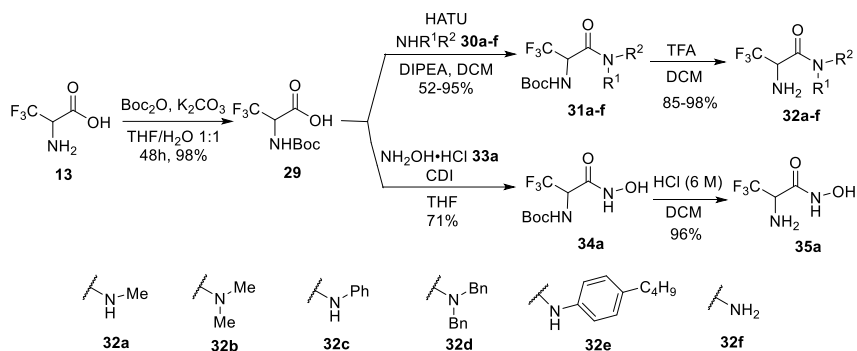
Scheme 3. Synthesis of triF–Ala derived amides 32a–f and hydroxamic acid 35a.

In a further effort to expand the library of triF–Ala analogues, we proceeded to parallel synthesis. Initially, the synthetic protocols for the application in parallel synthesis setup were established using model reactions. For the synthesis of hydroxamic acids **35b–d** the CDI coupling method proved to be a good choice. For the synthesis of acylsulfonamide **38a** the use of DMAP and EDC coupling was appropriate. For the synthesis of amide **32g** the already established protocol with HATU and DIPEA was applicable (Scheme 4).
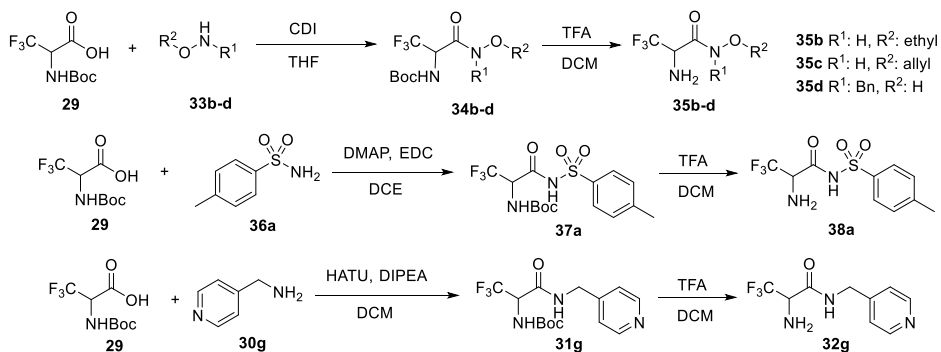
Scheme 4. Validation of reaction protocols for parallel synthesis.

Having the protocols established we proceeded to the synthesis of several compounds using the parallel synthesis blocks. In this setup we could run multiple reactions in 48 tubes' block then filter the whole set through fritted filter plates to an analytical 48 well plate which was submitted to purification with preparative HPLC (Fig. 11).
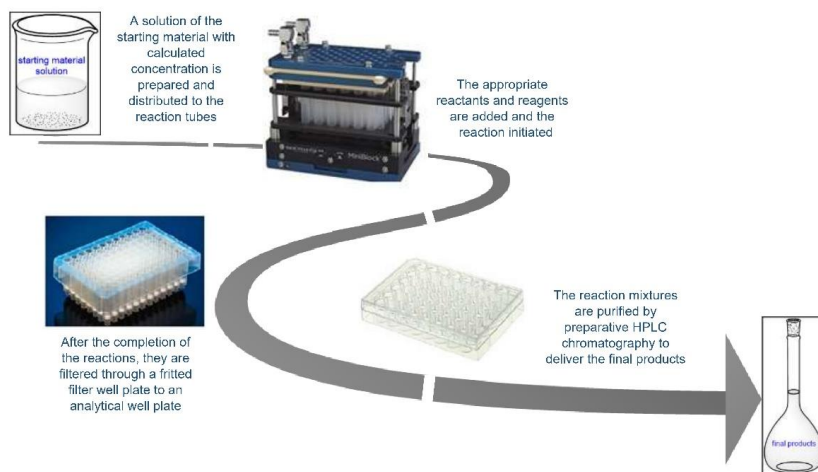
Fig. 11. Parallel synthesis workflow.

Following this workplan we managed to synthesize and isolate 42 compounds in short period. 11 hydroxamic acids were successfully synthesized and isolated, **35b–l** (additional to **35a** previously synthesized too), including aromatic and aliphatic N– and O– substituted compounds (Fig. 12).
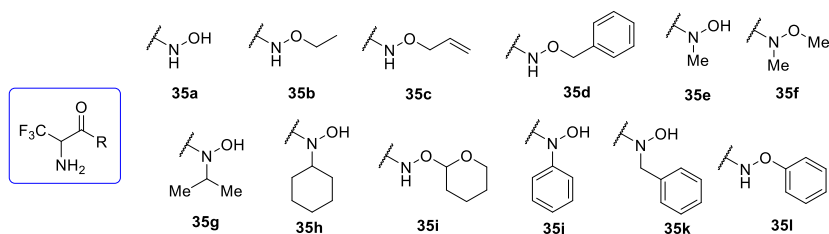
Fig. 12. Hydroxamic acids synthesized by parallel chemistry approach.

Different acylsulfonamides **38b–p** (plus **38a**) were prepared, most of them containing an aromatic or heteroaromatic moiety with various substituents like halogen (**38e, 38f, 38h, 38k, 38m**), cyano (**38n**), nitro (**38k, 38l**) etc. (Fig. 13).
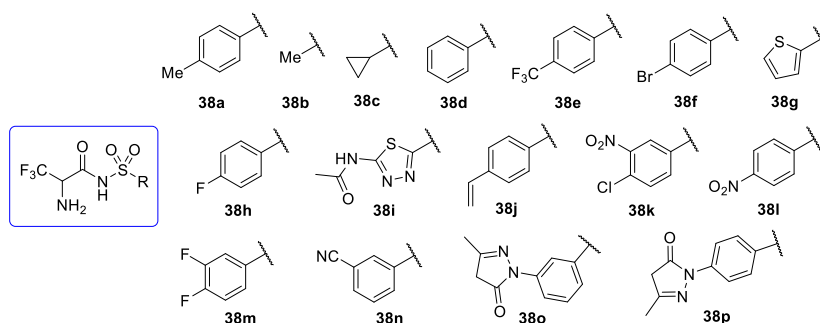
Fig. 13. *N*-Acylsulfonamides 38a–p synthesized by parallel chemistry approach.

Finally, 15 amides **32h–u** (plus **32g**) were synthesized using parallel synthesis setup compiling a versatile group of compounds, like pyridine with halogen or methyl substitution (**32h, 32j, 32o, 32t**) substrates, pyridine–methyl amides (**32g, 32u**), and various 5–membered heterocyclic amides (Fig. 14).
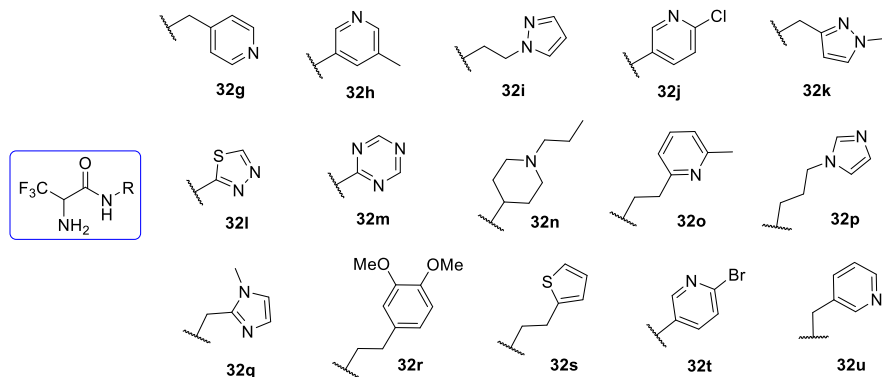
Fig. 14. Amides 32g–u synthesized by parallel chemistry approach.

As a part of triF–Ala analogues synthesis we aimed to obtain difluoroaspartic acid monoester **45**. For that, the synthesis of alcohol **41** was realized through a Barbier type reaction between benzaldehyde (**39**) and ethyl bromodifluoroacetate (**40**). The mesylation of alcohol **41** and substitution with azide provided intermediate **42**. The latter was reduced to amine which was Boc–protected *in situ* to give amine **43**. This was subjected to aromatic oxidation with sodium periodate and ruthenium chloride to transform the phenyl group to carboxyl group. The resulting acid **44** was deprotected to give the desired difluoro aspartic acid monoester **45**. To expand the library of triF–Ala analogues, Boc protected amine **43** was transformed to a free amine **46** for testing against OASS (Scheme 5).
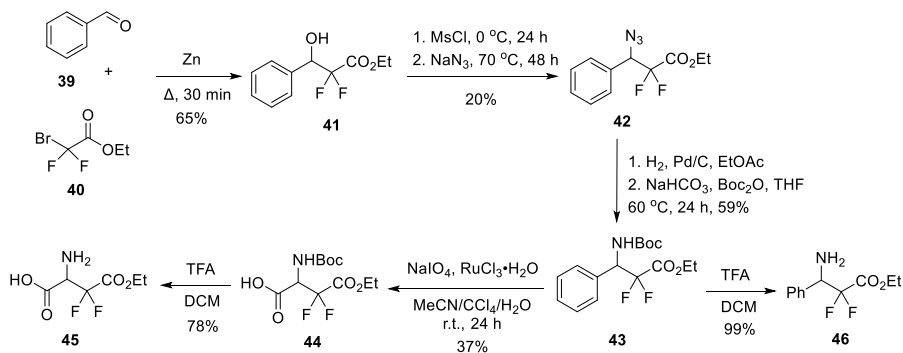
Scheme 5. Synthesis of difluoro aspartic acid monoester 45.

We also assume that difluoro aspartic acid monoester **45** might possibly act as mechanism–based inhibitor (Scheme 6) following two different pathways: with decarboxylation taking place early (**48B–52B**, path B) or late (**48A–53A**, path A) in the route, according to the proposed mechanism.
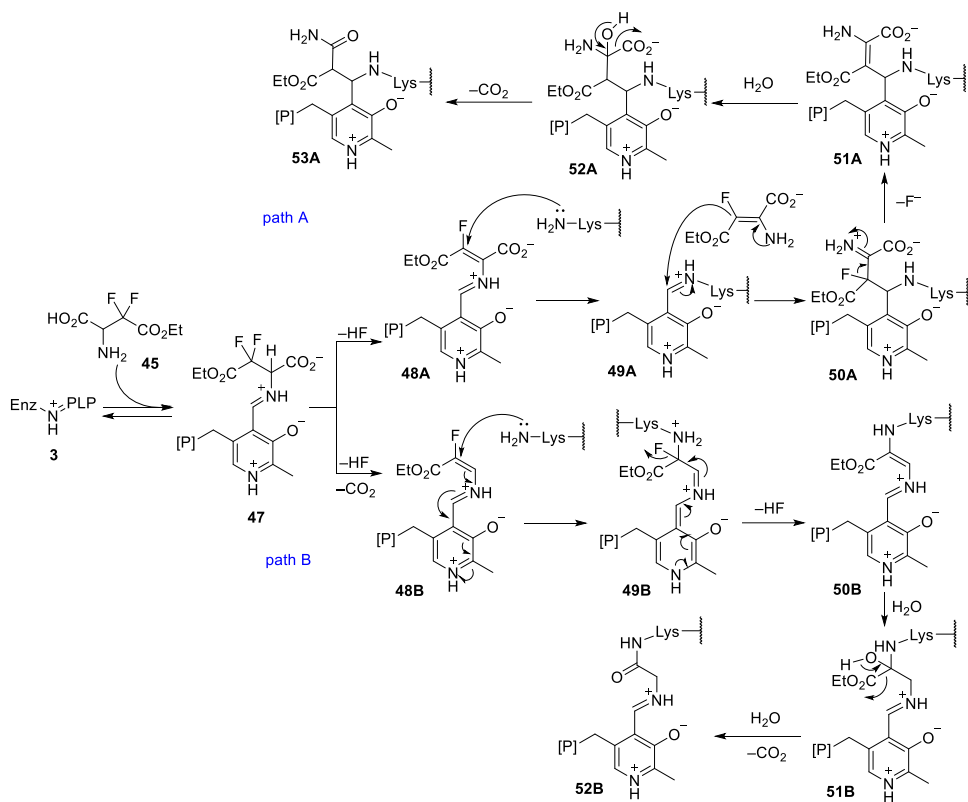
Scheme 6. Plausible mechanisms of inactivation of OASS by difluoro aspartic acid monoester 45.

Other targets within the triF–Ala analogues program were the compounds in which carboxylic acid was substituted with triazole **54** and tetrazole **55** (Fig. 15).
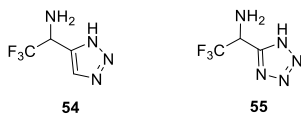
Fig. 15. Triazole and tetrazole analogues of triF–Ala.

To prepare the target compounds **54** and **55** first, we synthesized imine **58** by the condensation of *p*–methoxy benzylamine **56** with trifluoro acetaldehyde ethyl hemiacetal **57**. The nucleophilic addition of TMS–acetylene to imine **58** followed by desilylation provided alkyne **59**. The latter underwent copper mediated [2+3] cycloaddition with *p*–methoxy benzylazide **60** to give the protected triazole **61**. The PMB deprotection with TFA, to our surprise, occurred only from amino group providing triazole **62** (Scheme 7).
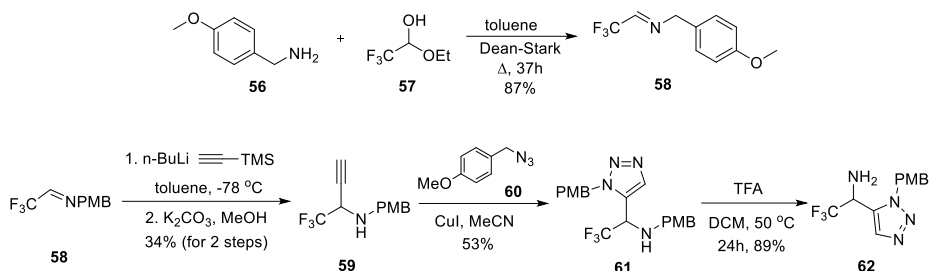
Scheme 7. Triazole 62 synthetic route.

The synthesis of the target compound **55** began by the preparation of PMB protected tetrazole **63** following the classic conditions reported in literature. Intermediate **63** was C–H metalated using *i*PrMgCl for the deprotonation and added to the imine **58** providing tetrazole **64** in a low yield (Scheme 8). Efforts to deprotect tetrazole **64** under various conditions (TFA/DCM, neat TFA 60°C, H$_2$/Pd, CAN, DDQ) led either to decomposition of the tetrazole (main product identified was *p*–methoxy benzylamine **56**) or to an inseparable mixture of tetrazole **64** with partially deprotected product.
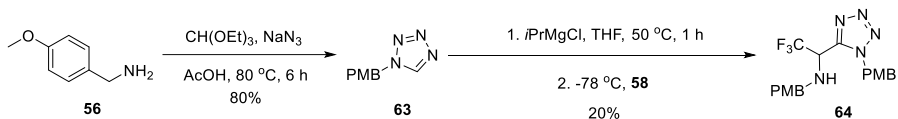
Scheme 8. Synthesis of tetrazole 64.

3. Evaluation of inhibitory potency of trifluoroalanine analogues

The compounds **32a–u**, **35a–l**, **38a–p**, **45**, **46**, **62** (Fig. 16) synthesized as described herein, were evaluated for their reactivity with OASS–A and OASS–B isozymes as well as for enzyme inhibition potency and inactivation kinetics. Assays were carried out on CysK and CysM of *Salmonella Typhimurium* recombinantly expressed in *Escherichia coli*. The enzyme was incubated with compounds at 1 mM concentration and the enzymatic activity was measured at time intervals.
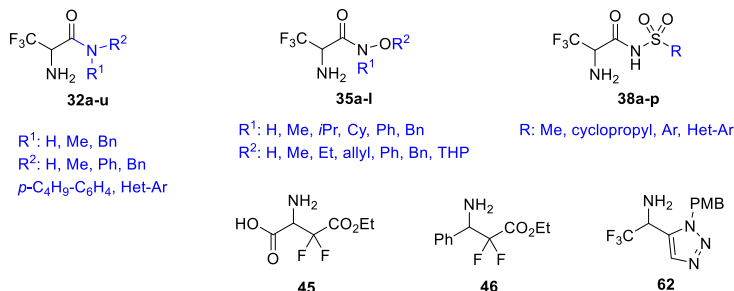
Fig. 16. Library of synthesized compounds that were tested for their reactivity with OASS.

To study the effect of the modification in the chain of triF–Ala, compounds **3–5** (Fig. 3) and **45–46** (Scheme 5) were investigated for reactivity with OAAS–A and OAAS –B. None of these compounds showed measurable improvement in reactivity compared to parent compound **13**, triF–Ala (IC$_{50}$=132 μM).

Next, the effect of bioisosteric replacement of the carboxylic acid moiety was examined. The first set of compounds, **32a–f** (Fig. 16) and **35a** (Fig. 12) were tested observing again only negligible effects on reactivity with an enzyme. Noteworthy, that hydroxamic acid **35a** caused small absorbance changes in OASS–A (Fig. 17), and about 14% decrease in enzyme activity.[5]
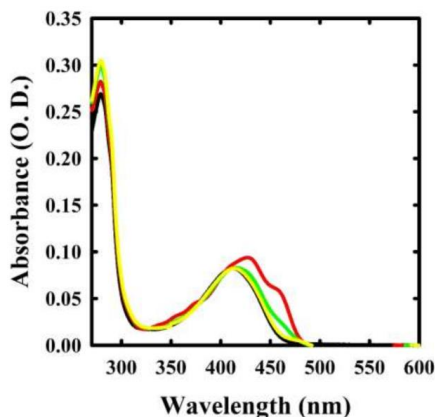
Fig. 17. Spectral changes for the reaction between OASS–A and 1 mM compound 35a. OASS–A in the absence of reagent (black line) and 1 min (red line), 30 min (green line) and 1 h (yellow line) after compound 22a addition.

From the next set of compounds, **35b–l, 38a–p,** and **32g–u** (Fig. 16) 5 compounds showed measurable OASS–A inhibitory properties (Fig. 18). Compounds **38i, 38p** and **32h** proved to be weak binders of the enzyme and did not cause significant inactivation, however, hydroxamic acid derivative **35k** and sulfonamide **38b** were the most potent compounds from this small library.
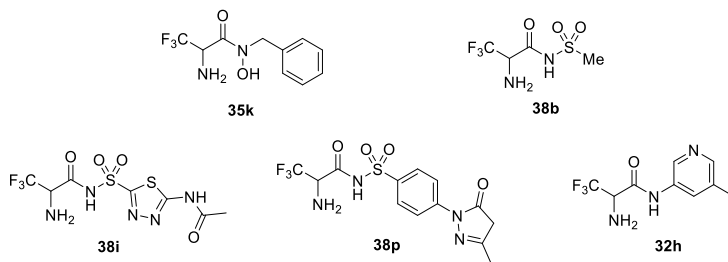
Fig. 18. Highest performing compounds.

Hydroxamic acid **35k** exhibited IC$_{50}$ (177±29 μM) and in inactivation assay, approximately 15% inhibition was observed at the first time point, although it is lost later, probably due the hydrolysis of the intermediate (Fig. 19).
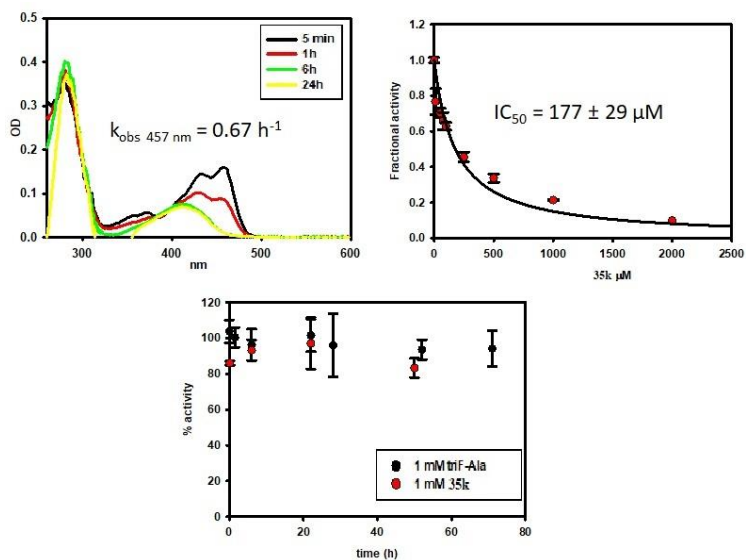
Fig. 19. 1 mM inhibitor 35k, following 5000–times dilution for the assay (0.2 µM inhibitor in the assay) in two replicates.

Sulfonamide **38b** also showed IC$_{50}$ (179±22 µM) for the inhbition of OASS–A and approximately 20% inhibition was observed during the inactivation assay at the first time point, although it is lost later, probably due the hydrolysis of the intermediate (Fig. 20).
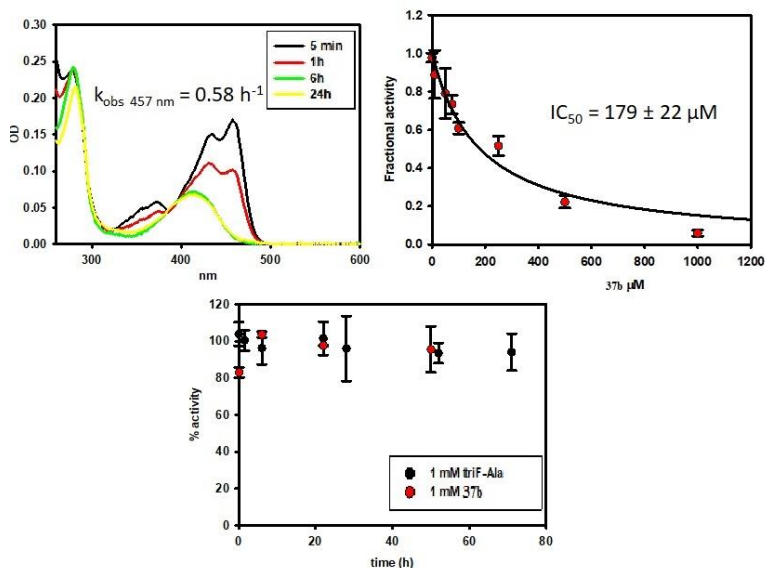
Fig. 20. 1 mM inhibitor 38b, following 5000–times dilution for the assay (0.2 µM inhibitor in the assay) in two replicates.

Based on the spectral and kinetics data collected from the reactivity experiments of triF–Ala with OASS and taking into consideration the mechanistic schemes already proposed for the reaction of triF–Ala with other PLP–dependent enzymes, we hypothesized that the inactivation mechanism of OASS–A is similar to the one proposed previously (Scheme 2). We propose that the mechanism follows the path B rather than path A, as decarboxylation does not take place in the catalytic cycle of OASS.

Inhibitors **35k** and **38b** comprise promising scaffolds for further development as these, in contrast to the parent triF–Ala (**13**), contain substructures amenable for derivatization to pick–up additional interactions with OASS. The work in this direction was suspended due to expiration of the program making the biological testing temporarily unavailable.

4. Development of new methods for the synthesis of PLP dependent enzyme inhibitors

4.1. Novel approach to C–quaternary alkynyl glycinols

One of the chemotypes that emerged as potential inhibitors of PLP–dependent enzymes was the alkynyl glycinols **65**. These, along with synthetically equivalent alkynyl glycine derivatives **66** (Fig. 21), are very useful building blocks for the synthesis of complex bioactive molecules. However, there are only a few methods for the direct synthesis of alkynyl glycinols avoiding the reduction of carboxyl groups in glycines **66**.
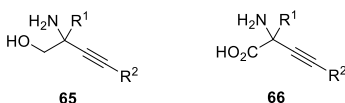
Fig. 21. Alkynyl glycinols 65 and alkynyl glycines 66.

The Ritter reaction of 1,2–diols was examined as method for the synthesis of alkynyl glycinols through the corresponding oxazolines. The first attempt for the direct access to oxazoline **70** only delivered a poor <10% yield (Scheme 9). The use of cobalt complexed alkynyl glycinols **68**, which can effectively stabilize the intermediate carbenium ion **A** provided oxazolines **70**, that serve as a precursor of alkynyl glycinol derivatives **65**.
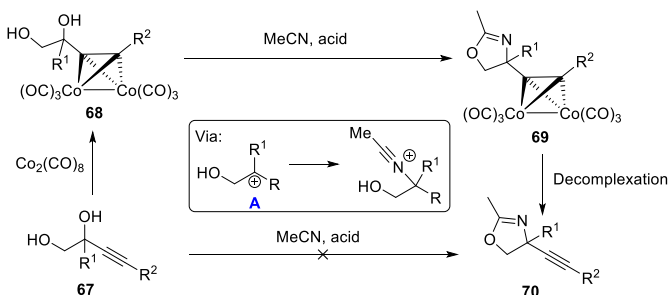
Scheme 9. Synthesis of oxazolines by Ritter reaction.

Preparation of cobalt complexed alkynyl glycols **68** and **73** was carried out in two steps, first by the addition of lithium acetylenides to hydroxy ketone derivatives **71** and then by the treatment of the provided alkynyl diols **72** with $Co_2(CO)_8$ (Scheme 10).
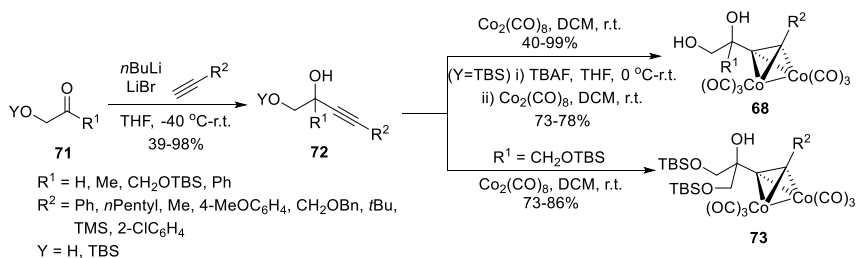
Scheme 10. Synthesis of cobalt complexed glycols 68 and 73.

Using either H_2SO_4 or $BF_3 \cdot EtO_2$ as acid promoters, cobalt complexed alkynyl glycols **68** gave the corresponding oxazolines **69** *via* the Ritter reaction with acetonitrile. The reaction tolerated a wide range of substituents at R^2 position, while substrates bearing a phenyl moiety at R^1 position did not give the expected oxazoline (Scheme 11).

R^1 = H, Me, CH_2OH
R^2 = Ph, *n*Pentyl, Me, 4-MeOC_6H_4, CH_2OBn,
  *t*Bu, TMS, 2-ClC_6H_4
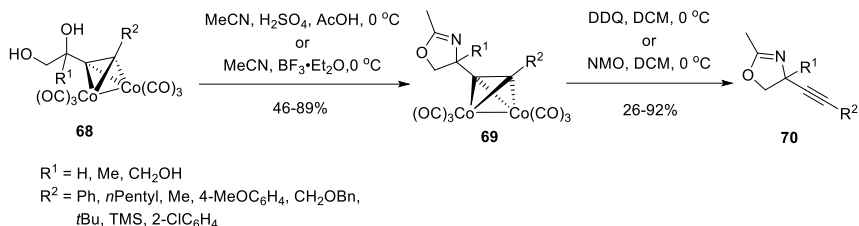
Scheme 11. The Ritter reaction and cobalt decomplexation towards oxazolines 70.

While the main route involved the deprotection of TBS protected alcohols before the formation of the cobalt complex, successful examples of protected alcohols undergoing the Ritter reaction with concomitant removal of the TBS group are reported (Scheme 12).

R^2 = Me, Ph, *n*Pentyl
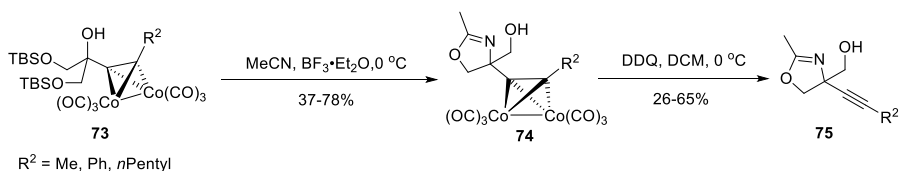
Scheme 12. The Ritter reaction and cobalt decomplexation towards oxazolines 75.

For the Co–decomplexation the use of DDQ proved to be more effective compared to NMO in most cases. Notably it is the first demonstration of DDQ as a reagent for the decomplexation of alkyne cobalt complexes (Schemes 11 and 12).

Selected oxazolines were submitted to acidic hydrolysis in mild conditions to obtain the final amino alcohols **76** with good yields (Scheme 13).

R^1 = Me, CH_2OH
R^2 = Ph, *n*Pentyl, Me, CH_2OBn
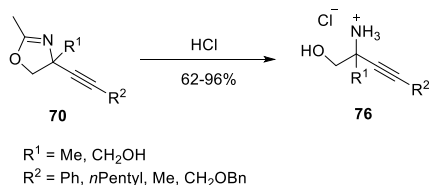
Scheme 13. Hydrolysis of oxazolines 70 to amino alcohols 76.

4.2. Functionalization of 1*N*–PMB protected tetrazoles

Our efforts to synthesize tetrazole containing analogue of triF–Ala **64** were the starting point to develop a new method for the direct C–H functionalization of tetrazole with improved yield compared to our initial effort presented in Scheme 8.

Our target was to raise the reaction yield (20%) of the addition of tetrazole to imine which suffered from the retro [2+3] cyclization reaction of metalated intermediate that leads to the cyanamide **80** (Scheme 14). The instability of metalated tetrazole **78** can take place even at temperature as low as –98°C, which constitute the major problem for the derivatization of tetrazole by C–H deprotonation.
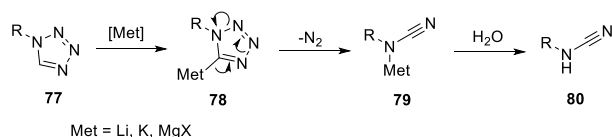
Scheme 14. Retro [2+3] cyclization of metalated tetrazoles.

It was known from the literature that tetrazole–derived Grignard reagents made by halogen–metal exchange showed improved stability.[11] This urged us to turn our research towards preparation of these reagents by C–H deprotonation. For these purposes we prepared 1*N*–PMB–protected tetrazole **63** which served as our test substrate (Table 1). We examined Grignard and turbo Grignard reagents using deuterium quench to determine the efficiency of the deprotonation. Range of bases were investigated, and it was the turbo Grignard (*i*PrMgCl·LiCl) that proved to be the most efficient, giving 99% of deuteration (Table 1, entries 1–2). Notably, under these conditions, the product of the retro [2+3] cycloaddition compound **81b** was not detected even after 1 hour at –60°C. Other Grignard reagents such as *i*PrMgCl and *i*PrMgBr were investigated; however, these turned out to be less efficacious compared to the turbo Grignard reagent (Table 1, entries 3–6).

Table 1.

Evaluation of deprotonating reagents.
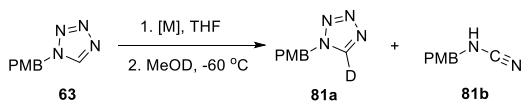
Entry	[M]	Time (min)	81a[a] yield %	81b
1	*i*PrMgCl·LiCl	15	98	n.d.[b]
2	*i*PrMgCl·LiCl	60	99	n.d.
3	*i*PrMgCl	15	53	n.d.
4	*i*PrMgCl	60	76	n.d.
5	*i*PrMgBr	15	57	n.d.
6	*i*PrMgBr	60	69	n.d.

[a]Yields were calculated based on the weight of crude material; NMR did not reveal any other compounds apart from **81a** and **81b**.

[b] n.d. = not detected

The reaction of tetrazole **63** with anisaldehyde **82a** was then examined. Using THF as a solvent, the expected product, alcohol **83a**, was obtained in very good yield (Table 2, entry 1). The reaction yield was not decreased when the reaction was warmed to room temperature after the addition of anisaldehyde (Table 2, entry 2). The use of different solvents (Et$_2$O, Toluene) lowered the reaction outcome, and they were excluded.

Table 2.

Optimization of reaction conditions.
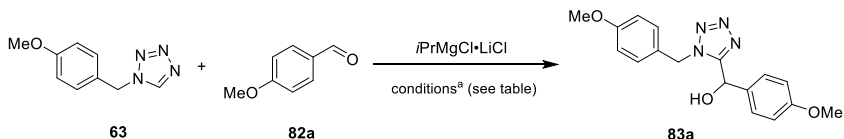
Entry	Solvent	Temperature (°C)	Time (h)	83a, yield %
1	THF	−60 °C	5	78[b]
2	THF	r.t.	24[c]	76
3	Et$_2$O	−60 °C	5	47
4	Toluene	−60 °C	5	22

[a]Tetrazole **63** (1.1 equiv), *i*PrMgCl·LiCl (1.3 equiv), 2 mmol scale. After the addition of *i*PrMgCl·LiCl, the reaction mixture was stirred for 30 min, and then aldehyde **82a** was added.
[b]88% yield of the product **83a** was obtained from the reaction performed on a 5 mmol scale.
[c]Addition of aldehyde **82a** performed at −60°C, then warmed to r.t.

The scope of substrates was then explored. Using various aromatic (**82b–e**) and aliphatic (**82f–g**) aldehydes, as well as structurally diverse ketones (**82h–n**) the corresponding alcohols **83b–n** were obtained in good to excellent yields (Scheme 15).
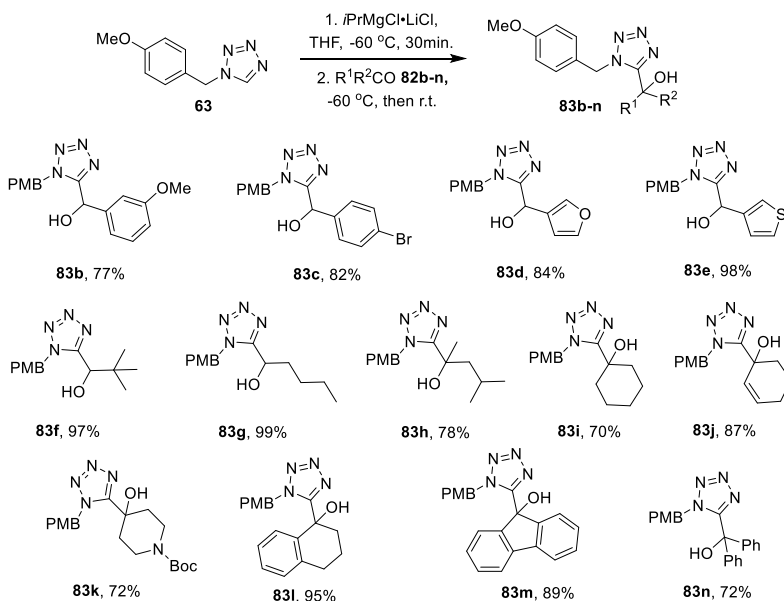
Scheme 15. Addition of tetrazole 63 to carbonyl electrophiles.

Weinreb amides **84a–c** and iodine were also successfully used as electrophiles, providing the corresponding ketones **85a–c** in good yields and the 5–iodo derivative **86** in almost quantitative yield (Scheme 16).
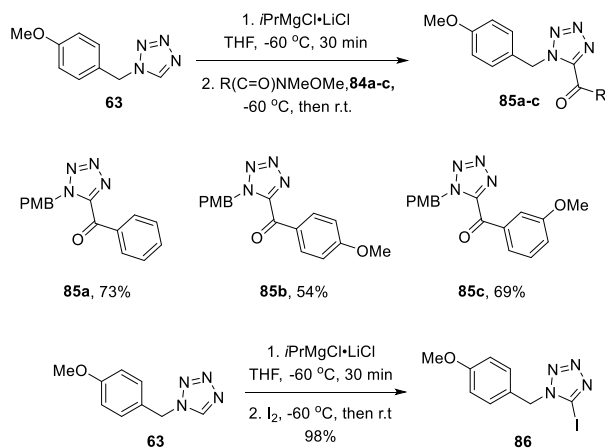
Scheme 16. Addition of tetrazole 63 to Weinreb amides and iodination of compound 63.

For the deprotection of 1N–PMB group three different methods were used, oxidative cleavage using CAN in MeCN/H$_2$O (method **A**), catalytic hydrogenation with PdCl$_2$ and H$_2$ in EtOH (method **B**), and acidic cleavage using TFA in DCM (method **C**). Each of these methods successfully delivered the desired free tetrazoles **87a–i** in good to excellent yield (Scheme 17).
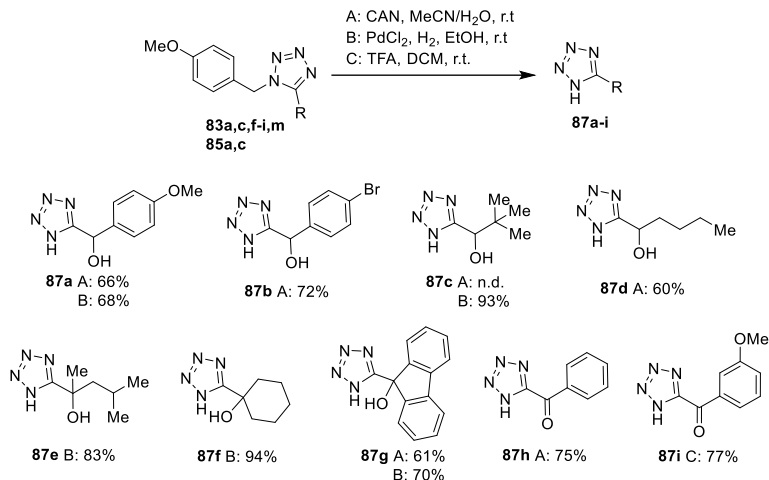
Scheme 17. Removal of the PMB protecting group.

4.3. Functionalization of tetrazoles bearing an electrochemically cleavable 1N–6–methylpyridyl–2–methyl protecting group

In order to broaden the utility of our tetrazole functionalization method, we aimed to incorporate a new electrochemically cleavable protecting group for tetrazole. Two substrates were prepared to be tested for that purpose, pyridylmethyl protected tetrazole **89** from the corresponding 2–aminomethyl pyridine (**88**), and 6–methyl–pyridylmethyl protected tetrazole **93** from 2,6–lutidine (**90**) through bromination followed by tetrazole **92** alkylation (Scheme 18).
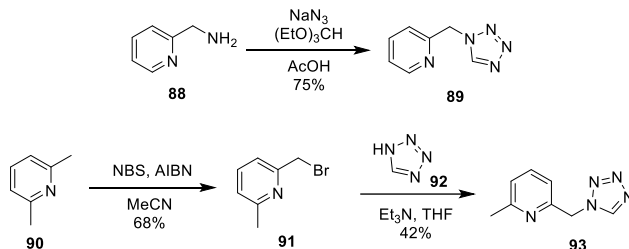
Scheme 18. Synthesis of pyridyl–protected tetrazoles.

The use of the turbo Grignard reagent for the deprotonation of the fifth position of the tetrazole resulted again in minor or complete absence of retro cyclisation–decomposition

product, which in the case of tetrazoles **89** and **93** proved to be **94c** instead of the cyanamide **94a** (Scheme 19).
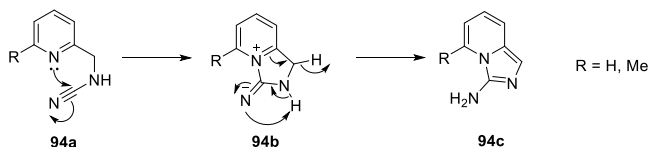
Scheme 19. Proposed mechanism for the formation of side product 94c.

Pyridylmethyl protected tetrazole **89** gave moderate deuterium incorporation at the fifth position (40–60%), along with the competitive deuteration product on CH_2 group and high recovery of tetrazole derivative **89**. Significant improvement in deuteration experiments was observed using 6–methyl–pyridylmethyl protected tetrazole **93** (97–98%). Importantly, no competitive deuteration or decomposition product was detected. Our assumption is that the methyl group at the C–6 of pyridine in compound **93** resulted in blockage of the relatively acidic C–H which can cause an equilibrium mixture of several metalated species.

6–Methyl–pyridylmethyl protected tetrazole **93**, underwent metalation and reaction with aromatic, aliphatic and heteroaromatic aldehydes **95a–e**. The resulting alcohols **96a–e** were obtained in good to excellent yields. The reaction with ketones **95f–j** was also successful providing the corresponding alcohols **96f–j** in moderate to good yields (Scheme 20).
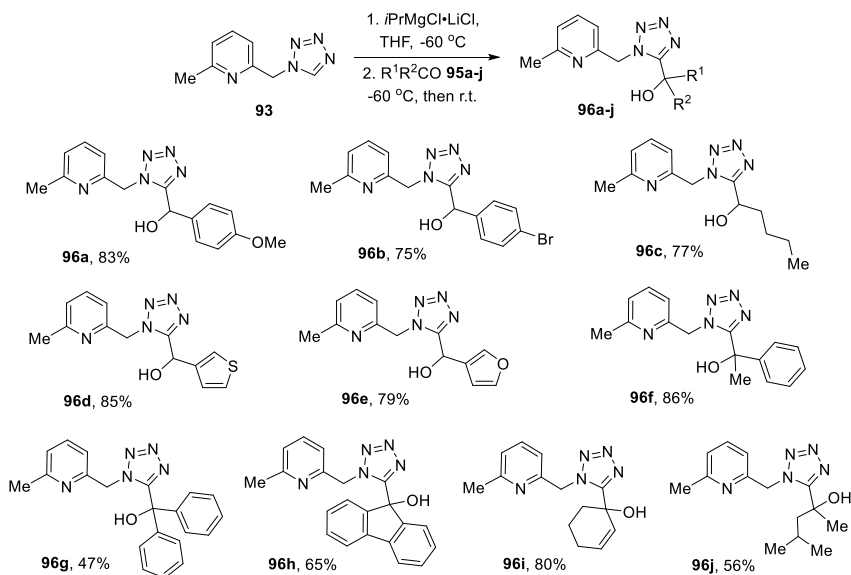
Scheme 20. Addition of tetrazole 93 to carbonyl electrophiles.

6–Methyl–pyridylmethyl group has been demonstrated as an electrochemically cleavable protection for thiols, carboxylic acids, and alcohols[14]. Similar electrochemical conditions were applied for the reductive cleavage of 6–methyl–pyridylmethyl group from tetrazole using compound **96a** as the model substrate. Range of electrodes, electrolytes was investigated at the fixed current and electric charge. The best result was achieved using

leaded bronze electrode as cathode, sacrificial zinc as anode, and TBA·BF$_4$ as electrolyte providing deprotected tetrazole **97a** in 67% isolated yield. These optimized deprotection conditions were further applied to tetrazoles **96a–c** and **96e-h** to obtain the 1*H*–tetrazoles **97b–g** in fair isolated yields as a result of the very polar nature of tetrazoles which made the isolation rather complicated (Scheme 21).
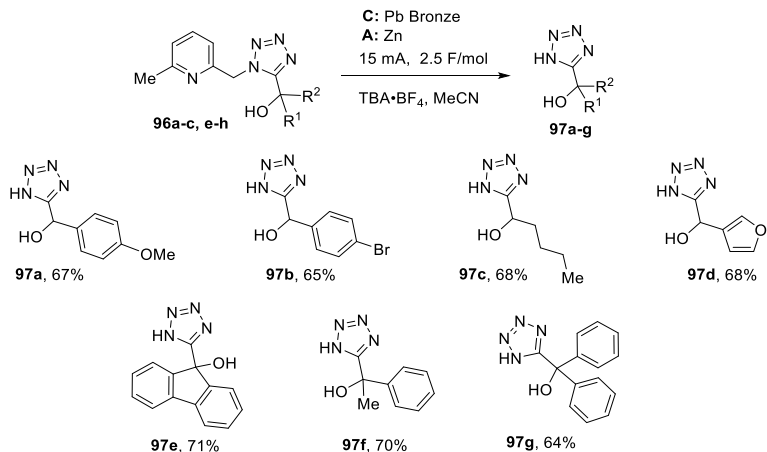
Scheme 21. Electrochemical removal of 6–methyl–pyridylmethyl protecting group.

The proposed mechanism for the electrochemical cleavage of 6–methyl–pyridylmethyl group from tetrazole **96** is depicted in Scheme 22. It starts with the reduction of 6–methyl–pyridylmethyl group at the cathode by sacrificing the Zn anode which leads to an anion radical **96A**. The latter fragments to radical **97b** and tetrazole anion [**97**]$^-$. The radical **97B** undergoes further reactions, like hydrogen abstraction, dimerization, oxidation and/or reduction to give a mixture of byproducts. The formation of pyridylmethyl radical **97B** is supported by the observation of 2,6–lutidine by LC/MS analysis of crude reaction mixture which can form either by hydrogen abstraction or a reduction followed by protonation.
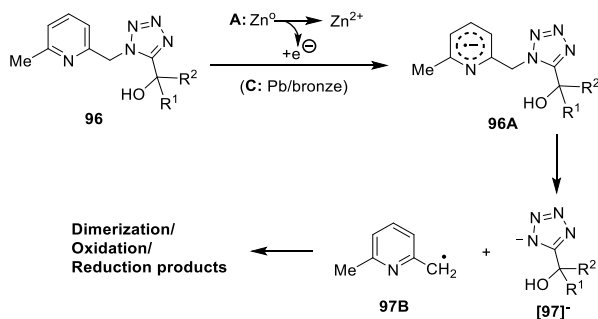
Scheme 22. Proposed mechanism for the electrochemical cleavage of 6–methyl–pyridylmethyl.

4.4. Addition of tetrazoles to imines, synthesis of amino acids' bioisosters

We turned our attention to the application of metalated tetrazole to produce amino acids' analogues bearing tetrazole as a bioisoster of the carboxylic acid. It has been reported in the literature that organometallic reagents can be added to *t*–butanesulfinyl imines in diastereoselective manner (Scheme 23).[12] The diastereoselectivity of this type of reactions is improved when DCM is used as a solvent.
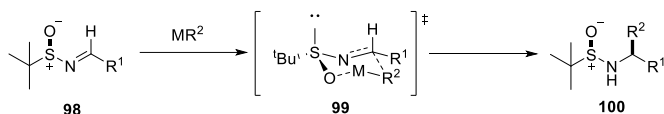
Scheme 23. Diastereoselective addition of organometallics to *t*–butanesulfinyl imines.

For the first test reactions enantiomeric imine **102a** was chosen, which was synthesized based on the literature procedure (Scheme 24).[13]
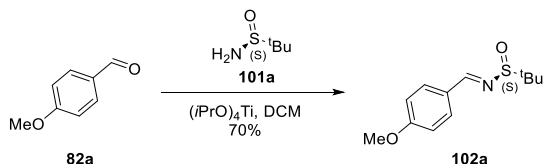
Scheme 24. Synthesis of *t*–butanesulfinyl imine 102a.

Then, we proceeded to the deprotonation of 1*N*–PMB protected tetrazole **63** using the turbo Grignard reagent followed by the addition of the metalated intermediate to *t*–butanesulfinyl imine **102a** using DCM instead of THF as a solvent. The outcome was a single product, **103a**, with high yield and only one diastereomer could be detected by H– and C–NMR (Scheme 25). The stereochemistry of newly formed center in product **103a** was assumed to be S–configuration according to the stereo–induction mechanism shown in the scheme 23, however an unambiguous proof is still needed.
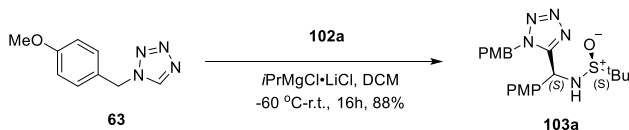
Scheme 25. Addition of tetrazole 63 to *t*–butanesulfinyl imine 102a.

After the first encouraging results we moved to expanding the scope of the reaction. A number of *t*–butanesulfinyl imines **102b–k** were synthesized as substrates for tetrazole **63** addition (Scheme 26).
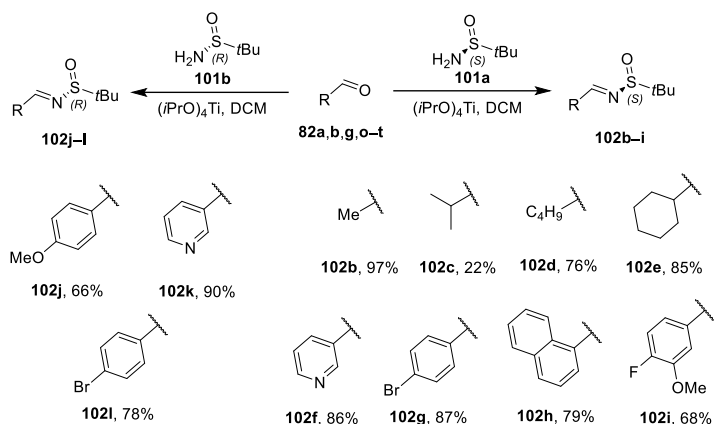
Scheme 26. Synthesis of *t*–butanesulfinyl imines 102b–l.

Applying the already optimized reaction conditions to the *t*–butanesulfinyl imines **102b–l** provided the desired tetrazole addition products **103b–l** in good to excellent yields (Scheme 27).
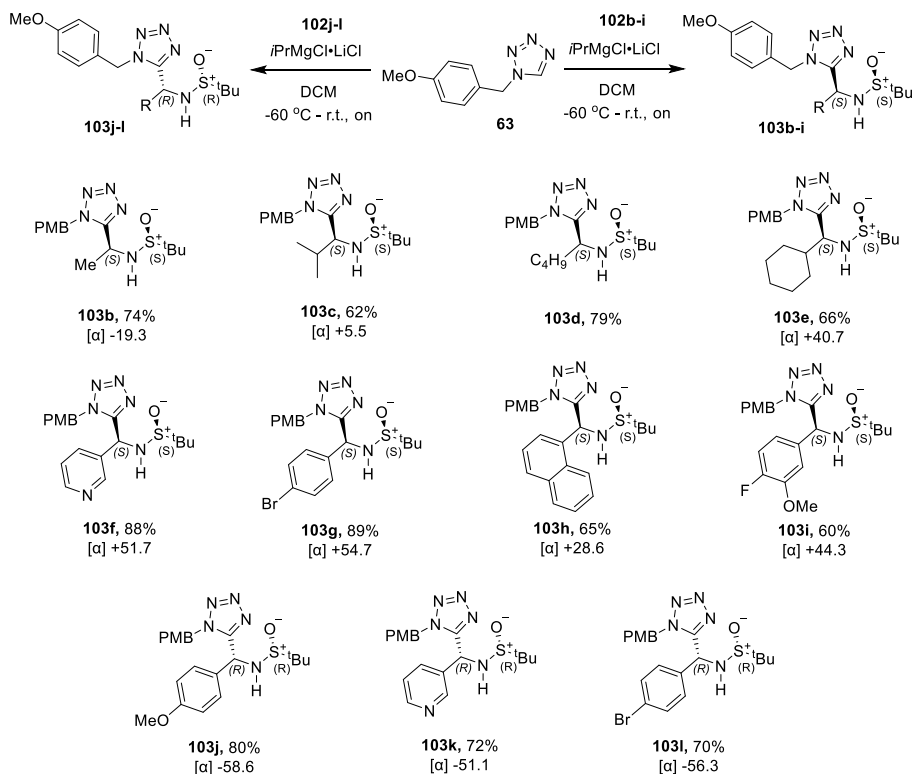
Scheme 27. Addition of tetrazole 63 to *t*–butanesulfinyl imines 102b–l.

The tetrazole **63** could be added to *t*–butyl (*E*)–(4–methoxybenzylidene) carbamate **105**, prepared by condensation of *p*–anisaldehyde (**82a**) and *t*–butyl carbamate (**104**), resulting in a single product, compound **106** (Scheme 28), extending the applicability of the reaction to different imines.
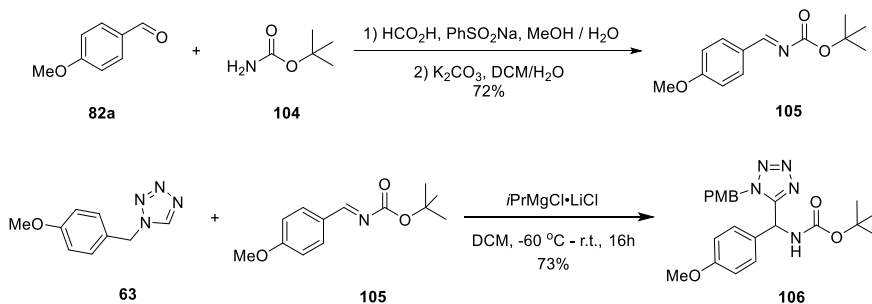
Scheme 28 Synthesis of tetrazole 106.

Concluding, the use of the turbo Grignard for the deprotonation of 1*N*–PMB protected tetrazole **63** and subsequent addition to *t*–butanesulfinyl imines **102a–l** gave access to compounds **103a–l** that upon deprotection would provide amino acid analogues **107**, bearing tetrazole as carboxylic acid bioisoster (Scheme 29).
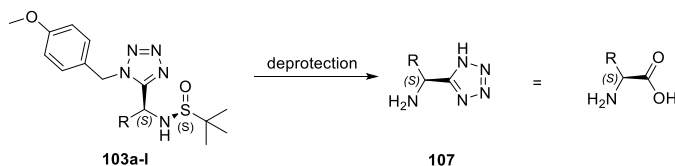
Scheme 29. Proposed route to amino acid analogues 107.

Conclusions

1. New chemotypes were identified as potential covalent inhibitors of PLP dependent enzymes. Hydroxamic acid and sulfonamide analogues of triF–Ala were the most potent compounds, though further study is required.

2. A new method was developed for the synthesis of *C*–quartenary alkynyl glycinols. The synthesis was realized *via* the Ritter reaction of cobalt complexed alkynyl glycols with acetonitrile to give oxazolines.
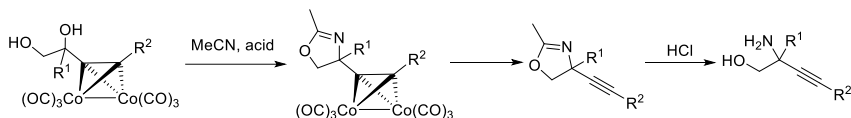
3. Direct C–H functionalization of tetrazoles can be achieved using the turbo Grignard reagent (*i*PrMgCl·LiCl complex). The use of turbo Grignard results in more stable metalated intermediate, avoiding the retro [2+3] cyclization and enabling the efficient addition of tetrazoles to electrophiles.
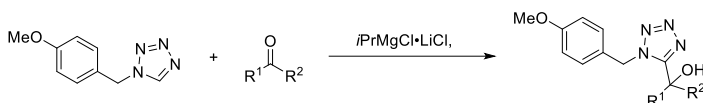
4. 6–Methyl–pyridylmethyl protected tetrazoles can undergo C–H deprotonation using the turbo Grignard reagent and participate in reactions with electrophiles. 6–Methyl–pyridylmethyl group can be removed under reductive electrochemical conditions.
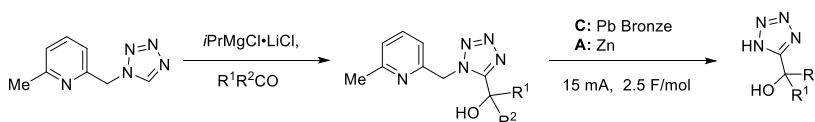
5. The reaction of deprotonated tetrazoles with enantiomeric *t*–butanesulfinyl imines can deliver the corresponding addition products in diastereoselective manner. This method can give access to amino acids' analogues bearing tetrazole moiety as carboxylic acid replacement.
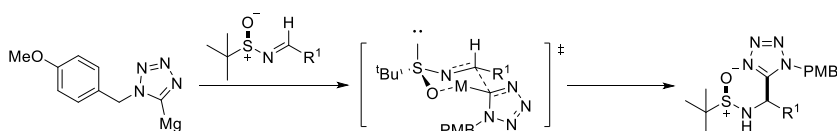
References

1. (a) Ventola, C. L., The antibiotic resistance crisis: part 1: causes and threats. *P T* **2015**, *40* (4), 277–283; (b) Hutchings M. I., Truman A. W., Wilkinson B., Antibiotics: past, present and future, *Current Opinion in Microbiology* **2019**, *51*, 72–80; (c) Church N. A., McKillip J. L., Antibiotic resistance crisis: challenges and imperatives. *Biologia* **2021**, *76*, 1535–1550; (d) Frieri, M.; Kumar, K.; Boutin, A., Antibiotic resistance. *J. Infect. Public Health.* **2017**, *10* (4), 369–378; (e) Browne K., Chakraborty S., Chen R., Willcox M. DP, StClair Black D., Walsh W. R., Kumar N., A New Era of Antibiotics: The Clinical Potential of Antimicrobial Peptides, *Int. J. Mol. Sci.* **2020**, *21*, 7047–7069

2. (a) Moellering, R. C., Discovering new antimicrobial agents. *Int. J. Antimicrob. Ag.* **2011**, *37* (1), 2–9. (b) Düzgüne N.; Sessevmez M.; Yildirim M. Bacteriophage Therapy of Bacterial Infections: The Rediscovered Frontier, *Pharmaceuticals* **2021**, *14*, 34–49.

3. Campanini, B.; Pieroni, M.; Raboni, S.; Bettati, S.; Benoni, R.; Pecchini, C.; Costantino, G.; Mozzarelli, A. Inhibitors of the Sulfur Assimilation Pathway in Bacterial Pathogens as Enhancers of Antibiotic Therapy. *Curr. Med. Chem.* **2015**, *22* (2), 187–213.

4. Mazumder, M.; Gourinath, S. Structure–Based Design of Inhibitors of the Crucial Cysteine Biosynthetic Pathway Enzyme O–Acetyl Serine Sulfhydrylase. *Curr. Top. Med. Chem.* **2016**, *16* (9), 948–959.

5. Franko, N.; Grammatoglou, K.; Campanini, B.; Costantino, G.; Jirgensons, A.; Mozzarelli, A. Inhibition of O–acetylserine sulfhydrylase by fluoroalanine derivatives. *J. Enzym. Inhib. Med. Chem.* **2018**, *33* (1), 1343–1351.

6. (a) Salsi, E.; Bayden, A. S.; Spyrakis, F.; Amadasi, A.; Campanini, B.; Bettati, S.; Dodatko, T.; Cozzini, P.; Kellogg, G. E.; Cook, P. F.; Roderick, S. L.; Mozzarelli, A. Design of O–Acetylserine Sulfhydrylase Inhibitors by Mimicking Nature. *J. Med. Chem.* **2010**, *53* (1), 345–356; (b) Nagpal, I.; Raj, I.; Subbarao, N.; Gourinath, S. Virtual Screening, Identification and In Vitro Testing of Novel Inhibitors of O–Acetyl–L–Serine Sulfhydrylase of Entamoeba histolytica. *Plos One* **2012**, *7* (2); (c) Kumar, V. U. J.; Poyraz, O.; Saxena, S.; Schnell, R.; Yogeeswari, P.; Schneider, G.; Sriram, D. Discovery of novel inhibitors targeting the Mycobacterium tuberculosis O–acetylserine sulfhydrylase (CysK1) using virtual high–throughput screening. *Bioorg. Med. Chem. Lett.* **2013**, *23* (5), 1182–1186; (d) Poyraz, O.; Jeankumar, V. U.; Saxena, S.; Schnell, R.; Haraldsson, M.; Yogeeswari, P.; Sriram, D.; Schneider, G. Structure–Guided Design of Novel Thiazolidine Inhibitors of O–Acetyl Serine Sulfhydrylase from Mycobacterium tuberculosis. *J. Med. Chem.* **2013**, *56* (16), 6457–6466; (e) Spyrakis, F.; Felici, P.; Bayden, A. S.; Salsi, E.; Miggiano, R.; Kellogg, G. E.; Cozzini, P.; Cook, P. F.; Mozzarelli, A.; Campanini, B. Fine tuning of the active site modulates specificity in the interaction of O–acetylserine sulfhydrylase isozymes with serine acetyltransferase. *Bba–Proteins. Proteom.* **2013**, *1834* (1), 169–181; (f) Pieroni, M.; Annunziato, G.; Beato, C.; Wouters, R.; Benoni, R.; Campanini, B.; Pertinhez, T. A.; Bettati, S.; Mozzarelli, A.; Costantino, G. Rational Design, Synthesis, and Preliminary Structure–Activity Relationships of alpha–Substituted–2–Phenylcyclopropane Carboxylic Acids as Inhibitors of Salmonella typhimurium O–Acetylserine Sulfhydrylase. *J Med Chem* **2016**, *59* (6), 2567–2578; (g) Marchetti, M.; De Angelis, F. S.; Annunziato, G.; Costantino, G.; Pieroni, M.; Ronda, L.; Mozzarelli, A.; Campanini, B.; Cannistraro, S.; Bizzarri, A. R.; Bettati, S. A Competitive O–Acetylserine Sulfhydrylase Inhibitor Modulates the Formation of Cysteine Synthase Complex. *Catalysts* **2021**, *11* (6). (h) Schnell R.; Oehlmann W.; Singh M.; Schneider G. Structural Insights into Catalysis and Inhibition of *O*–Acetylserine Sulfhydrylase from

Mycobacterium tuberculosis. Crystal structures of the enzyme alpha–aminoacrylate intermediate and an enzyme inhibitor complex. *J. Biol. Chem.* **2007**, *282*, 23473–23481.

7. (a) Amadasi, A.; Bertoldi, M.; Contestabile, R.; Bettati, S.; Cellini, B.; di Salvo, M. L.; Borri–Voltattorni, C.; Bossa, F.; Mozzarelli, A. Pyridoxal 5 '–phosphate enzymes as targets for therapeutic agents. *Curr. Med. Chem.* **2007**, *14* (12), 1291–1324; (b) Lowther, J.; Yard, B. A.; Johnson, K. A.; Carter, L. G.; Bhat, V. T.; Raman, M. C. C.; Clarke, D. J.; Ramakers, B.; McMahon, S. A.; Naismith, J. H.; Campopiano, D. J. Inhibition of the PLP–dependent enzyme serine palmitoyltransferase by cycloserine: evidence for a novel decarboxylative mechanism of inactivation. *Mol. Biosyst.* **2010**, *6* (9), 1682–1693; (c) Franco, T. M. A.; Favrot, L.; Vergnolle, O.; Blanchard, J. S. Mechanism–Based Inhibition of the Mycobacterium tuberculosis Branched–Chain Aminotransferase by D– and L–Cycloserine. *Acs Chem. Biol.* **2017**, *12* (5), 1235–1244. (d) Mozzarelli, A.; Bettati, S. Exploring the Pyridoxal 5′-Phosphate Dependent Enzymes. *Chem. Rec.* **2006**, 6, 275-287.

8. Maleckis A., Abdelkader E. H., Herath I. D., Otting G., Synthesis of fluorinated leucines, valines and alanines for use in protein NMR, *Org. Biomol. Chem.* **2022**, *20*, 2424–2432.

9. Tysoe, C.; Withers, S. G. Fluorinated Mechanism–Based Inhibitors: Common Themes and Recent Developments. *Curr. Top. Med. Chem.* **2014**, *14* (7), 865–874.

10. (a) Faraci, W. S.; Walsh, C. T. Mechanism of inactivation of alanine racemase by .beta.,.beta.,.beta.–trifluoroalanine. *Biochemistry* **1989**, *28* (2), 431–437; (b) Alexeev, D.; Baxter, R. L.; Campopiano, D. J.; Kerbarh, O.; Sawyer, L.; Tomczyk, N.; Watt, R.; Webster, S. P. Suicide inhibition of α–oxamine synthases: structures of the covalent adducts of 8–amino–7–oxononanoate synthase with trifluoroalanine. *Org. Biomol. Chem.* **2006**, *4* (7), 1209–1212.

11. Wiedemann, S. H.; Bio, M. M.; Brown, L. M.; Hansen, K. B.; Langille, N. F. Some Practical Methods for the Application of 5–Metallo–1–benzyl–1*H*–tetrazoles in Synthesis. *Synlett* **2012**, *23*, 2231–2236.

12. Cogan D. A.; Liu G.; Ellman J. Asymmetric Synthesis of Chiral Amines by Highly Diastereoselective 1,2–Additions of Organometallic Reagents to N–tert–Butanesulfinyl Imines. *Tetrahedron* **1999**, *55*, 8883–8904.

13. Bolshan Y.; Batey R. A. A Room–Temperature Protocol for the Rhodium(I)–Catalyzed Addition of Arylboron Compounds to Sulfinimines. *Organic Letters* **2005**, *7* (8), 1481–1484.

14. (a) Delerue-Matos, C.; Freitas, A. M. B.; Maia, H. L. S.; Medeiros, M. J.; Montenegro, M. I.; Pletcher, D. Electrochemical cleavage of some protecting groups from the sulphydryl function in aprotic solvents. *J. Electroanal. Chem.* **1991**, 315, 1−8; (b) Gosden, A.; Stevenson, D.; Young, G. T. Protection of thiol and phenolic hydroxy-groups as their 4-picolyl ethers, cleaved by electrolytic reduction. *Chem. Commun.* **1972**, 1123−1124; (c) Camble, R.; Garner, R.; Young, G. T. Amino-acids and peptides. Part XXX. Facilitation of peptide synthesis by the use of 4-picolyl esters for carboxy-group protection. *J. Chem. Soc. Section C: Organic* **1969**, 1911−1916; (d) Wieditz, S.; Schafer, H. J.; Schmidt, W.; Undheim, K.; Enzell, C. R.; Inoue, K. The picolyl group, an electroactive protection group for alcohols. *Acta Chem. Scand.* **1983**, 37b, 475.

ANNEXES

Publication No. 1

Grammatoglou K.; Bolsakova J.; Jirgensons A. *C*–Quaternary alkynyl glycinols via the Ritter reaction of cobalt complexed alkynyl glycols. *RSC Adv.*, **2017**, 7, 27530

PAPER

Check for updates

C-Quaternary alkynyl glycinols *via* the Ritter reaction of cobalt complexed alkynyl glycols†

K. Grammatoglou,‡ J. Bolsakova‡ and A. Jirgensons (ID) *

A novel approach to *C*-quaternary alkynyl glycinols based on the Ritter reaction of acetonitrile with cobalt complexed alkynyl glycols is presented. The reaction is promoted by acids such as H_2SO_4 or $BF_3 \cdot Et_2O$ to give oxazolines as the reaction products. These are subjected to cobalt complex cleavage in oxidative conditions and subsequent acidic hydrolysis providing amino alcohols. The substrates for the Ritter reaction can be easily assembled to introduce structural diversity at both variable positions. The Ritter reaction conditions for oxazoline formation is compatible with a range of substituents at the alkyne terminal position providing oxazolines in moderate to good yields. Methyl, hydroxymethyl and silyloxymethyl substituents at the reaction center of glycols are well tolerated, while a phenyl group in this position is detrimental to the reaction.

Introduction

C-Quaternary alkynyl glycinols **1** and synthetically equivalent alkynyl glycine **2** derivatives (Fig. 1) are versatile building blocks for the construction of complex biologically active molecules.[1–7] While there is a good arsenal of methods for the synthesis of *C*-quaternary alkynyl glycines **2**,[1,2] the direct access to *C*-quaternary alkynyl glycinols **1** is limited to few alternatives avoiding the reduction of carboxyl groups in glycines **2**. The literature search revealed only the Seyferth–Gilbert homologation of a serinal derivative;[8] aminolysis of alkynyl epoxides[7,9–12] and the insertion of a nitrene into a propargylic C–H bond[13] as synthetically useful approaches. Thus, a short synthesis of glycinol derivatives **1** from readily available variable building blocks is very desirable.

We have recently reported the synthesis of alkynyl glycinols **1** (R^1 = H) *via* intramolecular propargylic amination of bis-trichloroacetimidates derived from alkynyl glycols.[14] Our attempts to extend this approach for the synthesis of *C*-

quaternary derivatives were not successful. As an alternative, we turned our attention to the Ritter reaction of 1,2-diols which is a known method for the synthesis oxazolines and oxazines involving carbenium ion **A** and nitrilium ion **B** intermediates.[15–24] When alkynyl glycol **3** (R^1 = Me, R^2 = *n*Pent) was directly subjected to the Ritter reaction conditions (MeCN, AcOH, H_2SO_4) the expected oxazoline **6** was obtained in a very low yield (<10%) (Scheme 1). This prompted us to explore the Ritter reaction of cobalt complexed alkynyl glycols **4** (ref. 25 and 26) which has better ability to stabilize the intermediate carbenium ion **A**[27–29] providing oxazolines **5** as precursors of alkynyl glycinol derivatives **1**. Such approach gave the expected results which are summarized in this article.

Results and discussion

Cobalt complexed alkynyl glycols **4a–j** were prepared starting from hydroxy ketone derivatives **7a–j**. Addition of lithium
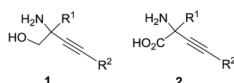
Fig. 1 C-Quaternary alkynyl glycinols **1** and glycines **2**.

Latvian Institute of Organic Synthesis, Aizkraukles 21, Riga LV-1006, Latvia. E-mail: aigars@osi.lv
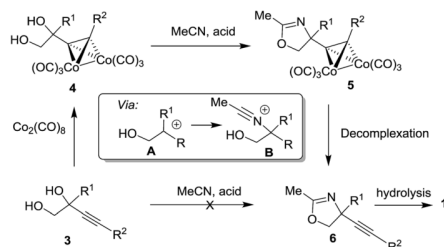
Scheme 1 The Ritter reaction for the synthesis of oxazolines **5** as precursors of amino alcohols **1**.

This journal is © The Royal Society of Chemistry 2017

Paper
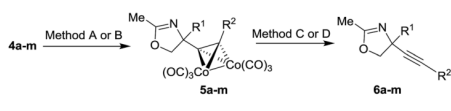
acetylenides provided alkynyl diols **3a–j** which were treated with Co₂(CO₈) (Table 1).

If *O*-TBS protected starting materials **7l–n** were used, the corresponding addition products **8a–c** were deprotected before the complex **4l–m** formation. Several *O*-TBS protected alkynyl glycols **8b–d** were transformed to the corresponding cobalt complexes **9a–c**.

Cobalt complexed alkynyl glycols **4a–d** gave the expected oxazolines **5a–d** in the Ritter reaction with acetonitrile using both H₂SO₄ and BF₃·EtO₂ as acid promoters (Table 2, entries 1–4). Except for the substrate **4c**, better yields were obtained under conditions involving BF₃·Et₂O. Using BF₃·Et₂O as acid, glycols **4e–h** were transformed to oxazolines **5e–h** (Table 2, entries 5–8). These results indicate that the Ritter reaction tolerates wide range of substituents at the terminal alkyne position in substrates **4**. Diols **4i,j** bearing Ph group at the reaction center were unsuitable substrates giving no yield of the expected oxazolines **5i,j** (Table 2, entries 9 and 10). Secondary alcohol **4k** could be successfully subjected to the Ritter reaction providing acetamide **5k** (Table 2, entry 11). Hydroxymethyl substituent at the reaction center of the substrates **4l,m** was tolerated to give the Ritter reaction products **5l,m** in moderate and good yields (Table 2, entries 12 and 13).

Several reaction conditions for the cleavage of cobalt complex **5a** were investigated to obtain the uncomplexed oxazoline **6a** (ethylenediamine, THF, 65 °C, yield of **6a**, 28%; NMO, CH₂Cl₂, r.t. yield of **6a**, 42%; DDQ, CH₂Cl₂, r.t. yield of **6a**, 84%).[30,31]

Table 2 The Ritter reaction of cobalt complexed alkynyl glycols **4** and the cleavage of cobalt complex[a]

Entry	R¹	R²	5, yield% (method)	6, yield% (method)
1	Me	*n*Pent	**5a**, 58 (A); 78 (B)	**6a**, 84 (C), 42 (D)
2	Me	*t*Bu	**5b**, 75 (A); 82 (B)	**6b**, 64 (C)
3	Me	TMS	**5c**, 89 (A); 84 (B)	**6c**, 88 (C)
4	Me	Ph	**5d**, 57 (A); 86 (B)	**6d**, 83 (C)
5	Me	2-ClPh	**5e**, 61 (B)	**6e**, 92 (C)
6	Me	4-MeOPh	**5f**, 63 (B)	**6f**, 85 (C)
7	Me	CH₂OBn	**5g**, 78 (B)	**6g**, 82 (C)
8	Me	Me	**5h**, 74 (B)	**6h**, 46 (C)
9	Ph	*n*Pent	**5i**, dec. (B)	—
10	Ph	Ph	**5j**, dec. (B)	—
11	H	*n*Pent	**5k**, 77 (B)	**6k**, 78 (C)
12	CH₂OH	*n*Pent	**5l**, 46 (B)	**6l**, 61 (C); 65 (D)
13	CH₂OH	Ph	**5m**, 81 (B)	**6m**, 26 (C); 65 (D)

[a] Reagents and conditions: method A: MeCN, H₂SO₄, AcOH, 0 °C; method B: BF₃·Et₂O, MeCN, 0 °C; method C: DDQ, CH₂Cl₂, 0 °C. Method D: NMO CH₂Cl₂, 0 °C.

The best yield of **6a** was obtained in oxidative conditions with DDQ which to our knowledge has not yet been reported as

Table 1 Synthesis of cobalt complexed alkynyl diols **4** and **9**[b]
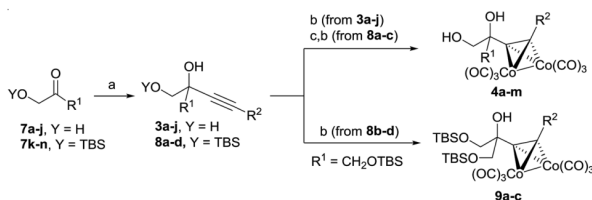
Entry	R¹	R²	Y	3 or 8, yield%	4, yield %[a]	9, yield%
1	Me	*n*Pent	H	**3a**, 98	**4a**, 98	—
2	Me	*t*Bu	H	**3b**, 47	**4b**, 75	—
3	Me	TMS	H	**3c**, 86	**4c**, >99	—
4	Me	Ph	H	**3d**, >99	**4d**, 94	—
5	Me	2-ClPh	H	**3e**, 90	**4e**, 92	—
6	Me	4-MeOPh	H	**3f**, 60	**4f**, 83	—
7	Me	CH₂OBn	H	**3g**, 39	**4g**, 70	—
8	Me	Me	H	**3h**, 47	**4h**, 70	—
9	Ph	*n*Pent	H	**3i**, 96	**4i**, 56	—
10	Ph	Ph	H	**3j**, 97	**4j**, 82	—
11	H	*n*Pent	TBS	**8a**, 82	**4k**, 40	—
12	CH₂OTBS (CH₂OH)[a]	*n*Pent	TBS	**8b**, 94	**4l**, 78	**9a**, 73
13	CH₂OTBS (CH₂OH)[a]	Ph	TBS	**8c**, 95	**4m**, 73	**9b**, 79
14	CH₂OTBS	Me	TBS	**8d**, 75	—	**9c**, 86

[a] R¹ = CH₂OTBS in compounds **8** was transformed to R¹ = CH₂OH in compounds **4**. [b] Reagents and conditions: (a) alkyne, *n*BuLi, LiBr, THF, −40 °C-r.t.; (b) Co₂(CO)₈, CH₂Cl₂, r.t.; (c) TBAF, THF, 0 °C-r.t.

76

the reagent for the decomplexation of alkyne cobalt complexes. Other cobalt complexes **5a–h,l–m** were also cleaved with DDQ to give uncomplexed oxazolines **6a–h,l–m** typically in good yields. The only exception was substrate **5m** which gave product **6m** in poor yield. For the cleavage of the complex **5m**, NMO was better suited as oxidant to provide product **6m** more efficiently.

O-TBS protected alkynyl glycols **9a–c** could also be used as substrates for the Ritter reaction (Table 3). The reaction proceeded with concomitant deprotection of *O*-TBS group to give oxazolines **5l–n**. The cleavage of cobalt complex **5n** was performed with DDQ to give uncomplexed oxazoline **6n** (Table 3, entry 3).

Selected oxazolines **6d,g,h,l,m** were transformed to amino alcohols **1** by using acidic hydrolysis in mild conditions (Table 4). The hydrolysis proceed with good yields of product **1d,g,h,l,m** formation which were purified by the trituration with EtOAc.

Experimental

General information

Commercially available reagents were used without further purification. All air or moisture-sensitive reactions were carried out under an argon atmosphere using oven-dried glassware. Flash chromatography was carried out using Merck Kieselgel 60 (230–400 mesh). Thin layer chromatography was performed on silica gel and was visualized by staining with $KMnO_4$. NMR spectra were recorded on a Varian Mercury spectrometer (400 MHz) and a Bruker Fourier spectrometer (300 MHz) with chemical shift values (δ) in ppm relative to TMS using the residual chloroform signal as an internal standard. Elemental analyses were performed using a Carlo-Erba EA1108 Elemental Analyser. HRMS were obtained using a Q-TOF micro high resolution mass spectrometer with ESI (ESI+/ESI−).

Preparation of diols/triols 3 and 8

Alcohols **3** and **8** were prepared according to the procedure described in the literature starting from the corresponding ketones **7**.[14]

Alcohols **3a**,[32] **3b**,[33] **3c**,[34] **3d**,[34] **3g**,[34] **3k**,[14] **3i,j**[35] **8a**[14] are known in literature.
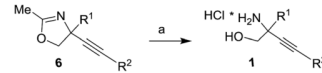
Table 3 The Ritter reaction of cobalt complexed alkynyl diols **9a–c** and the cleavage of cobalt complex in intermediate **5n**[a]

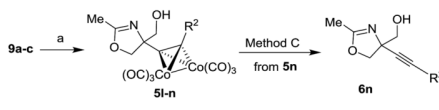| Entry	**9**, R^2	**5**, yield%	**6**, yield%
1	**9a**, *n*Pent,	**5l**, 37	See Table 2
2	**9b**, Ph	**5m**, 78	See Table 2
3	**9c**, Me	**5n**, 63	**6n**, 73 (C)

[a] Reagents and conditions: (a) BF$_3$·Et$_2$O, MeCN, 0 °C; method C: DDQ, CH$_2$Cl$_2$, 0 °C.

Table 4 Preparation of amino alcohols **1** *via* hydrolysis of oxazolines[a]

Entry	R^1	R^2	**1**, yield%
1	Me	Ph	**1d**, 96
2	Me	CH$_2$OBn	**1g**, 64
3	Me	Me	**1h**, 62
4	CH$_2$OH	*n*Pent	**1l**, 82
5	CH$_2$OH	Ph	**1m**, 77

[a] Reagents and conditions: (a) aq. 20% HCl, MeOH, r.t.

4-(2-Chlorophenyl)-2-methylbut-3-yne-1,2-diol (3e). White powder. M.p. 63–65 °C. ^{1}H NMR (400 MHz, CD$_3$OD) δ 7.50 (dd, J = 7.3, 2.1 Hz, 1H, –C$_6$H$_4$Cl), 7.43 (dd, J = 7.7, 1.6 Hz, 1H, –C$_6$H$_4$Cl), 7.30 (td, J = 7.7, 2.0 Hz, 1H, –C$_6$H$_4$Cl), 7.26 (td, J = 7.5, 1.5 Hz, 1H, –C$_6$H$_4$Cl), 3.63 (d, J = 11.0 Hz, 1H, –CH$_2$O–), 3.60 (d, J = 11.0 Hz, 1H, –CH$_2$O–), 1.54 (s, 3H, –CH$_3$). ^{13}C NMR (100 MHz, CD$_3$OD) δ 138.2, 135.9, 132.1, 131.7, 129.2, 125.4, 99.7, 82.5, 72.4, 71.1, 27.5. Anal. calcd for C$_{12}$H$_{14}$O$_3$: C, 62.72%; H, 5.26%; found: C, 62.71%; H, 5.23%.

4-(4-Methoxyphenyl)-2-methylbut-3-yne-1,2-diol (3f). Off white powder. M.p. 74–77 °C. ^{1}H NMR (400 MHz, CDCl$_3$) δ 7.36 (d, J = 8.9 Hz, 2H, –C$_6$H$_5$), 6.83 (d, J = 8.9 Hz, 2H, –C$_6$H$_5$), 3.81 (s, 3H, –OCH$_3$), 3.74 (dd, J = 11.0, 5.0 Hz, 1H, –CH$_2$O–), 3.56 (dd, J = 11.0, 8.8 Hz, 1H, –CH$_2$O–), 2.66 (s, 1H, –OH), 2.13 (dd, J = 8.8, 5.0 Hz, 1H, –OH), 1.55 (s, 3H, –CH$_3$). ^{13}C NMR (100 MHz, CDCl$_3$) δ 159.9, 133.4, 114.3, 114.1, 89.0, 84.7, 71.0, 69.2, 55.4, 20.2. Anal. calcd for C$_{12}$H$_{14}$O$_3$: C, 69.89%; H, 6.84%; found: C, 69.56%; H, 6.86%.

2-Methyl-pent-3-yne-1,2-diol (3h). Colourless oil. ^{1}H NMR (300 MHz, CDCl$_3$) δ 2.76 (d, J = 10.9 Hz, 1H, –CH$_2$OH), 2.61 (d, J = 10.9 Hz, 1H, –CH$_2$OH), 1.72 (s, 1H, –OH), 1.28 (s, 1H, –OH), 1.00 (s, 3H, –CH$_3$), 0.58 (s, 3H, –CH$_3$). ^{13}C NMR (100 MHz, CDCl$_3$) δ 109.9, 80.8, 70.9, 68.6, 25.5, 3.5. In HRMS conditions no signal observed. GC-MS (EI): *m/z*: 83 [M − CH$_2$OH]$^+$.

6-(Hept-1-yn-1-yl)-2,2,3,3,9,9,10,10-octamethyl-4,8-dioxa-3,9-disilaundecan-6-ol (8b). Colourless oil. ^{1}H NMR (300 MHz, CDCl$_3$) δ 3.61 (d, J = 9.5 Hz, 2H, –CH$_2$O–), 3.51 (d, J = 9.5 Hz, 2H, –CH$_2$O–), 2.80 (s, 1H, –OH), 2.11 (t, J = 7.1 Hz, 2H, –CH$_2$ (CH$_2$)$_3$CH$_3$), 1.52–1.37 (m, 2H, –CH$_2$CH$_2$(CH$_2$)$_2$CH$_3$), 1.29–1.14 (m, 4H, –CH$_2$CH$_2$(CH$_2$)$_2$CH$_3$), 0.82 (s, 18H, –SiC(CH$_3$)$_3$), 0.81–0.77 (m, 3H, –CH$_2$(CH$_2$)$_3$CH$_3$), 0.00 (d, J = 1.1 Hz, 12H, –Si(CH$_3$)$_2$). ^{13}C NMR (100 MHz, CDCl$_3$) δ 85.6, 79.8, 71.1, 65.9, 31.0, 28.2, 25.8, 22.2, 18.7, 18.3, 13.9, −5.4. In HRMS conditions no signal observed. GC-MS (EI): *m/z*: 357 [M − *t*Bu]$^+$.

Deprotection of silyl groups gave 2-(hept-1-yn-1-yl)propane-1,2,3-triol (3k). Colourless oil. ^{1}H NMR (400 MHz, CDCl$_3$) δ 3.70 (s, 4H, –CH$_2$OH), 2.18 (ddt, J = 9.2, 7.1, 3.7 Hz, 2H, –CH$_2$(CH$_2$)$_3$CH$_3$), 1.59–1.44 (m, 2H, –CH$_2$CH$_2$(CH$_2$)$_2$CH$_3$), 1.30 (qd, J = 3.6, 3.1, 1.5 Hz, 4H, –CH$_2$CH$_2$(CH$_2$)$_2$CH$_3$), 0.96–0.81 (m, 3H, –CH$_2$(CH$_2$)$_3$CH$_3$). ^{13}C NMR (100 MHz, CDCl$_3$) δ 87.9, 78.3,

71.5, 67.4, 31.0, 28.2, 22.1, 18.6, 13.9. In HRMS conditions no signal observed. GC-MS (EI): m/z: 155 [M − CH$_2$OH]$^+$.

2,2,3,3,9,9,10,10-Octamethyl-6-(phenylethynyl)-4,8-dioxa-3,9-disilaundecan-6-ol (8c). Colourless oil. ^{1}H NMR (400 MHz, CDCl$_3$) δ 7.44–7.39 (m, 2H, −C$_6$H$_5$), 7.30–7.26 (m, 3H, m, −C$_6$H$_5$), 3.80 (d, J = 9.5 Hz, 2H, −CH$_2$O−), 3.72 (d, J = 9.5 Hz, 2H, −CH$_2$O−), 3.04 (s, 1H, −OH), 0.90 (s, 18H, −SiC(CH$_3$)$_3$), 0.09 (d, J = 0.9 Hz, 12H, −Si(CH$_3$)$_2$). ^{13}C NMR (100 MHz, CDCl$_3$) δ 131.7, 128.1, 122.7, 89.3, 84.8, 71.6, 65.9, 25.8, 18.3, −5.4. HR-MS (ESI-TOF) m/z: calcd for C$_{23}$H$_{40}$O$_3$Si$_2$Na 443.2399; found [M + Na]$^+$ 443.2414.

Deprotection of silyl groups gave 2-(phenylethynyl)propane-1,2,3-triol (3l). Colourless oil. ^{1}H NMR (300 MHz, CDCl$_3$) δ 7.52–7.41 (m, 2H, o-C$_6$H$_5$−), 7.39–7.31 (m, 3H, m,p-C$_6$H$_5$−), 3.92–3.82 (m, 4H, −CH$_2$OH), 3.08 (s, 1H, −OH), 2.18 (dd, J = 8.6, 4.8 Hz, 2H, −CH$_2$OH). ^{13}C NMR (100 MHz, CDCl$_3$) δ 131.3, 127.9, 122.6, 88.9, 84.5, 71.5, 65.3. In HRMS conditions no signal observed. GC-MS (EI): m/z: 161 [M − −CH$_2$OH]$^+$.

2,2,3,3,9,9,10,10-Octamethyl-6-(prop-1-yn-1-yl)-4,8-dioxa-3,9-disilaundecan-6-ol (8d). Colourless oil. ^{1}H NMR (400 MHz, CDCl$_3$) δ 3.67 (d, J = 9.5 Hz, 2H, −CH$_2$O−), 3.58 (d, J = 9.5 Hz, 2H, −CH$_2$O−), 2.85 (s, 1H, −OH), 1.81 (s, 3H, −CH$_3$), 0.89 (s, 18H, −SiC(CH$_3$)$_3$), 0.06 (d, J = 1.7 Hz, 12H, Si(CH$_3$)$_2$). ^{13}C NMR (100 MHz, CDCl$_3$) δ 81.1, 79.2, 71.1, 65.8, 25.8, 18.3, 3.5, −5.3, −5.4. HR-MS (ESI-TOF) m/z: calcd for C$_{18}$H$_{48}$O$_3$Si$_2$Na 381.2247; found [M + Na]$^+$ 381.2257.

General procedure for the preparation of cobalt-complexed propargyl alcohols 4 and 9

To a solution of alkyne (1 mmol) in CH$_2$Cl$_2$ (5 mL), Co$_2$(CO)$_8$ (1.1 mmol) was added under argon atmosphere. The solution was stirred at room temperature until no evolution of CO$_2$ was observed (TLC showed the formation of the complex to be completed). The solvent was removed *in vacuo* and the residue was purified by column chromatography on silica gel eluting with a mixture of ethyl acetate and petroleum ether (1 : 30–1 : 4) to yield the Co$_2$(CO)$_6$-alkyne complex.

^{13}C-NMR for compounds **4** and **9** was not possible to record due to Co induced line broadening. Typically compounds **4** and **9** were not stable under conditions used for HRMS.

Hexacarbonyl[μ-η^4-(2-methylnon-3-yne-1,2-diol)]dicobalt (4a). Red powder. ^{1}H NMR (300 MHz, CDCl$_3$) δ 3.70 (d, J = 4.7 Hz, 2H, −CH$_2$O−), 2.90–2.73 (m, 2H, −CH$_2$CH$_2$(CH$_2$)$_2$CH$_3$), 2.26 (s, 1H, −OH), 2.06–1.95 (m, 1H, −OH), 1.73–1.31 (m, 9H, −CH$_3$, −CH$_2$CH$_2$(CH$_2$)$_2$CH$_3$, −(CH$_2$)$_2$(CH$_2$)$_2$CH$_3$), 0.93 (t, J = 6.2 Hz, 3H, −(CH$_2$)$_4$CH$_3$). Not stable under HR-MS conditions.

Hexacarbonyl[μ-η^4-(2,5,5-trimethylhex-3-yne-1,2-diol)]dicobalt (4b). Red powder. ^{1}H NMR (300 MHz, CDCl$_3$) δ 3.72 (d, J = 5.3 Hz, 2H, −CH$_2$O−), 2.25 (s, 1H, −OH), 2.15–2.02 (m, 1H, −OH), 1.62 (s, 3H, −CH$_3$), 1.35 (s, 9H, −C(CH$_3$)$_3$). Not stable under HR-MS conditions.

Hexacarbonyl[μ-η^4-(2-methyl-4-(trimethylsilyl)but-3-yne-1,2-diol)]dicobalt (4c). Red powder. ^{1}H NMR (300 MHz, CDCl$_3$) δ 3.66 (d, J = 5.9 Hz, 2H, −CH$_2$O−), 2.04 (s, 1H, −OH), 2.04 (t, J = 5.9 Hz, 1H, −OH), 1.57 (s, 3H, −CH$_3$), 0.33 (s, 9H, −Si(CH$_3$)$_3$). Not stable under HR-MS conditions.

Hexacarbonyl[μ-η^4-(2-methyl-4-phenylbut-3-yne-1,2-diol)] dicobalt (4d). Red powder. ^{1}H NMR (400 MHz, CDCl$_3$) δ 7.69–7.56 (m, J = 6.8 Hz, 2H, o-C$_6$H$_5$−), 7.40–7.29 (m, 3H, p,m-C$_6$H$_5$−), 3.89–3.74 (br, 2H, −CH$_2$O−), 2.58 (s, 1H, −OH), 2.08–1.99 (br, 1H, −OH), 1.67 (s, 3H, −CH$_3$). Not stable under HR-MS conditions.

Hexacarbonyl[μ-η^4-(4-(2-chlorophenyl)-2-methylbut-3-yne-1,2-diol)]dicobalt (4e). Red powder. ^{1}H NMR (300 MHz, CDCl$_3$) δ 8.01–7.94 (m, 1H, C$_6$H$_4$Cl−), 7.45–7.37 (m, 1H), 7.32–7.26 (m, 2H, C$_6$H$_4$Cl−, overlapping with CHCl$_3$ signal), 3.82 (d, J = 5.8 Hz, 2H, −CH$_2$O−), 2.87 (s, 1H, −OH), 2.05 (t, J = 5.8 Hz, 1H, −OH), 1.67 (s, 3H, −CH$_3$). Not stable under HR-MS conditions.

Hexacarbonyl[μ-η^4-(4-(4-methoxyphenyl)-2-methylbut-3-yne-1,2-diol)]dicobalt (4f). Red powder. ^{1}H NMR (300 MHz, CDCl$_3$) δ 7.61 (s, 2H, m-MeO−C$_6$H$_4$−), 6.90 (s, 2H, o-MeO−C$_6$H$_4$−), 4.14 (s, 1H, −CH$_2$OH), 3.85 (s, 4H, CH$_3$O−C$_6$H$_4$− (3H), and overlapping −CH$_2$OH (1H)), 2.59 (s, 1H, −OH), 2.18 (s, 1H, −OH), 1.69 (s, 3H, −CH$_3$). Not stable under HR-MS conditions.

Hexacarbonyl[μ-η^4-(5-(benzyloxy)-2-methylpent-3-yne-1,2-diol)]dicobalt (4g). Red powder. ^{1}H NMR (300 MHz, CDCl$_3$) δ 7.37 (m, 5H, C$_6$H$_5$−), 4.76 (d, J = 8.4 Hz, 4H, −CH$_2$O−CH$_2$−), 3.65 (d, J = 5.2 Hz, 1H, −CH$_2$OH), 3.53 (s, 1H, −CH$_2$OH), 3.10 (s, 1H, −OH), 2.19 (s, 1H, −OH), 1.53 (s, 3H, −CH$_3$). Not stable under HR-MS (ESI-TOF) m/z: calcd for C$_{19}$H$_{16}$O$_9$Co$_2$504.9382; found 504.9380.

Hexacarbonyl[μ-η^4-(2-methyl-pent-3-yne-1,2-diol)]dicobalt (4h). Red powder. ^{1}H NMR (300 MHz, CDCl$_3$) δ 3.72 (s, 2H, −CH$_2$OH), 2.72 (s, 3H, −CH$_3$), 2.31 (s, 1H, −OH), 2.06 (s, 3H, −CH$_3$). Not stable under HR-MS conditions.

Hexacarbonyl[μ-η^4-(2,4-diphenylbut-3-yne-1,2-diol)]dicobalt (4i). ^{1}H NMR (300 MHz, CDCl$_3$) δ 7.59 (d, J = 7.5 Hz, 2H, o-C$_6$H$_4$−), 7.41 (t, J = 7.5 Hz, 2H, m-C$_6$H$_4$−), 7.33 (d, J = 7.5 Hz, 1H, p-C$_6$H$_4$−), 4.36 (dd, J = 10.0, 4.5 Hz, 1H, −CH$_2$OH), 3.95 (t, J = 10.0 Hz, 1H, −CH$_2$OH), 3.10 (s, 1H, −OH), 2.75 (m, 2H, −CH$_2$(CH$_2$)$_3$CH$_3$), 2.19 (s, 1H, −OH), 1.69–1.58 (m, 2H, −CH$_2$CH$_2$(CH$_2$)$_2$CH$_3$), 1.52–1.30 (m, 4H, −CH$_2$CH$_2$(CH$_2$)$_2$CH$_3$), 0.95 (t, J = 6.9 Hz, 3H, −CH$_2$(CH$_2$)$_3$CH$_3$). Not stable under HR-MS conditions.

Hexacarbonyl[μ-η^4-(6-(hept-1-yn-1-yl)-2,2,3,3,9,9,10,10-octamethyl-4,8-dioxa-3,9-disilaundecan-6-ol)]dicobalt (4j). ^{1}H NMR (300 MHz, CDCl$_3$) δ 7.56 (d, J = 7.2 Hz, 4H, o-C$_6$H$_4$−), 7.42–7.29 (m, 6H, m,p-C$_6$H$_4$−), 4.60–4.43 (m, 1H, −CH$_2$OH), 4.25–4.03 (m, 1H, −CH$_2$OH), 3.39 (s, 1H, −OH), 1.84 (s, 1H, −OH). Not stable under HR-MS conditions.

Hexacarbonyl[μ-η^4-(non-3-yne-1,2-diol)]dicobalt (4k). Red powder. ^{1}H NMR (300 MHz, CDCl$_3$) δ 4.39 (s, 1H, −CH(OH)−), 3.62 (s, 2H, −CH$_2$OH), 2.21–2.09 (m, 2H, −CH$_2$(CH$_2$)$_3$CH$_3$), 1.44 (t, J = 7.2 Hz, 2H, −CH$_2$CH$_2$(CH$_2$)$_2$CH$_3$), 1.35–1.13 (m, 4H, −CH$_2$CH$_2$(CH$_2$)$_2$CH$_3$), 0.89–0.77 (m, 3H, −CH$_2$(CH$_2$)$_3$CH$_3$). Not stable under HR-MS conditions.

Hexacarbonyl[μ-η^4-(hept-1-yn-1-yl)propane-1,2,3-triol)]dicobalt (4l). ^{1}H NMR (300 MHz, CDCl$_3$) δ 3.62 (s, 4H, −CH$_2$OH), 2.11 (t, J = 7.2 Hz, 2H, −CH$_2$(CH$_2$)$_3$CH$_3$), 1.99 (s, 1H, −OH), 1.51–1.35 (m, 2H, −CH$_2$CH$_2$(CH$_2$)$_2$CH$_3$), 1.29–1.19 (m, 4H, −CH$_2$CH$_2$(CH$_2$)$_2$CH$_3$), 0.88–0.72 (m, 3H, −CH$_2$(CH$_2$)$_3$CH$_3$). Not stable under HR-MS conditions.

Hexacarbonyl[μ-η^4-(2-(phenylethynyl)propane-1,2,3-triol)]dicobalt (4m). ^{1}H NMR (300 MHz, CDCl$_3$) δ 7.46 (dd, J = 7.4, 2.2 Hz, 2H, o-C$_6$H$_4$−), 7.37–7.32 (m, 3H, m,p-C$_6$H$_4$−), 3.87 (dd, J =

6.3, 3.5 Hz, 4H, –CH$_2$OH), 3.08 (s, 1H, –OH), 1.57 (s, 1H, –OH). Not stable under HR-MS conditions.

Hexacarbonyl[μ-η^4-(6-(hept-1-yn-1-yl)-2,2,3,3,9,9,10,10-octamethyl-4,8-dioxa-3,9-disilaundecan-6-ol)]dicobalt (9a). Red powder. ^{1}H NMR (300 MHz, CDCl$_3$) δ 3.63 (dd, J = 24.5, 9.5 Hz, 4H, –CH$_2$OTBS), 2.80 (s, 1H, –OH), 2.75–2.65 (m, 2H, –CH$_2$–), 1.66–1.37 (m, 6H, (–CH$_2$–)$_3$), 1.31 (d, J = 3.0 Hz, 3H, –CH$_3$), 0.83 (s, 18H, –SiC(CH$_3$)$_3$), 0.00 (d, J = 3.1 Hz, 12H, –Si(CH$_3$)$_2$). Not stable under HR-MS conditions.

Hexacarbonyl[μ-η^4-(2,2,3,3,9,9,10,10-octamethyl-6-(phenyl ethynyl)-4,8-dioxa-3,9-disilaundecan-6-ol)]dicobalt (9b). Red powder. ^{1}H NMR (300 MHz, CDCl$_3$) δ 7.62 (dd, J = 7.7, 1.7 Hz, 2H, o-C$_6$H$_5$–), 7.30–7.23 (m, 3H, p,m-C$_6$H$_5$–), 3.89 (d, J = 9.6 Hz, 2H, –CH$_2$OTBS), 3.76 (d, J = 9.6 Hz, 2H, –CH$_2$OTBS), 3.20 (s, 1H, –OH), 0.85 (s, 18H, –SiC(CH$_3$)$_3$), 0.02 (d, J = 9.8 Hz, 12H, –Si(CH$_3$)$_2$). Not stable under HR-MS conditions.

Hexacarbonyl[μ-η^4-(2,2,3,3,9,9,10,10-octamethyl-6-(prop-1-yn-1-yl)-4,8-dioxa-3,9-disilaundecan-6-ol)]dicobalt (9c). Red powder. ^{1}H NMR (300 MHz, CDCl$_3$) δ 3.70 (dd, J = 21.3, 9.5 Hz, 4H, –CH$_2$OTBS), 2.85 (s, 1H, –OH), 2.65 (s, 3H, –CH$_3$), 0.91 (s, 18H, –SiC(CH$_3$)$_3$), 0.08 (d, J = 2.8 Hz, 12H, –Si(CH$_3$)$_2$). Not stable under HR-MS conditions.

Method A for the Ritter reaction

A solution of the cobalt complex of diol **4** (2.2 mmol) in CH$_3$CN (54 eq., 118.8 mmol, 6.2 mL) was cooled to 0–3 °C (ice/water bath) and AcOH (8 eq., 17.6 mmol, 1.0 mL) was added followed by dropwise addition of H$_2$SO$_4$ (9 eq., 19.9 mmol, 1.0 mL). The reaction mixture was allowed to stir at this temperature until complete conversion of the starting material was observed (TLC control, usually 8 min). The reaction mixture was diluted with Et$_2$O (30 mL) and poured into water (15 mL). The organic phase was separated and the aqueous phase was extracted with Et$_2$O (30 mL). The combined organic phase was washed with aq. NaHCO$_3$, dried over Na$_2$SO$_4$, filtered and evaporated. The crude residue was purified by chromatography on silica gel eluting with a mixture of ethyl acetate and petroleum ether (1 : 20–1 : 10) to afford oxazoline cobalt complex.

Method B for the Ritter reaction

A solution of the cobalt complex **4** or **9** (0.3 mmol) in MeCN (3 mL) was cooled to 0–3 °C (ice/water bath) and BF$_3$·Et$_2$O (0.38 mL, 10 eq., 2.96 mmol) was added dropwise. The reaction mixture was allowed to stir at this temperature until complete conversion of the starting material (TLC control, usually 5–10 min). The reaction mixture was diluted with DCM (15 mL) and aq. NaHCO$_3$ (7 mL) was added. The organic phase was separated and washed with brine (1 × 7 mL), dried over Na$_2$SO$_4$, filtered and evaporated. The crude residue was purified by chromatography on silica gel eluting with a mixture of ethyl acetate and petroleum ether (1 : 20–1 : 3) to afford oxazoline cobalt complex.

^{13}C-NMR for compounds **5** was not possible to record due to Co induced line broadening. Typically compounds **5** were not stable under conditions used for HRMS.

Hexacarbonyl[μ-η^4-(4-(hept-1-yn-1-yl)-2,4-dimethyloxazoline)] dicobalt (5a). Viscous colorless oil. ^{1}H NMR (400 MHz, CDCl$_3$) δ 4.28 (d, J = 8.4 Hz, 1H, –CH$_2$O–), 4.12 (d, J = 8.4 Hz, 2H, CDCl$_3$), 2.89–2.76 (m, 2H, –CH$_2$(CH$_2$)$_3$CH$_3$), 1.97 (s, 3H, –CH$_3$), 1.74–1.58 (m, 5H, –CH$_2$CH$_2$(CH$_2$)$_2$CH$_3$), 1.43 (qd, J = 15.2, 7.4 Hz, 4H, –(CH$_2$)$_2$(CH$_2$)$_2$CH$_3$), 0.93 (t, J = 7.1 Hz, 3H, –(CH$_2$)$_4$CH$_3$). Not stable under HR-MS conditions.

Hexacarbonyl[μ-η^4-(4-(3,3-dimethylbut-1-yn-1-yl)-2,4-dimethyl oxazoline)]dicobalt (5b). Viscous colorless oil with tendency to crystalize. ^{1}H NMR (300 MHz, CDCl$_3$) δ 4.28 (d, J = 8.4 Hz, 1H, –CH$_2$O–), 4.14 (d, J = 8.4 Hz, 1H, –CH$_2$O–), 1.97 (s, 3H, –CH$_3$), 1.68 (s, 3H, –CH$_3$), 1.35 (s, 9H, –C(CH$_3$)$_3$). Not stable under HR-MS conditions.

Hexacarbonyl[μ-η^4-(2,4-dimethyl-4-((trimethylsilyl)ethynyl) oxazoline)]dicobalt (5c). Viscous colorless oil. ^{1}H NMR (300 MHz, CDCl$_3$) δ 4.21 (d, J = 8.4 Hz, 1H, –CH$_2$O–), 4.15 (d, J = 8.4 Hz, 1H, –CH$_2$O–), 1.98 (s, 3H, –CH$_3$), 1.65 (s, 3H, –CH$_3$), 0.32 (s, 9H, –Si(CH$_3$)$_3$). Not stable under HR-MS conditions.

Hexacarbonyl[μ-η^4-(2,4-dimethyl-4-(phenylethynyl)oxazoline)] dicobalt (5d). Viscous colorless oil. ^{1}H NMR (400 MHz, CDCl$_3$) δ 7.74–7.68 (m, 2H, –C$_6$H$_5$), 7.41–7.27 (m, 3H, –C$_6$H$_5$), 4.40 (d, J = 8.4 Hz, 1H, –CH$_2$O–), 4.21 (d, J = 8.4 Hz, 1H, –CH$_2$O–), 2.02 (s, 3H, –CH$_3$), 1.70 (s, 3H, –CH$_3$). Not stable under HR-MS conditions.

Hexacarbonyl[μ-η^4-(4-((2-chlorophenyl)ethynyl)-2,4-dimethyl oxazoline)]dicobalt (5e). Viscous colorless oil. ^{1}H NMR (400 MHz, CDCl$_3$) δ 8.31–8.09 (br, 1H, –C$_6$H$_4$Cl), 7.53–7.28 (br, 3H, –C$_6$H$_4$Cl overlapping with CDCl$_3$), 4.50 (d, J = 8.2 Hz, 1H, –CH$_2$O–), 4.28 (d, J = 8.2 Hz, 1H, –CH$_2$O–), 2.02 (s, 3H, –CH$_3$), 1.68 (s, 3H, –CH$_3$). Not stable under HR-MS conditions.

Hexacarbonyl[μ-η^4-(4-((4-methoxyphenyl)ethynyl)-2,4-dimethyl-oxazoline)]dicobalt (5f). Red oil. ^{1}H NMR (300 MHz, CDCl$_3$) δ 7.69 (2H, –C$_6$H$_4$–), 6.92 (2H, C$_6$H$_4$–), 4.42 (1H, –CH$_2$O–), 4.24 (1H, –CH$_2$O–), 3.85 (3H, –OCH$_3$), 2.03 (3H, –CH$_3$), 1.71 (3H, –CH$_3$). Not stable under HR-MS conditions.

Hexacarbonyl[μ-η^4-(4-(3-(benzyloxy)prop-1-yn-1-yl)-2,4-dimethyl-oxazoline)]dicobalt (5g). Red oil. ^{1}H NMR (300 MHz, CDCl$_3$) δ 7.45–7.29 (m, 5H, C$_6$H$_5$–), 4.70 (t, J = 14.3 Hz, 4H, –CH$_2$O–CH$_2$–), 4.31 (d, J = 8.5 Hz, 1H, –CH$_2$O–), 4.13 (d, J = 8.5 Hz, 1H, –CH$_2$O–), 1.96 (s, 3H, –CH$_3$), 1.63 (s, 3H, –CH$_3$). Not stable under HR-MS conditions.

Hexacarbonyl[μ-η^4-(2,4-dimethyl-4-(prop-1-yn-1-yl)-oxazoline)] dicobalt 5h. Red oil. ^{1}H NMR (300 MHz, CDCl$_3$) δ 4.28 (1H, –CH$_2$O–), 4.15 (1H, –CH$_2$O–), 2.72 (s, 3H, –CH$_3$), 1.99 (s, 3H, –CH$_3$), 1.65 (s, 3H, –CH$_3$). Not stable under HR-MS conditions.

Hexacarbonyl[μ-η^4-(4-(hept-1-yn-1-yl)-2-methyl-oxazoline)] dicobalt (5k). Red oil. ^{1}H NMR (300 MHz, CDCl$_3$) δ 5.32 (dd, J = 8.7, 6.4 Hz, 1H, –CHN–), 4.58–4.45 (m, 1H, –CH$_2$O–), 4.18 (dd, J = 8.5, 5.6 Hz, 1H, –CH$_2$O–), 2.92–2.83 (m, 2H, –CH$_2$–), 2.01 (d, J = 1.0 Hz, 3H, –CH$_3$), 1.68 (dd, J = 15.6, 8.0 Hz, 2H, –CH$_2$–), 1.55–1.33 (m, 4H, –CH$_2$–CH$_2$–), 0.93 (dd, J = 13.7, 6.5 Hz, 3H, –CH$_3$). Not stable under HR-MS conditions.

Hexacarbonyl[μ-η^4-((4-(hept-1-yn-1-yl)-2-methyl-4,5-dihydro oxazol-4-yl)methanol)]dicobalt (5l). Red oil. ^{1}H NMR (300 MHz, CDCl$_3$) δ 4.46 (d, J = 8.4 Hz, 1H, –CH$_2$O–), 4.15 (d, J = 8.4 Hz, 1H, –CH$_2$O–), 3.84 (dd, J = 10.8, 4.4 Hz, 1H, –CH$_2$OH), 3.54 (dd, J =

20.4, 10.8 Hz, 1H, −CH$_2$OH), 3.09 (dd, J = 8.9, 4.4 Hz, 1H, −OH), 2.81–2.68 (m, 2H, −CH$_2$(CH$_2$)$_3$CH$_3$), 1.93 (s, 3H, −CH$_3$), 1.66–1.49 (m, 2H, −CH$_2$CH$_2$(CH$_2$)$_2$CH$_3$), 1.43–1.25 (m, 4H, −(CH$_2$)$_2$(CH$_2$)$_2$CH$_3$), 0.85 (t, J = 7.1 Hz, 3H, −CH$_3$). Not stable under HR-MS conditions.

Hexacarbonyl[μ-η⁴-((2-methyl-4-(phenylethynyl)-4,5-dihydro oxazol-4-yl)methanol)]dicobalt (5m). Red oil. ^{1}H NMR (300 MHz, CDCl$_3$) δ 7.45 (d, J = 6.5 Hz, 2H, o-C$_6$H$_5$−), 7.13 (d, J = 7.4 Hz, 3H, m,p-C$_6$H$_5$), 4.42 (d, J = 8.4 Hz, 1H, −CH$_2$O−), 4.12 (d, J = 8.4 Hz, 1H, −CH$_2$O−), 3.82–3.69 (m, 1H, −CH$_2$OH), 3.42 (t, J = 10.4 Hz, 1H, −CH$_2$OH), 2.36 (d, J = 6.1 Hz, 1H, −OH), 1.84 (s, 3H, −CH$_3$). Not stable under HR-MS conditions.

Hexacarbonyl[μ-η⁴-((2-methyl-4-(prop-1-yn-1-yl)-4,5-dihydro oxazol-4-yl)methanol)]dicobalt (5n). Red oil. ^{1}H NMR (300 MHz, CDCl$_3$) δ 4.50 (d, J = 8.2 Hz, 1H, −CH$_2$O−), 4.24 (d, J = 8.2 Hz, 1H, −CH$_2$O−), 4.00–3.84 (m, 2H, −CH$_2$OH), 3.76–3.60 (m, 1H, −OH), 2.72 (s, 3H, −CH$_3$), 2.06 (s, 3H, −CH$_3$). Not stable under HR-MS conditions.

General procedure for the cleavage of cobalt complexes 5, method C

DDQ (3 eq., 1.23 mmol) was added in portions to a solution of cobalt complexed oxazoline 5 (1 eq., 0.41 mmol) in CH$_2$Cl$_2$ (4 mL) at 0 °C (ice/water bath). The reaction mixture was stirred until complete conversion of the starting material (TLC control, 30 min – 2 h). The reaction mixture was diluted with CH$_2$Cl$_2$ (30 mL) and aq. NaHCO$_3$ (10 mL) was added. The organic phase was separated and washed with H$_2$O (1 × 10 mL). Organic phase was dried over Na$_2$SO$_4$, filtered and evaporated. The crude residue was purified by chromatography on silica gel eluting with a mixture of ethyl acetate and petroleum ether 1 : 4–1 : 1 to afford oxazoline 6.

General procedure for the cleavage of cobalt complexes 5, method D

N-Methylmorpholine N-oxide (NMO) (10 eq., 4.1 mmol) was added in portions to a solution of cobalt complexed oxazoline 5 (1 eq., 0.41 mmol) in CH$_2$Cl$_2$ (4 mL) at 0 °C (ice/water bath). The reaction mixture was stirred until complete conversion of the starting material (TLC control, usually 30 min). The reaction was quenched with aq. NaHCO$_3$ (10 mL) and extracted with ethyl acetate (2 × 8 mL). The organic phase was washed with brine (1 × 10 mL), dried over Na$_2$SO$_4$, filtered and evaporated. The crude residue was purified by chromatography on silica gel eluting with a mixture of ethyl acetate and petroleum ether (1 : 4–1 : 1) to afford oxazoline 6.

4-(Hept-1-yn-1-yl)-2,4-dimethyloxazoline (6a). Colorless oil. ^{1}H NMR (400 MHz, CDCl$_3$) δ 4.28 (d, J = 8.1 Hz, 1H, −CH$_2$O−), 4.02 (d, J = 8.1 Hz, 1H, −CH$_2$O−), 2.17 (t, J = 7.1 Hz, 2H, −CH$_2$(CH$_2$)$_3$CH$_3$), 1.98 (s, 3H, −CH$_3$), 1.54–1.44 (m, 5H, −CH$_3$, −CH$_2$CH$_2$(CH$_2$)$_2$CH$_3$), 1.37–1.24 (m, 4H, −(CH$_2$)$_2$(CH$_2$)$_2$CH$_3$), 0.89 (t, J = 7.1 Hz, 3H, −(CH$_2$)$_4$CH$_3$). ^{13}C NMR (100 MHz, CDCl$_3$) δ 165.0, 84.2, 82.8, 79.6, 64.4, 31.2, 29.3, 28.5, 22.3, 18.8, 14.2, 14.1. HR-MS (ESI-TOF) m/z: calcd for C$_{12}$H$_{20}$NO 194.1545; found [M + H]$^+$ 194.1548.

4-(3,3-Dimethylbut-1-yn-1-yl)-2,4-dimethyloxazoline (6b). Colorless oil. ^{1}H NMR (400 MHz, CDCl$_3$) δ 4.23 (d, J = 8.0 Hz, 1H, −CH$_2$O−), 4.02 (d, J = 8.0 Hz, 1H, −CH$_2$O−), 1.97 (s, 3H, −CH$_3$), 1.45 (s, 3H, −CH$_3$), 1.18 (s, 9H, −C(CH$_3$)$_3$). ^{13}C NMR (100 MHz, CDCl$_3$) δ 164.7, 92.1, 81.2, 79.8, 64.3, 31.2, 29.6, 27.4, 14.2. HR-MS (ESI-TOF) m/z: calcd for C$_{11}$H$_{18}$NO 180.1388; found 180.1389 [M + H]$^+$.

2,4-Dimethyl-4-((trimethylsilyl)ethynyl)oxazoline (6c). Colorless oil. ^{1}H NMR (400 MHz, CDCl$_3$) δ 4.32 (d, J = 8.2 Hz, 1H, −CH$_2$O−), 4.03 (d, J = 8.2 Hz, 1H, −CH$_2$O−), 1.98 (s, 3H, −CH$_3$), 1.49 (s, 3H, −CH$_3$), 0.14 (s, 9H, −Si(CH$_3$)$_3$). ^{13}C NMR (100 MHz, CDCl$_3$) δ 164.4, 107.1, 86.6, 78.4, 63.8, 28.1, 13.2, −0.9. HR-MS (ESI-TOF) m/z: calcd for C$_{10}$H$_{18}$NOSi 196.1158; found 196.1156 [M + H]$^+$.

2,4-Dimethyl-4-(phenylethynyl)oxazoline (6d). Colorless oil. ^{1}H NMR (400 MHz, CDCl$_3$) δ 7.42–7.36 (m, 2H, −C$_6$H$_5$), 7.28–7.22 (m, 3H, −C$_6$H$_5$), 4.41 (d, J = 8.2 Hz, 1H, −CH$_2$O−), 4.09 (d, J = 8.2 Hz, 1H, −CH$_2$O−), 1.99 (s, 3H, −CH$_3$), 1.58 (s, 3H, −CH$_3$). ^{13}C NMR (100 MHz, CDCl$_3$) δ 165.5, 131.8, 128.4, 128.3, 122.9, 91.7, 83.5, 79.5, 64.9, 29.1, 14.2. HR-MS (ESI-TOF) m/z: calcd for C$_{13}$H$_{14}$NO 200.1075; found 200.1075 [M + H]$^+$.

4-((2-Chlorophenyl)ethynyl)-2,4-dimethyloxazoline (6e). Colorless oil. ^{1}H NMR (400 MHz, CDCl$_3$) δ 7.45 (dd, J = 7.4, 1.9 Hz, 1H, −C$_6$H$_4$Cl), 7.37 (dd, J = 7.9, 1.3 Hz, 1H, −C$_6$H$_4$Cl), 7.22 (td, J = 7.7, 1.9 Hz, 1H, −C$_6$H$_4$Cl), 7.17 (td, J = 7.5, 1.4 Hz, 1H, −C$_6$H$_4$Cl), 4.49 (d, J = 8.2 Hz, 1H, −CH$_2$O−), 4.14 (d, J = 8.2 Hz, 1H, −CH$_2$O−), 2.02 (s, 3H, −CH$_3$), 1.63 (s, 3H, −CH$_3$). ^{13}C NMR (100 MHz, CDCl$_3$) δ 165.7, 136.2, 133.4, 129.4, 129.3, 126.4, 122.8, 96.9, 80.4, 79.4, 65.0, 28.9, 14.2. HR-MS (ESI-TOF) m/z: calcd for C$_{13}$H$_{13}$NOCl 234.0686; found 234.0684 [M + H]$^+$.

4-((4-Methoxyphenyl)ethynyl)-2,4-dimethyl-oxazoline (6f). Colorless oil. ^{1}H NMR (400 MHz, CDCl$_3$) δ 7.33 (d, J = 8.9 Hz, 2H, −C$_6$H$_4$OMe), 6.79 (d, J = 8.9 Hz, 2H, −C$_6$H$_4$OMe), 4.41 (d, J = 8.1 Hz, 1H, −CH$_2$O−), 4.09 (d, J = 8.1 Hz, 1H, −CH$_2$O−), 3.78 (s, 3H, −OCH$_3$), 2.00 (s, 3H, −CH$_3$), 1.58 (s, 3H, −CH$_3$). ^{13}C NMR (100 MHz, CDCl$_3$) δ 165.2, 159.5, 133.1, 133.1, 114.8, 113.7, 90.1, 83.2, 79.4, 64.7, 55.2, 28.9, 14.1. HR-MS (ESI-TOF) m/z: calcd for C$_{14}$H$_{15}$NO$_2$ 229.1181; found 230.1178 [M + H]$^+$.

4-(3-(Benzyloxy)prop-1-yn-1-yl)-2,4-dimethyloxazoline (6g). Brownish oil. ^{1}H NMR (300 MHz, CDCl$_3$) δ 7.30–7.21 (m, 5H, C$_6$H$_5$−), 4.51 (s, 2H, −OCH$_2$Ph), 4.28 (d, J = 8.2 Hz, 1H, −CH$_2$O−), 4.13 (s, 2H, −CH$_2$OBn), 3.98 (d, J = 8.2 Hz, 1H, −CH$_2$O−), 1.93 (s, 3H, −CH$_3$), 1.46 (s, 3H, −CH$_3$). ^{13}C NMR (100 MHz, CDCl$_3$) δ 165.5, 137.4, 128.4, 128, 127.8, 88.9, 79.3, 79.1, 71.6, 64.2, 57.5, 28.8, 13.9. HR-MS (ESI-TOF) m/z: calcd for C$_{15}$H$_{17}$NO$_2$ 243.1338; found 244.1335 [M + H]$^+$.

2,4-Dimethyl-4-(prop-1-yn-1-yl)-oxazoline (6h). Colorless oil. ^{1}H NMR (400 MHz, CDCl$_3$) δ 4.26 (d, J = 8.1 Hz, 1H, −CH$_2$O−), 3.98 (d, J = 8.1 Hz, 1H, −CH$_2$O−), 1.95 (s, 3H, −CH$_3$), 1.79 (s, 3H, −CH$_3$), 1.44 (s, 3H, −CH$_3$). ^{13}C NMR (100 MHz, CDCl$_3$) δ 164.9, 81.8, 79.4, 79.3, 64.2, 29.0, 13.9, 3.6. HR-MS (ESI-TOF) m/z: calcd for C$_8$H$_{11}$NO 137.0918; found 138.0919 [M + H]$^+$.

4-(Hept-1-yn-1-yl)-2-methyl-oxazoline (6k). Colorless oil. ^{1}H NMR (300 MHz, CDCl$_3$) δ 4.68 (d, J = 8.0 Hz, 1H, =NCH−), 4.33 (dd, J = 10.0, 8.0 Hz, 1H, −CH$_2$O−), 4.11–3.99 (m, 1H, −CH$_2$O−), 2.12 (td, J = 7.1, 2.0 Hz, 2H, −CH$_2$−), 1.93 (s, 3H, −CH$_3$), 1.49–

1.37 (m, 2H, −CH$_2$−), 1.30–1.22 (m, 4H, −CH$_2$CH$_2$−), 0.82 (t, J = 7.1 Hz, 3H, −CH$_3$). ^{13}C NMR (100 MHz, CDCl$_3$) δ 171.1, 84.9, 67.9, 60.4, 53.4, 31.0, 28.2, 22.1, 18.7, 14.2, 13.9. HR-MS (ESI-TOF) m/z: calcd for C$_{11}$H$_{17}$NO 179.1388; found 180.1384 [M + H]$^+$.

(4-(Hept-1-yn-1-yl)-2-methyl-4,5-dihydrooxazol-4-yl)methanol (6l). Colorless oil. ^{1}H NMR (300 MHz, CDCl$_3$) δ 4.30 (d, J = 8.2 Hz, 1H, −CH$_2$OH), 4.19 (d, J = 8.2 Hz, 1H, −CH$_2$OH), 3.66 (d, J = 11.3 Hz, 1H, −CH$_2$O−), 3.46 (d, J = 11.3 Hz, 1H, −CH$_2$O−), 2.13 (t, J = 7.2 Hz, 2H, −CH$_2$−), 1.95 (s, 3H, −CH$_3$), 1.43 (t, J = 7.2 Hz, 2H, −CH$_2$−), 1.33–1.16 (m, 4H, −CH$_2$CH$_2$−), 0.82 (t, J = 6.9 Hz, 3H, −CH$_3$). ^{13}C NMR (100 MHz, CDCl$_3$) δ 167.4, 86.5, 79.2, 75.2, 69.4, 67.4, 31.0, 28.2, 22.1, 18.7, 14.0, 13.9. HR-MS (ESI-TOF) m/z: calcd for C$_{12}$H$_{19}$NO$_2$ 209.1494; found [M + H]$^+$ 210.1492.

(2-Methyl-4-(phenylethynyl)-4,5-dihydrooxazol-4-yl)methanol (6m). Colorless oil. ^{1}H NMR (400 MHz, CDCl$_3$) δ 7.45–7.37 (m, 2H, −C$_6$H$_5$), 7.32–7.24 (m, 3H, −C$_6$H$_5$), 4.46 (d, J = 8.3 Hz, 1H, −CH$_2$OH), 4.40 (d, J = 8.3 Hz, 1H, −CH$_2$OH), 3.87 (d, J = 11.3 Hz, 1H, −CH$_2$O−), 3.64 (d, J = 11.3 Hz, 1H, −CH$_2$O−), 2.04 (s, 3H, −CH$_3$). ^{13}C NMR (100 MHz, CDCl$_3$) δ 167.9, 131.8, 128.5, 128.2, 122.2, 88.1, 85.5, 75.0, 69.8, 67.1, 14.0. HR-MS (ESI-TOF) m/z: calcd for C$_{13}$H$_{13}$NO$_2$ 215.1022; found [M + H]$^+$ 216.1025.

(2-Methyl-4-(prop-1-yn-1-yl)-4,5-dihydrooxazol-4-yl)methanol (6n). Colorless oil. ^{1}H NMR (300 MHz, CDCl$_3$) δ 4.28 (d, J = 8.2 Hz, 1H, −CH$_2$OH), 4.20 (d, J = 8.2 Hz, 1H, −CH$_2$OH), 3.66 (d, J = 11.3 Hz, 1H, −CH$_2$O−), 3.47 (d, J = 11.3 Hz, 1H, −CH$_2$O−), 1.95 (s, 3H, −CH$_3$), 1.78 (s, 3H, −CH$_3$). ^{13}C NMR (100 MHz, CDCl$_3$) δ 170.2, 81.2, 76.3, 67.3, 66.8, 56.9, 14.2, 3.7. HR-MS (ESI-TOF) m/z: calcd for C$_8$H$_{11}$NO$_2$ 153.0864; found [M + H]$^+$ 154.0868.

General procedure for the synthesis of alkynyl glycinols 1

Aqueous 6 M HCl (1 mL) was added dropwise to a solution of oxazoline **6** (0.15 mmol) in MeOH (1.5 mL) at room temperature. The reaction mixture was stirred at room temperature for 2 h and the solvent was evaporated. Toluene (1 mL) was added to the mixture and evaporated. This procedure was repeated one more time. The residue was suspended in EtOAc and filtered to give amino alcohol hydrochloride salt **1**.

1-Hydroxy-2-methyl-4-phenylbut-3-yn-2-aminium chloride (1c). Amorphous compound. ^{1}H NMR (400 MHz, methanol-d4) δ 7.50–7.43 (m, 2H, C$_6$H$_5$−), 7.43–7.26 (m, 3H, C$_6$H$_5$−), 3.83 (d, J = 11.5 Hz, 1H, −CH$_2$OH), 3.70 (d, J = 11.5 Hz, 1H, −CH$_2$OH), 1.64 (s, 3H, −CH$_3$). ^{13}C NMR (100 MHz, CD$_3$OD) δ 131.4, 129.1, 128.2, 121.1, 86.4, 84.7, 66.3, 52.7, 21.5. HR-MS (ESI-TOF) m/z: calcd for C$_{11}$H$_{13}$NO 175.23; found 159.0810 [M − OH]$^+$.

5-(Benzyloxy)-1-hydroxy-2-methylpent-3-yn-2-aminium chloride (1g). Amorphous compound. ^{1}H NMR (300 MHz, CD$_3$OD) δ 7.35–7.15 (m, 5H, C$_6$H$_5$−), 4.49 (s, 2H, −OCH$_2$Ph), 4.16 (s, 2H, −CH$_2$OBn), 3.66 (d, J = 11.4 Hz, 1H, −CH$_2$OH), 3.54 (d, J = 11.4 Hz, 1H, −CH$_2$OH), 1.48 (s, 3H, −CH$_3$). ^{13}C NMR (100 MHz, CD$_3$OD) δ 137.3, 128.0, 127.7, 127.6, 83.0, 82.5, 71.5, 66.2, 56.5, 54.4, 21.4. HR-MS (ESI-TOF) m/z: calcd for C$_{13}$H$_{18}$NO$_2$ 220.1336; found 220.1338 [M + H]$^+$.

1-Hydroxy-2-methylpent-3-yn-2-aminium chloride (1h). Amorphous compound. ^{1}H NMR (400 MHz, methanol-d_4) δ 3.67 (d, J = 11.5 Hz, 1H, −CH$_2$OH), 3.55 (d, J = 11.5 Hz, 1H, −CH$_2$OH),

1.85 (s, 3H, −CH$_3$), 1.49 (s, 3H, −CH$_3$), 1.36 (dt, J = 7.4, 3.9 Hz, 1H, −OH). ^{13}C NMR (101 MHz, CD$_3$OD) δ 83.4, 75.3, 66.4, 52.2, 21.6, 1.6. HR-MS (ESI-TOF) m/z: calcd for C$_{12}$H$_{12}$NO 114.0919; found 114.0922 [M + H]$^+$.

1-Hydroxy-2-(hydroxymethyl)non-3-yn-2-aminium chloride (1l). Amorphous compound. ^{1}H NMR (400 MHz, CD$_3$OD) δ 3.74 (d, J = 11.3 Hz, 2H, −CH$_2$OH), 3.67 (d, J = 11.3 Hz, 2H, −CH$_2$OH), 2.24 (t, J = 7.1 Hz, 2H, −CH$_2$(CH$_2$)$_3$CH$_3$), 1.61–1.46 (m, 2H, −CH$_2$CH$_2$(CH$_2$)$_2$CH$_3$), 1.44–1.27 (m, 4H, −CH$_2$CH$_2$(CH$_2$)$_2$CH$_3$), 0.89 (t, J = 7.1 Hz, 3H, −CH$_2$(CH$_2$)$_3$CH$_3$). ^{13}C NMR (101 MHz, CD$_3$OD) δ 88.9, 74.1, 62.9, 56.9, 30.6, 27.6, 21.8, 17.8, 12.8. HR-MS (ESI-TOF) m/z: calcd for C$_{10}$H$_{20}$NO$_2$ 186.1494; found. 186.1494 [M + H]$^+$.

1-Hydroxy-2-(hydroxymethyl)-4-phenylbut-3-yn-2-aminium chloride (1m). Amorphous compound. ^{1}H NMR (400 MHz, CD$_3$OD) δ 7.53–7.43 (m, 2H, o-C$_6$H$_5$−), 7.43–7.33 (m, 3H, p,m-C$_6$H$_5$−), 3.87 (d, J = 11.4 Hz, 2H, −CH$_2$OH), 3.83 (d, J = 11.4 Hz, 2H, −CH$_2$OH). ^{13}C NMR (101 MHz, CD$_3$OD) δ 131.5, 129.1, 128.2, 121.1, 87.5, 82.8, 62.7, 57.4. HR-MS (ESI-TOF) m/z: calcd for C$_{11}$H$_{14}$NO$_2$ 192.10; found 175.0759 [M − OH]$^+$.

Conclusions

In summary, we have developed a novel approach to C-quaternary alkynyl glycinols. This is based on the Ritter reaction of acetonitrile with cobalt complexed alkynyl glycols to give oxazolines. The substrates can be easy assembled to introduce the structural diversity at both variable positions. The Ritter reaction is compatible with a range of substituents at the alkyne terminal position providing oxazolines in moderate to good yields. Hydroxymethyl substituent at the reaction center in both unprotected or O-TBS protected form was well tolerated. The Ritter reaction proceeds also with bis-O-TBS protected alkynyl glycerols with concomitant cleavage of the TBS groups. However, the phenyl group at the reaction center of glycols was detrimental inducing low or no yield of the product formation. Cobalt alkyne complexes in the oxazolines produced by the Ritter reaction can be cleaved in oxidative conditions using DDQ, or NMO as reagents. Hydrolysis of oxazoline ring in mild acidic conditions efficiently provides amino alcohols. We believe that method presented in this paper will find an application for the synthesis of complex amino alcohol derivatives. A version based on catalytic amount of cobalt additive or a protocol for efficient cobalt recovery needs to be developed in the future. This would enable the use of the method for economic and eco-friendly manufacturing processes.

Acknowledgements

Notes and references

1 J. Bolsakova and A. Jirgensons, *Eur. J. Org. Chem.*, 2016, 4591.

81

2 T. Boibessot, D. Bénimélis, P. Meffre and Z. Benfodda, *Amino Acids*, 2016, **48**, 2081.

3 H. Fukumoto, K. Takahashi, J. Ishihara and S. Hatakeyama, *Angew. Chem., Int. Ed.*, 2006, **45**, 2731.

4 S. N. Osipov, P. Tsouker, L. Hennig and K. Burger, *Tetrahedron*, 2004, **60**, 271.

5 K. Morisaki, M. Sawa, J. Nomaguchi, H. Morimoto, Y. Takeuchi, K. Mashima and T. Ohshima, *Chem.–Eur. J.*, 2013, **19**, 8417.

6 V. M. Girijavallabhan, L. Chen, C. Dai, R. J. Feltz, L. Firmansjah, D. Li, S. H. Kim, J. A. Kozlowski, B. J. Lavey, A. Kosinski, *et al.*, *Bioorg. Med. Chem. Lett.*, 2010, **20**, 7283.

7 G. Pattenden and G. Rescourio, *Org. Biomol. Chem.*, 2008, **6**, 3428.

8 Z. Benfodda, D. Bénimélis, M. Jean, J.-V. Naubron, V. Rolland and P. Meffre, *Amino Acids*, 2015, **47**, 899.

9 G. Hattori, A. Yoshida, Y. Miyake and Y. Nishibayashi, *J. Org. Chem.*, 2009, **74**, 7603.

10 U. Schmidt, M. Respondek, A. Lieberknecht, J. Werner and P. Fischer, *Synthesis*, 1989, 256.

11 S. Hatakeyama, H. Matsumoto, H. Fukuyama, Y. Mukugi and H. Irie, *J. Org. Chem.*, 1997, **62**, 2275.

12 C. J. Brennan, G. Pattenden and G. Rescourio, *Tetrahedron Lett.*, 2003, **44**, 8757.

13 R. D. Grigg, J. W. Rigoli, S. D. Pearce and J. M. Schomaker, *Org. Lett.*, 2012, **14**, 280.

14 J. Sirotkina, L. Grigorjeva and A. Jirgensons, *Eur. J. Org. Chem.*, 2015, 6900–6908.

15 R. Bishop, in *Compr. Org. Synth. II*, Elsevier, Amsterdam, 2nd edn, 2014, pp. 239–295.

16 I. R. Morgan, A. Yazici, S. G. Pyne and B. W. Skelton, *J. Org. Chem.*, 2008, **73**, 2943.

17 M. Vangala and G. P. Shinde, *Beilstein J. Org. Chem.*, 2015, **11**, 2289.

18 J. L. Jiménez Blanco, E. M. Rubio, C. Ortiz Mellet and J. M. García Fernández, *Synlett*, 2004, 2230.

19 D. Noort, G. A. van der Marel, G. J. Mulder and J. H. van Boom, *Synlett*, 1992, 224.

20 D. M. Gordon and S. J. Danishefsky, *J. Org. Chem.*, 1991, **56**, 3713.

21 I. W. Davies, C. H. Senanayake, R. D. Larsen, T. R. Verhoeven and P. J. Reider, *Tetrahedron Lett.*, 1996, **37**, 813.

22 C. H. Senanayake, L. M. DiMichele, J. Liu, L. E. Fredenburgh, K. M. Ryan, F. E. Roberts, R. D. Larsen, T. R. Verhoeven and P. J. Reider, *Tetrahedron Lett.*, 1995, **36**, 7615.

23 E.-J. Tillmanns and J. Ritter, *J. Org. Chem.*, 1957, **22**, 839.

24 A. Toshimitsu, C. Hirosawa and K. Tamao, *Tetrahedron*, 1994, **50**, 8997.

25 S. Top and G. Jaouen, *J. Chem. Soc., Chem. Commun.*, 1979, 224.

26 S. Top and G. Jaouen, *J. Org. Chem.*, 1981, **46**, 78.

27 R. F. Lockwood and K. M. Nicholas, *Tetrahedron Lett.*, 1977, **18**, 4163.

28 K. M. Nicholas, *Acc. Chem. Res.*, 1987, **20**, 207.

29 B. J. Teobald, *Tetrahedron*, 2002, **58**, 4133.

30 G. B. Jones, J. M. Wright, T. M. Rush, G. W. Plourde, T. F. Kelton, J. E. Mathews, R. S. Huber and J. P. Davidson, *J. Org. Chem.*, 1997, **62**, 9379.

31 T. Sugihara, H. Ban and M. Yamaguchi, *J. Organomet. Chem.*, 1998, **554**, 163.

32 D. Kalaitzakis, T. Montagnon, I. Alexopoulou and G. Vassilikogiannakis, *Angew. Chem., Int. Ed.*, 2012, **51**, 8868.

33 B. Gabriele, R. Mancuso, V. Maltese, L. Veltri and G. Salerno, *J. Org. Chem.*, 2012, **77**, 8657.

34 S.-T. Chen and J.-M. Fang, *J. Org. Chem.*, 1997, **62**, 4349.

35 R. Spina, E. Colacino, J. Martinez and F. Lamaty, *Chem.–Eur. J.*, 2013, **19**, 3817.

82

Publication No. 2

N. Franko, K. Grammatoglou, B. Campanini, G. Costantino, A.
Jirgensons, A. Mozzarelli, Inhibition of O–acetylserine sulfhydrylase
by fluoroalanine derivatives. *Journal Of Enzyme Inhibition and
Medicinal Chemistry* **2018**, 33, 1, 1343–1351

Taylor & Francis
Taylor & Francis Group

RESEARCH PAPER

🔓 OPEN ACCESS [Check for updates]

Inhibition of *O*-acetylserine sulfhydrylase by fluoroalanine derivatives

Nina Franko[a]*, Konstantinos Grammatoglou[b]*, Barbara Campanini[a], Gabriele Costantino[a], Aigars Jirgensons[b] and Andrea Mozzarelli[a,c]

[a]Food and Drug Department, University of Parma, Parma, Italy; [b]Latvian Institute of Organic Synthesis, Riga, Latvia; [c]National Research Council, Institute of Biophysics, Pisa, Italy

ABSTRACT

O-acetylserine sulfhydrylase (OASS) is the pyridoxal 5′-phosphate dependent enzyme that catalyses the formation of L-cysteine in bacteria and plants. Its inactivation is pursued as a strategy for the identification of novel antibiotics that, targeting dispensable proteins, holds a great promise for circumventing resistance development. In the present study, we have investigated the reactivity of *Salmonella enterica* serovar Typhimurium OASS-A and OASS-B isozymes with fluoroalanine derivatives. Monofluoroalanine reacts with OASS-A and OASS-B forming either a stable or a metastable α-aminoacrylate Schiff's base, respectively, as proved by spectral changes. This finding indicates that monofluoroalanine is a substrate analogue, as previously found for other beta-halogenalanine derivatives. Trifluoroalanine caused different and time-dependent absorbance and fluorescence spectral changes for the two isozymes and is associated with irreversible inhibition. The time course of enzyme inactivation was found to be characterised by a biphasic behaviour. Partially distinct inactivation mechanisms for OASS-A and OASS-B are proposed.

Introduction

Sulfur is a fundamental component of many biomolecules, from amino acids to cofactors and compounds that control the redox homoeostasis. Only bacteria and plants can assimilate inorganic sulfur, either sulfate or thiosulfate, via a biosynthetic pathway leading to the formation of cysteine (Scheme 1(A))[1].

The final step is catalysed by *O*-acetylserine sulfhydrylase (OASS), a pyridoxal 5′-phosphate (PLP)-dependent enzyme that carries out a *β*-replacement reaction (Scheme 1(B)). First, *O*-acetylserine forms an external aldimine that undergoes the *β*-elimination of an acetoxy moiety leading to the aminoacrylate Schiff's base that is attacked by sulfide with the formation of the external aldimine of cysteine which is finally released to regenerate the internal aldimine.

OASS is present in bacteria as two isoforms, OASS-A and OASS-B, also named CysK and CysM after the coding genes. Their distribution, structural, and functional properties have been deeply investigated[2–8]. The enzyme that catalyses the synthesis of OAS, i.e. serine acetyltransferase (SAT), is able to form a high-affinity complex with OASS-A but not with OASS-B. Because SAT binding to OASS-A involves anchoring of its C-terminus in OASS-A active site, complex formation leads to the competitive inhibition of OASS-A activity. Both isoforms are present in bacteria but not in humans. Bacteria knocked-out for *cysK* and *cysM* exhibit a phenotype with reduced virulence, compromised fitness, and decreased antibiotic resistance[9,10]. For these reasons, OASS has been the target of multiple medicinal chemistry efforts to identify reversible inhibitors potentially useful as antibiotics or enhancers of antibiotic activity[11,12]. Initially, pentapeptides that mimic the inhibitory

interaction between OASS-A and the C-terminus of SAT were developed[13,14]. Then, more potent and isoform-specific peptidomimetic compounds based on cyclopropane derivatives were generated, with some of them exhibiting nanomolar K_i against OASS-A from *S*. Typhimurium[12,15].

The debate between pros and cons of reversible and irreversible enzyme inhibitors has been developing along the history of medicinal chemistry with alternative views[16,17]. Reversible inhibitors either directed to the active site or allosteric sites are thought to be more specific, thus less prone to toxicity effects due to unwanted off-target reactions, which are typical of irreversible inhibitors that exploit the intrinsic reactivity of protein residues, such as cysteines or cofactors. However, the concentration of irreversible inhibitors needed to inactivate enzymes is usually lower than the concentration required by reversible inhibitors and this can potentially lead to an increased therapeutic index. Two classes of irreversible inhibitors have been developed: mechanism-based inactivators and affinity labels[18,19].

Monohalogenated, dihalogenated and trihalogenated (either chloro-based or fluoro-based) alanines have been exploited as mechanism-based inhibitors of pyridoxal 5′-phosphate (PLP)-dependent enzymes, including γ-cystathionase[20,21], alanine racemase[22], tryptophan synthase and tryptophanase[23,24], 8-amino 7-oxononanotate synthase[25], ornithine decarboxylase[26], aspartate aminotransferase[27], and kynurenine transaminase[28]. The reaction mechanism and the extent of inactivation are different depending on the number of halogen substituents[29,30] and enzyme[25]. A widely accepted mechanism of inhibition by halogenated alanines includes the formation of an external aldimine with PLP

Scheme 1. Panel A: sulfur assimilation in bacteria. Thiosulfate is an alternative substrate to bisulfide and it can only be used by the OASS-B isozyme. SAT: serine acetyltransferase; RS$^-$: sulfur source, either SH$^-$ or S$_2$O$_3^-$. Panel B: catalytic cycle of OASS.
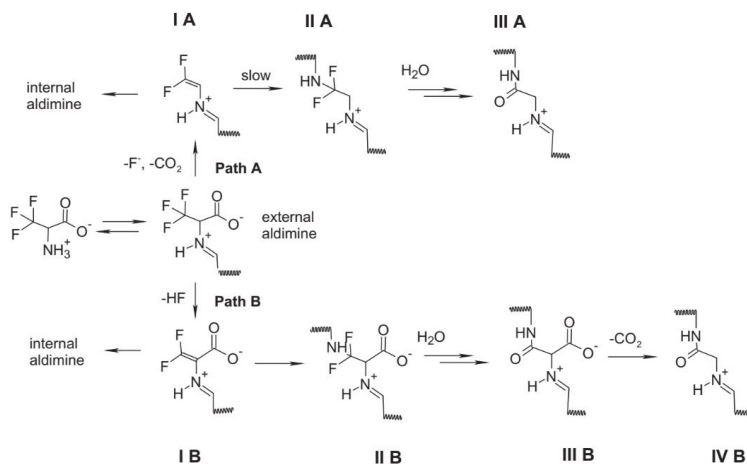
Scheme 2. Possible inactivation pathways of PLP-dependent enzymes by β,β,β-trifluoroalanine.

(transaldimination), followed by alpha-proton abstraction and elimination of either HF or HCl with the formation of an unsaturated Schiff's base, i.e. α-aminoacrylate-PLP complex (Scheme 2, path B). Another possible mechanism of inactivation is fluorodecarboxylation mechanism, leading to an unsaturated Schiff's base (Scheme 2, path A)[25,31]. In both types of inhibition, the unsaturated Schiff's base is the key partitioning intermediate and the following steps are strongly dependent on the active site environment and on the halogenated alanine, usually involving an attack of the active site lysine on the double bond, followed by chemical rearrangements that cause the release of further halogen ions and formation of stable derivatives that inactivate the enzyme.

In the present study, we investigated the reactivity of mono and trifluoroalanine derivatives with OASS-A and OASS-B in order to identify suitable mechanism-based irreversible inhibitors.

Material and methods

Reagents

If not otherwise specified, chemicals were purchased from Sigma-Aldrich (St. Louis, MO, USA) at the highest available quality. Ninhydrin was purchased from Apollo Scientific (Stockport, UK).

Protein preparation

Recombinant STOASS-A and STOASS-B were expressed in Escherichia coli BL21(DE3) and purified as described previously[32]. Briefly, His-tagged proteins were purified using ion metal affinity chromatography on immobilised Co^{2+} ions (Talon Technology, Clontech Laboratories, Inc., Mountain View, CA, USA). His-tag was removed at 37 °C by factor Xa in a 1:200 ratio with protein in 20 mM HEPES, 100 mM NaCl, and 4 mM CaCl$_2$, pH 7.5.

85

Proteins were more than 93% pure accordingly to SDS-PAGE (see Figure 1SM). Protein concentration was determined by extinction coefficients of the bound PLP, that are $9040\,M^{-1}\,cm^{-1}$ at 412 nm for OASS-A and $6800\,M^{-1}\,cm^{-1}$ at 414 nm for OASS-B. OASS-A was stored in 10 mM HEPES, pH 8.0 and OASS-B in 5 mM HEPES, pH 8.0.

Monitoring the reactions by absorbance spectroscopy

Absorbance spectra were recorded with a Cary4000 spectrophotometer (Agilent Technologies) on solutions containing 5–10 μM enzyme, 1 mM fluoroalanine derivative, 100 mM HEPES, pH 7.0, at room temperature. Spectra were corrected for buffer contribution. The time course of band disappearance at a fixed wavelength was fitted to a single exponential decay equation:

$$A_t = A_0 + A_i^{-k_{obs} \cdot t}, \tag{1}$$

where A_t is absorbance at time t, A_0 is the absorbance at infinite time, A_i is the total absorbance change and k_{obs} is the rate constant.

Monitoring the reactions by fluorescence spectroscopy

Fluorescence emission spectra were recorded with a FluoroMax-3 fluorimeter (HORIBA) on solutions containing 1 μM enzyme, 1 mM fluoroalanine, 100 mM HEPES, pH 7.0, at room temperature, upon excitation at 412 nm, with $slit_{ex} = slit_{em} = 6$ nm. Spectra were corrected for buffer and compound contribution.

Activity assays

Enzyme activity under steady-state conditions was measured by a discontinuous method, following the quantification of cysteine concentration by the method developed by Gaitonde[33], adjusted to 96-well plate format. Briefly, reaction was initiated by addition of 0.6 mM Na_2S to a solution containing 6 nM OASS-A/OASS-B, 1 mM OAS, 100 mM HEPES, pH 7.0, a 10-fold excess of BSA with respect to enzyme concentration to prevent enzyme adhesion to well wall and variable concentrations of potential inhibitors. Aliquots (60 μL) were withdrawn at time intervals and the reaction was stopped in PCR tubes containing 60 μL of acetic acid. 60 μL of ninhydrin were added by a multichannel pipette and the mixture was heated at 100 °C for 10 min in a thermal cycler. The solutions were cooled down on the ice and 46 μL were added to the wells of a 96-well plate containing 154 μL of cold ethanol. The absorbance at 550 nm was measured using a plate reader (Halo LED 96, Dynamica Scientific, Newport Pagnell, UK). Time courses were collected at least in duplicate. The amount of cysteine produced at each time point was calculated from a calibration curve, and data were fitted to a linear equation to calculate the initial rate of cysteine production. The fractional velocity was determined as a function of inhibitor concentration and IC_{50} was calculated using Equation (2):

$$\frac{v_i}{v_0} = \frac{1}{1 + \left(\frac{[I]}{IC50}\right)}, \tag{2}$$

where v_0 is the initial rate in the absence of inhibitor and v_i is the initial rate in the presence of inhibitor at concentration [I].

Inactivation kinetics

OASS (45 μM) was incubated with various concentrations of β,β,β-trifluoroalanine in 400 mM HEPES, pH 7.0, at room temperature. Enzyme activity at different time points was assayed as

described above upon a 5000-fold dilution with a solution containing 100 mM HEPES, 90 nM BSA, pH 7.0. Inactivation kinetics were collected at different concentrations of β,β,β-trifluoroalanine, and k_{obs} values were determined by fitting data to the equation of a single exponential decay:

$$\frac{v_i}{v_0} = A + B \cdot e^{-k_{obs} \cdot t}, \tag{3}$$

where v_0 is the initial rate in the absence of inhibitor, v_i is the initial rate in the presence of inhibitor at concentration [I], A is an off-set, B is the amplitude, and k_{obs} is the rate constant.

Enzyme activity was also measured upon 85 h of incubation in the presence of β,β,β-trifluoroalanine, removal of ligand by ultrafiltration, in the absence and presence of 1 μM PLP added to the activity assay mixture. The fractional activity was calculated with respect to enzyme incubated under the same conditions in the absence of β,β,β-trifluoroalanine.

Potency of inhibitor was determined as the ratio k_{inact}/K_I that for OASS-A was determined from Equation (4):

$$k_{obs} = \frac{k_{inact} \times [I]}{K_I + [I]}, \tag{4}$$

where k_{obs} is the observed rate constant of inactivation at inhibitor concentration [I], k_{inact} is inactivation rate constant and K_I is concentration of inhibitor that yields $k_{obs} = {}^1/_2\,k_{inact}$. k_{inact}/K_I for OASS-B was determined using Equation (5):

$$\frac{k_{obs}}{[I]} = \frac{k_{inact}}{K_I}. \tag{5}$$

Results and discussion

Monitoring the reaction of monofluoro- and trifluoroalanine with OASS-A and OASS-B by absorbance and fluorescence spectroscopy

The absorption spectra of OASS-A and OASS-B exhibit a band at 412 nm, attributed to the ketoenamine tautomer of the internal aldimine (Figure 1). When 1 mM monofluoroalanine (F-Ala) was added, the band shifted to 470 nm, a band attributed to the α-aminoacrylate Schiff's base (Figure 1(A))[5,6,34]. This species, that was stable for at least 21 h, is generated from the β-elimination reaction of HF, similar to the β-elimination reaction observed for the acetoxy moiety of the natural substrate OAS. When the same reaction was carried out on OASS-B, a rapid formation of the α-aminoacrylate was observed, followed by the slow reappearance of the band at 412 nm (Figure 1(B)) and a broad absorbance between 300 and 350 nm, where pyruvate absorbs. This finding indicates that the α-aminoacrylate Schiff's base of OASS-B decomposes to pyruvate and ammonia much faster than the α-aminoacrylate Schiff's base of OASS-A. The same behaviour was observed in the formation of aminoacrylate with O-acetylserine[3].

The same reaction was also monitored by fluorescence spectroscopy. The emission spectrum of OASS-A, upon excitation at 412 nm, was centred at 505 nm[8,35] and disappeared upon addition of F-Ala (Figure 2(A)), in agreement with the previous studies indicating that the fluorescence quantum yield of the α-aminoacrylate is much lower than that of the internal aldimine[8]. When the reaction with F-Ala was carried out on OASS-B (Figure 2(B)), only a shift to 550 nm of the emission peak was observed, in agreement with our previous work[7]. This emission was attributed to an α-aminoacrylate located in an active site with a different microenvironment compared to OASS-A isozyme.

Given the observed spectral changes, it can be concluded that F-Ala behaves as a substrate analog of OASS, as previously observed for β-chloroalanine[30] and that the intermediate α-aminoacrylate is oriented within the active site in such a way to disfavour the reaction with any active site residue. This finding is not surprising considering that OASS has evolved to stabilise an α-aminoacrylate intermediate ready to react with the incoming nucleophilic sulfide. In addition, it has been reported for alanine racemase[29,36] that the partition ratio between α-aminoacrylate hydrolysis and Michael addition on the adduct formed from the F-Ala is 820:1, a further indication of the very poor reactivity of this species in the enzyme active site.

We then investigated the reactivity of OASS-A and OASS-B with 1 mM β,β,β-trifluoroalanine (triF-Ala), a well-known suicide substrate of PLP-dependent enzymes[20,23–26,29,30]. The absorbance spectra collected as a function of time exhibited a complex behaviour (Figure 3). Immediately upon the addition of the reagent to OASS-A, two prominent peaks appeared, centred at 440 and 466 nm, and minor bands at 360 and 380 nm, as already observed for the reaction of triF-Ala with alanine racemase[30], indicative of a species with extended conjugation. Absorbance intensity was found to be nearly independent of reagent concentration between 1 and 10 mM (data not shown), suggesting that all

enzyme sites have reacted with the reagent forming a metastable species. The absorbance intensity at 466 nm slowly decreased with the k_{obs} of 0.43 h^{-1}, with formation of a band centred at 412 nm (Figure 3(C)).

The reaction of OASS-B with triF-Ala was accompanied by much smaller spectral changes in the range 400–500 nm (Figure 3(B)), independent of a ten-fold increase in triF-Ala concentration (data not shown). The time course for intermediate decay at 457 nm was similar to OASS-A (k_{obs} 0.48 h^{-1}) and was accompanied by the increase in the absorbance in the range 300–350 nm, suggesting the production of a keto-acid, possibly difluoropyruvate.

The reaction of triF-Ala with OASS-A was also monitored by fluorescence emission of the cofactor (Figure 4(A)). Immediately upon reaction, the emission band measured upon excitation at 412 nm was blue shifted to 495 nm with only a small decrease in emission intensity. This finding confirms that the species that is formed immediately upon exposure to triF-Ala is not the α-aminoacrylate Schiff's base, in agreement with absorbance data. The emission band slowly decreased as a function of time with a kinetics that parallels that observed for the disappearance of the absorption bands at 440 and 466 nm. However, after 6 h incubation, the initial emission spectrum is not recovered, differently
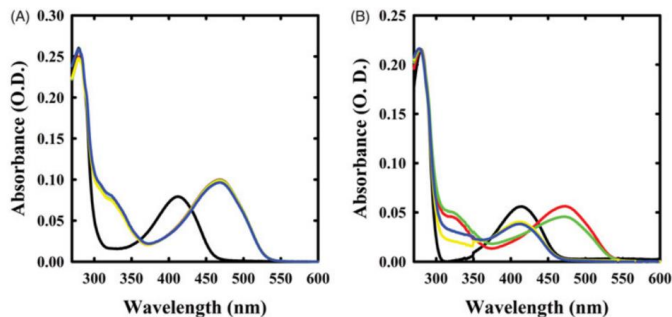
Figure 1. Spectral changes of OASS in the presence of F-Ala. Panel A: OASS-A in the absence of reagent (black line), 1 min (red line), 1 h (green line), 5 h (yellow line), and 21 h (blue line) after addition of 1 mM F-Ala. Panel B: OASS-B in the absence of reagent (black line), 1 min (red line), 1 h (green line), 3 h (yellow line), and 7 h (blue line) after addition of 1 mM F-Ala.
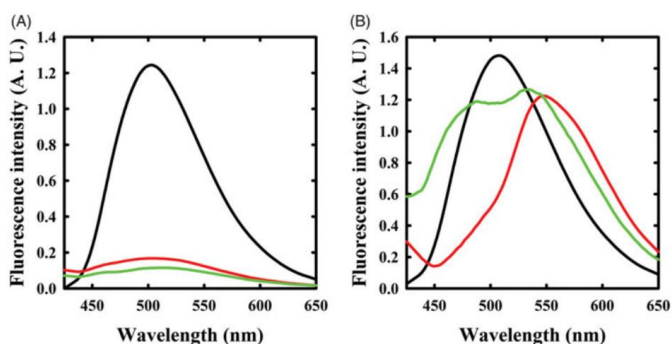
Figure 2. Fluorescence emission spectra of OASS upon excitation at 412 nm in the absence and presence of F-Ala. Panel A: OASS-A in the absence of reagent (black line), 1 min (red line), and 4 h (green line) after addition of 1 mM F-Ala. Panel B: OASS-B in the absence of reagent (black line), 1 min (red line), and 3 h (green line) after addition of 1 mM F-Ala.
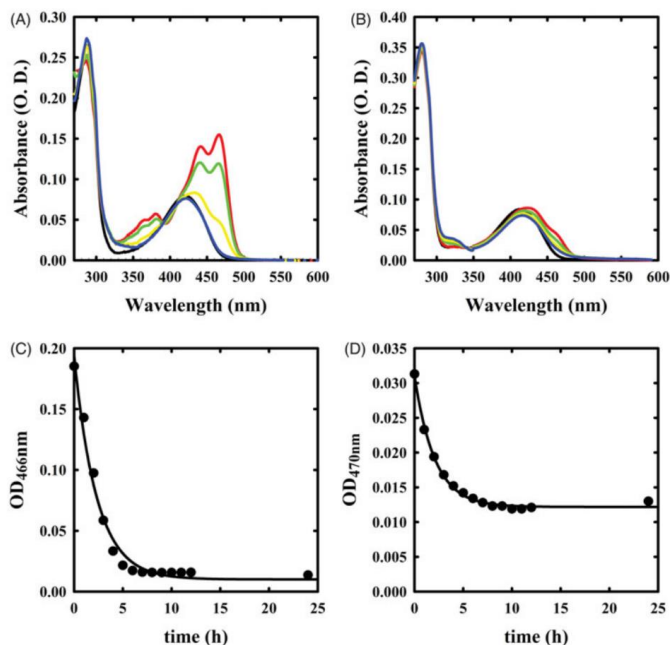
Figure 3. Absorbance spectra of OASS in the absence and presence of 1 mM triF-Ala. Panel A: absorbance spectrum of OASS-A in the absence of reagent (black line), 1 min (red line), 1 h (green line), 3 h (yellow line), and 7 h (blue line) after addition of the reagent. Panel B: absorbance spectrum of OASS-B in the absence of reagent (black line), 1 min (red line), 1 h (green line), 3 h (yellow line), and 7 h (blue line) after addition of the reagent. Panel C: time course of spectral changes of OASS-A, monitored at 466 nm. Panel D: time course of spectral changes of OASS-B, monitored at 457 nm starting 1 min after the addition of triF-Ala. Data were fitted to a monoexponential decay.
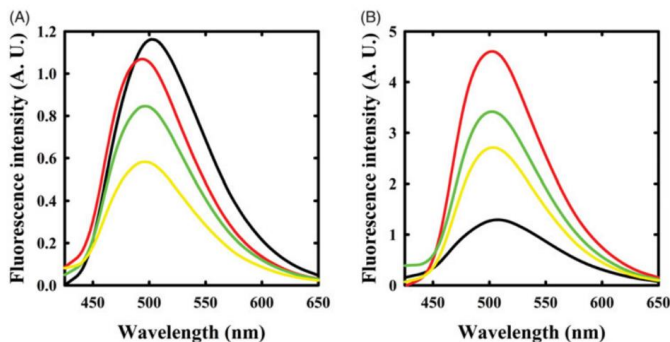
Figure 4. Fluorescence emission spectrum of OASS in the absence and presence of 1 mM triF-Ala. Emission spectra were recorded upon excitation at 412 nm. Panel A: OASS-A in the absence of reagent (black line), 1 min (red line), 4 h (green line), and 6 h (yellow line) after addition of the reagent. Panel B: OASS-B in the absence of reagent (black line), 1 min (red line), 3 h (green line), and 7 h (yellow line) after addition of the reagent.

from what was observed by absorbance spectroscopy. This suggests that the species that forms and absorbs at 412 nm is not the internal aldimine.

When the reaction of triF-Ala with OASS-B was monitored by recording emission spectra upon excitation at 412 nm (Figure 4(B)),

a different behaviour with respect to OASS-A was observed. The intensity of emission band immediately increases, then slowly decreases. Changes in intensity are accompanied by a small blue shift to 501 nm that shifts back slowly to 505 nm after 7 h of incubation. The intense emitting species might be an external

88
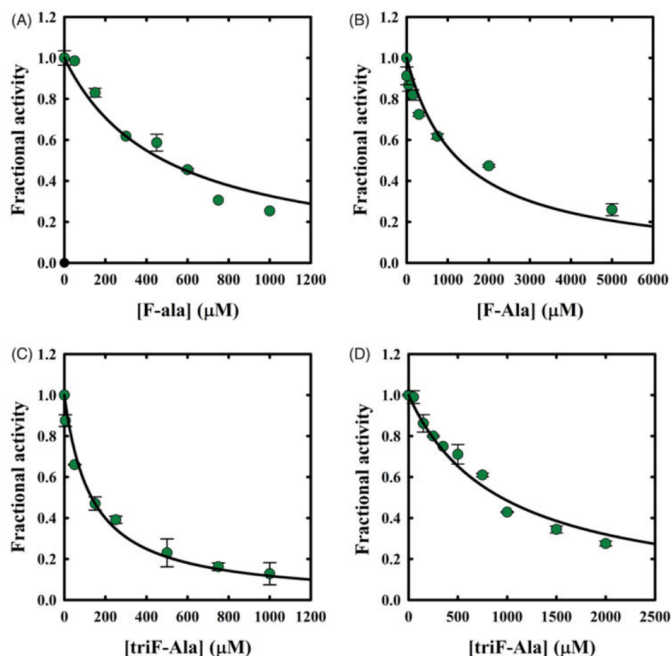
Figure 5. Dependence of OASS fractional activity on the concentration of fluoroalanine derivatives. (A) OASS-A and F-Ala; (B) OASS-B and F-Ala; (C) OASS-A and triF-Ala; (D) OASS-B and triF-Ala. The IC_{50} was obtained by fitting data points to Equation (2). The calculated IC_{50} values for F-Ala were $480 \pm 50 \mu M$ and $1290 \pm 230 \mu M$ for OASS-A and OASS-B, respectively, and for triF-Ala $130 \pm 10 \mu M$ and $940 \pm 60 \mu M$, for OASS-A and OASS-B, respectively.

aldimine, because in most PLP-dependent enzymes, including OASS, the external aldimine is endowed by high fluorescence intensity[7,8]. The small blue shift suggests the formation of a transient species.

Monitoring the reaction of F-Ala and triF-Ala with OASS-A and OASS-B by activity assays

The potential inhibitory action of F-Ala and triF-Ala on OASS-A and OASS-B was investigated by carrying out two distinct experiments. First, OASS-A and OASS-B were assayed within a few seconds from the exposure to increasing concentrations of F-Ala. IC_{50} values of $480 \pm 50 \mu M$ and $1290 \pm 230 \mu M$ were determined, respectively (Figure 5(A,B)). The same experiment was carried out for triF-Ala determining IC_{50} values of $130 \pm 10 \mu M$ and $940 \pm 60 \mu M$, for OASS-A and OASS-B, respectively (Figure 5(C,D)).

Whereas F-Ala inhibits OASS by competing with the substrate and is slowly degraded, as reported above and observed for other PLP-dependent enzymes, triF-Ala might inhibit OASS by irreversible inactivation. To detect whether this is the case, we monitored the kinetics of OASS-A inactivation in the presence of 1, 2.5, 10, 30, and 50 mM triF-Ala (Figure 6). At each time point, the enzyme activity was determined upon a 5000-fold dilution of the reaction mixture. The time course of enzyme inhibition was found to be clearly biphasic. The rate constant of the very fast phase cannot be measured, whereas its amplitude was found to be dependent on reagent concentration (Figure 6(B)) and

approaching saturation. The rate of the slow phase depends hyperbolically on reagent concentration, as expected for suicide substrates. The second-order rate constant k_{inact}/K_I was determined to be $3.95 \times 10^{-5} min^{-1} mM^{-1}$, indicating poor effectiveness in enzyme inactivation.

When the time dependence of spectral changes of OASS-A (Figure 3(A,C)) is compared with that of enzyme inactivation (Figure 6(A)), at least three phases in the reaction of triF-Ala with the enzyme are identified: (i) a fast phase completed in a few seconds in which a species is built-up absorbing at 440–470 nm; (ii) an intermediate phase completed in about 10 h where the species absorbing at 440–470 disappears with the concomitant appearance of a species at 412 and is accompanied by minor decrease in enzyme activity, and (iii) a very slow phase where most of enzyme inactivation takes place. It is worth stressing that the very fast phase of enzyme inhibition monitored by changes in the absorption spectrum (Figure 3(A)) is completely reversible within 8 h for inhibitor concentrations up to 1 mM (Figure 6(A)), thus the IC_{50}s (Figure 5) are a good estimate of the relative affinity of F-Ala and triF-Ala for the enzyme. The different phases observed monitoring the inactivation kinetics and absorbance spectra likely arise from the different ratio between enzyme concentration (10 μM in the absorbance spectra and 45 μM in the activity assays) and inactivator concentration.

We verified that the inhibition is irreversible by assaying the enzyme after 85-h reaction with 10 mM triF-Ala, complete removal of ligand by extensive ultrafiltration and incubation in the
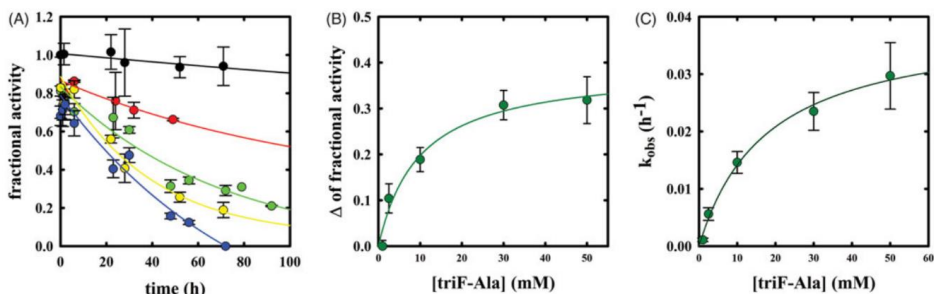
Figure 6. Panel A: Inactivation kinetics of OASS-A upon prolonged incubation time with 1 (black), 2.5 (red), 10 (green), 30 (yellow) and 50 mM (blue) triF-Ala. Panel B: Extent of OASS-A inactivation determined upon completion of the fast phase. Panel C: dependence of k_{obs} on the concentration of triF-Ala.
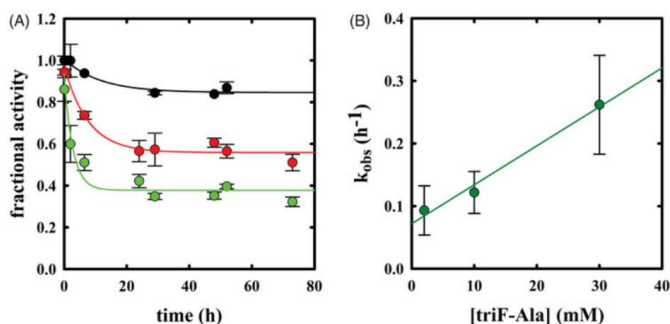
Figure 7. Panel A: Inactivation kinetics of OASS-B upon prolonged incubation time with 2 (black), 10 (red) and 30 mM (green) triF-Ala. Panel B: dependence of k_{obs} to the concentration of triF-Ala.

presence of saturating PLP concentration. We found that the remaining enzyme activity (about 25%) did not change upon ultrafiltration and incubation with PLP. This result indicates that enzyme inactivation brought about by triF-Ala does not involve displacement of the cofactor from the active site but is rather caused by an irreversible covalent modification of active site residue(s).

The kinetics of enzyme inactivation by triF-Ala was also measured on OASS-B (Figure 7(A)), observing again a biphasic enzyme inactivation. The amplitude of the fast phase is smaller but still dependent on reagent concentration, and the rate of the slow phase is about 10-fold faster than that observed for OASS-A and dependent on reagent concentration (Figure 7(B)). The dependence between k_{obs} and [I] appears to be linear, likely because the saturation conditions were not reached. k_{inact}/K_I was therefore estimated using the Equation (5) that describes single step inactivation and is $10.3 \times 10^{-5}\,min^{-1}\,mM^{-1}$.

In the case of OASS-B, there are two phases in the reaction of triF-Ala with OASS-B: a fast phase that occurs immediately upon addition of the reagent that can be followed by absorbance changes at 470 nm, followed by the slow disappearance of the shoulder at 470 nm that parallels the enzyme inactivation. Differently, from the OASS-A isozyme, the disappearance of the shoulder at 470 nm is accompanied not only by the recovery of the peak at 412 nm but also by the formation of a peak at about 320 nm, likely due to the accumulation of difluoropyruvate.

Table 1. Reactivity between OASS and alanine derivatives.

	R_1	R_2	Reactivity against OASS-A		Reactivity against OASS-B	
			% Inhibition*	Spectral changes	% Inhibition*	Spectral changes
1	CF_3CH_2	H	N.S.	No	18 ± 2	No
2	CF_3	Me	N.S.	No	N.S.	No
3	CHF_2CH_2	H	12 ± 1	No	16 ± 5	No
4	EtO_2CCF_2**	H	14 ± 1	No	N.S.	No

*% Inhibition was evaluated after 6 h incubation of the enzyme with 1 mM inhibitor, following 5000-times dilution for the assay (0.2 μM inhibitor in the assay) in two replicates. Percent inhibition of 10% or lower was considered not significant (N.S.).
**As TFA salt.

Several fluoroalanine derivatives were tested (Table 1) to assess the effect of chain extension branching and fluorine substitution (compounds **1–4**). None of these modifications resulted in an improvement in inactivation for both isozymes. In a further effort, series of trifluoroalanine derivatives where the carboxylic moiety

Table 2. Reactivity between OASS and β,β,β-trifluoroalanine carboxylate bioisosters.

$$F_3C \underset{NH_2}{\overset{\big|}{\diagdown}} R$$

		Reactivity against OASS-A		Reactivity against OASS-B	
	R	% Inhibition*	Spectral changes	% Inhibition*	Spectral changes
5	−C(=O)NHMe	N.S.	No	N.S.	No
6	−C(=O)NMe₂	N.S.	No	N.S.	No
7	−C(=O)NHPh	N.S.	No	N.S.	No
8	−C(=O)NBn₂	10 ± 2	No	N.S.	No
9	−C(=O)NH(p-₆H₁₃-Ph)	N.S.	No	12 ± 7	No
10	−C(=O)NHOH	15 ± 5	Yes	N.S.	No
11	−C(=O)NH₂	N.S.	No	N.S.	No
12	−P(=O)(OH)₂	N.S.	No	N.S.	No

*% Inhibition was evaluated after 6 h incubation of the enzyme with 1 mM inhibitor, following 5000-times dilution for the assay (0.2 μM inhibitor in the assay) in two replicates. Percent inhibition of 10% or lower was considered not significant (N.S.).

was substituted with bioisosters were tested (Table 2). These analogues were aimed to identify a scaffold with options to tune activity and selectivity of the inhibitor which is not possible for trifluoroalanine. A set of amides with different N-substitution patterns **5–11** was prepared. Again, negligible effects on enzyme activity were observed, with the exception of hydroxamic acid **10** that caused small absorbance changes in OASS-A (Figure 2SM) and about 14% decrease in enzyme activity.

On the basis of the spectral and kinetic data obtained by monitoring the reactivity of triF-Ala with OASS and taking into account reaction schemes previously proposed in the reaction of triF-Ala with other PLP-dependent enzymes[20,22,24,25,29,30,36], we propose an inactivation mechanism for OASS-A that is similar to the mechanism proposed for alanine racemase[30] (Scheme 2, path B). It is unlikely that the inactivation follows path A on Scheme 2 because decarboxylation does not occur in the catalytic cycle of OASS.

After the formation of the external aldimine, the elimination of HF leads to the formation of β,β-difluoro-α,β-unsaturated imine (intermediate **IB,** Scheme 2). The intermediate **IB** contains delocalised electrons that might account for the spectrum with bands at 440 and 466 nm. This species can be hydrolysed, with the release of difluoropyruvate and ammonia, leading to an internal aldimine. The ratio between hydrolysis and nucleophilic attack, which both lead to the decrease in the absorbance at 450–470 nm, is dictated by the concentration of inhibitor, geometry of active site residues and water accessibility. In the case of covalent modification, the species undergoes the Michael attack by the enzyme nucleophile, likely the active site lysine, leading to intermediate **IIB**. Formation of an intermediate absorbing at about 410–420 nm but distinct from the internal aldimine is supported by the fluorescence emission spectra (Figure 4(A)) where a decrease in the emission of a species at 495 nm was measured. Based on the literature data[25], we propose that this species is unstable and undergoes the addition of water on β-carbon, followed by the elimination of two fluoride ions, forming the intermediate **III B**. This step has been observed on alanine racemase after partial denaturation with sodium borohydride, suggesting that the active site needs to be open and accessible to water. The slow fluoride elimination is controlled by a conformational change occurring in the active site

that limits water accessibility. The final step might be the loss of the carboxylic moiety with formation of intermediate **IV B.**

Inactivation of OASS-B by triF-Ala follows the reaction scheme of the OASS-A isozyme although with different interconversion rates of intermediates. Indeed, in this case, external aldimine is the predominant species, as observed in the absorbance and fluorescence emission spectra. Elimination of HF leads to the formation of β,β-difluoro-α,β-unsaturated imine (**I B**) that does not accumulate to any significant extent. For this reason, the fraction of inactivated enzyme at this stage is small, differently from what observed for OASS-A isozyme where more intermediate accumulates. The Michael attack by the catalytic lysine leads to the elimination of difluoropyruvate, which absorbs at 320 nm, and ammonia. This reaction is more efficient for the OASS-B isozyme with respect to the OASS-A isozyme, thus preventing accumulation of the I B intermediate. Inactivation takes place by the same mechanism proposed for OASS-A by an attack of an active site nucleophile, likely the catalytic lysine, on the β-carbon.

Conclusions

The search for reversible and irreversible inhibitors of OASS-A and OASS-B is dictated by the relevance of these enzymes in the biosynthesis of cysteine in bacteria and by their absence in mammals. Cysteine depletion is associated with a decrease in bacterial fitness, thus enhancing antibiotics efficacy. Whereas reversible inhibitors for OASS-A and OASS-B with nanomolar/micromolar affinities have been identified[11,12,37], studies aiming at developing irreversible inhibitors are still lacking. The present investigation was aimed to fill this gap by exploring the reactivity of a class of compounds, fluoroalanine derivatives that are well-known inhibitors of PLP-dependent enzymes. We found that monofluoralanine is a weak substrate analogue for both isozymes, whereas trifluoroalanine acts as irreversible, although inefficient, inhibitor.

Disclosure statement

The authors report no conflict of interest.

Funding

References

1. Sekowska A, Kung H, Danchin A. Sulfur metabolism in *Escherichia coli* and related bacteria: facts and fiction. J Mol Microbiol Biotechnol 2000;2:145–77.
2. Cook PF, Wedding RT. Overall mechanism and rate equation for O-acetylserine sulfhydrylase. J Biol Chem 1977;252:3459.
3. Chattopadhyay A, Meier M, Ivaninskii S, et al. Structure, mechanism, and conformational dynamics of O-acetylserine sulfhydrylase from *Salmonella typhimurium*: comparison of A and B isozymes. Biochemistry 2007;46:8315–30.
4. Burkhard P, Jagannatha Rao G, Hohenester E, et al. Three-dimensional structure of O-acetylserine sulfhydrylase from *Salmonella typhimurium*. J Mol Biol 1998;283:121–33.
5. Cook PF, Wedding RT. A reaction mechanism from steady state kinetic studies for O-acetylserine sulfhydrylase from *Salmonella typhimurium* LT-2. J Biol Chem 1976;251:2023–9.

6. Tai CH, Nalabolu SR, Simmons JW, et al. Acid-base chemical mechanism of O-acetylserine sulfhydrylases-A and -B from pH studies. Biochemistry 1995;34:12311–22.
7. Salsi E, Guan R, Campanini B, et al. Exploring O-acetylserine sulfhydrylase-B isoenzyme from *Salmonella typhimurium* by fluorescence spectroscopy. Arch Biochem Biophys 2011;505: 178–85.
8. Benci S, Vaccari S, Mozzarelli A, Cook PF. Time-resolved fluorescence of O-acetylserine sulfhydrylase catalytic intermediates. Biochemistry 1997;36:15419–27.
9. Turnbull AL, Surette MG. L-Cysteine is required for induced antibiotic resistance in actively swarming *Salmonella enterica* serovar Typhimurium. Microbiology (Reading, Engl) 2008; 154:3410–19.
10. Turnbull AL, Surette MG. Cysteine biosynthesis, oxidative stress and antibiotic resistance in *Salmonella typhimurium*. Res Microbiol 2010;161:643–50.
11. Brunner K, Maric S, Reshma RS, et al. Inhibitors of the cysteine synthase CysM with antibacterial potency against dormant mycobacterium tuberculosis. J Med Chem 2016;59:6848–59.
12. Pieroni M, Annunziato G, Beato C, et al. Rational design, synthesis, and preliminary structure-activity relationships of α-substituted-2-phenylcyclopropane carboxylic acids as inhibitors of *Salmonella typhimurium* O-acetylserine sulfhydrylase. J Med Chem 2016;59:2567–78.
13. Spyrakis F, Felici P, Bayden AS, et al. Fine tuning of the active site modulates specificity in the interaction of O-acetylserine sulfhydrylase isozymes with serine acetyltransferase. Biochim Biophys Acta Proteins Proteomics 2013;1834:169–81.
14. Salsi E, Bayden AS, Spyrakis F, et al. Design of O-acetylserine sulfhydrylase inhibitors by mimicking nature. J Med Chem 2010;53:345–56.
15. Amori L, Katkevica S, Bruno A, et al. Design and synthesis of trans-2-substituted-cyclopropane-1-carboxylic acids as the first non-natural small molecule inhibitors of O-acetylserine sulfhydrylase. Medchemcomm 2012;3:1111.
16. Singh J, Petter RC, Baillie TA, Whitty A. The resurgence of covalent drugs. Nat Rev Drug Discov 2011;10:307–17.
17. Baillie TA. Targeted covalent inhibitors for drug design. Angew Chem Int Ed Engl 2016;55:13408–21.
18. Copeland RA. Evaluation of enzyme inhibitors in drug discovery: a guide for medicinal chemists and pharmacologists. John Wiley & Sons Inc 2005;46:214–247.
19. Silverman RB. Mechanism-based enzyme inactivators. Meth Enzymol 1995;249:240–83.
20. Silverman RB, Abeles RH. Mechanism of inactivation of gamma-cystathionase by beta,beta,beta-trifluoroalanine. Biochemistry 1977;16:5515–20.
21. Alston TA, Muramatsu H, Ueda T, Bright HJ. Inactivation of gamma-cystathionase by gamma-fluorinated amino acids. FEBS Lett 1981;128:293–7.
22. Azam MA, Jayaram U. Inhibitors of alanine racemase enzyme: a review. J Enzyme Inhib Med Chem 2016;31:517–26.
23. Phillips RS, Dua RK. Indole protects tryptophan indole-lyase, but not tryptophan synthase, from inactivation by trifluoroalanine. Arch Biochem Biophys 1992;296:489–96.
24. Silverman RB, Abeles RH. Inactivation of pyridoxal phosphate dependent enzymes by mono- and polyhaloalanines. Biochemistry 1976;15:4718–23.
25. Alexeev D, Baxter RL, Campopiano DJ, et al. Suicide inhibition of α-oxamine synthases: structures of the covalent adducts of 8-amino-7-oxononanoate synthase with trifluoroalanine. Org Biomol Chem 2006;4:1209.
26. Withers SG, Tysoe C. Fluorinated mechanism-based inhibitors: common themes and recent developments. Curr Top Med Chem 2014; 14:865–74.
27. John RA, Tudball N. Evidence for induced fit of a pseudo-substrate of aspartate aminotransferase. Eur J Biochem 1972;31:135–8.
28. Passera E, Campanini B, Rossi F, et al. Human kynurenine aminotransferase II-reactivity with substrates and inhibitors. FEBS J 2011;278:1882–900.
29. Wang EA, Walsh C. Characteristics of beta, beta-difluoroalanine and beta, beta, beta -trifluoroalanine as suicide substrates for Escherichia coli B alanine racemase. Biochemistry 1981;20:7539–46.
30. Faraci WS, Walsh CT. Mechanism of inactivation of alanine racemase by beta, beta, beta-trifluoroalanine. Biochemistry 1989;28:431–7.
31. Poulin R, Lu L, Ackermann B, et al. Mechanism of the irreversible inactivation of mouse ornithine decarboxylase by alpha-difluoromethylornithine. Characterization of sequences at the inhibitor and coenzyme binding sites. J Biol Chem 1992;267:150–8.
32. Tian H, Guan R, Salsi E, et al. Identification of the structural determinants for the stability of substrate and aminoacrylate external schiff bases in O-acetylserine sulfhydrylase-A. Biochemistry 2010;49:6093–103.
33. Gaitonde MK. A spectrophotometric method for the direct determination of cysteine in the presence of other naturally occurring amino acids. Biochem J 1967;104:627–33.
34. Cook PF, Hara S, Nalabolu S, Schnackerz KD. pH Dependence of the absorbance and 31P NMR spectra of O-acetylserine sulfhydrylase in the absence and presence of O-acetyl-L-serine. Biochemistry 1992;31:2298–303.
35. Benci S, Bettati S, Vaccari S, et al. Conformational probes of O-acetylserine sulfhydrylase: fluorescence of tryptophans 50 and 161. J Photochem Photobiol B Biol 1999;48:17–26.
36. Wang E, Walsh C. Suicide substrates for the alanine racemase of Escherichia coli B. Biochemistry 1978;17:1313–21.
37. Annunziato G, Pieroni M, Benoni R, et al. Cyclopropane-1,2-dicarboxylic acids as new tools for the biophysical investigation of O-acetylserine sulfhydrylases by fluorimetric methods and saturation transfer difference (STD) NMR. J Enzyme Inhib Med Chem 2016;31:78–87.

K. Grammatoglou, A. Jirgensons, Functionalization of
1*N*-Protected Tetrazoles by Deprotonation with the Turbo Grignard
Reagent. *J. Org. Chem.* **2022**, 87, 3810−3816

Functionalization of 1N-Protected Tetrazoles by Deprotonation with the Turbo Grignard Reagent

Konstantinos Grammatoglou and Aigars Jirgensons*

Cite This: *J. Org. Chem.* 2022, 87, 3810−3816

Read Online

ACCESS | Metrics & More | Article Recommendations | Supporting Information

ABSTRACT: 1N-PMB-protected tetrazole undergoes C−H deprotonation with the turbo Grignard reagent, providing a metalated intermediate with increased stability. This can be used for the reaction with electrophiles such as aldehydes, ketones, Weinreb amides, and iodine. C−H deprotonation with the turbo Grignard reagent is compatible with the PMB-protecting group at the tetrazole, which can be cleaved using oxidative hydrogenolysis and acidic conditions. The method enables the tetrazole functionalization at the fifth position by overcoming the difficulties associated with retro [2 + 3] cycloaddition of the metalated intermediates.
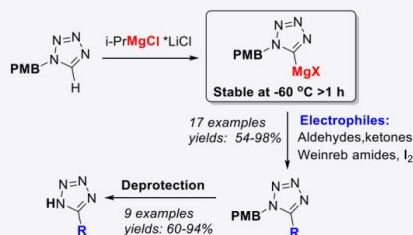
Tetrazole is an important substructure for the construction of value-added compounds with a range of applications. In medicinal chemistry, tetrazole is used as a bioisosteric replacement for carboxylic acids, owing to the weak NH acidity, as well as a bioisoster for cis-amide bonds.[1−5] As such, the tetrazole unit is represented in several approved drugs and drug candidates.[6−8] Other applications of tetrazole-containing compounds are explosives,[9,10] anion binders,[11−13] and organo-catalysts.[14,15] In addition, 5-(1-hydroxyalkyl)tetrazoles have been demonstrated as precursors of alkylidenecarbenes, which undergo rearrangements to acetylenes or C−H insertion reactions.[16,17]

The synthesis of tetrazole derivatives **3** involves two general approaches: construction of the cycle via cycloaddition or electrocyclization reactions[18,19] and the modification of N-protected tetrazole at the fifth position (Scheme 1).[16,20−24] The latter can be done via C−H deprotonation of tetrazole **1** or halogen-metal exchange of halogen derivative **2** to generate organometallic intermediates **4**, which are subjected to further modifications.[16,18,21−26] A well-known problem for the modification of tetrazole is the low stability of organometallic intermediates **4**, which tend to eliminate nitrogen forming cyanamide **5** as the byproduct (Scheme 1).[23,24] This is why the C−H deprotonation/reactions of tetrazoles should be done at very low temperatures (−100 °C) or why the deprotonation should be done in the presence of an electrophile.[22] Importantly, tetrazole-derived Grignard reagents (**4**, Met = "Mg") made by halogen-metal exchange showed considerably improved stability ($t_{1/2}$ = 3 h at −20 °C).[22] This method, however, requires 2-bromotetrazole derivative **2** as a starting material.

In this paper, we report direct functionalization of tetrazole **6** by C−H deprotonation with the turbo Grignard reagent,

providing an organomagnesium intermediate **7** with increased stability. The application of the metalated tetrazole was demonstrated by the reaction with electrophiles such as aldehydes, ketones, Weinreb amides, and iodine to give the corresponding products **8−10**, which can be deprotected to provide tetrazole derivatives **11**.

The 1N-PMB-protected tetrazole **6** was prepared from p-methoxybenzyl amine (**12**) in the reaction with triethylorthoformate and sodium azide according to the literature procedure (Table 1).[27] The efficiency of C−H deprotonation of tetrazole **6** with the turbo Grignard reagent was explored in THF, followed by the quench with CD$_3$OD. The composition of the products was investigated by NMR of a crude mixture (Table 1). Almost quantitative deprotonation was achieved at −60 °C as indicated by the clean formation of deuterated tetrazole d-**6** (Table 1, entries 1−3, see also Supporting Information for ^{1}H NMR). The metalated intermediate was stable at −60 °C for at least 60 min, which was in accordance with literature results on the Grignard reagent prepared by Mg insertion into the C−Br bond (Scheme 1). Warming the solution of the metalated intermediate to 0 °C resulted in considerable decomposition via retro [2 + 3] cycloaddition, leading to a mixture of deuterated tetrazole d-**6** and cyanamide **13** (Table 1, entry 4). Warming to room temperature led to cyanamide **13** as the major reaction product (Table 1, entry 5). Other Grignard

94

Scheme 1. Modification of the Tetrazole at the Fifth Position via the Metalated Intermediate
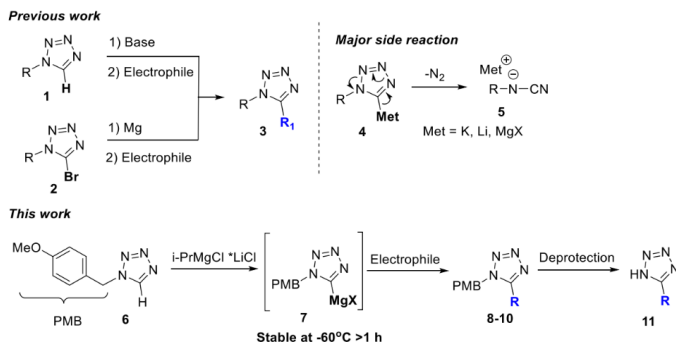
Table 1. Deprotonation of 1N-PMB-Protected Tetrazole with the Turbo Grignard Reagent[a]

entry	[M]	temp (°C)	time (min)	d-6 (%)[b]	13[b]
1	iPrMgCl·LiCl	−60	15	98	nd
2	iPrMgCl·LiCl	−60	30	99	nd
3	iPrMgCl·LiCl	−60	60	99	nd
4	iPrMgCl·LiCl	0[c]	30	54	35
5	iPrMgCl·LiCl	rt[c]	30	0	95
6	iPrMgCl	−60	15	53	nd
7	iPrMgCl	−60	30	78	nd
8	iPrMgCl	−60	60	76	nd
9	iPrMgBr	−60	15	57	nd
10	iPrMgBr	−60	30	57	nd
11	iPrMgBr	−60	60	69	nd

[a]1 mmol of tetrazole **6**, 1.2 mmol of iPrMgCl·LiCl, 4 equiv of CD$_3$OD. [b]Yields were calculated based on the weight of crude material; NMR did not reveal any other compounds apart from **6**,*d*-**6**, and **13**. [c]Deprotonation was performed at −60 °C; then cooling was removed to reach the indicated temperature.

reagents such as *i*PrMgCl and *i*PrMgBr were investigated; however, these turned out to be less efficient compared to the turbo Grignard (Table 1, entries 6−11).

Next, the reaction of tetrazole **6** with anisaldehyde **14a** was investigated (Table 2). Using THF as a solvent, deprotonation and addition to aldehyde **14a** provided the expected product **8a** in a very good isolated yield (Table 2, entry 1). After the addition of aldehyde **14a**, the reaction mixture can also be warmed to room temperature without impairing the yield of **8a** (Table 2, entry 2). Et$_2$O and toluene were also explored as solvents; however, they were found to be inappropriate for the formation of the product **8a** (Table 2, entries 3 and 4).

The range of aldehydes and ketones were explored as reaction partners for metalated intermediate prepared *in situ* from tetrazole **6** (Scheme 2). Alcohols **8b−n** were obtained in good to excellent yields from aromatic aldehydes **14b−e**, aliphatic aldehydes **14f−g**, and structurally diverse ketones **14h−n**.

Weinreb amides **15a−c** were also shown as competent reaction partners for metalated tetrazole **6**, giving ketones **9a−c** in good yields (Scheme 3).

Table 2. Deprotonation of Tetrazole 6 and the Reaction with Anisaldehyde 14a[a]

entry	solvent	temp (°C), time (h)	8a, yield (%)
1	THF	−60, 5	78[b]
2	THF	rt, 24[c]	76
3	Et$_2$O	−60, 5	47
4	toluene	−60, 5	22

[a]Tetrazole (1.1 equiv), iPrMgCl·LiCl (1.3 equiv), 2 mmol scale. After the addition of iPrMgCl·Cl, the reaction mixture was stirred for 30 min, and then aldehyde **14** was added. [b]88% yield of the product **8a** was obtained from the reaction performed on a 5 mmol scale. [c]Addition of aldehyde performed at −60 °C, then warmed to rt.

In addition, the iodination of tetrazole **6** gave 5-iodo-derivative **10** in an excellent yield (Scheme 4). Product **10** is a versatile building block for further functionalization, e.g., Suzuki−Miyaura reaction.[28,29]

95

Scheme 2. Addition of Metalated Tetrazole to Aldehydes and Ketones
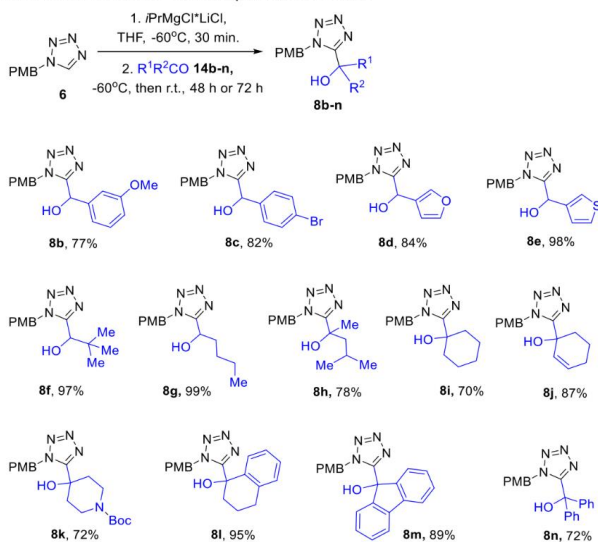
Scheme 3. Reaction of Metalated Tetrazole with Weinreb Amides
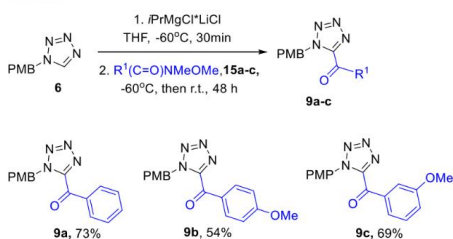
Scheme 4. Iodination of Metalated Tetrazole
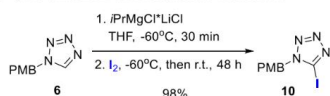
Deprotection of the 1N-PMB group in tetrazole derivatives was demonstrated for the protected derivatives **8** and **9** (Scheme 5). Oxidative cleavage (conditions A) of the PMB-protecting group provided tetrazole derivatives **11a,b,d,g,h**. Catalytic hydrogenation (conditions B) was applied for PMB deprotection to give tetrazoles **11a,c,e−g**. Acidic cleavage (conditions C) could also be used to obtain tetrazole **11i** from the protected precursor **9c**.

In summary, 1N-PMB-protected tetrazole undergoes C−H deprotonation with the turbo Grignard (iPrMgCl·LiCl) reagent providing a metalated intermediate with increased stability. To our knowledge, this is the first example of the application of the turbo Grignard on the deprotonation of tetrazoles. The metalated intermediate can be used for the reaction with electrophiles such as aldehydes, ketones, Weinreb amides, and iodine. C−H deprotonation is compatible with the PMB-protecting group at the tetrazole, which can be cleaved using oxidative, hydrogenolysis, and acidic conditions. Overall, the method enables the tetrazole functionalization at the fifth position by overcoming the difficulties associated with retro [2 + 3] cycloaddition of metalated intermediates.

■ EXPERIMENTAL SECTION

General Information. Commercially available reagents were used without further purification. All air- or moisture-sensitive reactions were carried out under an argon atmosphere using oven-dried glassware. Flash chromatography was carried out using Merck Kieselgel 60 (230−400 mesh). Thin-layer chromatography was performed on silica gel and was visualized by staining with $KMnO_4$. NMR spectra were recorded on a Varian Mercury spectrometer (400 MHz) and a Bruker Fourier spectrometer (300 MHz) with chemical shift values (δ) in ppm relative to TMS using the residual chloroform signal as an internal standard. Elemental analyses were performed using a Carlo-Erba EA1108 Elemental Analyzer. HRMS were obtained using a Q-TOF micro high-resolution mass spectrometer with ESI (ESI+/ESI−).

Synthesis of Starting Materials. 1-(4-Methoxybenzyl)-1H-tetrazole (**6**) is known in the literature.[30] It was synthesized according to the literature procedure.

N-Methoxy-N-methylbenzamide (**15a**) is known in the literature.[31] It was synthesized according to the literature procedure.

N,4-Dimethoxy-N-methylbenzamide (**15b**) is known in the literature.[32] It was synthesized according to the literature procedure.

N,3-Dimethoxy-N-methylbenzamide (**15c**) is known in the literature.[32] It was synthesized according to the literature procedure.

Deprotonation Studies of 1N-PMB-Protected Tetrazole. One mmol of 1N-PMB-protected tetrazole was dissolved in 5 mL

96

Scheme 5. Deprotection of the 1N-PMB Group in Tetrazole Derivatives
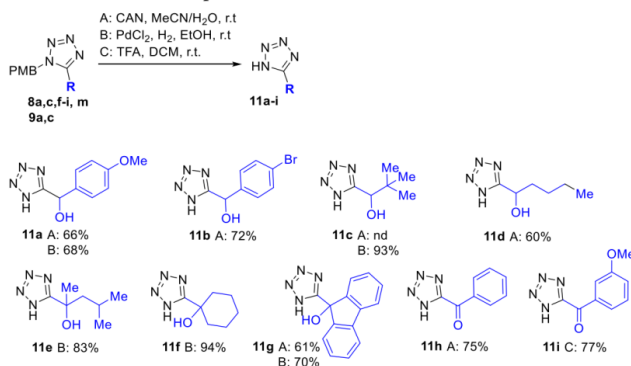
of THF and cooled to −60 °C. The turbo Grignard (*i*-PrMgCl·LiCl) reagent (1.2 equiv) was added dropwise, and stirring continued at this temperature for the specified time (Table 1). The reaction was quenched with CD₃OD (4 equiv) and after 10 min, AcOH was added (4 equiv); the reaction was left to reach room temperature. The reaction mixture was washed with brine and concentrated, and ¹H NMR was recorded.

General Protocol for the Reaction with Electrophiles. One mmol of 1N-PMB-protected tetrazole (1.1 equiv) was dissolved in 5 mL of THF and cooled to −60 °C. The isopropyl magnesium chloride−lithium chloride complex (1.3 equiv) was added dropwise, and after 30 min, at the same temperature, the corresponding electrophile (1 equiv), dissolved in 1 mL of THF, was added dropwise. The reaction mixture was slowly left to reach room temperature, and the stirring was continued for 24 h. NH₄Cl was added to quench the reaction, and the aqueous phase was extracted with EtOAc (×3) The combined organic phase was washed with brine, dried, and evaporated. The crude was purified with column chromatography on silica.

Deprotection Protocols. *Method A.* 1N-PMB-tetrazole (0.5 mmol, 1 equiv) was dissolved in 2 mL of MeCN and cooled to 0 °C. Ceric ammonium nitrate (CAN) (5 equiv) was dissolved in 1 mL of H₂O and added to the tetrazole solution. After 15 min, the cooling bath was removed, and the stirring continued for 3 h. Water was added, and the solution was extracted with EtOAc (4 × 5 mL). The combined organic phase was washed with brine, dried with Na₂SO₄, filtered, and evaporated. The crude was purified with chromatography on silica gel using gradient eluent DCM/MeOH/AcOH 98:1:1−92:5:3.

Method B. 1N-PMB-tetrazole (0.5 mmol, 1 equiv) was dissolved in 8 mL of EtOH in a pressure tube. PdCl₂ (5% mmol) was added, and the mixture was stirred under H₂ pressure (4 atm) overnight. The mixture was filtered through a Celite pad, evaporated, and purified with chromatography on silica gel using gradient eluent DCM/MeOH/AcOH 98:1:1−92:5:3.

Method C. 1N-PMB-tetrazole (0.5 mmol, 1 equiv) was dissolved in 2 mL of DCM, TFA (30 equiv) was added, and the mixture was stirred overnight. The solvent was evaporated, and the crude was purified with chromatography on silica gel using gradient eluent DCM/MeOH/AcOH 98:1:1−92:5:3.

Characterization of the Reaction Products. *(1-(4-Methoxybenzyl)-1H-tetrazol-5-yl)(4-methoxyphenyl)methanol (8a).* With a reaction time of 48 h, purification by flash chromatography (PE/EA = 2:1) gave a thick yellow oil (225.2 mg, 78%).

Product **8a** (1.44 g, 88% yield) was obtained by the general procedure starting from 1.0 g (5.2 mmol) of tetrazole **6** and 0.68 g (5.0 mmol) of aldehyde **14a**; the reaction was performed for 72 h.

¹H NMR (300 MHz, CDCl₃): δ 7.12 (d, *J* = 8.7 Hz, 2H), 6.96 (d, *J* = 8.7 Hz, 2H), 6.75 (dd, *J* = 15.6, 8.7 Hz, 4H), 6.11 (s, 1H), 5.40 (d, *J* = 14.8 Hz, 1H), 5.25 (d, *J* = 14.9 Hz, 1H), 4.36 (sb, 1H), 3.76 (s, 3H), 3.74 (s, 3H). ¹³C{¹H} NMR (101 MHz, CDCl₃): δ 159.8, 159.7, 156.0, 130.1, 129.6, 127.7, 125.2, 114.2, 114.1, 66.6, 55.3, 55.3, 51.1. HR-MS (ESI-TOF) *m/z*: calcd for C₁₇H₁₉N₄O₃, 327.1457; found, 327.1454.

(1-(4-Methoxybenzyl)-1H-tetrazol-5-yl)(3-methoxyphenyl)-methanol (8b). With a reaction time of 48 h, purification by flash chromatography (PE/EA = 2:1) gave a yellow gum (222.4 mg, 77%). ¹H NMR (400 MHz, CDCl₃): δ 7.22 (dd, *J* = 8.4, 7.7 Hz, 1H), 6.98 (d, *J* = 8.7 Hz, 2H), 6.86−6.79 (m, 3H), 6.74 (d, *J* = 8.8 Hz, 2H), 6.18 (d, *J* = 5.1 Hz, 1H), 5.40 (d, *J* = 14.9 Hz, 1H), 5.27 (d, *J* = 14.9 Hz, 1H), 4.32 (d, *J* = 5.2 Hz, 1H), 3.75 (s, 3H), 3.72 (s, 3H). ¹³C{¹H} NMR (101 MHz, CDCl₃): δ 160.0, 159.8, 155.6, 139.3, 130.0, 129.6, 125.2, 118.4, 114.4, 114.2, 111.7, 66.8, 55.3, 51.1. HR-MS (ESI-TOF) *m/z*: calcd for C₁₇H₁₈N₄O₃Na, 349.1277; found, 349.1275.

(4-Bromophenyl)(1-(4-methoxybenzyl)-1H-tetrazol-5-yl)-methanol (8c). Purification by flash chromatography (PE/EA = 2:1) gave a white solid (261.7 mg, 82%). Mp: 98−100 °C. ¹H NMR (400 MHz, CDCl₃): δ 7.36 (d, *J* = 8.5 Hz, 2H), 7.05 (d, *J* = 8.3 Hz, 2H), 6.92 (d, *J* = 8.7 Hz, 2H), 6.71 (d, *J* = 8.7 Hz, 2H), 6.18 (s, 1H), 5.42 (d, *J* = 14.9 Hz, 1H), 5.33 (d, *J* = 14.9 Hz, 1H), 3.75 (s, 3H). ¹³C{¹H} NMR (101 MHz, CDCl₃): δ 159.8, 155.4, 136.8, 131.9, 129.5, 127.8, 124.9, 122.7, 114.2, 66.1, 55.3, 51.2. HR-MS (ESI-TOF) *m/z*: calcd for C₁₆H₁₆BrN₄O₂, 375.0457; found, 375.0454.

Furan-3-yl(1-(4-methoxybenzyl)-1H-tetrazol-5-yl)methanol (8d). With a reaction time of 72 h, purification by flash chromatography (PE/EA = 2:1) gave a yellow gum (212 mg, 84%). ¹H NMR (400 MHz, CDCl₃): δ 7.38−7.34 (m, 2H), 7.11 (d, *J* = 8.7 Hz, 2H), 6.81 (d, *J* = 8.8 Hz, 2H), 6.24 (dd, *J* = 1.8, 1.0 Hz, 1H), 6.10 (d, *J* = 5.0 Hz, 1H), 5.52 (d, *J* = 14.8 Hz, 1H), 5.45 (d, *J* = 14.9 Hz, 1H), 4.09 (d, *J* = 5.7 Hz, 1H), 3.77 (s, 3H). ¹³C{¹H} NMR (101 MHz, CDCl₃): δ 159.9, 155.0, 144.1, 140.3, 129.6, 125.2, 123.8, 114.3, 108.7, 60.8, 55.3, 51.2. HR-MS (ESI-TOF) *m/z*: calcd for C₁₄H₁₄N₄O₃Na, 309.0964; found, 309.0959.

(1-(4-Methoxybenzyl)-1H-tetrazol-5-yl)(thiophen-3-yl)methanol (8e). With a reaction time of 48 h, purification by flash chromatography (PE/EA = 3:1) gave a yellow solid (270 mg, 98%). Mp: 68−70 °C. ¹H NMR (400 MHz, CDCl₃): δ 7.28−7.26 (m, 1H), 7.19 (dt, *J* = 3.0, 1.2 Hz, 1H), 7.01 (d, *J* = 8.7 Hz, 2H), 6.86 (dd, *J* = 5.0, 1.3 Hz, 1H), 6.77 (d, *J* = 8.7 Hz, 2H), 6.25 (dd, *J* = 5.5, 1.1 Hz, 1H), 5.43 (d, *J* = 14.8 Hz, 1H), 5.36 (d, *J* = 14.8 Hz, 1H), 4.41 (d, *J* = 5.5 Hz, 1H), 3.76 (s, 3H). ¹³C{¹H} NMR (101 MHz, CDCl₃): δ 159.8, 155.3, 139.2, 129.7, 127.2, 125.7, 125.2, 122.9, 114.2, 63.9, 55.3, 51.2. HR-MS (ESI-TOF) *m/z*: calcd for C₁₄H₁₄N₄O₂SNa, 325.0735; found, 325.0722.

97

1-(1-(4-Methoxybenzyl)-1H-tetrazol-5-yl)-2,2-dimethylpropan-1-ol (**8f**). With a reaction time of 48 h, purification by flash chromatography (PE/EA = 4:1) gave a white solid (245 mg, 97%). Mp: 109−112 °C. ^{1}H NMR (400 MHz, CDCl$_3$): δ 7.23 (d, J = 8.9 Hz, 2H), 6.85 (d, J = 8.7 Hz, 2H), 5.65 (d, J = 14.8 Hz, 1H), 5.52 (d, J = 14.8 Hz, 1H), 4.72 (d, J = 7.3 Hz, 1H), 3.78 (s, 3H), 2.97 (d, J = 7.3 Hz, 1H), 0.98 (s, 9H). ^{13}C{^{1}H} NMR (101 MHz, CDCl$_3$): δ 160.0, 154.8, 129.6, 126.1, 114.5, 73.5, 55.4, 51.6, 36.7, 25.7. HR-MS (ESI-TOF) m/z: calcd for C$_{14}$H$_{20}$N$_4$O$_2$Na, 299.1484; found, 299.1482.

1-(1-(4-Methoxybenzyl)-1H-tetrazol-5-yl)pentan-1-ol (**8g**). Purification by flash chromatography (PE/EA = 3:1) gave a white solid (228.4 mg, 99%). Mp: 54−57 °C. ^{1}H NMR (400 MHz, CDCl$_3$): δ 7.22 (d, J = 8.7 Hz, 2H), 6.85 (d, J = 8.7 Hz, 2H), 5.64 (d, J = 14.9 Hz, 1H), 5.58 (d, J = 14.9 Hz, 1H), 4.98−4.90 (m, 1H), 3.78 (s, 3H), 3.43 (d, J = 6.8 Hz, 1H), 1.89−1.72 (m, 2H), 1.43−1.14 (m, 4H), 0.82 (t, J = 7.0 Hz, 3H). ^{13}C{^{1}H} NMR (101 MHz, CDCl$_3$): δ 159.9, 156.1, 129.5, 125.8, 114.4, 65.2, 55.3, 51.1, 35.4, 27.2, 22.2, 13.8. HR-MS (ESI-TOF) m/z: calcd for C$_{14}$H$_{20}$N$_4$O$_2$Na, 299.1484; found, 299.1483.

2-(1-(Methoxybenzyl)-1H-tetrazol-5-yl)-4-methylpentan-2-ol (**8h**). With a reaction time of 72 h, purification by flash chromatography (PE/EA = 4:1) gave an offwhite solid (209.2 mg, 78%). Mp: 98−100 °C. ^{1}H NMR (400 MHz, CDCl$_3$): δ 7.26 (d, J = 8.7 Hz, 2H), 6.85 (d, J = 8.7 Hz, 2H), 5.75 (d, J = 3.9 Hz, 2H), 3.78 (s, 3H), 2.45 (s, 1H), 1.89 (dd, J = 14.3, 6.3 Hz, 1H), 1.75 (dd, J = 14.4, 5.9 Hz, 1H), 1.65 (s, 3H), 1.64−1.55 (m, 1H), 0.78 (d, J = 6.6 Hz, 3H), 0.71 (d, J = 6.6 Hz, 3H). ^{13}C{^{1}H} NMR (101 MHz, CDCl$_3$): δ 159.8, 158.6, 129.7, 127.0, 114.3, 72.9, 55.4, 52.1, 50.9, 29.6, 24.3, 24.1, 24.0. HR-MS (ESI-TOF) m/z: calcd for C$_{15}$H$_{22}$N$_4$O$_2$Na, 313.1640; found, 313.1642.

1-(1-(4-Methoxybenzyl)-1H-tetrazol-5-yl)cyclohexan-1-ol (**8i**). With a reaction time of 48 h, purification by flash chromatography (PE/EA = 3:1) gave a white solid (194 mg, 70%). Mp: 130−133 °C. ^{1}H NMR (400 MHz, CDCl$_3$): δ 7.22 (d, J = 8.7 Hz, 2H, Ar), 6.84 (d, J = 8.7 Hz, 2H), 5.74 (s, 2H), 3.78 (s, 3H), 2.48 (s, 1H), 2.09−1.94 (m, 2H), 1.86−1.73 (m, 2H), 1.65 (tq, J = 9.7, 3.5 Hz, 5H), 1.34 (dddd, J = 10.1, 8.3, 6.3, 3.4 Hz, 1H). ^{13}C{^{1}H} NMR (101 MHz, CDCl$_3$): δ 159.6, 159.0, 129.3, 127.0, 114.2, 70.8, 55.3, 51.8, 37.1, 24.8, 21.1. HR-MS (ESI-TOF) m/z: calcd for C$_{15}$H$_{20}$N$_4$O$_2$Na, 311.1484; found, 311.1491.

1-(1-(4-Methoxybenzyl)-1H-tetrazol-5-yl)cyclohex-2-en-1-ol (**8j**). With a reaction time of 48 h, purification by flash chromatography (PE/EA = 2:1) gave a yellow gum (208 mg, 87%). ^{1}H NMR (400 MHz, CDCl$_3$): δ 7.24 (d, J = 8.9 Hz, 2H), 6.85 (d, J = 8.7 Hz, 2H), 6.07 (ddd, J = 10.0, 4.4, 3.1 Hz, 1H), 5.81−5.77 (m, 1H), 5.73 (d, J = 3.8 Hz, 2H), 3.78 (s, 3H), 2.77 (s, 1H), 2.15−1.91 (m, 4H), 1.83−1.74 (m, 2H). ^{13}C{^{1}H} NMR (101 MHz, CDCl$_3$): δ 159.7, 158.1, 133.3, 129.5, 127.7, 126.7, 114.2, 68.6, 55.3, 51.7, 36.2, 24.6, 18.0. HR-MS (ESI-TOF) m/z: calcd for C$_{15}$H$_{18}$N$_4$O$_2$Na, 309.1327; found, 309.1325.

tert-Butyl 4-hydroxy-4-(1-(4-methoxybenzyl)-1H-tetrazol-5-yl)piperidine-1-carboxylate (**8k**). With a reaction time of 48 h, purification by flash chromatography (PE/EA = 2:1) gave a white solid (237.5 mg, 72%), dec > 80 °C. ^{1}H NMR (400 MHz, CDCl$_3$): δ 7.20 (d, J = 8.7 Hz, 2H), 6.84 (d, J = 8.7 Hz, 2H), 5.75 (s, 2H), 3.81 (t, J = 3.4 Hz, 2H), 3.78 (s, 3H), 3.68−3.54 (m, 1H), 3.24 (m, 2H), 2.15−1.99 (m, 2H), 1.75 (d, J = 14.0 Hz, 2H), 1.43 (s, 9H). ^{13}C{^{1}H} NMR (101 MHz, CDCl$_3$): δ 160.2, 158.6, 155.0, 129.8, 126.9, 114.7, 80.4, 69.2, 55.8, 52.3, 39.3, 36.7, 28.8. HR-MS (ESI-TOF) m/z: calcd for C$_{19}$H$_{27}$N$_5$O$_4$Na, 412.1961; found, 412.1968.

1-(1-(4-Methoxybenzyl)-1H-tetrazol-5-yl)-1,2,3,4-tetrahydronaphthalen-1-ol (**8l**). With a reaction time of 72 h, purification by flash chromatography (PE/EA = 4:1) gave a red oil (289 mg, 95%). ^{1}H NMR (400 MHz, CDCl$_3$): δ 7.18 (t, J = 7.5, 1.3 Hz, 1H), 7.11 (dd, J = 7.8, 1.3 Hz, 1H), 7.03 (td, J = 7.5, 7.0, 1.3 Hz, 1H), 6.94 (d, J = 8.7 Hz, 2H), 6.82 (dd, J = 7.8, 1.3 Hz, 1H), 6.73 (d, J = 8.7 Hz, 2H), 5.43 (d, J = 14.7 Hz, 1H), 5.07 (d, J = 14.7 Hz, 1H), 3.70 (s, 3H), 2.84−2.62 (m, 2H), 2.04−1.68 (m, 4H). ^{13}C{^{1}H} NMR (101 MHz, CDCl$_3$): δ 159.7, 159.6, 137.4, 136.7, 129.6, 129.5, 129.0,

128.4, 127.0, 126.0, 114.2, 71.8, 55.3, 51.9, 38.3, 29.2, 18.5. HR-MS (ESI-TOF) m/z: calcd for C$_{19}$H$_{20}$N$_4$O$_2$Na, 359.1484; found, 359.1486.

9-(1-(4-Methoxybenzyl)-1H-tetrazol-5-yl)-9H-fluoren-9-ol (**8m**). With a reaction time of 48 h, purification by flash chromatography (PE/EA = 8:1) gave a white solid (274.5 mg, 89%). Mp: 156−160 °C. ^{1}H NMR (400 MHz, CDCl$_3$): δ 7.65 (d, J = 7.6 Hz, 2H), 7.40 (td, J = 7.3, 1.5 Hz, 2H), 7.28−7.18 (m, 4H), 6.54 (d, J = 8.8 Hz, 2H), 6.43 (d, J = 8.7 Hz, 2H), 5.23 (sb, 1H), 4.67 (s, 2H), 3.68 (s, 3H). ^{13}C{^{1}H} NMR (101 MHz, CDCl$_3$): δ 159.4, 156.6, 144.6, 139.9, 130.6, 129.1, 129.0, 125.1, 124.9, 120.8, 113.8, 78.5, 55.3, 50.9.HR-MS (ESI-TOF) m/z: calcd for C$_{22}$H$_{18}$N$_4$O$_2$Na, 393.1327; found, 393.1337.

(1-(4-Methoxybenzyl)-1H-tetrazol-5-yl)diphenylmethanol (**8n**). With a reaction time of 48 h, purification by flash chromatography (PE/EA = 8:1) gave a colorless gum (236 mg, 72%). ^{1}H NMR (400 MHz, CDCl$_3$): δ 7.36−7.28 (m, 6H), 7.26−7.20 (m, 4H), 6.95 (d, J = 8.7 Hz, 2H), 6.69 (d, J = 8.7 Hz, 2H), 5.40 (s, 2H), 3.74 (s, 4H). ^{13}C{^{1}H} NMR (101 MHz, CDCl$_3$): δ 159.5, 158.0, 142.3, 129.9, 128.6, 128.5, 127.1, 126.0, 113.9, 77.5, 55.3, 52.0. HR-MS (ESI-TOF) m/z: calcd for C$_{22}$H$_{20}$N$_4$O$_2$Na, 395.1484; found, 395.1483.

(1-(4-Methoxybenzyl)-1H-tetrazol-5-yl)(phenyl)methanone (**9a**). With a reaction time of 48 h, purification by flash chromatography (PE/EA = 15:1) gave a colorless gum (182.5 mg, 73%), ^{1}H NMR (400 MHz, CDCl$_3$): δ 8.41−8.33 (m, 2H), 7.72−7.63 (m, 1H), 7.57−7.48 (m, 2H), 7.36 (d, J = 8.7 Hz, 2H), 6.84 (d, J = 8.8 Hz, 2H), 5.88 (s, 2H), 3.76 (s, 3H). ^{13}C{^{1}H} NMR (101 MHz, CDCl$_3$): δ 181.8, 160.1, 149.2, 135.2, 135.1, 131.2, 130.3, 128.9, 125.9, 114.4, 55.4, 52.8. HR-MS (ESI-TOF) m/z: calcd for C$_{16}$H$_{14}$N$_4$O$_2$Na, 317.1014; found, 317.1007.

(1-(4-Methoxybenzyl)-1H-tetrazol-5-yl)(4-methoxyphenyl)methanone (**9b**). With a reaction time of 48 h, purification by flash chromatography (PE/EA = 12:1) gave a white solid (149 mg, 54%). Mp: 97−99 °C. ^{1}H NMR (400 MHz, CDCl$_3$): δ 8.40 (d, J = 9.1 Hz, 2H), 7.35 (d, J = 8.7 Hz, 2H), 6.99 (d, J = 9.1 Hz, 2H), 6.83 (d, J = 8.8 Hz, 2H), 5.86 (s, 2H), 3.90 (s, 3H), 3.75 (s, 3H). ^{13}C{^{1}H} NMR (101 MHz, CDCl$_3$): δ 179.8, 165.4, 160.1, 149.4, 133.9, 130.3, 128.1, 126.0, 114.4, 114.3, 55.8, 55.4, 52.6. HR-MS (ESI-TOF) m/z: calcd for C$_{17}$H$_{16}$N$_4$O$_3$Na, 347.1120; found, 347.1115.

(1-(4-Methoxybenzyl)-1H-tetrazol-5-yl)(3-methoxyphenyl)methanone (**9c**). With a reaction time of 48 h, purification by flash chromatography (PE/EA = 12:1) gave a subyellow solid (189.4 mg, 69%). Mp: 79−81 °C. ^{1}H NMR (400 MHz, CDCl$_3$): δ 8.00 (ddd, J = 7.7, 1.6, 1.0 Hz, 1H), 7.86 (dd, J = 2.7, 1.6 Hz, 1H), 7.43 (t, J = 8.0 Hz, 1H), 7.36 (d, J = 8.8 Hz, 2H), 7.23 (ddd, J = 8.3, 2.7, 1.0 Hz, 1H), 6.84 (d, J = 8.7 Hz, 2H), 5.87 (s, 2H), 3.84 (s, 3H), 3.76 (s, 3H). ^{13}C{^{1}H} NMR (101 MHz, CDCl$_3$): δ 181.5, 160.1, 159.9, 149.2, 136.2, 130.3, 129.9, 125.9, 124.3, 122.3, 114.6, 114.5, 55.7, 55.4, 52.8. HR-MS (ESI-TOF) m/z: calcd for C$_{17}$H$_{16}$N$_4$O$_3$Na, 347.1120; found, 347.1105.

5-Iodo-1-(4-methoxybenzyl)-1H-tetrazole (**10**). With a reaction time of 48 h, purification by flash chromatography (PE/EA = 4:1) gave an off-white solid (263 mg, 98%). Mp: 120−122 °C. ^{1}H NMR (400 MHz, CDCl$_3$): δ 7.21 (d, J = 8.8 Hz, 2H), 6.82 (d, J = 8.7 Hz, 2H), 5.44 (s, 2H), 3.73 (s, 3H). ^{13}C{^{1}H} NMR (101 MHz, CDCl$_3$): δ 160.2, 129.7, 124.7, 114.5, 102.5, 55.4, 52.5. HR-MS (ESI-TOF) m/z: calcd for C$_9$H$_9$IN$_4$ONa, 338.9719; found, 338.9721.

(4-Methoxyphenyl)(1H-tetrazol-5-yl)methanol (**11a**). Purification by flash chromatography (DCM/MeOH/AcOH = 98:1:1−92:5:3) gave a white solid (method A: 63 mg, 66%; method B: 77.2 mg, 68%). Mp: 121−125 °C. ^{1}H NMR (400 MHz, CD$_3$OD): δ 7.35 (d, J = 8.6 Hz, 2H), 6.92 (d, J = 8.8 Hz, 2H), 6.10 (s, 1H), 3.77 (s, 3H). ^{13}C{^{1}H} NMR (101 MHz, CD$_3$OD): δ 159.9, 159.7, 132.3, 127.5, 113.7, 66.9, 54.3. HR-MS (ESI-TOF) m/z: calcd for C$_9$H$_9$N$_4$O$_2$, 205.0726; found, 205.0728.

(4-Bromophenyl)(1H-tetrazol-5-yl)methanol (**11b**). Purification by flash chromatography (DCM/MeOH/AcOH = 98:1:1−92:5:3) gave a white solid (method A: 88.2 mg, 72%). Mp: 175−180 °C. ^{1}H NMR (300 MHz, CD$_3$OD): δ 7.54 (d, J = 8.5 Hz, 2H), 7.39 (d, J = 8.5 Hz, 2H), 6.14 (s, 1H). ^{13}C{^{1}H} NMR (101 MHz, CD$_3$OD): δ

160.7, 141.0, 132.8, 129.4, 123.2, 67.9. HR-MS (ESI-TOF) m/z: calcd for $C_8H_6BrN_4O$, 252.9725; found, 252.9734.

2,2-Dimethyl-1-(1H-tetrazol-5-yl)propan-1-ol (11c). Purification by flash chromatography (DCM/MeOH/AcOH = 98:1:1−92:5:3) gave a white solid (method A: n.d.; method B: 79 mg, 93%). Mp: 208−212 °C. ^1H NMR (400 MHz, CD_3OD): δ 4.62 (s, 1H), 0.85 (s, 9H). $^{13}C\{^1H\}$ NMR (101 MHz, CD_3OD): δ 158.3, 72.7, 35.2, 24.5. HR-MS (ESI-TOF) m/z: calcd for $C_6H_{11}N_4O$, 155.0933; found, 155.0935.

1-(1H-Tetrazol-5-yl)pentan-1-ol (11d). Purification by flash chromatography (DCM/MeOH/AcOH = 98:1:1−92:5:3) gave a yellow amorphous solid (method A: 46 mg, 60%). ^1H NMR (400 MHz, CD_3OD): δ 5.04 (dd, J = 7.5, 5.4 Hz, 1H), 1.98−1.84 (m, 2H), 1.45−1.32 (m, 4H), 0.98−0.88 (m, 3H). $^{13}C\{^1H\}$ NMR (101 MHz, CD_3OD): δ 161.4, 66.0, 37.3, 28.1, 23.4, 14.3. HR-MS (ESI-TOF) m/z: calcd for $C_6H_{11}N_4O$, 155.0933; found, 155.0933.

4-Methyl-2-(1H-tetrazol-5-yl)pentan-2-ol (11e). Purification by flash chromatography (DCM/MeOH/AcOH = 98:1:1−92:5:3) gave a colorless oil (method B: 75.6 mg, 83%). ^1H NMR (400 MHz, CD_3OD): δ 1.98−1.74 (m, 2H), 1.63 (s, 3H), 1.63 (s, 1H), 0.88 (d, J = 6.7 Hz, 3H), 0.66 (d, J = 6.7 Hz, 3H). $^{13}C\{^1H\}$ NMR (101 MHz, CD_3OD): δ 164.2, 71.5, 52.3, 29.6, 25.3, 24.5, 24.0. HR-MS (ESI-TOF) m/z: calcd for $C_7H_{13}N_4O$, 169.1089; found, 169.1091.

1-(1H-Tetrazol-5-yl)cyclohexan-1-ol (11f). Purification by flash chromatography (DCM/MeOH/AcOH = 98:1:1−92:5:3) gave a white solid (method B: 87.8 mg, 94%). Mp: 128−131 °C. ^1H NMR (400 MHz, CD_3OD): δ 2.05−1.95 (m, 2H), 1.93−1.73 (m, 4H), 1.62 (ddq, J = 26.0, 13.5, 4.2 Hz, 3H), 1.50−1.35 (m, 1H). $^{13}C\{^1H\}$ NMR (101 MHz, CD_3OD): δ 163.3, 68.6, 36.8, 24.8, 21.0. HR-MS (ESI-TOF) m/z: calcd for $C_7H_{11}N_4O$, 167.0933; found, 167.0936.

9-(1H-Tetrazol-5-yl)-9H-fluoren-9-ol (11g). Purification by flash chromatography (DCM/MeOH/AcOH = 98:1:1−92:5:3) gave a yellow solid (method A: 76.4 mg, 61%; method B: 89 mg, 70%). Mp: 110−115 °C. ^1H NMR (400 MHz, CD_3OD): δ 7.79 (dt, J = 7.5, 0.9 Hz, 2H), 7.48−7.40 (m, 4H), 7.32 (td, J = 7.5, 1.1 Hz, 2H). $^{13}C\{^1H\}$ NMR (101 MHz, CD_3OD): δ 161.5, 147.9, 141.2, 131.1, 129.5, 125.7, 121.5, 79.2. HR-MS (ESI-TOF) m/z: calcd for $C_{14}H_9N_4O$, 249.0776; found, 249.0778.

Phenyl(1H-tetrazol-5-yl)methanone (11h). Purification by flash chromatography (DCM/MeOH/AcOH = 98:1:1−92:5:3) gave a light green solid (method A: 69 mg, 75%). Mp: 136−140 °C. ^1H NMR (400 MHz, CD_3OD): δ 8.48 (dd, J = 8.5, 1.3 Hz, 2H), 7.85−7.67 (m, 1H), 7.65−7.50 (m, 1H). $^{13}C\{^1H\}$ NMR (101 MHz, CD_3OD): δ 180.4, 154.2, 134.7, 134.5, 130.4, 128.5. In HRMS conditions, no signal was observed. LC-MS: 175.25.

(3-Methoxyphenyl)(1H-tetrazol-5-yl)methanone (11i). Purification by flash chromatography (DCM/MeOH/AcOH = 98:1:1−92:5:3) gave a green amorphous solid (method C: 78 mg, 77%). ^1H NMR (300 MHz, $CDCl_3$): δ 8.88 (sbr, 1H), 8.22 (d, J = 7.7 Hz, 1H), 7.99 (s, 1H), 7.40 (t, J = 8.0 Hz, 1H), 7.24−7.16 (m, 1H), 3.82 (s, 3H). $^{13}C\{^1H\}$ NMR (101 MHz, $CDCl_3$): δ 180.3, 159.9, 154.1, 135.2, 130.0, 124.2, 122.5, 114.5, 55.6. HR-MS (ESI-TOF) m/z: calcd for $C_9H_7N_4O_2$, 203.0569; found, 203.0569.

■ ASSOCIATED CONTENT

ⓈI Supporting Information

The Supporting Information is available free of charge at https://pubs.acs.org/doi/10.1021/acs.joc.1c02926.

    Copies of NMR spectra (PDF)

■ AUTHOR INFORMATION

Corresponding Author

    Aigars Jirgensons − *Latvian Institute of Organic Synthesis, LV-1006 Riga, Latvia;* ● orcid.org/0000-0002-8937-8792; Email: aigars@osi.lv

Author

    Konstantinos Grammatoglou − *Latvian Institute of Organic Synthesis, LV-1006 Riga, Latvia*

Complete contact information is available at:
https://pubs.acs.org/10.1021/acs.joc.1c02926

Notes

The authors declare no competing financial interest.

■ ACKNOWLEDGMENTS

■ REFERENCES

(1) Malik, M. A.; Wani, M. Y.; Al-Thabaiti, S. A.; Shiekh, R. A. Tetrazoles as carboxylic acid isosteres: chemistry and biology. *J. Incl. Phenom. Macrocycl. Chem.* **2014**, *78*, 15.

(2) Ballatore, C.; Huryn, D. M.; Smith, A. B., 3rd Carboxylic acid (bio)isosteres in drug design. *ChemMedChem* **2013**, *8*, 385.

(3) Ostrovskii, V. A.; Trifonov, R. E.; Popova, E. A. Medicinal chemistry of tetrazoles. *Russ. Chem. Bull.* **2012**, *61*, 768.

(4) Allen, F. H.; Groom, C. R.; Liebeschuetz, J. W.; Bardwell, D. A.; Olsson, T. S. G.; Wood, P. A. The Hydrogen Bond Environments of 1H-Tetrazole and Tetrazolate Rings: The Structural Basis for Tetrazole−Carboxylic Acid Bioisosterism. *J. Chem. Inf. Model* **2012**, *52*, 857.

(5) Matta, C. F.; Arabi, A. A.; Weaver, D. F. The bioisosteric similarity of the tetrazole and carboxylate anions: Clues from the topologies of the electrostatic potential and of the electron density. *Eur. J..Med. Chem.* **2010**, *45*, 1868.

(6) Myznikov, L. V.; Vorona, S. V.; Zevatskii, Y. E. Biologically active compounds and drugs in the tetrazole series. *Chem. Heterocycl. Compd.* **2021**, *57*, 224.

(7) Zou, Y.; Liu, L.; Liu, J.; Liu, G. Bioisosteres in drug discovery: focus on tetrazole. *Future Med. Chem.* **2020**, *12*, 91.

(8) Vitaku, E.; Smith, D. T.; Njardarson, J. T. Analysis of the Structural Diversity, Substitution Patterns, and Frequency of Nitrogen Heterocycles among U.S. FDA Approved Pharmaceuticals. *J. Med. Chem.* **2014**, *57*, 10257.

(9) Wurzenberger, M. H. H.; Endraß, S. M. J.; Lommel, M.; Klapötke, T. M.; Stierstorfer, J. Comparison of 1-Propyl-5H-tetrazole and 1-Azidopropyl-5H-tetrazole as Ligands for Laser Ignitable Energetic Materials. *ACS Appl. Energy Mater.* **2020**, *3*, 3798.

(10) Yin, P.; Zhang, Q;; Shreeve, J. N. M. Dancing with Energetic Nitrogen Atoms: Versatile N-Functionalization Strategies for N-Heterocyclic Frameworks in High Energy Density Materials. *Acc. Chem. Res.* **2016**, *49*, 4.

(11) Pinter, T.; Jana, S.; Courtemanche, R. J. M.; Hof, F. Recognition Properties of Carboxylic Acid Bioisosteres: Anion Binding by Tetrazoles, Aryl Sulfonamides, and Acyl Sulfonamides on a Calix[4]arene Scaffold. *J. Org. Chem.* **2011**, *76*, 3733.

(12) Pinter, T.; Simhadri, C.; Hof, F. Dissecting the Complex Recognition Interfaces of Potent Tetrazole- and Pyrrole-Based Anion Binders. *J. Org. Chem.* **2013**, *78*, 4642.

(13) McKie, A. H.; Friedland, S.; Hof, F. Tetrazoles are Potent Anion Recognition Elements That Emulate the Disfavored Anti Conformations of Carboxylic Acids. *Org. Lett.* **2008**, *10*, 4653.

(14) Shmatova, O. I.; Nenajdenko, V. G. Synthesis of Tetrazole-Derived Organocatalysts via Azido-Ugi Reaction with Cyclic Ketimines. *J. Org. Chem.* **2013**, *78*, 9214.

(15) Knudsen, K. R.; Mitchell, C. E. T.; Ley, S. V. Asymmetric organocatalytic conjugate addition of malonates to enones using a proline tetrazole catalyst. *Chem. Commun.* **2006**, 66.

(16) Alexakos, P. D.; Wardrop, D. J. N-Morpholinomethyl-5-lithiotetrazole: A Reagent for the One-Pot Synthesis of 5-(1-Hydroxyalkyl)tetrazoles. *J. Org. Chem.* **2019**, *84*, 12430.

(17) Wardrop, D. J.; Komenda, J. P. Dehydrative Fragmentation of 5-Hydroxyalkyl-1H-tetrazoles: A Mild Route to Alkylidenecarbenes. *Org. Lett.* **2012**, *14*, 1548.

(18) Neochoritis, C. G.; Zhao, T.; Domling, A. Tetrazoles via Multicomponent Reactions. *Chem. Rev.* **2019**, *119*, 1970.

(19) Roh, J.; Vávrová, K.; Hrabálek, A. Synthesis and Functionalization of 5-Substituted Tetrazoles. *Eur. J. Org. Chem.* **2012**, *2012*, 6101.

(20) Zhang, Y.; Lee, J. C. H.; Reese, M. R.; Boscoe, B. P.; Humphrey, J. M.; Helal, C. J. 5-Aryltetrazoles from Direct C−H Arylation with Aryl Bromides. *J. Org. Chem.* **2020**, *85*, 5718.

(21) Tüllmann, C. P.; Steiner, S.; Knochel, P. Preparation and Reactions of (1H-Tetrazol-5-yl)zinc Pivalates. *Synthesis* **2020**, *52*, 2357.

(22) Wiedemann, S. H.; Bio, M. M.; Brown, L. M.; Hansen, K. B.; Langille, N. F. Some Practical Methods for the Application of 5-Metallo-1-benzyl-1H-tetrazoles in Synthesis. *Synlett* **2012**, *23*, 2231.

(23) Satoh, Y.; Marcopulos, N. Application of 5-Lithiotetrazoles in Organic-Synthesis. *Tetrahedron Lett.* **1995**, *36*, 1759.

(24) Raap, R. Reactions of 1-Substituted 5-Tetrazolyllithium Compounds; Preparation of 5-Substituted 1-Methyltetrazoles. *Can. J. Chem.* **1971**, *49*, 2139.

(25) Satoh, Y.; De Lombaert, S.; Marcopulos, N.; Moliterni, J.; Moskal, M.; Tan, J.; Wallace, E. Synthesis of tetrazole analogs of alpha-amino acids by alkylation of a Schiff base of alpha-amino-methyltetrazole. *Tetrahedron Lett.* **1998**, *39*, 3367.

(26) Satoh, Y.; Moliterni, J. Homologation of 1-(benzyloxymethyl)-1H-tetrazole via lithiation. *Synlett* **1998**, *1998*, 528.

(27) Grigoriev, Y. V.; Voitekhovich, S. V.; Karavai, V. P.; Ivashkevich, O. A. Synthesis of tetrazole and its derivatives by heterocyclization reaction involving primary amines, orthoesters, and azides. *Chem. Heterocycl. Compd.* **2017**, *53*, 670.

(28) Carpenter, J.; Wang, Y.; Wu, G.; Feng, J.; Ye, X. Y.; Morales, C. L.; Broekema, M.; Rossi, K. A.; Miller, K. J.; Murphy, B. J.; Wu, G.; Malmstrom, S. E.; Azzara, A. V.; Sher, P. M.; Fevig, J. M.; Alt, A.; Bertekap, R. L., Jr.; Cullen, M. J.; Harper, T. M.; Foster, K.; Luk, E.; Xiang, Q.; Grubb, M. F.; Robl, J. A.; Wacker, D. A. Utilization of an Active Site Mutant Receptor for the Identification of Potent and Selective Atypical 5-HT2C Receptor Agonists. *J. Med. Chem.* **2017**, *60*, 6166.

(29) Abe, M.; Nishikawa, K.; Fukuda, H.; Nakanishi, K.; Tazawa, Y.; Taniguchi, T.; Park, S.-y.; Hiradate, S.; Fujii, Y.; Okuda, K.; Shindo, M. Key structural features of cis-cinnamic acid as an allelochemical. *Phytochemistry* **2012**, *84*, 56.

(30) Yang, H.; Ouyang, Y.; Ma, H.; Cong, H.; Zhuang, C.; Lok, W.-T.; Wang, Z.; Zhu, X.; Sun, Y.; Hong, W.; Wang, H. Design and synthesis of novel PRMT1 inhibitors and investigation of their binding preferences using molecular modelling. *Bioorg. Med. Chem. Lett.* **2017**, *27*, 4635.

(31) Peixoto, P. A.; Boulangé, A.; Leleu, S.; Franck, X. Versatile Synthesis of Acylfuranones by Reaction of Acylketenes with α-Hydroxy Ketones: Application to the One-Step Multicomponent Synthesis of Cadiolide B and Its Analogues. *Eur. J. Org. Chem.* **2013**, *2013*, 3316.

(32) Bourne, C.; Roy, S.; Wiley, J. L.; Martin, B. R.; Thomas, B. F.; Mahadevan, A.; Razdan, R. K. Novel, potent THC/anandamide (hybrid) analogs. *Bioorg. Med. Chem. Lett.* **2007**, *15*, 7850.

100

Publication No. 4

K. Grammatoglou, M. Dārziņa, A. Jirgensons, Functionalization of Tetrazoles Bearing the Electrochemically Cleavable 1*N*-(6–Methylpyridyl–2–methyl) Protecting Group. *ACS Omega* **2022**, 7, 18103−18109

Functionalization of Tetrazoles Bearing the Electrochemically Cleavable 1N-(6-Methylpyridyl-2-methyl) Protecting Group

Konstantinos Grammatoglou, Madara Dārziņa, and Aigars Jirgensons*
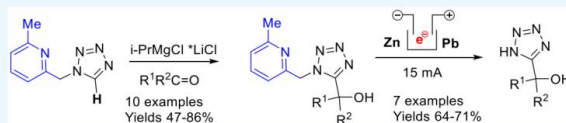
Cite This: ACS Omega 2022, 7, 18103−18109

Read Online

ACCESS | Metrics & More | Article Recommendations | Supporting Information

ABSTRACT: 6-Methylpyridyl-2-methyl protected tetrazoles can be C−H deprotonated using the turbo-Grignard reagent and involved in the reactions with aldehydes and ketones. The protecting group can be cleaved under reductive electrochemical conditions using Pb bronze as a cathode and Zn as a sacrificial anode.

INTRODUCTION

Tetrazoles do not exist in nature; however, the tetrazole motif is found in a number of useful compounds with an application in pharmacology,[1] catalysis,[2] and material science.[3] Representative examples of pharmacologically relevant tetrazole derivatives are the antihypertensive drug losartan,[4] antiasthmatic drug tomelukast (LY171883),[5] antibiotic tedizolid,[6] the multidrug resistance efflux pump inhibitor encequidar,[7] and an experimental antitumor agent BMS-317180[8] (Figure 1).

The importance of tetrazole containing compounds has motivated researchers to develop numerous methods for their synthesis.[9] Among them, C−H functionalization of tetrazoles via metalation is an attractive approach to install substituents at the fifth position. It should be noted, however, that lithiated tetrazoles suffer from low stability due to a rapid retro $[2 + 3]$ cycloaddition forming the cyanamide even at −78 °C.[9a-c] Organomagnesiun intermediates are considerably more stable ($t_{1/2}$ = 3 h at −20 °C), which enables the use of routine lab operations for their derivatization.[9c] Recently, we have reported generation organomagnesiun intermediates by C−H deprotonation of 1N-PMB protected tetrazole (1, PG = PMB), which was subsequently subjected to the reaction with electrophiles (Scheme 1).[10] To extend the utility of this approach, 1N-pyridyl-2-methyl protected tetrazoles 1a and 1b were investigated as substrates to give C−H functionalization products, which can be deprotected by the electrochemical reduction (Scheme 1).

RESULTS AND DISCUSSION

Methylpyridylmethyl protected tetrazole 1a was obtained according to a known method.[11] The 6-methyl analogue 1b was prepared by the alkylation of tetrazole (4) with bromomethylpyridine derivative 3 (Scheme 2). The reaction provided 1N alkylation product 1b as the major isomer

together with 2N alkylation product 5, which was separated by chromatography.

The deprotonation efficiency of substrates 1a and 1b was determined by the deuterium quench of the metalated intermediates generated by the reaction with the turbo-Grignard reagent (Table 1).

Pyridylmethyl protected tetrazole 1a gave moderate deuterium incorporation at the fifth position according to the NMR spectra of a reaction mixture (Table 1, entries 1 and 2). A high recovery of tetrazole 1a as well as product deuterated at the CH₂ group were observed. Imidazopyridine 6a was isolated from the reaction mixture as a minor impurity resulting from cyanamide 7a, a product of metalated tetrazole decomposition. Considerable improvement in a deuterium quench experiment was observed using methylpyridylmethyl protected tetrazole 1b as a substrate. High deuterium incorporation at the fifth position was observed after deprotonation with turbo-Grignard reagent at −60 °C (Table 1, entries 3−5). An increase of the temperature after the metalation step led to the formation of imidazopyridine 6b. This formed as a major product if the reaction mixture was warmed to room temperature. Better performance of methylpyridylmethyl protected tetrazole 1b compared to that of substrate 1a can be explained by blocking the relatively acidic C−H at the sixth position of pyridine, which could cause an equilibrium mixture of several metalated species.
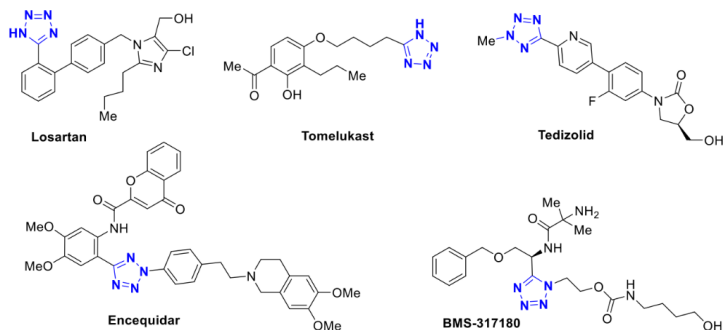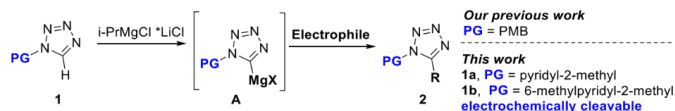
Figure 1. Representative examples of pharmacologically relevant tetrazole derivatives.

Scheme 1. Functionalization of Tetrazoles Bearing an Electrochemically Cleavable Protecting Group

Scheme 2. Synthesis of Methylpyridylmethyl Protected Tetrazole 1b
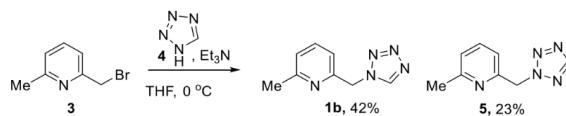
Table 1. Deprotonation Studies of Pyridyl Protected Tetrazoles 1a and 1b with Turbo-Grignard Reagent[a]
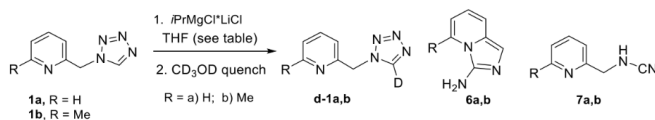
entry	temp.	time (min)	d-1, yield[b]	6, yield[b]
1	−60 °C	15	d-**1a**, ∼40%	**6a**, trace
2	−60 °C	60	d-**1a**, ∼60%	**6a**, trace
3	−60 °C	15	d-**1b**, 90%	**6a**, trace
4	−60 °C	30	d-**1b**, 97%	**6b**, n.d.
5	−60 °C	60	d-**1b**, 98%	**6b**, n.d.
6	0 °C[c]	30	d-**1b**, 55%	**6b**, ∼30%
7	r.t.[c]	30	d-**1b**, 0%	**6b**, 98%

[a]0.7 mmol of tetrazole and 1.2 equiv of turbo-Grignard reagent at −60 °C for the indicated time; quench with 3 equiv of MeOD, add 3 equiv of AcOH, and warm to r.t. [b]Yields were calculated on the basis of the weight of the crude material and the reduction of the integral intensity of the 5-CH group in the NMR spectra. [c]Deprotonation was performed at −60 °C, and then, the reaction was cooled to reach the indicated temperature.

Methylpyridylmethyl protected tetrazole **1b**, after metalation, was subjected to the reaction with aldehydes **8a−e** and ketones **8f−j** (Scheme 3). The addition of the metalated intermediate to aromatic aldehydes **8a** and **8b**, aliphatic aldehyde **8c**, and heteroaromatic aldehydes **8d** and **8e** was very productive, providing alcohols **9a−i**. The reaction with ketones **8f−j** was also successful to give alcohols **9f−9j** in moderate to good yields.

The pyridylmethyl group has been demonstrated to have electrochemically cleavable protection for thiols,[12,13] carboxylic acids,[14] and alcohols.[13,15] Similar electrochemical conditions were applied for the reductive cleavage of the methylpyridylmethyl group from tetrazole using compound **9a** as the model substrate. A range of electrodes and electrolytes was investigated at the fixed current and electric charge (Table 2). The best result was achieved using leaded bronze electrode as cathode, sacrificial zinc as anode, and TBA·BF$_4$ (tetrabutyla-

103

Scheme 3. Synthesis of Alcohols 9a−j by the Addition of Tetrazole 1b to Carbonyl Compounds

Table 2. Conditions for the Electrochemical Cleavage of the Methylpiridylmethyl Group in Tetrazole 9a

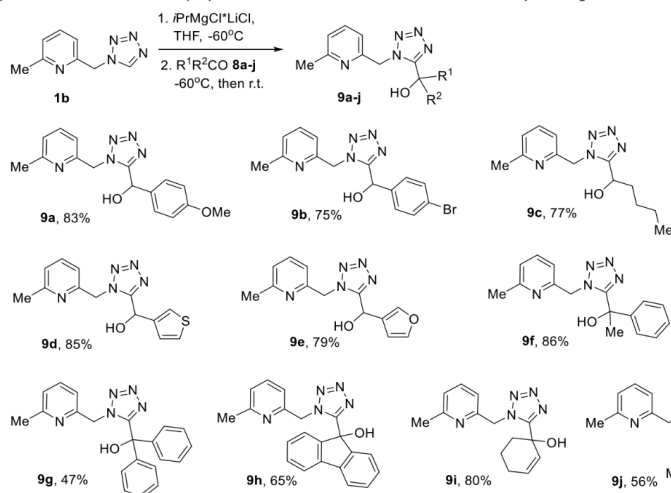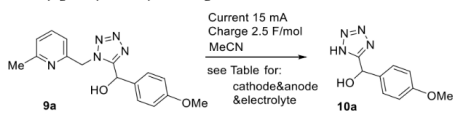| entry	cathode	anode	electrolyte	conversion of 9a to 10a, %[a]
1	Pb/bronze	Mg	TBABF₄	57
2	Pb	Mg	TBABF₄	24
4	Pb	Mg	LiClO₄	0
5	BDD	Mg	TBABF₄	24
6	Pb/bronze	Zn	TBABF₄	87 (67)[b]
7	Pb/bronze	Zn	TBAClO₄	42
8	Pb/bronze	Zn	TBAPF₆	6
9	Pb	Zn	TBABF₄	45
10	BDD	Zn	TBABF₄	76 (50)[b]

[a]Determined by the ratio of 10a and 9a in HPLC of the reaction mixture. [b]Isolated yield, %.

Scheme 4. Electrochemical Deprotection of the Methylpiridylmethyl Group in Tetrazoles 9b−g
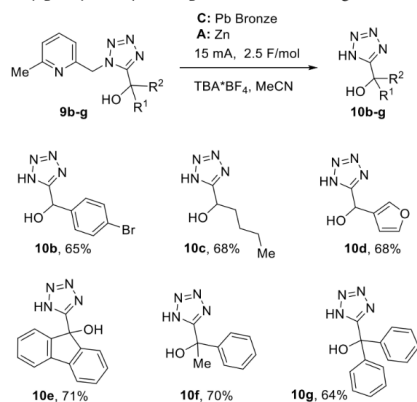
monium tetrafluoroborate) as electrolyte, providing deprotected tetrazole 10a in good isolated yield (Table 2, entry 6). A good conversion of the starting material 9a to deprotected tetrazole 10a was also observed using boron-doped diamond (BDD) as cathode and sacrificial zinc as anode (Table 2, entry 10).

The best electrochemical conditions found for the substrate 9a deprotection with Pb bronze cathode and the sacrificial Zn anode were applied for the deprotection of tetrazoles 9b−g (Scheme 4). The resulting free tetrazoles 10b−g were obtained in fair isolated yields despite high conversion of the starting materials 9b−g. The major loss of the product was due to the very polar nature of tetrazoles 10b−g, which complicated the isolation.

The proposed mechanism for the electrochemical cleavage of the 6-methyl-pyridylmethyl group from tetrazole 9 is provided in Scheme 5 in analogy to the cleavage of the O-(4-nitro)benzyl group.[16] The reduction of the pyridylmethyl group at the cathode by sacrificing the Zn anode leads to an anion radical **A**, which fragments to pyridylmethyl radical **B** and tetrazole anion [**10**]⁻. The pyridyl radical **B** undergoes further reactions, like hydrogen abstraction, dimerization, oxidation, and/or reduction to give a mixture of byproducts. The formation of pyridylmethyl radical **B** is supported by the observation of 2,6-lutidine by LC/MS analysis of the crude reaction mixture, which can form by either hydrogen abstraction or a reduction followed by a protonation.

Scheme 5. Proposed Mechanism for Electrochemical Cleavage of the Methylpyridylmethyl Group
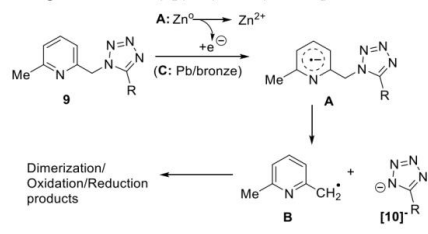
■ CONCLUSIONS

6-Methylpyridyl-2-methyl protected tetrazoles can be C−H deprotonated using the turbo-Grignard reagent and involved in the reactions with aldehydes and ketones. The protecting group can be cleaved in reductive electrochemical conditions using Pb bronze as a cathode and Zn as a sacrificial anode. This expands the utility of tetrazole functionalization via C−H deprotonation, particularly for the cases where selective protecting group cleavage should be achieved. To our knowledge, this is the first example for the protection of tetrazole with an electrochemically cleavable protecting group.

■ EXPERIMENTAL SECTION

General Information. Commercially available reagents were used without further purification. All air- or moisture-sensitive reactions were carried out under an argon atmosphere using oven-dried glassware. Flash chromatography was carried out using Merck Kieselgel 60 (230−400 mesh). Thin layer chromatography was performed on silica gel and was visualized by staining with KMnO$_4$. NMR spectra were recorded on a *Varian Mercury* spectrometer (400 MHz) and a *Bruker Fourier* spectrometer (300 MHz) with chemical shift values (δ) in ppm relative to TMS using the residual chloroform signal as an internal standard. Elemental analyses were performed using a Carlo-Erba EA1108 Elemental Analyzer. HRMS spectra were obtained using a Q-TOF micro high resolution mass spectrometer with ESI (ESI+/ESI−).

Synthesis of Starting Materials. *1H-Tetrazole (4).* 4 (11.4 g, 73%) was synthesized according to a literature procedure.[17]

2-(Bromomethyl)-6-methylpyridine (3). 3 (13.1 g, 68%) was synthesized according to a known method.[18]

2-(1H-Tetrazol-1-ylmethyl)pyridine (1a). 1a was synthesized according to a known method.[11]

2-Methyl-6-(1H-tetrazol-1-ylmethyl)pyridine (1b). A mixture of 1H-tetrazole (4) (2.9 g, 1.2 equiv), dry THF (150 mL), and 2-(bromomethyl)-6-methylpyridine (3) (6.5 g, 1 equiv) was cooled at 0 °C. Triethylamine (19.47 mL, 2.5 equiv) was added, and the mixture was left stirring overnight. Brine (450 mL) was added to quench the reaction, and the mixture was transferred to a separatory funnel and then extracted with ethyl acetate. The combined organic extracts were dried over sodium sulfate, filtered, and concentrated by a rotary evaporator. Concentration of the extract gave two isomers 1b and 5, which were separated by column chromatography on silica gel. The desired isomer 1b was obtained in high purity (>96%) as an off-white solid.

General Protocol for the Reaction of Tetrazole 1b with Electrophiles. The tetrazole (1b, 1.1. equiv) was dissolved in THF (0.12 M) and cooled to −60 °C. An isopropyl magnesium chloride−lithium chloride complex (1.2 equiv) was added dropwise and, after 30 min, at the same temperature, the corresponding electrophile (1 equiv), dissolved in THF (0.7 M), was added dropwise. The reaction mixture was slowly left to reach room temperature and stirring continued for 24−72 h. NH$_4$Cl was added to quench the reaction; the aqueous phase was extracted with EtOAc (3×), and the combined organics were washed with brine, dried, and evaporated. The crude was purified with column chromatography on silica.

General Protocol for Electrolytic Removal of the 6-Methyl-pyridylmethyl Protecting Group. A single cell with leaded bronze as a cathode and zinc as an anode was charged with 0.28−0.3 mmol of the corresponding tetrazole 9 and supporting electrolyte TBABF$_4$ (1 equiv) under an inert atmosphere. Dry MeCN (7.5 mL) was added, and the reaction was started by applying constant current (15 mA, total charge of 2.5 F/mol). After the end of the reaction, AcOH (1 equiv) was added and the mixture was diluted with EtOAc and water. The aqueous phase was extracted with EtOAc, and the combined organics were washed with 1 N aqueous HCl and brine, dried, and evaporated; product 10 was purified by column chromatography eluted with a mixture of petroleum ether/ethyl acetae/acetic acid (1:1:0.04).

Characterization of the Products. *2-(1H-Tetrazol-1-ylmethyl)pyridine (1a).* 1a, 1.2 g, 76%. ^{1}H NMR (400 MHz, CDCl$_3$) δ 8.87 (s, 1H, −C$\underline{H}$−), 8.58 (ddd, J = 4.8, 1.9, 1.0 Hz, 1H, Ar), 7.73 (td, J = 7.7, 1.8 Hz, 1H, Ar), 7.36−7.26 (m, 2H, Ar), 5.71 (s, 2H, −C$\underline{H}_2$−). ^{13}C NMR (101 MHz, CDCl$_3$) δ 152.46, 150.13, 143.11, 137.59, 123.95, 122.74, 53.30.

2-Methyl-6-(1H-tetrazol-1-ylmethyl)pyridine (1b). 1b, off-white solid (2.55 g, 42%), mp 53−55 °C. ^{1}H NMR (300 MHz, CDCl$_3$) δ 8.87 (s, 1H, −C$\underline{H}$−), 7.59 (t, J = 7.7 Hz, 1H, Ar), 7.10 (dd, J = 17.0, 7.7 Hz, 2H, Ar), 5.64 (s, 2H, −C$\underline{H}_2$−), 2.51 (s, 3H, −C$\underline{H}_3$). ^{13}C NMR (101 MHz, CDCl$_3$) δ 159.40, 151.78, 143.15, 137.78, 123.66, 119.75, 53.52, 24.46. Element. Anal. for C$_8$H$_9$N$_5$: N, 39.98; C, 54.85; H, 5.18. Found: N, 39.99; C, 54.85; H, 5.11. HR-MS (ESI-TOF) m/z: Calcd for C$_8$H$_9$N$_5$Na 198.0756; Found [M + Na]$^+$ 198.0758.

4-(Methoxyphenyl)(1-((6-methylpyridin-2-yl)methyl)-1H-tetrazol-5-yl)methanol (9a). 9a, white solid (83%), mp 91−95 °C. ^{1}H NMR (400 MHz, CDCl$_3$) δ 7.60 (t, J = 7.7 Hz, 1H, pyr.), 7.28 (dd, J = 8.9, 0.8 Hz, 1H, Ar), 7.19 (d, J = 7.1 Hz, 1H, pyr.), 7.11 (d, J = 7.8 Hz, 1H, pyr.), 6.82 (d, J = 8.8 Hz, 2H, Ar), 6.38 (s, 1H, −C$\underline{H}$−OH), 5.45 (d, J = 14.8 Hz, 1H, −C$\underline{H}_2$−), 5.34 (d, J = 14.8 Hz, 1H, −C$\underline{H}_2$−), 3.73 (s, 3H, −OC$\underline{H}_3$), 2.44 (s, 3H, −C$\underline{H}_3$). ^{13}C NMR (101 MHz, CDCl$_3$) δ 159.55, 158.87, 156.90, 151.36, 138.83, 131.38, 127.21, 124.26, 120.87, 114.13, 66.12, 55.33, 52.14, 23.54. HR-MS (ESI-TOF) m/z: Calcd for C$_{16}$H$_{17}$N$_5$O$_2$Na 334.1280; Found [M + Na]$^+$ 334.1279.

(4-Bromophenyl)(1-((6-methylpyridin-2-yl)methyl)-1H-tetrazol-5-yl)methanol (9b). 9b, light green solid (75%), mp 131−135 °C. ^{1}H NMR (400 MHz, chloroform-d) δ 7.71 (t, J = 7.7 Hz, 1H, pyr.), 7.51 (d, J = 8.5 Hz, 2H, Ar), 7.37 (d, J = 7.9 Hz, 1H, Ar), 7.31 (d, J = 7.6 Hz, 1H, pyr.), 7.22 (d, J = 7.8 Hz, 1H, pyr.), 6.46 (s, 1H, −C$\underline{H}$−OH), 5.58 (d, J = 14.8 Hz, 1H, −C$\underline{H}_2$−), 5.45 (d, J = 14.8 Hz, 1H, −C$\underline{H}_2$−), 2.53 (s, 3H, −C$\underline{H}_3$). ^{13}C NMR (101 MHz, CDCl3) δ 158.90, 156.34, 151.09, 139.00, 138.39, 131.85, 127.77, 124.43, 122.41, 120.99,

65.92, 52.19, 23.51. HR-MS (ESI-TOF) m/z: Calcd for $C_{15}H_{15}BrN_5O$ 360.0460; Found $[M + H]^+$ 360.0470.

1-(1-((6-Methylpyridin-2-yl)methyl)-1H-tetrazol-5-yl)-pentan-1-ol (9c). **9c**, white solid (77%), mp 105−108 °C. ^1H NMR (400 MHz, chloroform-d) δ 7.68 (t, J = 7.7 Hz, 1H, pyr.), 7.33 (d, J = 7.6 Hz, 1H, pyr.), 7.18 (d, J = 7.8 Hz, 1H, pyr.), 7.06 (sb, 1H, −O$\underline{H}$), 5.80 (d, J = 14.6 Hz, 1H, −C$\underline{H}_2$−), 5.68 (d, J = 14.6 Hz, 1H, −C$\underline{H}_2$−), 5.18 (dd, J = 7.9, 5.2 Hz, 1H, −C$\underline{H}$−OH), 2.50 (s, 3H, −C$\underline{H}_3$), 2.21−1.94 (m, 2H, −C$\underline{H}_2$−), 1.60−1.35 (m, 4H, −C$\underline{H}_2$−C$\underline{H}_2$−), 0.92 (t, J = 7.2 Hz, 3H, −C$\underline{H}_3$). ^{13}C NMR (101 MHz, CDCl3) δ 158.86, 157.26, 151.66, 138.78, 124.21, 121.01, 64.90, 52.27, 35.58, 27.44, 23.73, 22.47, 14.00. HR-MS (ESI-TOF) m/z: Calcd for $C_{13}H_{20}N_5O$ 262.1668; Found $[M + H]^+$ 262.1667.

(1-((6-Methylpyridin-2-yl)methyl)-1H-tetrazol-5-yl)-(thiophen-3-yl)methanol (9d). **9d**, subwhite solid (85%), mp 76−80 °C. ^1H NMR (400 MHz, CDCl$_3$) δ 7.97 (sb, 1H, −O$\underline{H}$) 7.62 (t, J = 7.7 Hz, 1H, pyr.), 7.32 (dt, J = 2.7, 1.3 Hz, 1H, thioph.), 7.28 (dd, J = 5.0, 3.1 Hz, 1H, thioph.), 7.20 (d, J = 7.6 Hz, 1H, pyr.), 7.13 (d, J = 7.8 Hz, 1H, pyr.), 6.97 (dd, J = 5.0, 1.3 Hz, 1H, thioph.), 6.47 (d, J = 1.2 Hz, 1H, −C$\underline{H}$−OH), 5.55 (d, J = 14.8 Hz, 1H, −C$\underline{H}_2$−), 5.41 (d, J = 14.8 Hz, 1H, −C$\underline{H}_2$−), 2.43 (s, 3H, −C$\underline{H}_3$). ^{13}C NMR (101 MHz, CDCl$_3$) δ 158.79, 156.24, 151.33, 140.75, 138.80, 126.98, 125.65, 124.22, 122.31, 120.82, 63.80, 52.24, 23.52. HR-MS (ESI-TOF) m/z: Calcd for $C_{13}H_{14}N_5OS$ 288.0919; Found $[M + H]^+$ 288.0909.

Furan-3-yl(1-((6-methylpyridin-2-yl)methyl)-1H-tetrazol-5-yl)methanol (9e). **9e**, light brown solid (79%), mp 71−75 °C. ^1H NMR (400 MHz, CDCl$_3$) δ 7.69 (t, J = 7.7 Hz, 1H, pyr.), 7.52 (q, J = 1.2 Hz, 1H, furan), 7.42 (t, J = 1.8 Hz, 1H, furan), 7.31 (d, J = 7.6 Hz, 1H, pyr.), 7.18 (d, J = 7.8 Hz, 1H, pyr.), 6.40 (d, J = 1.3 Hz, 2H, furan), 5.64 (s, 2H, −C$\underline{H}_2$−), 2.48 (s, 3H, −C$\underline{H}_3$). ^{13}C NMR (101 MHz, CDCl$_3$) δ 158.92, 156.00, 151.31, 143.92, 140.23, 138.90, 125.18, 124.35, 121.02, 108.84, 61.01, 52.32, 23.54. HR-MS (ESI-TOF) m/z: Calcd for $C_{13}H_{14}N_5O_2$ 272.1147; Found $[M + H]^+$ 272.1151.

1-(1-((6-Methylpyridin-2-yl)methyl)-1H-tetrazol-5-yl)-1-phenylethan-1-ol (9f). **9f**, yellow crystalline (86%), mp 106−109 °C. ^1H NMR (400 MHz, CDCl$_3$) δ 7.64 (t, J = 7.7 Hz, 1H, pyr.), 7.48−7.41 (m, 2H, Ar), 7.37−7.25 (m, 3H, Ar), 7.21 (d, J = 7.6 Hz, 1H, pyr.), 7.15 (d, J = 7.8 Hz, 1H, pyr.), 5.38 (d, J = 14.8 Hz, 1H, −C$\underline{H}_2$−), 5.12 (d, J = 14.8 Hz, 1H, −C$\underline{H}_2$−), 2.51 (s, 3H, −C$\underline{H}_3$), 2.16 (s, 3H, −C$\underline{H}_3$). ^{13}C NMR (101 MHz, CDCl$_3$) δ 159.48, 158.60, 151.44, 144.76, 138.93, 128.69, 127.85, 124.80, 124.23, 120.92, 71.11, 52.21, 31.99, 23.38. HR-MS (ESI-TOF) m/z: Calcd for $C_{16}H_{18}N_5O$ 296.1511; Found $[M + H]^+$ 296.1516.

(1-((6-Methylpyridin-2-yl)methyl)-1H-tetrazol-5-yl)-diphenyl Methanol (9g). **9g**, subyellow solid (47%), mp 108−112 °C. ^1H NMR (400 MHz, CDCl$_3$) δ 7.66 (t, J = 7.7 Hz, 1H, pyr.), 7.47−7.41 (m, 4H, Ar), 7.38−7.26 (m, 7H, Ar(6H) + pyr.(1H)), 7.12 (d, J = 7.8 Hz, 1H, pyr.), 5.72 (s, 2H, −C$\underline{H}_2$−), 2.31 (s, 3H, −C$\underline{H}_3$). ^{13}C NMR (101 MHz, CDCl$_3$) δ 159.04, 158.58, 151.64, 144.28, 139.09, 128.17, 127.96, 127.11, 124.33, 121.17, 76.65, 52.97, 23.16. HR-MS (ESI-TOF) m/z: Calcd for $C_{21}H_{20}N_5O$ 358.1668; Found $[M + H]^+$ 358.1666.

9-(1-((6-Methylpyridin-2-yl)methyl)-1H-tetrazol-5-yl)-9H-fluoren-9-ol (9h). **9h**, yellow solid (65%), mp 165−170 °C. ^1H NMR (400 MHz, CDCl$_3$) δ 8.33 (s, 1H, −O$\underline{H}$), 7.72−7.64 (m, 3H, pyr.(1H) + Ar(2H)), 7.40 (ddd, J = 7.5, 6.9, 1.7 Hz, 2H, Ar), 7.33−7.16 (m, 6H. pyr.(2H) + Ar(4H)), 5.98 (s, 2H,

−C$\underline{H}_2$−), 2.58 (s, 3H, −C$\underline{H}_3$). ^{13}C NMR (101 MHz, CDCl$_3$) δ 158.54, 157.81, 151.94, 146.88, 139.84, 138.89, 130.00, 128.44, 124.25, 124.11, 120.78, 120.75, 79.37, 53.03, 23.85. HR-MS (ESI-TOF) m/z: Calcd for $C_{21}H_{18}N_5O$ 356.1511; Found $[M + H]^+$ 356.1508.

1-(1-((6-Methylpyridin-2-yl)methyl)-1H-tetrazol-5-yl)-cyclohex-2-en-1-ol (9i). **9i**, beige solid (80%), mp 92−95 °C. ^1H NMR (400 MHz, CDCl$_3$) δ 7.67 (t, J = 7.7 Hz, 1H, pyr.), 7.44 (sb, 1H, −O$\underline{H}$), 7.29 (d, J = 7.6 Hz, 1H, pyr.), 7.17 (d, J = 7.8 Hz, 1H, pyr.), 6.03 (dt, J = 9.9, 3.7 Hz, 1H, −C$\underline{H}$=CH−), 5.95 (d, J = 14.5 Hz, 1H, −C$\underline{H}_2$−), 5.85 (d, J = 14.5 Hz, 1H, −C$\underline{H}_2$−), 5.79 (dd, J = 10.0, 1.0 Hz, 1H, −CH=C$\underline{H}$−), 2.51 (s, 3H, −C$\underline{H}_3$), 2.27 (ddd, J = 13.2, 10.3, 3.6 Hz, 1H, −C$\underline{H}_2$−), 2.18 (dddd, J = 9.3, 5.7, 3.3, 2.2 Hz, 2H, −C$\underline{H}_2$−), 2.10 (dddd, J = 13.3, 7.2, 3.2, 1.1 Hz, 1H, −C$\underline{H}_2$−), 2.01−1.83 (m, 2H, −C$\underline{H}_2$−). ^{13}C NMR (101 MHz, CDCl$_3$) δ 160.01, 158.61, 152.27, 138.70, 131.13, 129.20, 124.05, 120.93, 68.58, 53.11, 37.21, 24.62, 23.79, 18.08. HR-MS (ESI-TOF) m/z: Calcd for $C_{14}H_{17}N_5O$ 272.1511; Found $[M + H]^+$ 272.1513.

4-Methyl-2-(1-((6-methylpyridin-2-yl)methyl)-1H-tetrazol-5-yl)pentan-2-ol (9j). **9j**, thick yellow oil (56%). ^1H NMR (400 MHz, chloroform-d) δ 7.69 (t, J = 7.7 Hz, 1H, pyr.), 7.35 (d, J = 7.5 Hz, 1H, pyr.), 7.18 (d, J = 7.8 Hz, 1H, pyr.), 5.99 (d, J = 14.2 Hz, 1H, −C$\underline{H}_2$−), 5.82 (d, J = 14.3 Hz, 1H, −C$\underline{H}_2$−), 2.52 (s, 3H, −C$\underline{H}_3$), 2.05 (dd, J = 14.2, 6.7 Hz, 1H, −C$\underline{H}_2$−), 1.95 (dd, J = 14.2, 5.5 Hz, 1H, −C$\underline{H}_2$−), 1.86−1.75 (m, 1H, −C$\underline{H}$−), 1.72 (s, 1H, −C$\underline{H}_3$), 0.98 (d, J = 6.7 Hz, 3H, −C$\underline{H}_3$), 0.73 (d, J = 6.7 Hz, 3H, −C$\underline{H}_3$). ^{13}C NMR (101 MHz, CDCl3) δ 160.53, 158.50, 152.28, 138.93, 124.22, 121.35, 72.49, 52.93, 51.62, 31.57, 24.61, 24.41, 23.68, 23.63. HR-MS (ESI-TOF) m/z: Calcd for $C_{14}H_{22}N_5O$ 276.1824; Found $[M + H]^+$ 276.1834.

(4-Methoxyphenyl)(1H-tetrazol-5-yl)methanol (10a). **10a**, 67%. ^1H NMR (300 MHz, CD$_3$OD) δ 7.35 (d, J = 8.7 Hz, 2H, Ar), 6.92 (d, J = 8.7 Hz, 2H, Ar), 6.10 (s, 1H, −C$\underline{H}$−OH), 3.77 (s, 3H, −OC$\underline{H}_3$).[10]

(4-Bromophenyl)(1H-tetrazol-5-yl)methanol (10b). **10b**, 65%. ^1H NMR (300 MHz, CD$_3$OD) δ 7.54 (d, J = 8.5 Hz, 2H, Ar), 7.39 (d, J = 8.4 Hz, 2H, Ar), 6.14 (s, 1H, −C$\underline{H}$−OH).[10]

1-(1H-Tetrazol-5-yl)pentan-1-ol (10c). **10c**, 68%. ^1H NMR (300 MHz, CD$_3$OD) δ 5.04 (t, J = 6.5 Hz, 1H, −C$\underline{H}$−OH), 2.00−1.77 (m, 2H, −C$\underline{H}_2$−), 1.38 (dd, J = 7.4, 3.9 Hz, 4H, −C$\underline{H}_2$−C$\underline{H}_2$−), 1.09−0.81 (m, 3H, −C$\underline{H}_3$).[11]

Furan-3-yl(1H-tetrazol-5-yl)methanol (10d). **10d**, white amorphous solid (68%). ^1H NMR (400 MHz, CD$_3$OD) δ 7.58 (s, 1H, −C=C$\underline{H}$−), 7.49 (t, J = 1.9 Hz, 1H, −CH−O−), 6.45 (t, J = 1.9 Hz, 1H, C−CH=), 6.14 (s, 1H, −C$\underline{H}$−OH). ^{13}C NMR (101 MHz, CD$_3$OD) δ 159.10, 143.68, 140.15, 125.50, 108.37, 60.22. HR-MS (ESI-TOF) m/z: Calcd for $C_6H_6N_4O_2$ 165.0413; Found $[M − H]^−$ 165.0417.

9-(1H-Tetrazol-5-yl)-9H-fluoren-9-ol (10e). **10e**, 71%. ^1H NMR (400 MHz, CD$_3$OD) δ 7.79 (dd, J = 7.6, 0.9 Hz, 2H), 7.49−7.39 (m, 4H), 7.32 (td, J = 7.5, 1.1 Hz, 2H).[10]

1-Phenyl-1-(1H-tetrazol-5-yl)ethan-1-ol (10f). **10f**, white solid (70%), mp 142−146 °C. ^1H NMR (400 MHz, MeOD) δ 7.51 (d, J = 7.2 Hz, 2H), 7.33 (t, J = 7.5 Hz, 2H), 7.25 (t, J = 7.3 Hz, 1H), 2.02 (s, 3H, −C$\underline{H}_3$). ^{13}C NMR (101 MHz, CD$_3$OD) δ 164.03, 145.86, 129.40, 128.72, 125.99, 72.19, 30.08. HR-MS (ESI-TOF) m/z: Calcd for $C_9H_{10}N_4O$ 189.0776; Found $[M − H]^−$ 189.0780.

Diphenyl(1H-tetrazol-5-yl)methanol (10g). **10g**, white solid (64%), mp 146−150 °C. ^1H NMR (400 MHz,

106

CD$_3$OD) δ 7.43−7.37 (m, 4H), 7.37−7.28 (m, 6H). ^{13}C NMR (101 MHz, CD$_3$OD) δ 163.45, 145.20, 129.15, 129.09, 128.27, 77.81. HR-MS (ESI-TOF) m/z: Calcd for C$_{14}$H$_{12}$N$_4$O 251.0933; Found [M − H]$^-$ 251.0943.

■ ASSOCIATED CONTENT

ⓢ Supporting Information

The Supporting Information is available free of charge at https://pubs.acs.org/doi/10.1021/acsomega.2c01633.

^{1}H NMR and ^{13}C NMR spectra for compounds **1a,b**, **6b**, **9a−j**, and **10a−g**; ^{1}H NMR spectra for crude mixtures from the deuterium incorporation experiments in Table 1 (PDF)

■ AUTHOR INFORMATION

Corresponding Author

Aigars Jirgensons − *Latvian Institute of Organic Synthesis, LV-1006 Riga, Latvia*; ● orcid.org/0000-0002-8937-8792; Email: aigars@osi.lv

Authors

Konstantinos Grammatoglou − *Latvian Institute of Organic Synthesis, LV-1006 Riga, Latvia*

Madara Dārziņa − *Latvian Institute of Organic Synthesis, LV-1006 Riga, Latvia*

Complete contact information is available at: https://pubs.acs.org/10.1021/acsomega.2c01633

Notes

The authors declare no competing financial interest.

■ ACKNOWLEDGMENTS

■ REFERENCES

(1) (a) Vitaku, E.; Smith, D. T.; Njardarson, J. T. Analysis of the Structural Diversity, Substitution Patterns, and Frequency of Nitrogen Heterocycles among U.S. FDA Approved Pharmaceuticals. *J. Med. Chem.* **2014**, *57*, 10257−10274. (b) Zou, Y.; Liu, L.; Liu, J.; Liu, G. Bioisosteres in drug discovery: focus on tetrazole. *Future Med. Chem.* **2020**, *12*, 91−93. (c) Myznikov, L. V.; Vorona, S. V.; Zevatskii, Y. E. Biologically active compounds and drugs in the tetrazole series. *Chem. Heterocycl. Compd.* **2021**, *57*, 224−233. (d) Ostrovskii, V. A.; Trifonov, R. E.; Popova, E. A. Medicinal chemistry of tetrazoles. *Russ. Chem. Bull.* **2012**, *61*, 768−780. (e) Ballatore, C.; Huryn, D. M.; Smith, A. B. 3rd. Carboxylic acid (bio)isosteres in drug design. *ChemMedChem* **2013**, *8*, 385−395. (f) Herr, R. J. 5-Substituted-1H-tetrazoles as carboxylic acid isosteres: medicinal chemistry and synthetic methods. *Bioorg. Med. Chem.* **2002**, *10*, 3379−3393.

(2) (a) Knudsen, K. R.; Mitchell, C. E. T.; Ley, S. V. Asymmetric organocatalytic conjugate addition of malonates to enones using a proline tetrazole catalyst. *Chem. Commun.* **2006**, 66−68. (b) Shmatova, O. I.; Nenajdenko, V. G. Synthesis of Tetrazole-Derived Organocatalysts via Azido-Ugi Reaction with Cyclic Ketimines. *J. Org. Chem.* **2013**, *78*, 9214−9222.

(3) (a) Pinter, T.; Jana, S.; Courtemanche, R. J. M.; Hof, F. Recognition Properties of Carboxylic Acid Bioisosteres: Anion Binding by Tetrazoles, Aryl Sulfonamides, and Acyl Sulfonamides on a Calix[4]arene Scaffold. *J. Org. Chem.* **2011**, *76*, 3733−3741. (b) Pinter, T.; Simhadri, C.; Hof, F. Dissecting the Complex Recognition Interfaces of Potent Tetrazole- and Pyrrole-Based Anion Binders. *J. Org. Chem.* **2013**, *78*, 4642−4648. (c) Yin, P.; Zhang, Q.; Shreeve, J. N. M. Dancing with Energetic Nitrogen Atoms: Versatile N-Functionalization Strategies for N-Heterocyclic Frameworks in High Energy Density Materials. *Acc. Chem. Res.* **2016**, *49*, 4−16. (d) McKie, A. H.; Friedland, S.; Hof, F. Tetrazoles are Potent Anion Recognition Elements That Emulate the Disfavored Anti Conformations of Carboxylic Acids. *Org. Lett.* **2008**, *10*, 4653−4655. (e) Wurzenberger, M. H. H.; Endraß, S. M. J.; Lommel, M.; Klapötke, T. M.; Stierstorfer, J. Comparison of 1-Propyl-5H-tetrazole and 1-Azidopropyl-5H-tetrazole as Ligands for Laser Ignitable Energetic Materials. *ACS Appl. Energy Mater.* **2020**, *3*, 3798−3806.

(4) Belz, G. G.; Butzer, R.; Kober, S.; Mang, C.; Mutschler, E. Time course and extent of angiotensin II antagonism after irbesartan, losartan, and valsartan in humans assessed by angiotensin II dose response and radioligand receptor assay. *Clin. Pharmacol. Ther.* **1999**, *66*, 367−373.

(5) Feinstein, D. L. Contrasting the neuroprotective and gliotoxic effects of PPARγ agonists. *Drug Discovery Today Ther. Strateg.* **2004**, *1*, 29−34.

(6) Gao, F.; Xiao, J.; Huang, G. Current scenario of tetrazole hybrids for antibacterial activity. *Eur. J. Med. Chem.* **2019**, *184*, 111744.

(7) Zhang, J.; Wang, S.; Ba, Y.; Xu, Z. Tetrazole hybrids with potential anticancer activity. *Eur. J. Med. Chem.* **2019**, *178*, 341−351.

(8) Davulcu, A. H.; McLeod, D. D.; Li, J.; Katipally, K.; Littke, A.; Doubleday, W.; Xu, Z.; McConlogue, C. W.; Lai, C. J.; Gleeson, M.; Schwinden, M.; Parsons, R. L. Process Research and Development for a Tetrazole-Based Growth Hormone Secretagogue (GHS) Pharmaceutical Development Candidate. *J. Org. Chem.* **2009**, *74*, 4068−4079.

(9) (a) Raap, R. Reactions of 1-Substituted 5-Tetrazolyllithium Compounds; Preparation of 5-Substituted 1-Methyltetrazoles. *Can. J. Chem.* **1971**, *49*, 2139−2142. (b) Satoh, Y.; Marcopulos, N. Application of 5-Lithiotetrazoles in Organic-Synthesis. *Tetrahedron Lett.* **1995**, *36*, 1759−1762. (c) Wiedemann, S. H.; Bio, M. M.; Brown, L. M.; Hansen, K. B.; Langille, N. F. Some Practical Methods for the Application of 5-Metallo-1-benzyl-1H-tetrazoles in Synthesis. *Synlett* **2012**, *23*, 2231−2236. (d) Roh, J.; Vavrova, K.; Hrabalek, A. Synthesis and Functionalization of 5-Substituted Tetrazoles. *Eur. J. Org. Chem.* **2012**, *2012*, 6101−6118. (e) Alexakos, P. D.; Wardrop, D. J. N-Morpholinomethyl-5-lithiotetrazole: A Reagent for the One-Pot Synthesis of 5-(1-Hydroxyalkyl)tetrazoles. *J. Org. Chem.* **2019**, *84*, 12430−12436. (f) Neochoritis, C. G.; Zhao, T.; Domling, A. Tetrazoles via Multicomponent Reactions. *Chem. Rev.* **2019**, *119*, 1970−2042. (g) Tullmann, C. P.; Steiner, S.; Knochel, P. Preparation and Reactions of (1H-Tetrazol-5-yl)zinc Pivalates. *Synthesis-Stuttgart* **2020**, *52*, 2357−2363. (h) Zhang, Y.; Lee, J. C. H.; Reese, M. R.; Boscoe, B. P.; Humphrey, J. M.; Helal, C. J. 5-Aryltetrazoles from Direct C-H Arylation with Aryl Bromides. *J. Org. Chem.* **2020**, *85*, 5718−5723.

(10) Grammatoglou, K.; Jirgensons, A. Functionalization of 1N-Protected Tetrazoles by Deprotonation with the Turbo Grignard Reagent. *J. Org. Chem.* **2022**, *87*, 3810−3816.

(11) Brandão, G. C.; Rocha Missias, F. C.; Arantes, L. M.; Soares, L. F.; Roy, K. K.; Doerksen, R. J.; Braga de Oliveira, A.; Pereira, G. R. Antimalarial naphthoquinones. Synthesis via click chemistry, in vitro activity, docking to PfDHODH and SAR of lapachol-based compounds. *Eur. J. Med. Chem.* **2018**, *145*, 191−205.

(12) Delerue-Matos, C.; Freitas, A. M. B.; Maia, H. L. S.; Medeiros, M. J.; Montenegro, M. I.; Pletcher, D. Electrochemical cleavage of some protecting groups from the sulphydryl function in aprotic solvents. *J. Electroanal. Chem.* **1991**, *315*, 1−8.

(13) Gosden, A.; Stevenson, D.; Young, G. T. Protection of thiol and phenolic hydroxy-groups as their 4-picolyl ethers, cleaved by electrolytic reduction. *Chem. Commun.* **1972**, 1123−1124.

(14) Camble, R.; Garner, R.; Young, G. T. Amino-acids and peptides. Part XXX. Facilitation of peptide synthesis by the use of 4-picolyl esters for carboxy-group protection. *J. Chem. Soc. Section C: Organic* **1969**, 1911−1916.

(15) Wieditz, S.; Schafer, H. J.; Schmidt, W.; Undheim, K.; Enzell, C. R.; Inoue, K. The picolyl ester, an electroactive protection group for alcohols. *Acta Chem. Scand.* **1983**, *37b*, 475.

(16) Montenegro, M. I. The electrochemical cleavage of protecting groups. *Electrochim. Acta* **1986**, *31*, 607−620.

(17) Wang, X.; Liu, J.; Wang, D.; Bi, X.; Zhao, W. Synthesis and Characterization of Sodium 5-Chlorotetrazolate Dihydrate by Chlorination of 1H-Tetrazole. *Z. Anorg. Allg. Chem.* **2015**, *641*, 631−635.

(18) Zhang, J.; Leitus, G.; Ben-David, Y.; Milstein, D. Facile Conversion of Alcohols into Esters and Dihydrogen Catalyzed by New Ruthenium Complexes. *J. Am. Chem. Soc.* **2005**, *127*, 10840−10841.

108

Addition of tetrazoles to imines–synthesis of amino acids' bioisosters

experimental part

General procedure for the synthesis of *t*–butanesulfinyl imines: To a solution of (R)– or (S)–*t*–butanesulfinamide (0.605 g,5 mmol) and the corresponding carbonyl compound (4.5 mmol) in dry THF (20 mL) under argon at 23 °C, titanium isopropoxide (2.005 g, 1.885 mL, 9 mmol) was slowly added. The reaction mixture was stirred for 12 h at the same temperature. The resulting mixture was hydrolyzed with brine (30 mL), extracted with ethyl acetate (3x15 mL), dried over anhydrous MgSO₄, and evaporated *in vacuo*. The residue was purified by column chromatography (Petroleum ether/Ethyl acetate 4:1) to obtain the title compound.

General procedure for the addition of tetrazole to *t*–butanesulfinyl imine: A solution of the tetrazole **63** (3 eq.) in dry DCM (0.2 M) was cooled to –60 °C. Turbo Grignard reagent (3.05 eq., 1 M in THF) was added to the mixture dropwise and it was stirred for 30 min at this temperature. Then, a solution of the corresponding electrophile (1 eq.) in DCM (0.35 M) was added dropwise and stirring continued at –60 °C for 30 min. The reaction was then left to reach r.t. slowly and stirred overnight. The reaction was quenched with sat. aq. NH₄Cl and extracted with DCM. The organic phase was dried over anhydrous MgSO₄ and evaporated *in vacuo*. The residue was purified by column chromatography (Petroleum ether/Ethyl acetate 6:1) to obtain the title compound.

(S, E)–N–(4–Methoxybenzylidene)–2–methylpropane–2–sulfinamide (**102a**): White solid (4.1 g, 70%). Synthesized according to the literature.[1]

(S, E)–N–Ethylidene–2–methylpropane–2–sulfinamide (**102b**): Yellow oil (2 g, 97%). Synthesized according to the literature.[2]

(S, E)–2–Methyl–N–(2–methylpropylidene) propane–2–sulfinamide (**102c**): Colourless oil (1.4 g, 98%). Synthesized according to the literature.[3]

(S, E)–2–Methyl–N–pentylidenepropane–2–sulfinamide (**102d**): Yellow oil (1.1 g, 76%). Synthesized according to the literature.[4]

(S, E)–N–(Cyclohexylmethylene)–2–methylpropane–2–sulfinamide (**102e**): Colourless oil (1.5 g, 85%). Synthesized according to the literature.[5]

(S, E)–2–Methyl–N–(pyridin–3–ylmethylene) propane–2–sulfinamide (**102f**): Yellow oil (966 mg, 87%). Synthesized according to the literature.[6]

(S, E)–N–(4–Bromobenzylidene)–2–methylpropane–2–sulfinamide (**102g**): Yellow oil (1.6 g, 87%). Synthesized according to the literature.[7]

(S, E)–2–Methyl–N–(naphthalen–1–ylmethylene) propane–2–sulfinamide (**102h**): Yellow oil (1.5 g, 79%). Synthesized according to the literature.[8]

(S, E)–N–(4–Fluoro–3–methoxybenzylidene)–2–methylpropane–2–sulfinamide (**102i**): Yellow oil (680 mg, 68%). $[\alpha]_D$ = +68.3 (CHCl$_3$, c = 1). ^{1}H NMR (400 MHz, CDCl$_3$) δ 8.50 (s, 1H, –C$\underline{H}$=N–), 7.50 (dd, J = 8.2, 2.0 Hz, 1H, Ar), 7.36 (ddd, J = 8.3, 4.5, 2.0 Hz, 1H, Ar), 7.16 (dd, J = 10.7, 8.3 Hz, 1H, Ar), 3.94 (s, 3H, C$\underline{H}_3$O–), 1.26 (s, 9H, –C(C$\underline{H}_3$)$_3$). ^{13}C NMR (101 MHz, CDCl$_3$) δ 161.8, 154.0, 148.5, 130.9, 123.9, 116.7, 112.8, 57.9, 56.4, 22.7. HR–MS (ESI–TOF) m/z: calculated for C$_{12}$H$_{17}$FNO$_2$S ([M+H]$^+$): 258.0964; found 258.0970.

(R, E)–N–(4–Methoxybenzylidene)–2–methylpropane–2–sulfinamide (**102j**): White solid (776 mg, 66%). Synthesized according to the literature.[9]

(R, E)–2–Methyl–N–(pyridin–3–ylmethylene) propane–2–sulfinamide (**102k**): Yellow oil (1 g, 90%). Synthesized according to the literature.[6]

(R, E)–N–(4–Bromobenzylidene)–2–methylpropane–2–sulfinamide (**102l**): Yellow oil (1.1 g, 78%). Synthesized according to the literature.[7]

(S)–N–((S)–(1–(4–Methoxybenzyl)–1H–tetrazol–5–yl) (4–methoxyphenyl) methyl)–2–methylpropa–ne–2–sulfinamide (**103a**): White solid (220 mg, 88%). $[\alpha]_D$ = +56.8 (CHCl$_3$, c = 1). MP: Dec. > 55°C. ^{1}H NMR (400 MHz, CDCl$_3$) δ 7.07 (d, J = 8.8 Hz, 2H, Ar), 6.99 (d, J = 8.7 Hz, 2H, Ar), 6.79 (dd, J = 8.8, 7.3 Hz, 4H, Ar), 5.67 (d, J = 5.7 Hz, 1H, –C$\underline{H}$–NH–), 5.47 – 5.32 (m, 2H, –C$\underline{H}_2$–), 4.08 (d, J = 5.7 Hz, 1H, –CH–N$\underline{H}$–), 3.77 (s, 3H, C$\underline{H}_3$O–), 3.76 (s, 3H, C$\underline{H}_3$O–), 1.17 (s, 9H, –C(C$\underline{H}_3$)$_3$). ^{13}C NMR (101 MHz, CDCl$_3$) δ 160.2, 160.1, 155.3, 129.2, 129.1, 128.6, 125.1, 114.7, 65.9, 57.0, 55.5, 55.4, 52.4, 50.9, 22.5. HR–MS (ESI–TOF) m/z: calculated for C$_{21}$H$_{27}$N$_5$O$_3$SNa ([M+Na]$^+$): 452.1732; found 452.1727.

(S)–N–((S)–1–(1–(4–Methoxybenzyl)–1H–tetrazol–5–yl)   ethyl)–2–methylpropane–2–sulfinamide (**103b**): Colourless gum (178 mg, 74%). $[\alpha]_D$ = –19.3 (CHCl$_3$, c = 1). ^{1}H NMR (400 MHz, CDCl$_3$) δ 7.20 – 7.11 (m, 2H, Ar), 6.92 – 6.83 (m, 2H, Ar), 5.67 (d, J = 15.3 Hz, 1H, –C$\underline{H}_2$–), 5.43 (d, J = 15.3 Hz, 1H, –C$\underline{H}_2$–), 4.73 – 4.61 (m, 1H, –C$\underline{H}$–NH–), 3.79 (s, 3H, C$\underline{H}_3$O–), 3.74 (d, J = 8.3 Hz, 1H, –CH–N$\underline{H}$–), 1.60 (d, J = 6.8 Hz, 3H C$\underline{H}_3$–), 1.17 (s, 9H, –C(C$\underline{H}_3$)$_3$). ^{13}C NMR (101 MHz, CDCl$_3$) δ 160.2, 156.1, 129.2, 125.3, 114.8, 56.9, 55.5, 50.8, 45.8, 22.6, 21.9. HR–MS (ESI–TOF) m/z: calculated for C$_{15}$H$_{23}$N$_5$O$_2$SNa ([M+Na]$^+$): 360.1470; found 360.1483.

(S)–N–((S)–1–(1–(4–Methoxybenzyl)–1H–tetrazol–5–yl)–2–methylpropyl)–2–methylpropane–2–sulfinamide (**103c**): White solid (158 mg, 62%). $[\alpha]_D$ = +5.5 (CHCl$_3$, c = 1). MP: 92 – 95°C. ^{1}H NMR (400 MHz, CDCl$_3$) δ 7.20 (d, J = 8.7 Hz, 2H, Ar), 6.87 (d, J = 8.8 Hz, 2H, Ar), 5.61 (d, J = 15.2 Hz, 1H, –C$\underline{H}_2$–), 5.51 (d, J = 15.3 Hz, 1H, –C$\underline{H}_2$–), 4.32 (t, J = 7.6 Hz, 1H, –C$\underline{H}$–NH–), 3.87 (d, J = 7.6 Hz, 1H, –CH–N$\underline{H}$–), 3.78 (s, 3H, C$\underline{H}_3$O–), 2.23 – 2.10 (m, 1H, CH$_3$–C$\underline{H}$–CH$_3$), 1.09 (s, 9H, –C(C$\underline{H}_3$)$_3$), 0.93 (d, J = 6.7 Hz, 3H, C$\underline{H}_3$), 0.67

(d, J = 6.7 Hz, 3H, C$\underline{H}_3$). ^{13}C NMR (101 MHz, CDCl$_3$) δ 160.3, 155.4, 129.5, 125.5, 114.7, 56.8, 55.5, 54.9, 50.9, 33.5, 22.4, 19.0, 18.8.

HR–MS (ESI–TOF) m/z: calculated for C$_{17}$H$_{27}$N$_5$O$_2$SNa ([M+Na]$^+$): 388.1783; found 388.1797.

(S)–N–((S)–1–(1–(4–Methoxybenzyl)–1H–tetrazol–5–yl)–pentyl)–2–methylpropane–2–sulfinamide (**103d**): Colourless gum (195 mg, 79%). (CHCl$_3$, c = 1). ^{1}H NMR (400 MHz, CDCl$_3$) δ 7.15 (d, J = 8.7 Hz, 2H, Ar), 6.84 (d, J = 8.8 Hz, 2H, Ar), 5.65 (d, J = 15.3 Hz, 1H, –C$\underline{H}_2$–), 5.45 (d, J = 15.3 Hz, 1H, –C$\underline{H}_2$–), 4.52 (ddd, J = 8.7, 7.6, 6.1 Hz, 1H, –C$\underline{H}$–NH–), 3.82 (d, J = 7.7 Hz, 1H, –CH–N$\underline{H}$–), 3.75 (s, 3H, C$\underline{H}_3$O–), 2.01 – 1.83 (m, 2H, –C$\underline{H}_2$CH$_2$CH$_2$CH$_3$), 1.10 (s, 11H, –C(C$\underline{H}_3$)$_3$ overlapping with –CH$_2$C$\underline{H}_2$CH$_2$CH$_3$), 0.96 – 0.79 (m, 2H, –CH$_2$CH$_2$C$\underline{H}_2$CH$_3$), 0.68 (t, J = 7.3 Hz, 3H, –CH$_2$CH$_2$CH$_2$C$\underline{H}_3$). ^{13}C NMR (101 MHz, CDCl$_3$) δ 160.2, 155.7, 129.2, 125.5, 114.7, 56.7, 55.4, 50.8, 49.5, 35.6, 27.7, 22.4, 22.1, 13.7.

HR–MS (ESI–TOF) m/z: calculated for C$_{18}$H$_{30}$N$_5$O$_2$S ([M+H]$^+$): 380.2120; found 380.2116.

(S)–N–((S)–Cyclohexyl(1–(4–methoxybenzyl)–1H–tetrazol–5–yl)–methyl)–2–methylpropane–2–sulfinamide (**103e**): White solid (190 mg, 66%). [α]$_D$ = +40.7 (CHCl$_3$, c = 1). MP: dec > 55°C. ^{1}H NMR (400 MHz, CDCl$_3$) δ 7.19 (d, J = 8.7 Hz, 2H, Ar), 6.87 (d, J = 8.8 Hz, 2H, Ar), 5.58 (d, J = 15.3 Hz, 1H, –C$\underline{H}_2$–), 5.50 (d, J = 15.2 Hz, 1H, –C$\underline{H}_2$–), 4.34 (t, J = 7.7 Hz, 1H, –C$\underline{H}$–NH–), 3.87 (d, J = 7.5 Hz, 1H, –CH–N$\underline{H}$–), 3.79 (s, 3H, C$\underline{H}_3$O–), 1.89 (dt, J = 12.6, 3.2 Hz, 1H, Cyclohexane), 1.82 – 1.65 (m, 2H, Cyclohexane), 1.63 – 1.50 (m, 2H, Cyclohexane), 1.26 – 1.11 (m, 3H, Cyclohexane), 1.07 (s, 9H, –C(C$\underline{H}_3$)$_3$), 1.02 – 0.82 (m, 2H, Cyclohexane), 0.81 – 0.67 (m, 1H, Cyclohexane). ^{13}C NMR (101 MHz, CDCl$_3$) δ 160.3, 155.5, 129.5, 125.5, 114.7, 56.8, 55.5, 54.6, 50.9, 42.7, 29.5, 29.3, 25.9, 25.7, 25.7, 22.4.

HR–MS (ESI–TOF) m/z: calculated for C$_{20}$H$_{31}$N$_5$O$_2$SNa ([M+Na]$^+$): 428.2096; found 428.2106.

(S)–N–((S)–(1–(4–Methoxybenzyl)–1H–tetrazol–5–yl)(pyridin–3–yl)methyl)–2–methylpropane–2–sulfinamide (**103f**): White solid (249 mg, 88%). [α]$_D$ = +51.7 (CHCl$_3$, c = 1). MP: 95 – 99°C. ^{1}H NMR (400 MHz, CDCl$_3$) δ 8.56 (d, J = 4.8 Hz, 1H, Py), 8.28 (s, 1H, Py), 7.65 (d, J = 8.0 Hz, 1H, Pyr), 7.16 (d, J = 8.1 Hz, 2H, Ar), 6.89 (d, J = 8.4 Hz, 2H, Ar), 5.84 (d, J = 6.6 Hz, 1H, –C$\underline{H}$–NH–), 5.73 (d, J = 15.3 Hz, 1H, –C$\underline{H}_2$–), 5.64 (d, J = 15.3 Hz, 1H, –C$\underline{H}_2$–), 4.71 (d, J = 6.6 Hz, 1H, –CH–N$\underline{H}$–), 3.85 (s, 3H, C$\underline{H}_3$O–), 1.24 (s, 9H, –C(C$\underline{H}_3$)$_3$). ^{13}C NMR (101 MHz, CDCl$_3$) δ 160.3, 154.7, 150.2, 148.7, 135.6, 132.8, 129.2, 125.0, 123.9, 114.8, 57.3, 55.5, 51.1, 48.9, 22.5.

HR–MS (ESI–TOF) m/z: calculated for C$_{29}$H$_{25}$N$_6$O$_2$S ([M+H]$^+$): 401.1760; found 401.1765.

(S)–N–((S)–(4–Bromophenyl)(1–(4–methoxybenzyl)–1H–tetrazol–5–yl)methyl)–2–methylpropane–2–sulfinamide (**103g**): White solid (277 mg, 89%). [α]$_D$ = +54.7 (CHCl$_3$, c = 1). MP: dec > 60°C. ^{1}H NMR (400 MHz, CDCl$_3$) δ 7.37 (d, J = 8.5 Hz, 2H, Ar), 7.00 (d, J

= 8.7 Hz, 2H, Ar), 6.96 (d, J = 8.2 Hz, 2H, Ar), 6.80 (d, J = 8.7 Hz, 2H, Ar), 5.69 (d, J = 6.4 Hz, 1H, –C$\underline{H}$–NH–), 5.55 (d, J = 15.4 Hz, 1H, –C$\underline{H}_2$–), 5.44 (d, J = 15.4 Hz, 1H, –C$\underline{H}_2$–), 4.18 (d, J = 6.4 Hz, 1H, –CH–N$\underline{H}$–), 3.79 (s, 3H, C$\underline{H}_3$O–), 1.16 (s, 9H, –C(C$\underline{H}_3$)$_3$). ^{13}C NMR (101 MHz, CDCl$_3$) δ 160.3, 154.9, 135.7, 132.4, 129.4, 129.2, 125.0, 123.5, 114.7, 57.2, 55.54, 51.5, 51.1, 22.5.

HR–MS (ESI–TOF) m/z: calculated for C$_{20}$H$_{24}$BrN$_5$O$_2$SNa ([M+Na]$^+$): 500.0732; found 500.0747.

(S)–N–((S)–(1–(4–Methoxybenzyl)–1H–tetrazol–5–yl)(naphthalen–1–yl)methyl)–2–methylpropane–2–sulfinamide (**103h**): White solid (190 mg, 65%). [α]$_D$ = +28.6 (CHCl$_3$, c = 1). MP: dec > 60ºC. ^{1}H NMR (400 MHz, CDCl$_3$) δ 7.98 – 7.92 (m, 1H, Ar), 7.89 – 7.85 (m, 1H, Ar), 7.83 (dt, J = 8.3, 1.1 Hz, 1H, Ar), 7.55 – 7.48 (m, 2H, Ar), 7.33 (dd, J = 8.2, 7.2 Hz, 1H, Ar), 7.22 (dd, J = 7.3, 1.2 Hz, 1H, Ar), 6.80 (d, J = 8.8 Hz, 2H, Ar), 6.60 (d, J = 8.7 Hz, 2H, Ar), 6.47 (d, J = 4.5 Hz, 1H, –C$\underline{H}$–NH–), 5.33 (d, J = 15.3 Hz, 1H, –C$\underline{H}_2$–), 5.22 (d, J = 15.3 Hz, 1H, –C$\underline{H}_2$–), 4.07 (d, J = 4.5 Hz, 1H, –CH–N$\underline{H}$–), 3.70 (s, 3H, C$\underline{H}_3$O–), 1.21 (s, 9H, –C(C$\underline{H}_3$)$_3$). ^{13}C NMR (101 MHz, CDCl$_3$) δ 159.8, 155.1, 134.1, 131.4, 130.3, 130.1, 129.1, 129.1, 127.5, 126.8, 126.5, 125.2, 124.3, 122.4, 114.3, 56.9, 55.3, 50.9, 49.8, 22.5.

HR–MS (ESI–TOF) m/z: calculated for C$_{24}$H$_{27}$N$_5$O$_2$SNa ([M+Na]$^+$): 472.1783; found 472.1794.

(S)–N–((S)–(4–Fluoro–3–methoxyphenyl)(1–(4–methoxybenzyl)–1H–tetrazol–5–yl)methyl)–2–methylpropane–2–sulfinamide (**103i**): White solid (167 mg, 60%). [α]$_D$ = +44.3 (CHCl$_3$, c = 1). MP: dec > 60ºC. ^{1}H NMR (400 MHz, CDCl$_3$) δ 7.03 (d, J = 8.7 Hz, 2H, Ar), 6.93 (dd, J = 10.9, 8.3 Hz, 1H, Ar), 6.80 (d, J = 8.8 Hz, 2H, Ar), 6.69 (dd, J = 7.9, 2.2 Hz, 1H, Ar), 6.64 (ddd, J = 8.4, 4.1, 2.2 Hz, 1H, Ar), 5.69 (d, J = 6.1 Hz, 1H, –C$\underline{H}$–NH–), 5.54 (d, J = 15.4 Hz, 1H, –C$\underline{H}_2$–), 5.45 (d, J = 15.4 Hz, 1H, –C$\underline{H}_2$–), 4.16 (d, J = 6.1 Hz, 1H, –CH–N$\underline{H}$–), 3.77 (s, 3H, C$\underline{H}_3$O–), 3.73 (s, 3H, C$\underline{H}_3$O–), 1.17 (s, 9H, –C(C$\underline{H}_3$)$_3$). ^{13}C NMR (101 MHz, CDCl$_3$) δ 160.1, 154.9, 153.8, 151.3, 148.2, 148.1, 132.9, 132.9, 129.1, 125.0, 120.0, 119.9, 116.5, 116.3, 114.6, 112.8, 112.8, 57.0, 56.2, 55.4, 51.7, 50.9, 22.4. ^{19}F NMR (376 MHz, CDCl$_3$) δ –133.8.

HR–MS (ESI–TOF) m/z: calculated for C$_{21}$H$_{26}$FN$_5$O$_3$SNa ([M+Na]$^+$): 470.1638; found 470.1646.

(R)–N–((R)–(1–(4–Methoxybenzyl)–1H–tetrazol–5–yl)(4–methoxyphenyl)methyl)–2–methylpropa–ne–2–sulfinamide (**103j**): White solid (318 mg, 80%). [α]$_D$ = –58.6 (CHCl$_3$, c = 1). MP: dec > 55ºC. ^{1}H NMR (400 MHz, CDCl$_3$) δ 7.08 (d, J = 8.8 Hz, 2H, Ar), 6.99 (d, J = 8.7 Hz, 2H, Ar), 6.80 (dd, J = 8.8, 7.4 Hz, 4H, Ar), 5.67 (d, J = 5.8 Hz, 1H, –C$\underline{H}$–NH–), 5.42 (d, J = 15.3 Hz, 1H, –C$\underline{H}_2$–), 5.36 (d, J = 15.3 Hz, 1H, –C$\underline{H}_2$–), 4.05 (d, J = 5.8 Hz, 1H, –CH–N$\underline{H}$–), 3.78 (s, 3H, C$\underline{H}_3$O–), 3.77 (s, 3H, C$\underline{H}_3$O–), 1.17 (s, 9H, –C(C$\underline{H}_3$)$_3$). ^{13}C NMR (101 MHz, CDCl$_3$) δ 160.3, 160.2, 155.3, 129.9, 129.2, 129.1, 128.6, 125.1, 114.7, 57.0, 55.5, 55.4, 52.4, 50.9, 22.6.

HR–MS (ESI–TOF) m/z: calculated for C$_{21}$H$_{27}$N$_5$O$_3$SNa ([M+Na]$^+$): 452.1732; found 452.1729.

(R)–N–((R)–(1–(4–Methoxybenzyl)–1H–tetrazol–5–yl)(pyridin–3–yl)methyl)–2–methylpropane–2–sulfinamide (**103k**): White solid (205 mg, 72%). [α]$_D$ = –51.2 (CHCl$_3$, c = 1). MP: 94 – 98°C. ^{1}H NMR (400 MHz, CDCl$_3$) δ 8.49 (dd, J = 4.8, 1.6 Hz, 1H, Py), 8.20 (d, J = 2.2 Hz, 1H, Py), 7.59 (dt, J = 7.9, 2.0 Hz, 1H, Py), 7.19 (ddd, J = 8.0, 4.8, 0.9 Hz, 1H, Py), 7.07 (d, J = 8.7 Hz, 2H, Ar), 6.81 (d, J = 8.7 Hz, 2H, Ar), 5.76 (d, J = 6.4 Hz, 1H, –CH–NH–), 5.65 (d, J = 15.3 Hz, 1H, –CH$_2$–), 5.55 (d, J = 15.4 Hz, 1H, –CH$_2$–), 4.51 (d, J = 6.5 Hz, 1H, –CH–NH–), 3.77 (s, 3H, CH$_3$O–), 1.16 (s, 9H, –C(CH$_3$)$_3$). ^{13}C NMR (101 MHz, CDCl$_3$) δ 160.2, 154.6, 150.1, 148.6, 135.6, 132.7, 129.1, 124.9, 123.9, 114.7, 57.3, 55.4, 51.1, 49.0, 22.4.

HR–MS (ESI–TOF) m/z: calculated for C$_{19}$H$_{25}$N$_6$O$_2$S ([M+H]$^+$): 401.1760; found 401.1762.

(R)–N–((R)–(4–Bromophenyl)(1–(4–methoxybenzyl)–1H–tetrazol–5–yl)methyl)–2–methylpropane–2–sulfinamide (**103l**): White solid (238 mg, 70%). [α]$_D$ = –56.4 (CHCl$_3$, c = 1). MP: dec > 60°C. ^{1}H NMR (400 MHz, CDCl$_3$) δ 7.35 (d, J = 8.6 Hz, 2H, Ar), 6.98 (dd, J = 18.1, 8.6 Hz, 4H, Ar), 6.79 (d, J = 8.8 Hz, 2H, Ar), 5.69 (d, J = 6.4 Hz, 1H, –CH–NH–), 5.54 (d, J = 15.4 Hz, 1H, –CH$_2$–), 5.45 (d, J = 15.5 Hz, 1H, –CH$_2$–), 4.26 (d, J = 6.5 Hz, 1H, –CH–NH–), 3.78 (s, 3H, CH$_3$O–), 1.15 (s, 9H, –C(CH$_3$)$_3$). ^{13}C NMR (101 MHz, CDCl$_3$) δ 160.3, 154.9, 135.7, 132.3, 129.4, 129.2, 125.0, 123.4, 114.7, 57.2, 55.5, 51.4, 51.0, 22.5.

HR–MS (ESI–TOF) m/z: calculated for C$_{20}$H$_{24}$BrN$_5$O$_2$SNa ([M+Na]$^+$): 500.0732; found 500.0736.

t–Butyl (E)–(4–methoxybenzylidene) carbamate (**105**): White solid (0.8 g, 72%). Synthesized according to the literature.[10]

t–Butyl ((1–(4–methoxybenzyl)–1H–tetrazol–5–yl)(4–methoxyphenyl)methyl)carbamate (**106**): White solid (212 mg, 73%). [α]$_D$ = 0.0 (CHCl$_3$, c = 1). MP: 142 – 145°C. ^{1}H NMR (400 MHz, CDCl$_3$) δ 7.03 (d, J = 8.8 Hz, 2H, Ar), 6.98 (d, J = 8.7 Hz, 2H, Ar), 6.80 – 6.70 (m, 4H, Ar), 5.96 (d, J = 8.2 Hz, 1H, –CH–NH–), 5.75 (d, J = 8.3 Hz, 1H, –CH–NH–), 5.38 (d, J = 15.2 Hz, 1H, –CH$_2$–), 5.29 (d, J = 15.3 Hz, 1H, –CH$_2$–), 3.76 (s, 3H, CH$_3$O–), 3.75 (s, 3H, CH$_3$O–), 1.39 (s, 9H, –C(CH$_3$)$_3$). ^{13}C NMR (101 MHz, CDCl$_3$) δ 160.0, 159.9, 155.1, 154.9, 129.3, 129.0, 128.5, 124.9, 114.5, 114.5, 80.7, 55.4, 50.8, 49.1, 28.4.

HR–MS (ESI–TOF) m/z: calculated for C$_{22}$H$_{27}$N$_5$O$_4$Na ([M+Na]$^+$): 448.1961; found 448.1964.

1.   Maji M. S.; Fröhlich R.; Studer A. Desymmetrization of Metalated cyclohexadienes with Chiral *N–tert*–Butanesulfinyl Imines. *Organic Letters* **2008**, *10* (9), 1847–1850.
2.   Toop H. D.; Brusnahan J. S.; Morris J. C. Concise Total Synthesis of Dioncophylline E through an *ortho*–Arylation Strategy. *Angew. Chem. Int. Ed.* **2017**, *56*, 8536.

3. Liu G.; Cogan D. A.; Ellman J. A. Catalytic Asymmetric Synthesis of *tert*–Butane–sulfinamide. Application to the Asymmetric Synthesis of Amines. *J. Am. Chem. Soc.* **1997**, *119*, 41, 9913–9914.

4. Morales S.; Guijarro F. G.; Ruano J. L. G.; Cid M. B. A General Aminocatalytic Method for the Synthesis of Aldimines. *J. Am. Chem. Soc*. **2014**, *136*, 3, 1082–1089.

5. Bolshan Y.; Batey R. A. A Room–Temperature Protocol for the Rhodium(I)–Catalyzed Addition of Arylboron Compounds to Sulfinimines. *Org. Lett*. **2005**, *7*, 8, 1481–1484.

6. Liu G.; Cogan D. A.; Owens T. D.; Tang T. P.; Ellman J. A. Synthesis of Enantiomerically Pure N–tert–Butanesulfinyl Imines (*tert*–Butanesulfinimines) by the Direct Condensation of *tert*–Butanesulfinamide with Aldehydes and Ketones. *J. Org. Chem*. **1999**, *64*, 4, 1278–1284.

7. Plobeck N.; Powell D. Asymmetric synthesis of diarylmethylamines by diastereoselective addition of organometallic reagents to chiral *N–tert–*butanesulfinimines: switchover of diastereofacial selectivity. *Tetrahedron: Asymmetry* **2002**, *13*, 3, 303–310.

8. Vazquez–Chavez J.; Luna–Morales S.; Cruz–Aguilar D. A.; Díaz–Salazar H.; Vallejo Narváez W. E.; Silva–Gutiérrez R. S.; Hernández–Ortega S.; Rocha–Rinza T.; Hernández–Rodríguez M. The effect of chiral N–substituents with methyl or trifluoromethyl groups on the catalytic performance of mono– and bifunctional thioureas. *Org. Biomol. Chem*., **2019**, *17*, 10045–10051.

9. Kells K. W.; Chong J. M. Stille Coupling of Stereochemically Defined α–Sulfonamido–organostannanes. *J. Am. Chem. Soc*. **2004**, *126*, 48, 15666–15667

10. Wenzel A. G.; Jacobsen E. N. Asymmetric Catalytic Mannich Reactions Catalyzed by Urea Derivatives: Enantioselective Synthesis of β–Aryl–β–Amino Acids. *J. Am. Chem. Soc*. **2002**, *124*, 44, 12964–12965.

Konstantinos Grammatoglou dzimis 1980. gadā Grieķijā, Salonikos. Aristoteļa Universitātē (Saloniki) ieguvis bakalaura (2013) un maģistra (2015) grādu ķīmijā. No 2015. līdz 2022. gadam strādājis Latvijas Organiskās sintēzes institūta Organiskās sintēzes metodoloģijas grupā. Patlaban ir pētnieks *Symeres* Groningenā, Nīderlandē. Zinātniskās intereses saistītas ar organisko ķīmiju, mazo molekulu un bioloģiski aktīvu savienojumu sintēzi. Ir četru oriģinālpublikāciju, kas publicētas starptautiski citējamos žurnālos (impaktfaktors 5,756), līdzautors.

Konstantinos Grammatoglou was born in 1980 in Thessaloniki, Greece. He obtained his Bachelor's degree in 2013 and his Master's degree in 2015 from Aristotle University of Thessaloniki. From 2015 until 2022, he has been a Research Assistant at Latvian Institute of Organic Synthesis in Organic Synthesis Methodology group, Riga. He is currently a Research Scientist at *Symeres* in Groningen, Netherlands. His research interests are organic chemistry research, synthesis of small molecules and synthesis of bioactive compounds. He is a co-author of four original publications in international journals (IF up to 5.756).